STUDIES ON *NYMPHAEA PUBESCENS* WILLD. (NYMPHAEACEAE) - A PLANT DRUG OF AQUATIC FLORA INTEREST

Thesis submitted to

THE TAMILNADU DR. M.G.R. MEDICAL UNIVERSITY
GUINDY, CHENNAI-600 032, INDIA

In partial fulfillment of the requirements for the Degree of

DOCTOR OF PHILOSOPHY
in
PHARMACY

by

E. SELVA KUMARI, M.Pharm.

Under the Guidance of

Dr. A. SHANTHA, B.Pharm., M.Sc.,(Pharm.), Ph.D.

Professor and Head
Department of Pharmaceutical Analysis
C.L.Baid Metha College of Pharmacy
Thorapakkam, Chennai-600 097
India

December 2012

Dedicated to

my

lovable Almighty

ACKNOWLEDGEMENT

I express my true gratefulness to my ever loving God, who has given me the wisdom with his grace and capability to complete this work successfully.

I got inward bound and brainwave to endure research investigations to this extent, I concede my inmost special gratitude and thanks to **Dr. A. Shantha, B.Pharm., M.Sc.(Pharm.)., Ph.D.,** Professor, Department of Pharmaceutical Analysis, C.L.Baid Metha College of Pharmacy, Chennai, India, for the active guidance, innovative ideas, creative works, indulgement and enthusiastic guidance, valuable suggestions, a source of inspiration where the real treasure of my work.

I owe my sincere thanks with bounteous pleasure to my doctoral committee members **Prof. N. Ramesh Kumar, M.Pharm.,** Department of Pharmaceutical Chemistry, C.L.Baid Metha College of Pharmacy, Chennai and **Dr. P. Muthuswamy, M.Pharm., Ph.D,** Tutor, Madras Medical College, Chennai, whose encouragement, guidance and support from the initial to the final level enabled me to develop an understanding of the subject.

I wish to express my deep sense of gratitude to **Harish L Metha,** Secretary and Correspondance, C.L.Baid Metha College of Pharmacy, Chennai, for having given me an opportunity and encouragement in all the ways in completing the study.

I extend my thanks to **Dr. Grace Rathinam, M.Pharm., Ph.D., Principal**, C.L.Baid Metha College of Pharmacy, for providing all the necessary facilities to carry out this work.

My special wisdom of thanks to **Mr.T.Purushoth Prabhu**, M.Pharm., Assistant Professor, Department of Pharmacognosy, C.L.Baid Metha College of Pharmacy, for helping and for his untiring efforts throughout the research work.

I would like to express my heartfelt thanks to **Dr. R. Radha,** M.Pharm.,Ph.D., Assistant Professor and **Dr. R. Vijayabarathi,** M.Pharm.,Ph.D., Tutor, College of

Pharmacy, Madras Medical College, Chennai, for their guidance throughout my research work.

I take this opportunity to express my sincere thanks to my fellow colleagues and my committee members **R.Vijayageetha, M.Pharm., B.Rama, M.Pharm., T.Uma, M.Pharm., and S.Yamuna, M.Pharm.,** Assistant Professors, C.L.Baid Metha College of Pharmacy, Chennai. All of them encouraged me in various ways.

I express my sincere thanks to **Prof., Dr. P. Jayaraman,** Director, Plant Anatomy Research Centre, Thambaram, Chennai, for his help, interest and encouragement in Pharmacognostic studies.

My heartful thanks to **Dr. P. Kalaiselvi.,** M.Phil., Ph.D., Professor, Department of Medical Biochemistry, Late **D. Rajalakshmi,** Research Scholar**,** Department of Medical Biochemistry, IBMS, University of Madras, Chennai, for their complete guidance and precious help for the completion of molecular studies.

I extend my thanks to **Dr. N. Adhiraj,** Research Associate, KMCH College of Pharmacy, Coimbature, for the lab facilities for carrying out the anticancer activity.

I immensely thank **Dr. D. Chamundeeswari**, M.Pharm., Ph.D., Principal, College of Pharmacy, Sri Ramachandra University, Chennai, for the HPTLC studies.

I express my heartful thanks to **Mr.Veera Bhadra Rao**, Research Scholar, Department of Chemistry, Pondicherry University, Puducherry, for the interpretation of the spectrums.

I would like to express my thanks to **Mr. Shanthakumar,** M.Pharm., Department of Pharmacology, C.L.Baid Metha College of Pharmacy, for his help in Pharmacological studies.

I express my special thanks to **Prof. Dr. V.Gopal, M.Pharm., Ph.D.,** Principal and Academic Registrar, MTPG & RIHS, Puducherry, for his valuable support and help to complete my research work.

The acknowledgement would not be complete without a heartfelt thanks to **Prof. Dr. S. Kavimani, M.Pharm., Ph.D.,** Professor and Head of the Department,

Department of Pharmacology, MTPG & RIHS, Puducherry, for his valuable help throughout the research work.

I express my heartfelt thanks to **Dr. S. Ravi Shankar**, Assistant Professor, Madras Christian College, Chennai, for his timely help for the compilation of the thesis.

I immensely express my gratitude to all my colleagues and friends, for their encouragement, either directly or indirectly during course of my study.

I express my respectful regards to my husband **Dr**. **C. Sreenath kumar**, for his complete support throughout my research work.

I submit my fragrance of love for ever to my daughter **S. Rebecca Janice**, for her co-operation throughout my research work.

Finally I express my heartful gratitude and love to my Father, Mother, Brothers and my family members for their energetic support in my entire study.

CONTENTS

LIST OF TABLES

LIST OF FIGURES

LIST OF SPECTRA

Spectra No.		Title of the spectra
1	-	GCMS of ethanolic extract from root and rhizome of *Nymphaea pubescens*
2	-	GCMS of ethanolic flower extract of *Nymphaea pubescens*
3	-	IR Spectrum of compound I
4	-	^{1}H NMR spectrum of compound I
5	-	^{13}C NMR spectrum of compound I
6	-	^{13}C DEPT-135 NMR Spectrum of compound I
7	-	HMBC Spectrum of compound I
8	-	Mass spectrum of compound I
9	-	IR spectrum of compound II
10	-	^{1}H NMR spectrum of compound II
11	-	^{13}C NMR spectrum of compound II
12	-	^{13}C DEPT-135 NMR spectrum of compound II
13	-	HMBC spectrum of compound II
14	-	Mass Spectrum of compound II
15	-	UV Spectrum of compound III
16	-	IR spectrum of compound III
17	-	^{1}H NMR spectrum of compound III
18	-	Mass spectroscopy of compound III
19	-	UV spectrum of compound IV
20	-	IR spectrum of compound IV
21	-	^{1}H NMR spectrum of compound IV
22	-	Mass spectroscopy of compound IV

ABBREVIATIONS

2DNMR	-	2 Dimensional Nuclear Magnetic Resonance
ABTS	-	2,2'-Azino-bis (3-ethylbenzo-thiazoline-6-sufonic acid diammonium salt
ALX	-	Alloxan
COSY	-	Correlation Spectroscopy
DAL	-	Dalton Ascites Lymphoma
dATP	-	Deoxyadenosine Triphosphate
DEPT	-	Distortionless enhancement of polarization technique
DMSO	-	Dimethylsulfoxide
DPPH	-	Diphenyl -1-Picryl Hydrazyl
EDTA	-	Ethylene Diamine Tetra acetic Acid
Fe-NTA	-	Ferric Nitrilo Tri Acetate
GCMS	-	Gas Chromatography–Mass Spectrometry
GCMSMS	-	Gas Chromatography-Mass Spectrometry Mass Spectrometry
GLC-MS	-	Gas Liquid Chromatography- Mass Spectrometry
GPx	-	Glutathione Peroxidase
HeLa	-	Henrietta Lack
HIP	-	Human Islet Amyloid Polypeptide
HMBC	-	Heteronuclear multiple bond coherence
HPTLC	-	High Performace Thin Layer Chromatography
HSQC	-	Heteronuclear Single Quantum Coherence.
IDDM	-	Insulin dependent diabetes mellitus
IR	-	Infra Red
IRS	-	Insulin Receptor Substrate
LCMS	-	Liquid Chromatography-Mass Spectrometry
LCMSMS	-	Liquid Chromatography-Mass Spectrometry Mass Spectrometry
LD	-	Lethal Dose
LDL	-	Low Density Lipoprotein

LPO	-	Lipid peroxidation
MPTP	-	Mitochondrion Permeability Transition Pores
NAD	-	Nicotinamide Adenine Dinucleotide
NCD	-	Non Communicable disease
NIDDM	-	noninsulin-dependent diabetes mellitus
NMR	-	Nuclear Magnetic Resonance
OGTT	-	Oral Glucose Tolerance Test
PARP	-	Adenine Ribosyl Polymerase Enzyme
PDX	-	Pancreas Duodenum Homeobox
p-NDA	-	*p*-Nitroso dimethyl aniline
PTP1B	-	Phospho Tyrosine Phosphatase 1B
RTK	-	Receptor Tyrosine Kinase
SDS	-	Sodium Dodecyl Sulphate
SOCS	-	Suppressor of Cytokine Signalling
SOD	-	Superoxide Dismutase
STZ	-	Streptozotocin
TEMED	-	Tetramethylethylenediamine
TLC	-	Thin Layer Chromatography
UCP1	-	Uncoupling Protein
UV	-	Ultra violet
VLDL	-	Very Low Density Lipoprotein
WEF	-	World Economic Forum
WHO	-	World Health Organization

INTRODUCTION

Pharmacognostic science, considered the mother of all the sciences, owes its birth to the advent on earth of the earliest man, who had no choice but to search his surroundings for some product to relieve his pain and cure the disease. His experiments with the surrounding materials, led him to use natural products. With the passage of time, the natural medicine developed into well organized and well researched systems of medicine, throughout the World. In the old and new testaments of the Bible, there are over a dozen of plants were mentioned as a food and medicines- "Their fruits of the tree along the bank of the river will be for food and their leaves for medicine -Ezekiel-47:12".

India with its earliest history of civilization and vast natural resources, named its traditional medicinal methods as Ayurveda, Siddha and Unani systems and also Homeopathy which was imported later from Germany. Likewise in other parts of the World, the systems of traditional medicine practiced were named according to their own conventional sensibilities and philosophies. Eg., China's system was called the Chinese medicine. As caught the fancy of the people and almost threw natural remedies into discredit, even though the traditional system refused to die and continue to be practiced globally among 75-80% of the total population.

Allopathic drugs though with the rapid advances made in their immediate professional surroundings, overlooked the fact that the phytochemicals had made valuable contribution to drug discovery by giving a lead in all kinds of new chemicals, from which modern medicines were designed and prepared. It is now a matter of common knowledge that no fewer than 25% of plant based drugs are being used in the USA. The global market for herbal drugs presently is said to be $80 billion. It is particularly noteworthy that more than 60 crude drugs have recently been incorporated in the European and British Pharmacopoeias [1].

We are all acquainted with the prevalent mode of Allopathic treatment. In the treatment of acute distressing conditions and in emergencies, allopathic drugs are of considerable value. These drugs can instantly relieve acute pain and distress. Moreover, with the great strides made in the field of surgery, many valuable lives

have been saved, thus reducing the mortality rate. But the treatment of chronic diseases with drugs of the orthodox system, poses a grave problem. Allopathic drugs are fundamentally palliative. In 2009, H1N1 or "Swine Flu", was reported as rampant throughout America and parts of Mexico. When younger children were given the H1N1 vaccine, some experienced side effects like muscle aches, sore throat, headaches, and fever. Some medicines caused increased cases of autism in children. Moreover, the long term use of the modern medicine is often associated with the risk of side-effects. Thus in relieving a diseased condition, other abnormal physiological and pathological conditions may develop. In other words a drug-induced disease is produced. Such diseases are called *Iatrogenic* Disease ("*Iatrogenic*" means "Physician-Induced"), which are far more difficult to treat than natural diseases.

When the corticosteroids were introduced into the market they were called the "Wonder-Drugs". Arthritis found a miraculous relief in their agonizing pains, and the inflammatory condition of the affected joints was greatly reduced. But, the relief was short-lived. As soon as the drug was stopped the symptoms came back. Moreover, the long-term use of Cortisones had serious side-effects. Kidney dysfunction, diabetes, peptic ulcers were aggravated. Some patients developed cataract and some women developed an unwanted growth of facial hair. Antibiotics, which plays a greater role in modern medicine is now threatening the life with many adverse effects and development of multi and extreme drug resistant strains (http://www.homeoint.org /site/ahmad/allopathy.htm).

But there are number of advantages associated with using herbal medicines as opposed to pharmaceutical products. Examples include reduced risk of side effects, effectives with chronic conditions, lower cost and widespread availability. Medicinal plants play an important role in the development of potent therapeutic agents. During 1950-1970 approximately 100 plants based new drugs were introduced in the USA drug market including Deserpidine (Depletion of neurotransmiters, Inhibition of ATP/Mg^{2+} pump – Antihypertensive and Antipsychotic drug), Rescinnamine (Angiotensin converting enzyme inhibitor – Antihypertensive and Antipsychotic drug), Reserpine (Depletion of monoamine neurotransmitters – Antihypertensive and Antipsychotic drug), Vinblastine (Inhibiting the assembly of microtubules in M phase

– Anticancer drug) and Vincristine (Mitotic inhibitory drug – Anticancer drug) which are derived from higher plants. From 1971 to 1990 new drugs such as Etoposide (Induction of DNA damage – Anticancer drug), Guggulsterone (Induces apoptosis in leukemic cells – Anticancer drug), Teniposide (Topoisomerase II inhibitor – anticancer drug), Plaunotol (Leakage of K^+ ions in bacterial cell – Antibacterial drug) and Artemisinin (Interference with parasite transport proteins, disruption of parasite mitochondrial function, modulation of host immune function and inhibition of angiogenesis – Antimalarial drug) appeared all over the world. 2% of drugs were introduced from 1991 to 1995 including Paclitaxel (Mitotic inhibitor – Anticancer drug), Topotecan and Irinotecan (Topoisomerase inhibitors – Anticancer drug) etc. The above mentioned drugs are the plant based origin that provides outstanding contribution to modern therapeutics [2].

The rationalization of the new multidrug and multitarget concept of therapy in classical medicine is likely to have great implications on the future basic research in phytomedicine and evidence-based phytotherapy. It requires concerted cooperation between phytochemists, molecular biologists, pharmacologists and clinicians, with the aim of using modern high-tech methods for standardization of phytopreparations, of integrating new molecular biological assays into the screening of plant extracts and plant constituents and of increasing studies on the efficacy proof of phytopreparations using controlled clinical trials. This should be paralleled or followed by pharmacokinetic and bioavailability studies[3].

Even though the 21st century is characterised by rapid changes and hyper competition in the modern therapeutics, the rapid globalization and industrialization occurring in developing countries resulted in considerable increase in lifestyle related disease.

From the 1940's to the late 1990's heart disease, cancer and degenerative diseases (eg., diabetes, cirrhosis, kidney failure, chronic obstructive pulmonary disease) accounted for the maximum number of death. Of the 57 million deaths that occurred globally in 2008, 36 million, almost two thirds were due to non communicable diseases comprising mainly cardiovascular diseases, cancer, diabetes

and chronic lung diseases (http://www.who.int/nmh/publications/ncd_report_full_en.pdf). A report, jointly published by the World Health Organization and the World Economic Forum says, India will incur an accumulated loss of $236.6 billion by 2015 on account of unhealthy lifestyles and faulty diet.

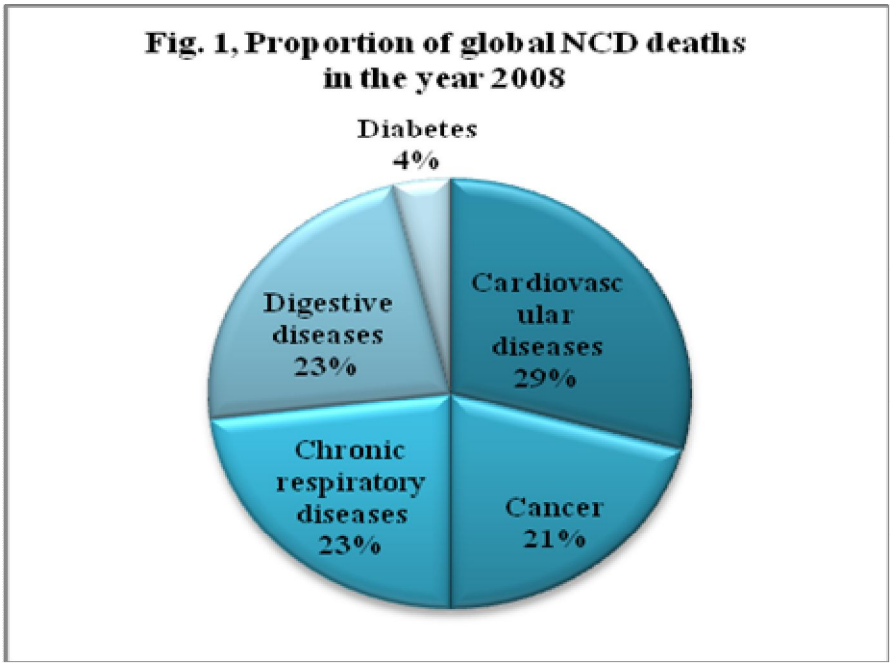

Indirect evidence suggests that free radicals and excited state species play a key role in both normal biological function and in the pathogenesis of certain diseases. There is significant circumstantial evidence that active oxygen is involved in some of the fundamental mechanisms in pathogenesis and in the etiology of diseases like diabetes and cancer and they are the common diseases with tremendous impact on health worldwide. These are heterogeneous, multifactorial, severe and chronic diseases[4]. Thus the challenge facing these life style related diseases, it is the right time to exploit the vast diversity of chemical structures and biological activities of natural product leads.

REVIEW OF LITERATURE

Literature survey was carried out on *Nymphaea pubescens* (Nymphaeaceae) regarding ethnobotanical uses, ethnopharmacology, pharmacognosy, phytochemistry, pharmacological studies and geographical distribution.

Nymphaea is the most speciose, phenotypically diverse and geographically widespread genus of Nymphaeales. The family Nymphaeaceae comprises of six genera's such as *Barclaya*, *Euryale*, *Nuphar*, *Nymphaea*, *Ondinea* and *Victoria*. *Nymphaea* occurs almost worldwide, comprising 45-50 species in five subgenera such as *Anecphya*, *Brachyceras*, *Hydrocallis*, *Lotos* and *Nymphaea*. The subgenera lotos consist of three species such as *Nymphaea petersiana*, *Nymphaea lotus* and *Nymphaea pubescens*. The phylogenetic analysis of *N.pubescens* and *N.lotus* reveals that based on the chloroplast trnT-trnF region, the two species are well separated genetically[5]. Sequence divergence between *N.lotus* and *N.pubescens* provides clear evidence for the distintinctness of *N.pubescens*. A perusal of literature shows that only six species occurs in India and they are *Nymphaea nouchali*, *N.pubescens*, *N.rubra*, *N.tetragona*, *N.alba* and *N.candida*[6].

Plant Profile

Taxonomical Hierarchy

Kingdom	-	Plantae
Phylum	-	Embryophyta
Class	-	Dicotyledons
Order	-	Nymphaeales
Family	-	Nymphaeaceae
Genus	-	*Nymphaea*
Subgenus	-	Lotos
Species	-	*pubescens*

Vernacular Names

Hindi	-	Kanval, Kokka
Kanadam	-	Bilenaydilie, Biletavare
Malayalam	-	Ampal
Sanskrit	-	Kumudam
Tamil	-	Vellambal, Allitamarai
Telugu	-	Allikada, Tellakaluva
English	-	Water lily

General characters

Nymphaea pubescens is a large perennial aquatic herb with short, erect, roundish, tuberous rhizome, leaves floating, peltate, sharply sinuate-toothed, flowers large, floating, solitary, white in colour with pink striations, fruits spongy many seeded berries, seeds minute greyish black when dry with longitudinal striations[7].

Floral diagram

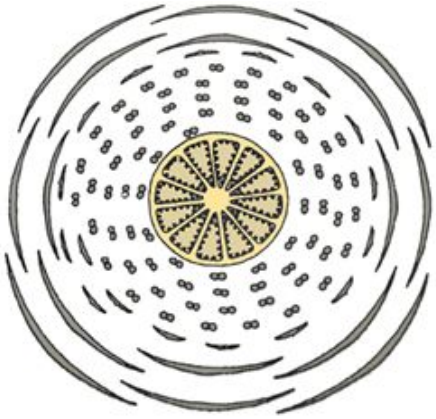

Fig.2 Floral diagram of the flower of *Nymphaea pubescens*

Floral formula

$$\oplus \ \mathrm{⚥} \quad K_4 \quad C_\alpha \quad A_\alpha \quad \underline{G}_\alpha$$

Geographical Distribution

Nymphaea pubescens is common in shallow lakes and ponds throughout temperate and tropical Asia: Bangladesh, India, Pakistan, Sri Lanka, Yunnan, Taiwan, Philippines, Cambodia, Laos, Myanmar, Thailand, Vietnam, Indonesia and Malaysia.

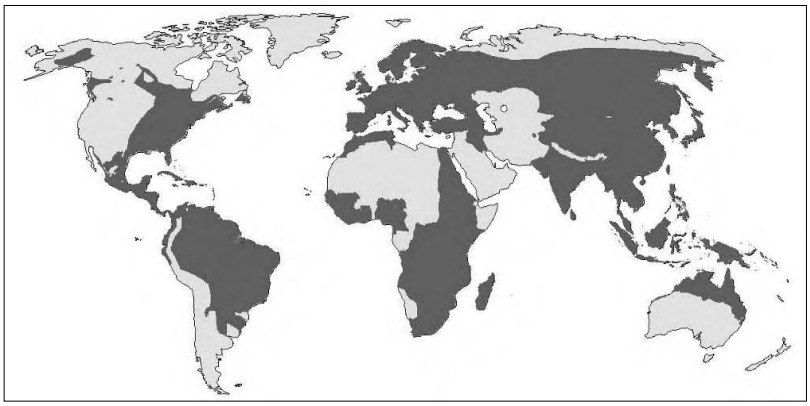

Fig.3 Distribution of *Nymphaea*

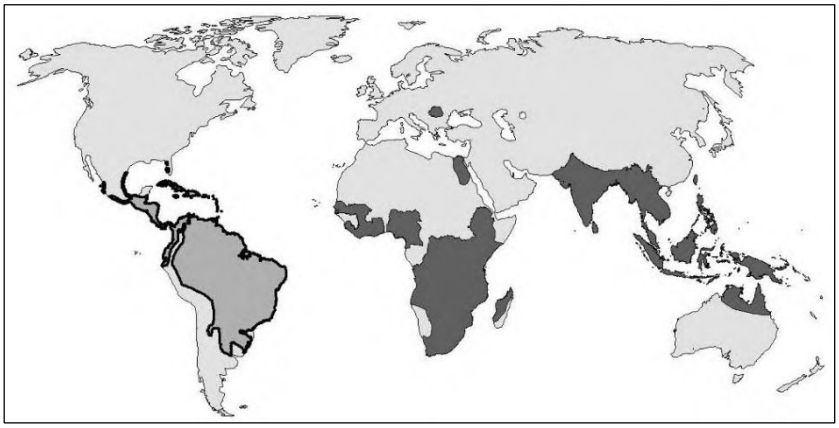

Subg. Hydrocallis Subg. Lotus

Fig.4 Distribution of *Nymphaea* subgenera

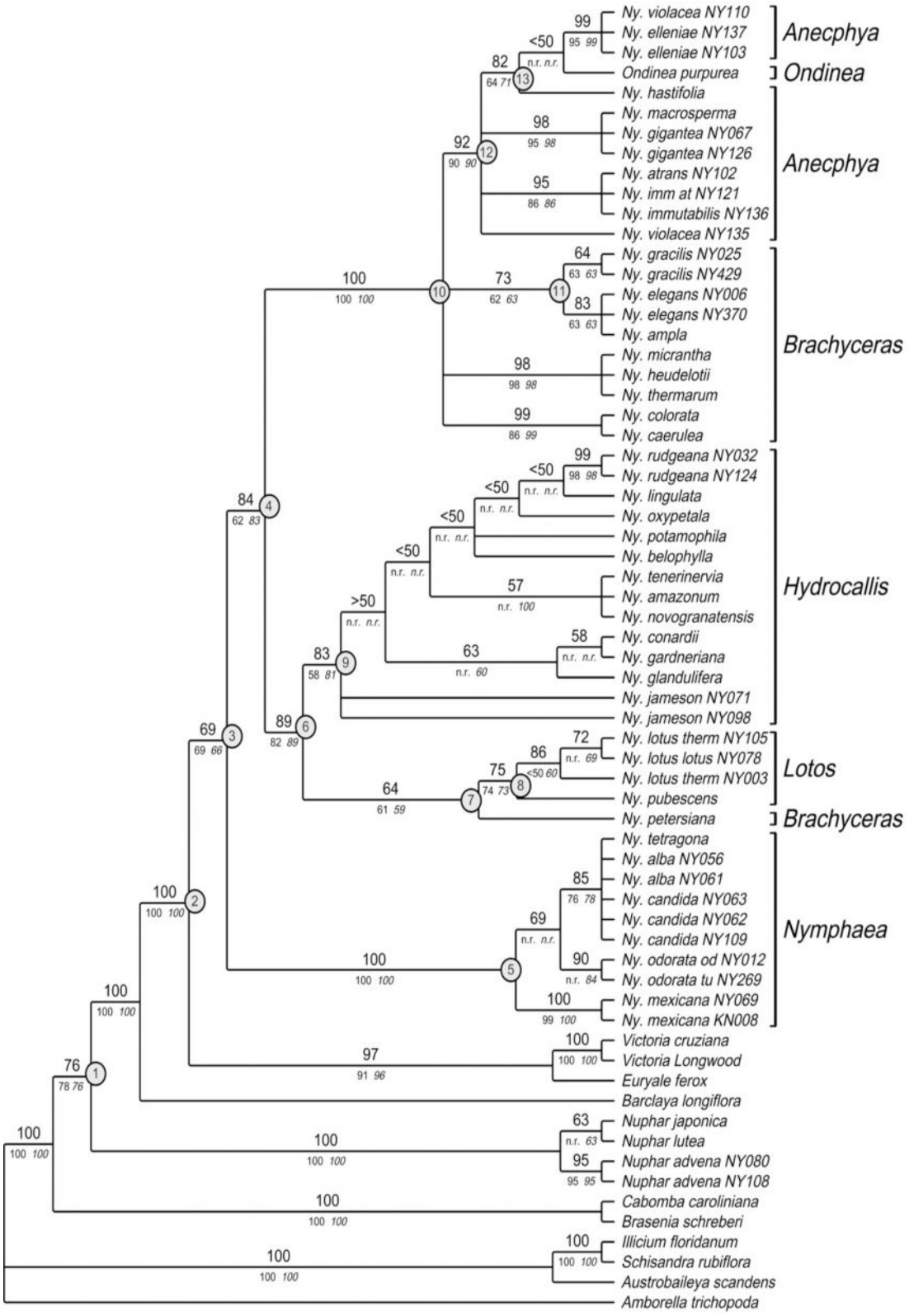

Fig.5 Maximum parsimony tree of trnT-trnF in *Nymphaea* and the Nymphaeales

Ethnobotany

The rhizomes are rich in starch and used as vegetable. The peduncles and tender leaves are also used as salad. Boiled rhizomes and parched seeds eaten in times of scarcity. Dried seeds are made into flour which is mixed in wheat flour for making bread in China, East Indies and Phillipine islands. Rhizome employed for tanning. Powdered rhizomes given in the treatment of dyspepsia, diarrhoea and for bleeding piles. Macerated leaves used as a lotion in eruptive fevers. They are also used for erysipelas[8].

Ethnopharmacology

The powdered root stock is given for dyspepsia, diarrhea, piles and urinary ailments. A decoction of the flower is given for palpitation of the heart. It is also supposed to be a blood purifier and aphrodisiac. The rhizome is prescribed for cystitis, nephritis, enteritis, fevers and insomnia[9]. The whole plant is being used for the treatment of diabetes and eyedisorder[10]. In Africa, the different species of *Nymphaea* is being used in the management of cancer[11].

Pharmacognosy

Nymphaeaceae includes many species, which yield edible fruits and rhizomes. However no detailed pharmacognostic studies of the plants has been done. Certain monographs provide the uses and applications of the plants and its folklore claims[12]. But this plant does not find a place in any of the pharmacognostic treatise.

Phytochemistry

Gertrude Maud Robinson and Robert Robinson (1934) isolated anthocyanins from the flowers of *Nymphaea gigantea* and identified as Delphinidin 3:5 dimonosides[13].

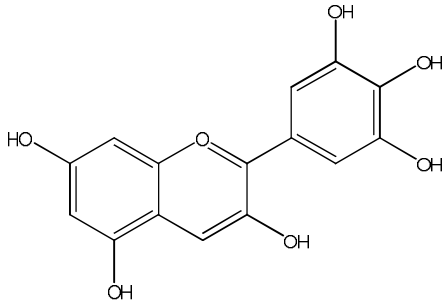

Bendz and Jonsson (1971) isolated anthocyanins from the leaves of *N. candida* and identified as Delphinidin-3-galactoside, Delphinidin-7-galactoside, Cyanidin-3-galactoside by UV spectroscopic and chromatographic studies[14].

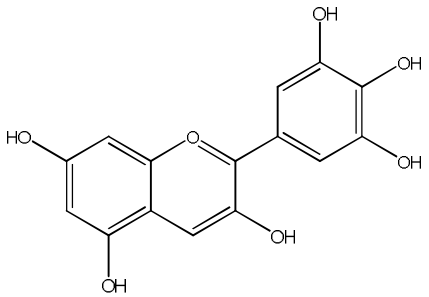

Delphinidin

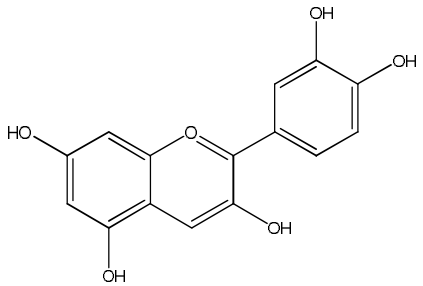

Cyanidin

Vidya Joshi *et al*. (1974) isolated β-Sitosterol, Gallic acid, alkaloid – Nupharin, Nymphaeine and cardiac glycoside - Nymphalin from the alcoholic extract from the flowers of *Nymphaea alba* and the structure was elucidated by I.R and NMR spectroscopic studies[15].

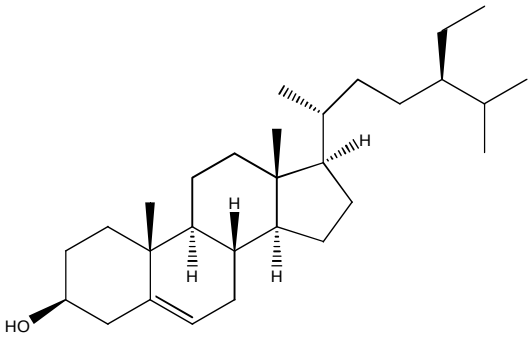

β-Sitosterol

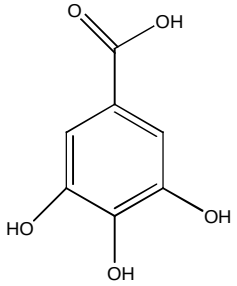

Gallic acid

Emboden (1982) reported alkaloids such as Nupharidin and Apomorphine based compounds from the flowers of *Nymphaea ampla*[16].

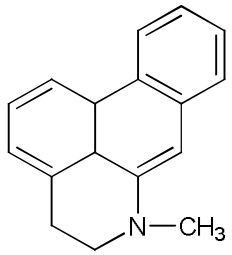

Aporphine

Hooper and Chandler (1984) isolated sterols - Campesterol, Stigmasterol, β-Sitosterol and Triterpenes–α & β-Amyrin, Taraxasterol, Friedlin, Allobetulin, Erythrodiol, Betulin from the leaves, stems and roots of *Nymphaea odorata*. The structure was confirmed by comparing their retention times with the marker compounds on three different gas liquid chromatography columns[17].

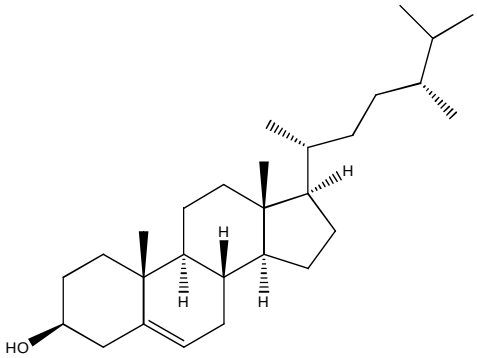

Campesterol

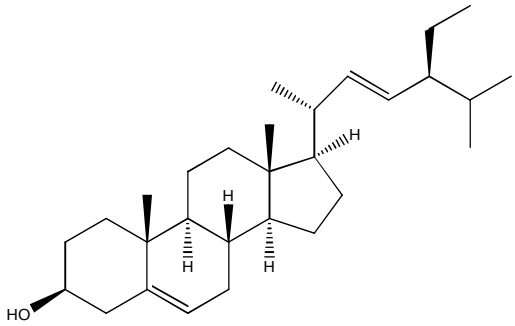

Stigmasterol

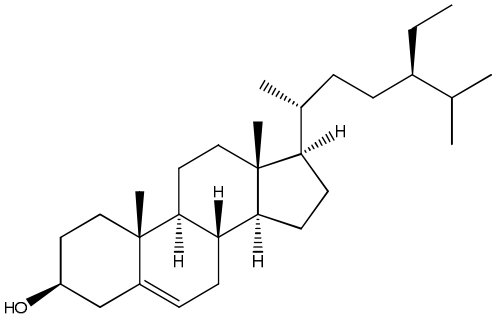

β-Sitosterol

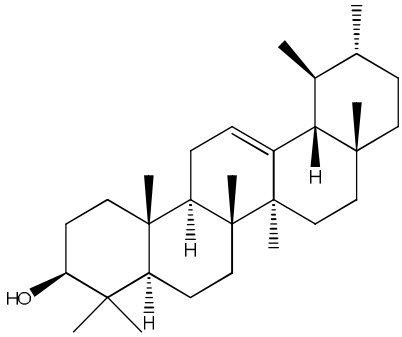

α-Amyrin

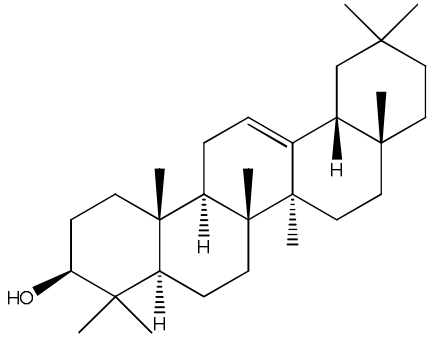

β-amyrin

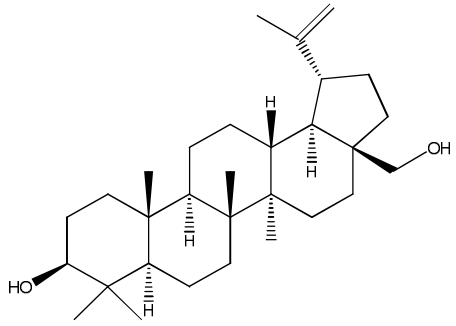

Betulin

Kurihara *et al*. (1993) isolated antimicrobial hydrolysable tannin against fish pathogenic bacteria, Geraniin from the leaves of *Nymphaea tetragona* and the structure was elucidated by ^{1}H, ^{13}C and DEPT NMR studies[18].

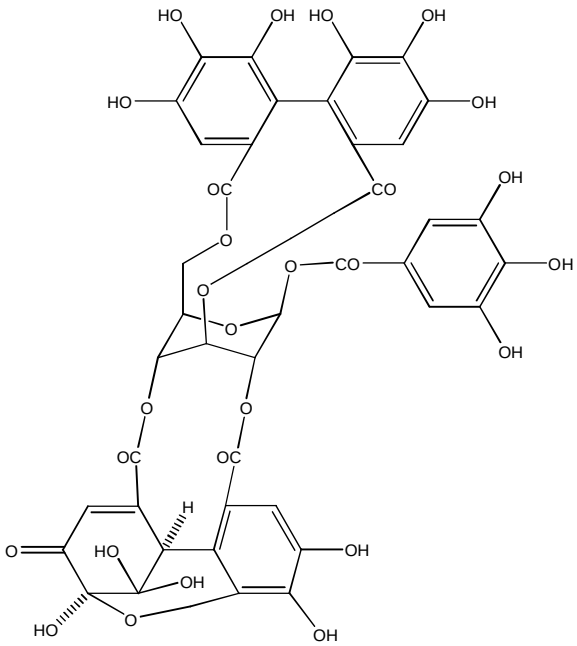

Geraniin

Fossen and Andersen (1997) isolated acylated anthocyanins Delphinidin 3-o-β-Galactopyranoside, Delphinidin 3-o-(6”-o-acetyl-β-galactopyranoside), Delphinidin 3-o-(2”-o-galloyl-6”-o-acetyl-β-galactopyranoside) from the leaves of *Nymphaea X marliaceae* and the structures were elucidated by chromatographic, ^{1}H, ^{13}C, homo

and hetero nuclear two dimensional NMR and Electrospray mass spectroscopic studies[19].

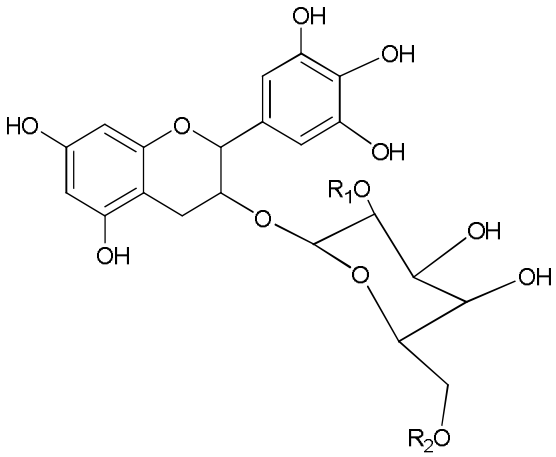

	R^1	R^2
Delphinidin 3-o-β-galactopyranoside	H	H
Delphinidin 3-o-(6”-o-acetyl-β-galactopyranoside)	H	Acetyl
Delphinidin 3-o-(2”-o-galloyl-6”-o-acetyl-β-galactopyranoside	Galloyl	Acetyl

Fossen *et al*. (1998) isolated five anthocyanins Delphinidin 3-o-β-galactopyranoside, Delphinidin 3-0-(2”-0-galloyl-β-galactopyranoside), Delphinidin 3-0-(6”-o-acetyl - β - galactopyranoside), Delphinidin 3 – 0 - (2”- o – galloyl - 6”- o – acetyl–β-galactopyranoside), Cyanidin 3-0-(2”-0-galloyl-6”-o-acetyl-β-galactopyranoside) from red flowers of *Nymphaea marliaceae* var. Escarboucle and the structures were identified by HPLC, electrospray MS and homo and hetero nuclear two dimensional NMR techniques[20].

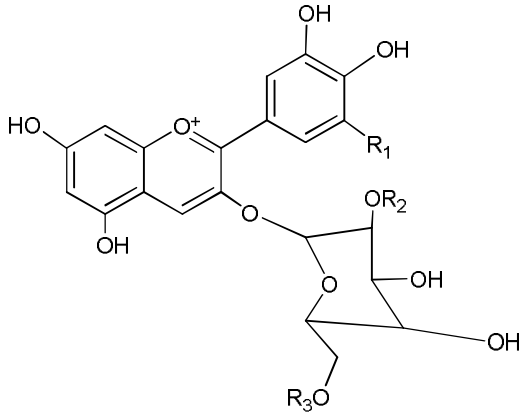

	R1	**R2**	**R3**
Delphinidin 3-o-β-Galactopyranoside	OH	H	H
Delphinidin 3-0-(2”-0-galloyl-β-galactopyranoside	OH	Galloyl	H
Delphinidin 3-0-(6”-o-acetyl- β-galactopyranoside)	OH	H	Acetyl
Delphinidin 3-0-(2”-0-galloyl-6”-o-acetyl-β-galactopyranoside)	OH	Galloyl	Acetyl
Cyanidin 3-0-(2”-0-galloyl-6”-o-acetyl-β-galactopyranoside)	H	Galloyl	Acetyl

Fossen *et al*. (1999) isolated seven flavonols Myricetin 3-rhamnoside, Myricetin 3-(20-acetyl rhamnoside), Quercetin-3-rhamnoside, Kaempferol 3-rhamnoside, Quercetin 3-(30-acetyl rhamnoside), Quercetin 3-(20-acetyl rhamnoside) and Kaempferol 3-(20-acetyl rhamnoside) from the blue flowers of *Nymphaea caerulea* and their structures were elucidated by HPLC, homo and heteronuclear two-dimensional NMR techniques and electrospray mass spectroscopy studies[21].

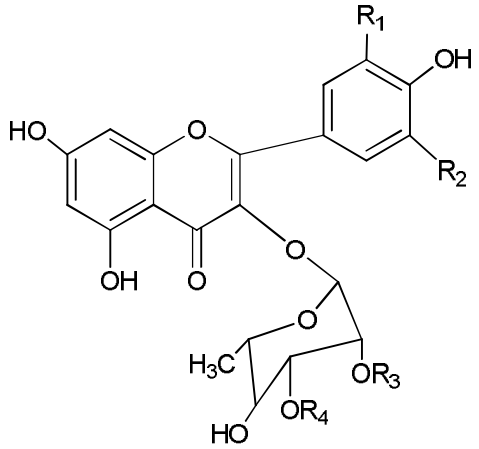

	R^1	R^2	R^3	R^4
Myricetin 3-rhamnoside	OH	OH	H	H
Myricetin 3-(20-acetyl rhamnoside)	OH	OH	CH_3CO	H
Quercetin-3-rhamnoside	OH	H	H	H
Kaempferol 3-rhamnoside	H	H	H	H
Quercetin 3-(30-acetyl rhamnoside)	OH	H	H	CH_3CO
Quercetin 3-(20-acetyl rhamnoside)	OH	H	CH_3CO	H
Kaempferol 3-(20-acetyl rhamnoside)	H	H	CH_3CO	H

Zhan *et al*. (2003) fractioned the ethanolic extract from the leaves of *Nymphaea odorata* and identified two lignans Nymphaeoside A and Icariside E_4 together with six flavonol glycosides Kaempferol-3-o-α-L-rhamnopyranoside, Quercetin-3-o-α-α-rhamnopyranoside, Myricetin 3-o-α-L-rhamnopyranoside, Quercetin 3-o-(6”-o-acetyl)- β-D-galactopyranoside, Myricetin 3-o-β-D-galactopyranoside, Myricetin 3-o-(6”-o-acetyl)- β-D-galactopyranoside and their structures were elucidated by HMBC and HSQC NMR, IR and Mass spectroscopic studies[22].

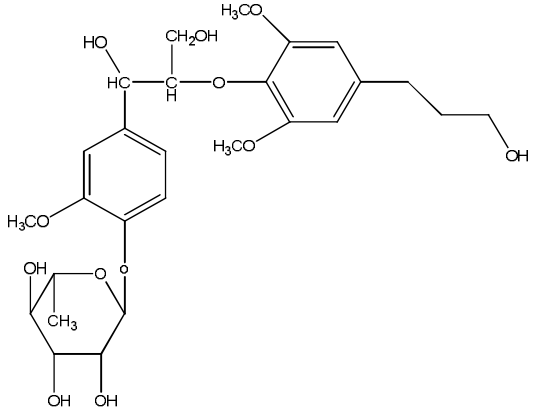

Nymphaeoside A

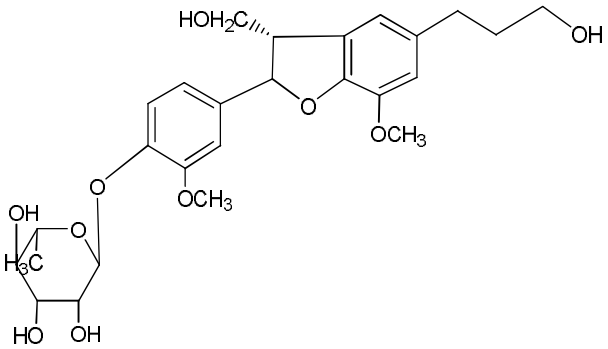

Icariside E_4

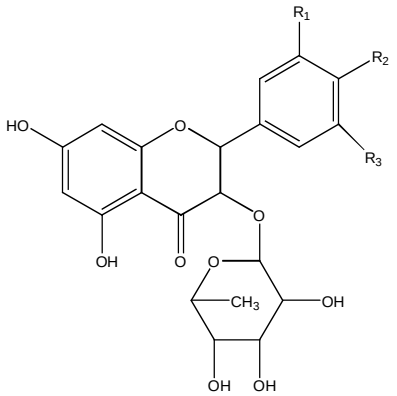

	R1	**R2**	**R3**
Kaempferol 3-o-α-L-rhamnopyranoside	H	OH	H
Quercetin 3-o-α-L-rhamnopyranoside	OH	OH	H
Myricetin 3-o-(6”-o-acetyl)- β-D-galactopyranoside	OH	OH	OH

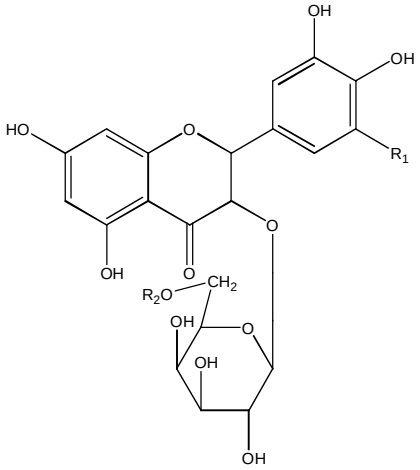

	R1	**R2**
Quercetin 3-o-(6”-o-acetyl)- β-D-galactopyranoside	H	OH
Myricetin 3-o-β-D-galactopyranoside	OH	OH
Myricetin 3-o--(6”-o-acetyl)- β-D-galactopyranoside	OH	OH

Elegami *et al*. (2003) isolated 1,2,3,4,6-pentagalloyl glucose, Myricetin-3-o-rhamnoside, Myricetin-3’-o-(6”-p-coumaroyl) glucoside, Nympholide A & B, a macrocyclic flavonol glycoside from the leaves of *Nymphaea lotus* and their structures were elucidated by 2D NMR studies[23].

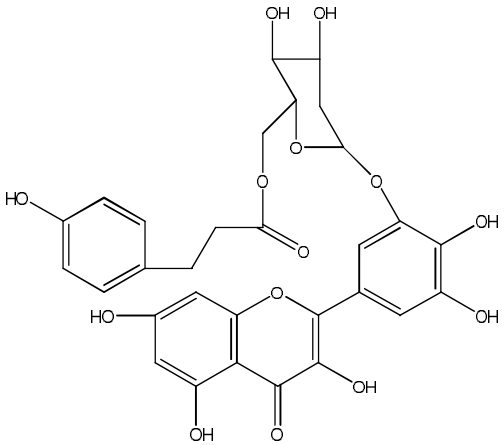

6”-p-coumaroyl myricetin 3-o- glucoside

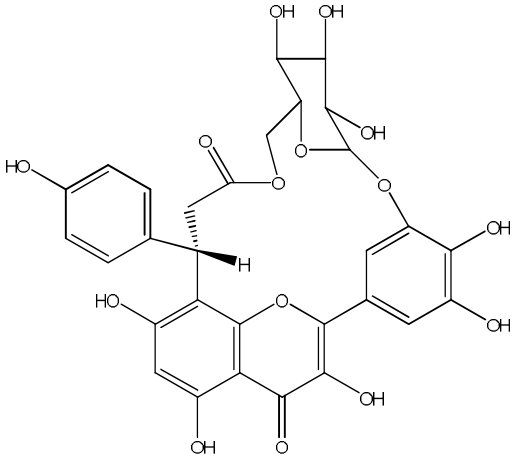

Nympholide A

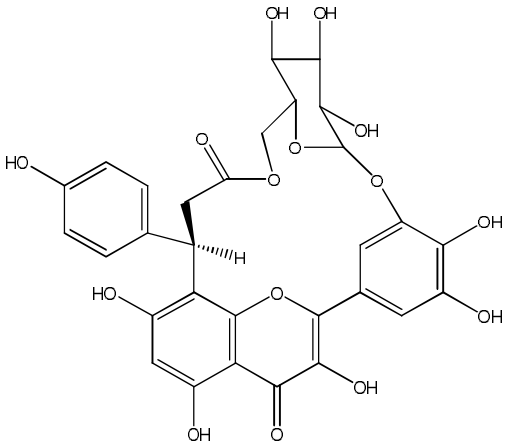

Nympholide B

Marquina *et al*. (2005) isolated glycosyl flavones 7, 3', 4'-trihydroxy-5-O-β-D-(2"-acetyl) - xylopyranosyl - isoflavone, 7,3',4-trihydroxy-5-O-α-L-rhamnopyranosyl-isoflavone, Kaempferol-3-Rhamnopyranoside, Quercetin–3-Rhamnoside, Quercetin–3- xylopyranoside, Quercetin-3-glucopyranoside, Methyl gallate, Methyl oleanolate-3-O-β-D-glucopyranoside, 28-O-β-D-glucopyranosyl-oleanate from *Nymphaea ampla*, *N.pulchella*, *N.gracilis* and *N.elegans* and their structures were elucidated by 1D and 2D NMR, FABMS studies[24].

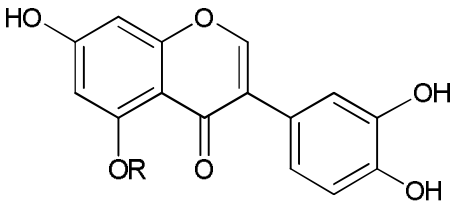

	R
7,3' ,4' -trihydroxy-5-O-β-D-(2"-acetyl)-xylopyranosyl-isoflavone	Xyl-(2"-OAC)
7,3' ,4' -trihydroxy-5-O-α-L-Rhamnopyranosyl-isoflavone	H
Kaempferol-3-Rhamnopyranoside	Rha

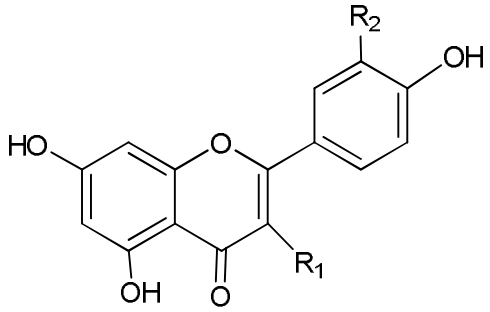

	R^1	R^2
Quercetin-3-Rhamnoside	Rha	H
Quercetin-3-Xylopyranoside	xylopyranoside	OH
Quercetin-3-Glucopyranoside	glucopyranoside	OH

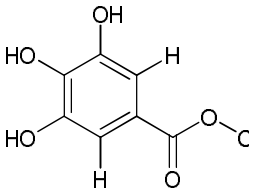

Methyl gallate

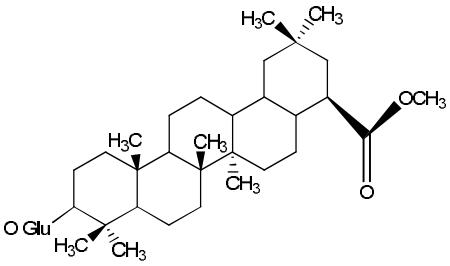

Methyl oleanolate-3-O-β-D-glucopyranoside

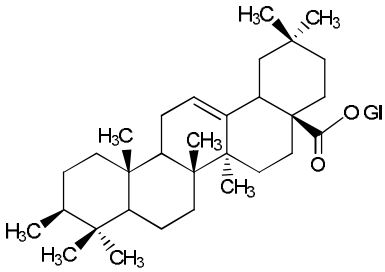

28-O-β-D-glucopyranosyl-oleanate

Agnihotri *et al*. (2008) isolated 2S,3S,4S-trihydroxy pentanoic acid, myricetin 3-o-(3”-o-acetyl)-a-l-rhamnoside, Myricetin 3-o-α-l-rhamnoside, Myricetin 3-o-β-D-glucoside, quercetin 3-o-(3”-o-acetyl)-a-l-rhamnoside, Quercetin 3-o-α-l-rhamnoside, Quercetin 3-o-β-l-glucoside, Kaempferol 3-o-(3”-o-acetyl)-a-l-rhamnoside, Kaempferol 3-o-β-D-glucoside, naringenin, (S)-naringenin 5-o-β-d-glucoside, isosalipurposide, β-sitosterol, β-sitosterol palmitate, 24-methylene cholesterol palmitate, 4a-methyl-5a-ergosta-7, 24(28)-diene-3β, 4β-diol, ethyl gallate, gallic acid, p-coumaric acid from the flowers of *Nymphaea caerulea* and their structures were elucidated by 1D and 2D NMR, IR and Mass spectroscopic studies[25].

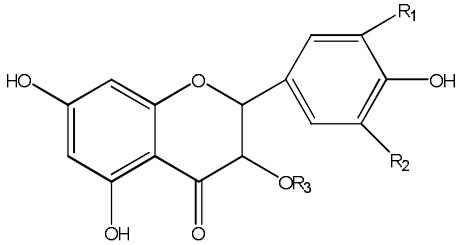

	R^1	R^2	R^3
Myricetin 3-o-(3”-o-acetyl)-a-L-rhamnoside	OH	OH	Rha-(3”-o-Ac)
Myricetin 3-o-α-L-rhamnoside	OH	OH	Rhamnoside
Myricetin 3-o-β-D-glucoside	OH	OH	Glucose
Quercetin 3-o-(3”-o-acetyl)-a-L-rhamnoside	OH	H	Rha-(3”-o-Ac)
Quercetin 3-o-α-L-rhamnoside	OH	H	Rhamnoside
Quercetin 3-o-β-L-glucoside	OH	H	Glucose
Kaempferol 3-o-(3”-o-acetyl)-a-L-rhamnoside	H	H	Rha-(3”-o-Ac)
Kaempferol 3-o-β-D-glucoside	H	H	Glucose

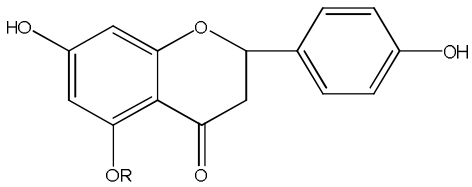

	R
Naringenin	H
(S)-Naringenin 5-o-β-d-glucoside	Glucose

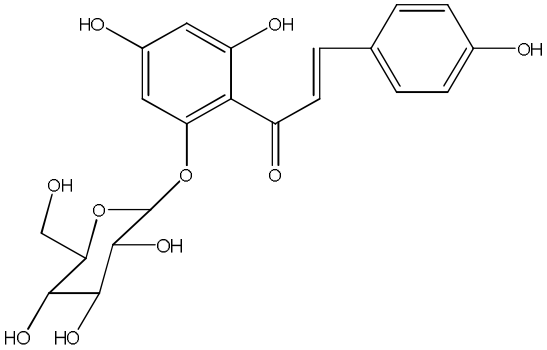

Isosalipurposide

Raja *et al*. (2010) isolated Nymphayol from *Nymphaea stellata* and the structure was identified by UV, IR, NMR and Mass spectroscopic studies. Nymphayol has been scientifically proved to be responsible for the traditionally claimed antidiabetic activity. It reverses the damaged endocrine tissue and stimulates secretion of insulin in the β-cells[26].

Verma (2011) isolated Nymphasterol from methanolic fraction of ethanolic extract of seeds of *Nymphaea stellata* and was characterized as 24-methyl-cholesta-5-ene-3-ol-(23,24,29)-cyclopropane, a steroidal compound and the structure was elucidated on the basis of UV, IR, 1D and 2D NMR and mass spectrometric studies[27].

NELUMBO NUCIFERA

Yang *et al*. (1972) isolated alkaloids-Nuciferine, n-Nuciferine, oxoushinsunine and n-Norarmepavine from lotus receptacle. Identification of these bases was carried out by their spectral data and direct comparison with authentic samples. The biscoclaurine and quaternary water soluble base only occurs in the embryo[28].

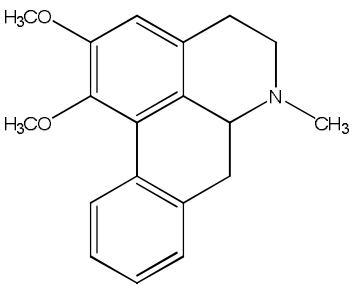

Nuciferine

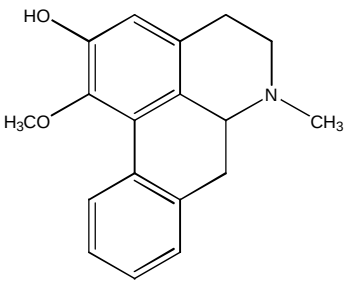

O-Nornuciferine

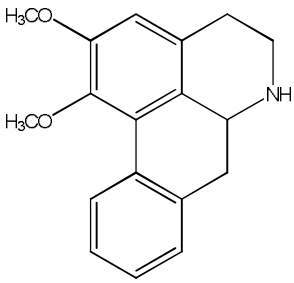

N-Nornuciferine

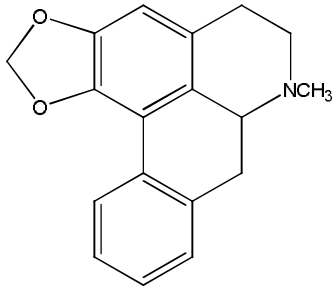

Roemerine

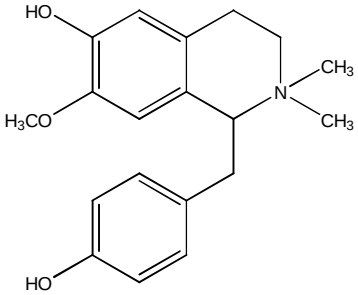

Lotusine

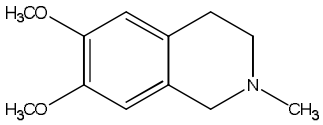

Methyl corypalline

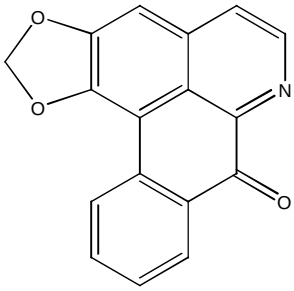

Oxoushinsunine

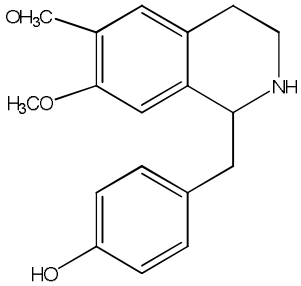

N-Norarmepavine

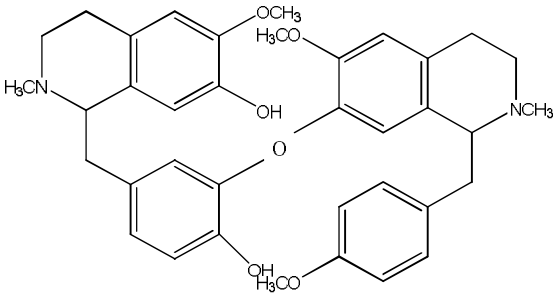

Isoleinsinine

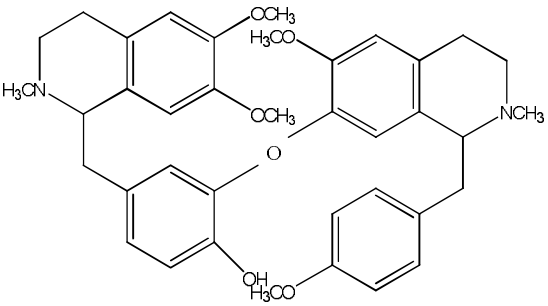

Neferine

Kunitomo *et al.* (1973) reported alkaloids from the leaves of *Nelumbo nucifera* using GLC-MS. They are dehydroroemerine, dehydroroemerine, dehydronuciferine, dehydroanonaine and N-methylisococlaurine besides the known roemerine, nuciferine, anonaine, pronuciferine, N-nornuciferine, nornuciferine, armepavine and N-methylcoclaurine[29].

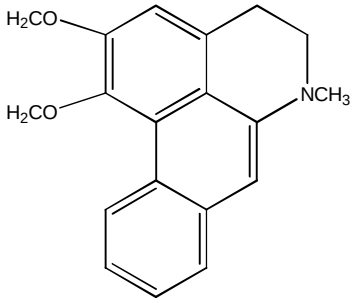

Dehyro roemerine

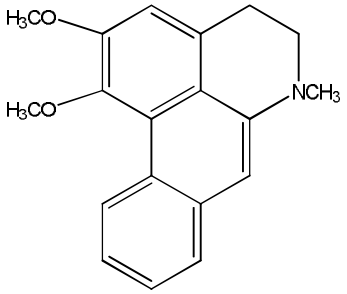

Dehydronuciferine

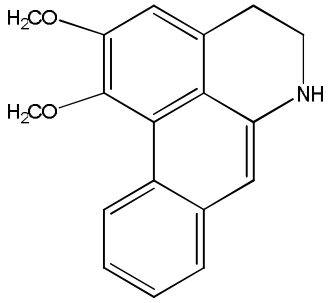

Dehydroanonaine

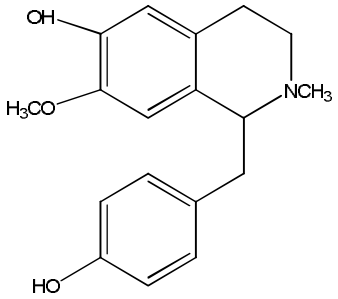

n-Methyl isococlaurine

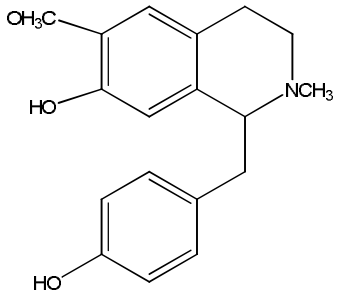

n-Methyl coclaurine

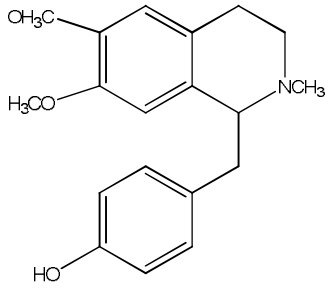

Armepavine

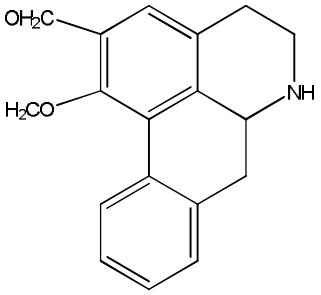

Anonaine

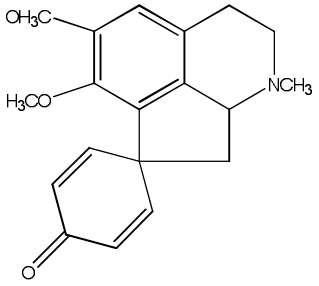

Pronuciferine

Yang and Kailan (2004) determined the spectral assignments by using a series of NMR experiments including ^{1}H, ^{1}H-COSY, HSQC and HMBC. The absolute configuration of neferine (C-1 and C-1') was determined as R and S and that of isoliensinine (C-1 and C-1') was determined as R and R[30].

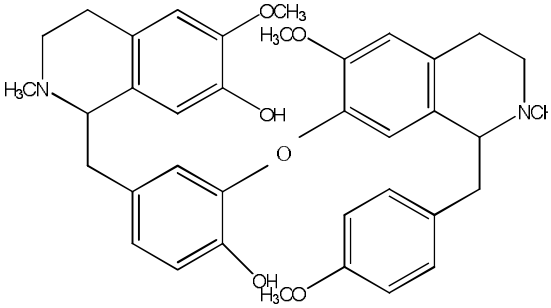

Isoleinsinine

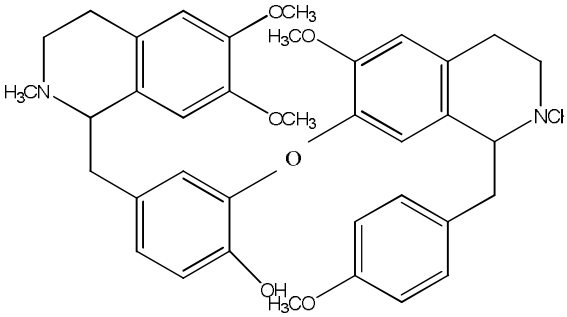

Neferine

Wu *et al*. (2004) isolated liensinine, isoliensinine and neferine from the embryo of the seed of *Nelumbo nucifera* by preparative counter chromatography using upright coil planet with four multilayer coils connected in series with 1600 ml capacity[31].

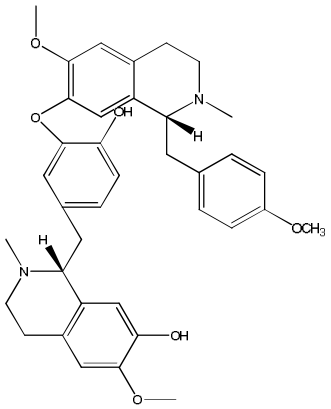

Liensinine

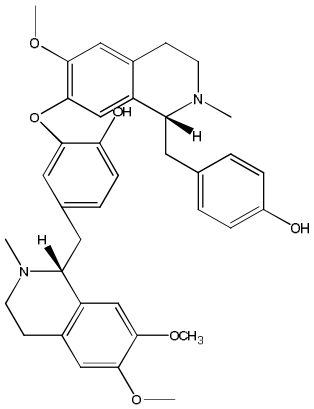

Isoliensinine

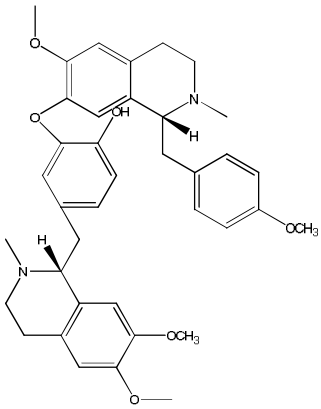

Neferine

Yang (2005) reported alkaloid Lotusine identified by a series of NMR experiments including ^{1}H-^{1}H, COSY, HSQC and HMBC. It is one of the major constituents of the Chinese medicine Lotus plumule and has hypertension and antibacterial activity[32].

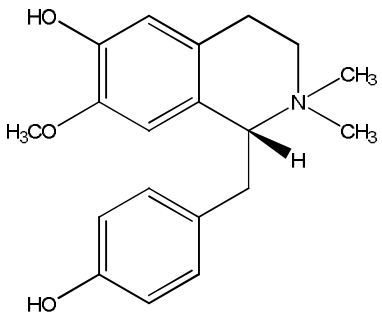

Lotusine

Kashiwada *et al*. (2005) isolated (+)-1(R)-coclaurine and (-)-(S)-norcoclaurine together with Quercetin-3-O-β-D-glucuronide from the leaves of *Nelumbo nucifera* and identified as anti-HIV principles[33].

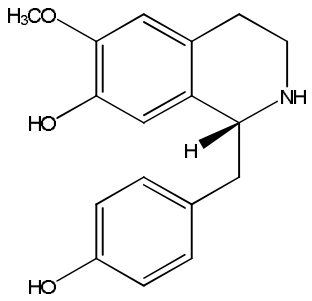

Coclaurine

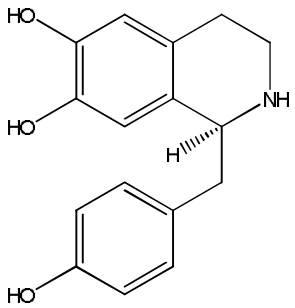

Norcoclaurine

NUPHAR SPECIES

Wrobel and Iwanow (1972) isolated and reported alkaloid nupharolutine from the rhizomes of *Nuphar luteum*. By spectroscopic and chemical methods it is shown to be a hydroxyl derivative of deoxynupharidine. The mass spectra of the new base and several isomers are reported[34].

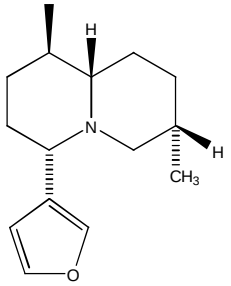

Deoxynupharidine

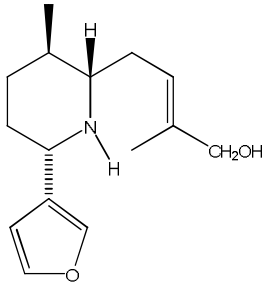

Nuphamine

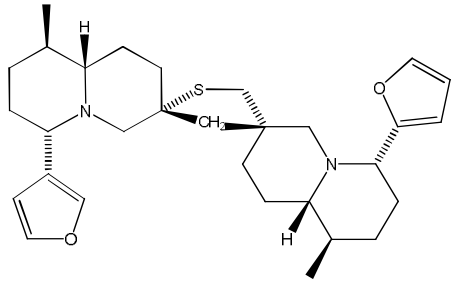

Neothiobinupharidine

Wrobel *et al*. (1972) isolated and reported an alkaloid neothionupharidine from *Nuphar luteum* by mass spectroscopic studies[35].

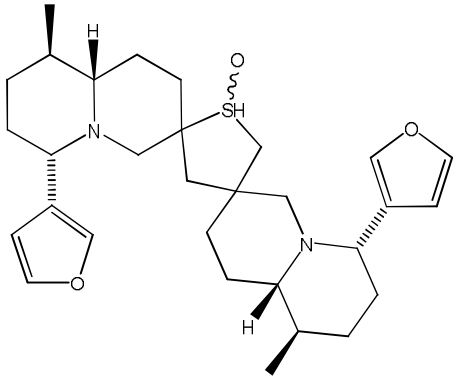

Neothionupharidine

Agnieszka *et al*. (1986) isolated, identified (IR, ^{1}H NMR and Mass spectroscopic studies) and reported four alkaloids Syn -6-Hydroxythiobinupharidine, Syn-6-Hydroxythiobinupharidine sulphoxide, Syn 6,6'-dihydroxythiobinupharidine and Anti-thiobinupharidine sulphoxide from *Nuphar lutea*[36].

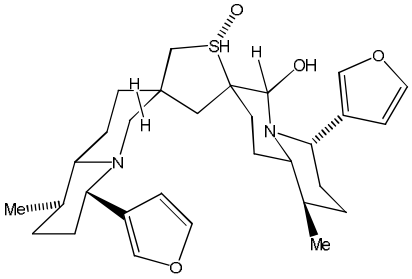

Syn -6-Hydroxythiobinupharidine

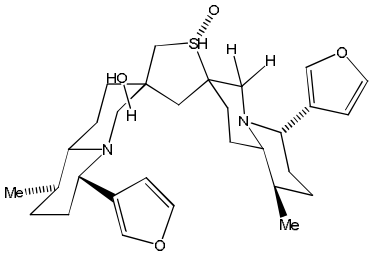

Syn-6-Hydroxythiobinupharidine sulphoxide

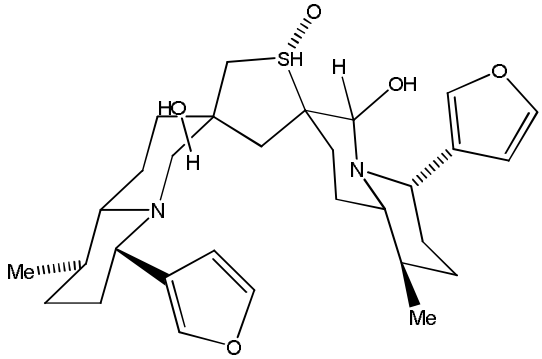

Syn 6,6'-dihydroxythiobinupharidine

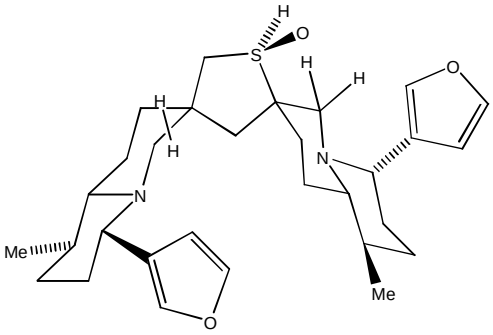

Anti-thiobinupharidine sulphoxide

Cybulski *et al*. (1988) isolated and reported an alkaloid nuphacristine (C_{15} alkaloid) from the rhizomes of *Nuphar luteum* and the structure and stereochemistry of nuphacristine have been established on the basis of spectral analysis (IR, ^{1}H NMR and Mass spectroscopic studies) and chemical informations[37].

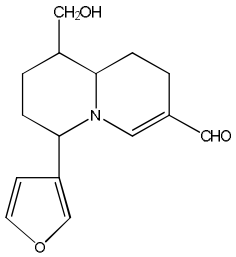

nuphacristine

Nishizawa *et al*. (1990) reported antibacterial activity for the solution containing gallotannin 1, 2, 3, 4 – tetrakis - (3, 4, 5-trihydroxybenzoyl) – α – D - glycopyranose, a second gallotannin and two ellagitannins from the roots of Candian water lily, *Nuphar variegatum*[38].

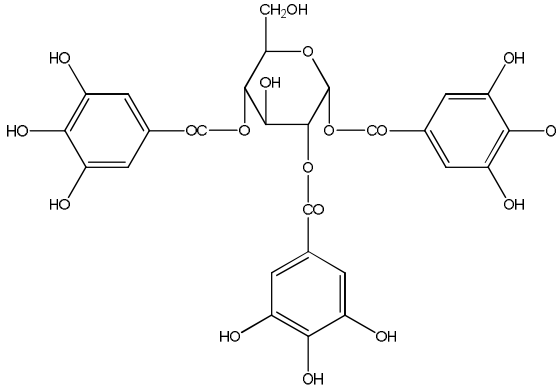

1,2,4-Trigalloyl-α-D-glucose

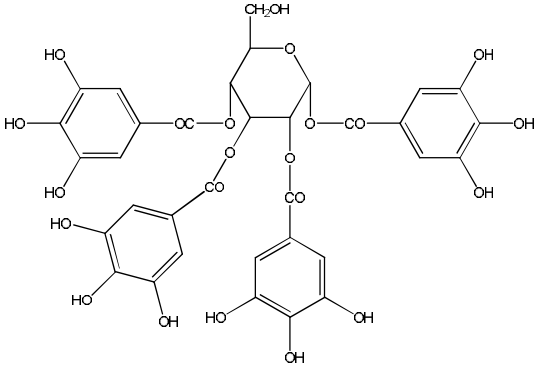

1,2,3,4-Tetra Trigalloyl-α-D-glucose

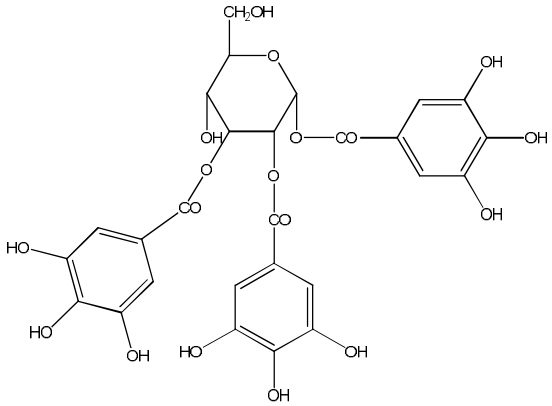

1,2,3-tri-o-galloyl- α-D-glucose

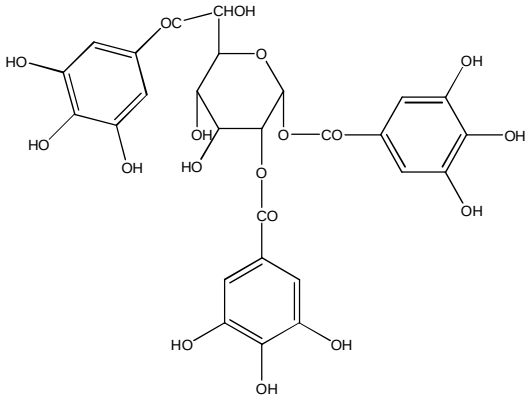

1,2,6-tri-o- galloyl- α-D-glucose

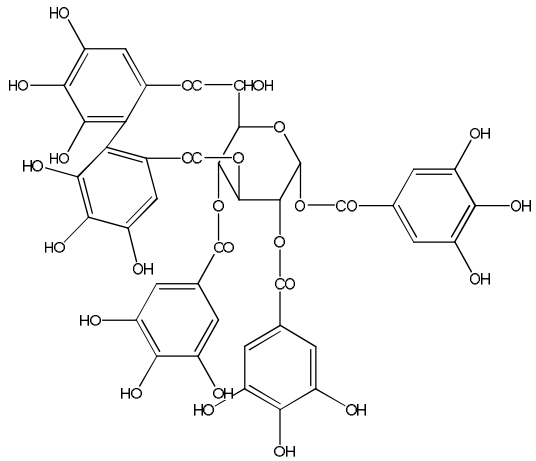

Nupharin B

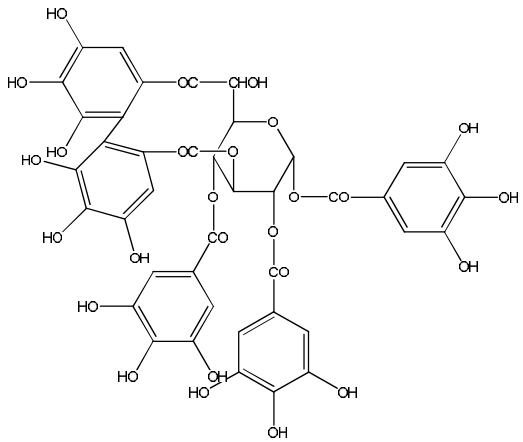

Nupharin A

Zhao and Zhao (1994) isolated and reported a novel cerebroside n-α-hydroxyl-cis-octadecaenoyl-1-β-glucopyranosylspingosine from the rhizome and adventitious roots of *Euryale ferox* and the structure was elucidated by spectroscopic methods and characterized as an isomeric mixture and its trans isomer[39].

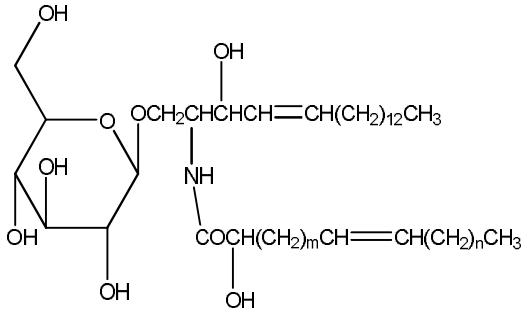

Miyazawa *et al.* (1998) reported four insecticidal alkaloids (-)-epi-deoxynupharidine, (-)-Castoramine, (-)-Nupharolutine, Nuphamine from the rhizomes of *Nuphar japonicum* against larvae of *Drosophila melanogaster*[40].

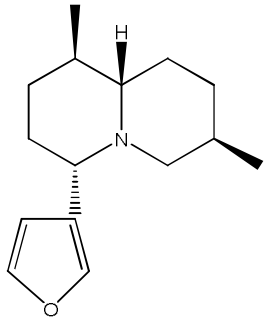

(-)-epi-deoxynupharidine

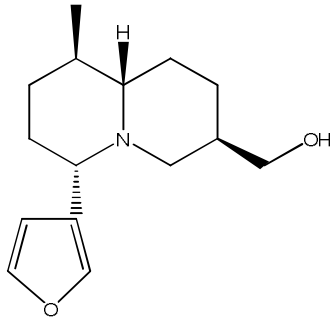

(-)-Castoramine

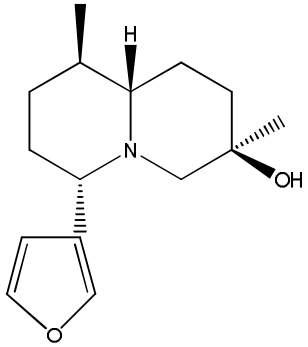

(-)-Nupharolutine

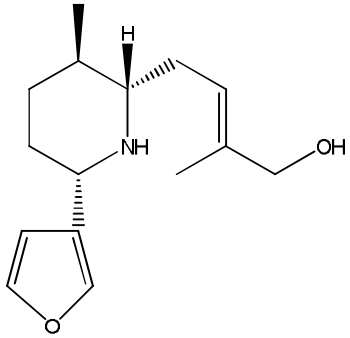

Nuphamine

Pharmacology

Bhandarkar and khan (2004) investigated the hepatoprotective activity of *Nymphaea stellata* flower against carbon tetra chloride induced hepatic damage. The

oral administration of varying dosage to rats for ten days afforded the good hepatoprotection against carbon tetrachloride induced elevation in serum marker enzymes, serum bilirubin, liver peroxidation and reduction in liver glutathione, liver glutathione peroxidase, glycogen, superoxide dismutase and catalase activity[41].

Khan and Sultana (2005) investigated the prophylactic effect of *Nymphaea alba* against ferric nitrilo triacetate (Fe-NTA) induced renal oxidative stress, hyperproliferative response and renal carcinogenesis in wistar rats. Treatment with Fe-NTA (9mg/kg body weight, Intraperitoneally) enhanced iron-ascorbate-induced renal lipid peroxidation, xanthine oxidase and hydrogen peroxide generation with reduction in renal glutathione content, antioxidant enzymes such as glutathione peroxidase, glutathione reductase. It also elevated the levels of blood urea nitrogen, serum creatinine, ornithine decarboxylase activity and thymidine incorporation into renal DNA. It also enhanced renal carcinogenesis by increasing the percentage incidence of renal tumors. Treatment of rats orally with *Nymphaea alba*100 and 200mg / kg body weight resulted in significant decrease in glutamyl transpeptidase, lipid peroxidation, xanthine oxidase, hydrogen peroxide generation, blood urea nitrogen, serum creatinine, DNA synthesis and incidence of tumors. *Nymphaea alba* is a potent chemopreventive agent and suppress hyperproliferative response and renal carcinogenesis in wistar rats[42].

Sowemimo *et al*. (2007) reported the toxicity and mutagenic activity of *Nymphaea lotus*. The ethanolic extract was studied using the brine shrimp lethality tests, inhibition of telomerase activity and induction of chromosomal aberrations *invivo* in rat lymphocytes[11].

Rajagopal and Sasikala (2008) screened the antidiabetic activity of hydro-ethanolic extracts of *Nymphaea stellata* flowers in normal and alloxan induced diabetes rats. The effect of oral administration of the hydro ethanolic extract for 30 days on the level of blood glucose, glycosylated hemoglobin, total cholesterol, triglycerides, phospholipids, low density lipoprotein, very low density lipo protein, high density lipoprotein, hexokinase, lactate dehydrogenase and glucose-6-phosphatase in normal and alloxan induced diabetic rats were evaluated. The hydro ethanolic extract decreases the elevated blood glucose level, glycosylated

hemoglobin, cholesterol, triglycerides, phopholipids, LDL, VLDL, hexokinase and it showed a significant increase in liver glycogen, insulin, glucose-6-phosphatase and HDL level. *Nymphaea stellata* flowers possess promising antidiabetic effect in diabetic rats[43].

Karthiyayini *et al*. (2011) screened the antidiabetic activity on the ethanolic and aqueous flower extract of *Nymphaea pubescens* Willd in alloxan induced diabetic rats.There was statistically significant reduction ($P<0.001$) in blood glucose level in the diabetic rats with the maximum activity at 6 hours and the percentage reductions were found to be 21.97% and 19.94% at the dose of 400 mg/kg with ethanol and aqueous extracts respectively, when compared with diabetic control groups[44].

Shajeela *et al*. (2012) investigated the antidiabetic, hypolipidaemic and antioxidant effects of *Nymphaea pubescens* extract in alloxan induced diabetic rats[45].

Rajan Rushender *et al*. (2012) investigated the in-vitro antidiabetic activity of *Nymphaea pubescens* by α-amylase and α-glucosidase inhibition assay[46].

Dalmeida and Mohan (2012) investigated the total phenolic content, total flavonoid content and anti-oxidant activity of *Nymphaea pubescens*[47].

AIM AND OBJECTIVE

There are about 45,000 medicinal plant species present in India and among these the waterlilies are a group of fascinating aquatic plants with potent medicinal properties and they are important in the fact that they are considered to be one of the primitive groups of flowering plants still existing in the world. Among five genera's from Nymphaeaceae family occurs throughout the world, three genera's are found in India such as *Nelumbo*, *Nymphaea* and *Nuphar* and they were being used medicinally. *Nymphaea* is one of the few genera's of Nymphaeaceae recognized for economic values including medicinal properties.

There are about fifty species from the genus *Nymphaea* and six species occurs in India such as *Nymphaea pubescens*, *N. rubra*, *N. tetragona*, *N. alba*, *N. stellata* and *N. candida*. These are mostly used for the treatment of skin disease, wound healing, diabetes, cancer, as blood purifier and bleeding piles.

A comprehensive search of the literature from the primary and secondary sources of genus *Nymphaea* revealed that only a few species have been investigated for their medicinal properties. *Nymphaea pubescens* is the common aquatic plant, have not been explored scientifically. However folklore claims are available for the drug claiming some alluring medicinal properties.

Availability of sustainable quantam of the biomass, lacuna in pharmacognostical, phytochemical and pharmacological parameters and its folklore claims have formed the rationale to undertake the scientific evaluation of the *Nymphaea pubescens* in molecular and computational aspects.

The present work is aimed to carry out the pharmacognostical, phytochemical and pharmacological studies of *Nymphaea pubescens* Willd, which includes development of morphological and microscopical diagnostic feature, characterisation of active constituents, analyzing physico-chemical properties of isolated compound and scientific assessment of folklore claim by biological assay including molecular studies and computational screening for the isolated compounds.

The objectives of the present scientific investigation of the flower petals, roots and rhizomes of *Nymphaea pubescens* are

- To develop the diagnostic feature by morphological, microscopical, micrometry measurements of cell content, histochemical and powder microscopical studies.
- Physical evaluation by analytical parameters.
- Extraction of the plant material.
- To identify the phytoconstituents by performing preliminary phytochemical analysis.
- To develop TLC and HPTLC fingerprints for qualitative and quantitative estimation.
- GCMS analysis of the extracts for identifying the phytoconstituents by matching with the spectrum libraries.
- To isolate the phytoconstituents using Column chromatography and identify the same by using UV, IR, NMR (^{1}H, ^{13}C, ^{13}C DEPT-135 & HMBC) and Mass spectroscopic studies.
- Bio assay guided isolation of the plant extract.
- To analyze physico-chemical parameters of the isolated compounds by computational methods using ACD / ilabs and www.molinformation. com software's.
- Chemotaxonomical analysis.
- Acute toxicity studies of the plant extracts.
- *In-vivo* antidiabetic activity of the root and rhizome ethanolic extract in type II diabetes induced animal model.

- Molecular estimation of apoptotic proteins such as BCl-2 and Caspase-3 by Gel electrophoresis and Western blot analysis.
- Molecular docking of the isolated compounds with insulin deactivation signaling protein tyrosine phosphatase 1B.
- *In-vitro* and *In-vivo* anticancer activity of the ethyl acetate fraction from the ethanolic flower extract of *Nymphaea pubescens* against *Hela* cells and Dalton Ascitic Lymphoma induced swiss albino mice.
- *In-vitro* anti-oxidant activity of the ethyl acetate fraction by ABTS, DPPH, Hydrogen peroxide and *p*-NDA scavenging method.

The scientific study including structural interpretation, molecular screening and molecular docking by computational method in the field of indigenous medicine would put a firm foundation for characterization and scientific validation of the folklore claims that provides a standardizing protocol for *Nymphaea pubescens*, since scientific standardization of the herbal drug is the need of the hour.

SCOPE & PLAN OF WORK

Historically natural products are the core of the drug leads and they are the source of novel viable chemical moieties in drug research. Increased interest in the research of pharmacognosy in drug development, natural products is the driving force in modernizing pharmacognosy.

Pharmacognostic research today focuses on the discovery of novel and unique molecules and on revealing unknown targets of lead molecule in nature. New and improved research protocols concerning the selection of plant drug based on ethnomedical information or folklore claims, pharmacognostic standardization, chromatographic studies, bio assay guided fractionation, hyphenated techniques, isolation procedures, structural elucidations, *In-vivo* and *in-vitro* pharmacological bioassays, molecular screening, toxicity studies and screening of isolated compounds by computational molecular docking studies provides the outstanding contribution to the future drug discovery.

Hence the research work on the aquatic plant *Nymphaea pubescens* was selected based on above mentioned advancements in revealing the novel lead compound for drug discovery.

The research work on *Nymphaea pubescens* Willd was divided into three parts.

Part I : Pharmacognostic studies

- Authentication of plant drug.
- Organoleptic and microscopical evaluation of the flower, root and rhizome of *Nymphaea pubescens*.
- Histochemical studies of the root and rhizome of *Nymphaea pubescens* to identify the presence of primary and secondary metabolites in specific cellular region.
- Powder microscopical studies.

- Linear measurements of fibres and starch grains.
- Analytical parameters such as Total ash, sulphated ash, acid insoluble ash, water soluble ash, ethanol soluble extractive, water soluble extractive and loss on drying.
- Behavior of the crude powdered drug with different chemical reagents.
- Fluorescence analysis of crude drug.

Part II – Phytochemical studies

- Extraction of plant material.
- Preliminary phytochemical analysis of the extracts.
- Developing TLC and HPTLC fingerprints of the extracts.
- GCMS analysis of the extracts.
- Isolation of phytoconstituents by column chromatography using neutral alumina for alkaloids and silica gel G for other phytoconstituents.
- Bio-assay guided isolation of ethanolic flower extract.
- Quantification of the isolated compound by HPTLC.
- Structural interpretation of isolated compounds by spectroscopic methods (UV, IR, ^{1}H, ^{13}C, ^{13}C DEPT-135, HMBC NMR and Mass spectroscopic studies.
- Analyzing physico-chemical parameters of the isolated compounds by computational methods using ACD / ilabs and www.molinformation .com software.
- Chemotaxanomical analysis.

Part III – Pharmacological studies

- Ethical clearance.
- Acute toxicity studies for the extracts.
- *In-vivo* antidiabetic activity in the Streptozotocin and Nicotinamide induced type II diabetes animal models.
- Molecular estimation of apoptotic proteins such as Caspase - 3, Bax and Bcl-2 by Gel electrophoresis and Western Blot analysis.
- Molecular docking of the isolated compounds with insulin deactivation signaling protein tyrosine phosphatase 1B.
- *In-vitro* and *In-vivo* anticancer activity of the ethyl acetate fraction from the ethanolic flower extract of *Nymphaea pubescens* against *HeLa* cells and Dalton Ascitic Lymphoma induced swiss albino mice.
- *In-vitro* anti-oxidant activity of the ethyl acetate fraction by ABTS, DPPH, Hydrogen peroxide and *p*-NDA scavenging method.
- Statistical analysis by one way ANOVA followed by Tukey multiple comparison test using the SPSS (Version 15.0) program followed by PSD.

PART-1 PHARMACOGNOSY

MATERIALS & METHODS

The pharmacognostic evaluation provides the simplest and quickest means to establish the identity and purity and thereby ensure quality of an herbal drug. It is often necessary to substantiate the findings by morphology, microscopy and physicochemical analysis to obtain the standardization protocol for the evaluation of herbal drug.

Nymphaea pubescens Willd. (Fig. 6) is a perennial aquatic rhizomatous stoloniferous herbs, leaves large orbicular with long fleshy warty petiole and the leaves are green above and pubescent below, sinus to 8cm deep, margins sharply dendate (Fig.7A&B).

The flower consists of numerous stamens, arranged spirally. The stamens are transformed into petals through gradual modifications of the stamens. The stamens are flat and dorsiventral. The filaments and the anthers are equally flat. The pollen chambers are located on the adaxial side of the stamen. The chambers are vertically elongated and dehiscence of the anther is also along vertical line. Sepals are oblong, obtuse and green in colour. Petals are white in colour. The sepals and petals are marked with pink striations in its centre (Fig. 6).

The fruit is a large berry (Fig 8B). The seeds are attached on the surface of septa (Fig. 8C). The rhizome is thick spherical fleshy and soft (Fig. 7C). Roots contains numerous root hairs which tapering towards the end (Fig. 7D).

As seen in transverse section, the anther consists of two adaxial theca (dithecous) and each theca is two chambered (Fig 9A). The outer wall of the pollen chamber consists of outer epidermis, middle layer of endothecium and inner layer of endodermis. The epidermis is thin and the cells are spindle shaped and thin walled (Fig. 9B&C). The endothecial cells are wide and radially elongated. They possess annular thickenings which offer rigidity to the anther wall. The anther wall is 6.0 µm thick; pollen grains are elliptical to spherical. The exine (outer wall) of the pollen is smooth and no distinct marking are evident (Fig. 9C). The starch grains are 30µm in diameter.

The root exhibits hydromorphic features. It consists of a thin epidermal layer of shrunken cells. The cortex is wide and aerenchymatous. Is consists of several layers of air-chambers, which are large and polygonal in outline. The air-chambers are separated from each other's by thin uniseriate partition filaments (Fig. 10A). The vascular cylinder is circular measuring 700µm in diameter. It consists of about 10 radial arms of exarch xylem strands and 10 clusters of phloem alternating with the xylem. The xylem and phloem strands are radial in arrangement (Fig. 10B&C). The xylem strands have 7-10 cells, which are angular and thin walled. The metaxylem elements are upto 80 µm in diameter. The ground tissue of the vascular cylinder has small, thin walled, compact parenchyma cells.

The rhizome is thick spherical fleshy and soft. It is 1cm in diameter. It is covered by membranous sheath which is peeled off easily. The sheath consists of small thin walled parenchyma cells. Inner to the membranous covering is a dark band of thick walled cells which are compact and dense. The dark zone is 200µm thick. The cells of this zone consist of sclerenchyma with lignified walls filled with dense tannin which renders the zone dark color. Inner to the dark sclerotic zone, the entire rhizome has homogenous parenchymatous tissue. Throughout rhizome are diffusely distributed sclereids of various shape and size, they are circular, amoeboid, elongated and irregular. The sclereids have very thick lignified wall and narrow lumen. Tanniferous cells are also seen, especially along the outer zone (Fig.11,12 &13).

The vascular strands are seen scattered in the ground tissue. They are variable in shape and size. The vascular bundles have a few reduced xylem elements and well developed phloem elements. No bundle sheath is seen.

Almost all ground tissue is filled with dense starch grains. The starch grains are solitary and simple. Some of these are circular and concentric with central hilum and others are elongated, elliptical or spindle shaped with exeutic hilum. When the starch grains are viewed under the polarized light microscope "+" shaped dark marking is seen in the concentric type and "y" shaped markings are seen in the elongated type (Fig.14). The starch grains are 30µm (circular type) and 50µm (elongated type) in size.

The histochemical studies give a preliminary idea about the type of compounds and their accumulation in the plant tissues. Histochemical studies of root showed the presence of alkaloids inbetween the vascular bundle, tannins in the phloem cells and partition filaments, protein in phloem cells and pith and starch in the partition filament in the ground tissue. In rhizome the alkaloids, proteins and starch histochemically stained in the parenchymatous cells and in the ground tissue and tannin in the inner sclerotic zone (Table-1; Fig. 15 &16). This is of great interest for quality control in basic research and biosynthetic accumulation of phytoconstituent in the aquatic plant *Nymphaea pubescens*.

Powder microscopy is an evaluation parameter in a quality control process used for medicinal plants to study the specific microscopic characters using different staining reagent for the detection of adulterants and its purity. The powder microscopic analysis of the powdered root and rhizome of *Nymphaea pubescens* showed the presence of lignified fibres, starch grains, xylem vessels pitted and sclereids (Fig. 17). These cellular characters give the diagnostic features of *Nymphaea pubescens*.

The linear measurement of fibres showed 240-560 µm in length and 64-112 µm in width. The diameter of starch grains shows 30-82 µm (Table-2). These values are found to be constant for this species. Quantitative microscopic data's are useful for identifying the different species of genus and also helpful in the determination of the authenticity of the plant.

The physico-chemical parameters are mainly used in judging the purity and quality of the drug. Ash values of a drug give an idea about the earthy matter or inorganic composition or other impurities present along with the drug. Total ash value was found to be slightly high (when compared to sulphated ash, acid insoluble ash and water soluble ash (Table-3).

Extractive values give an idea about the chemical constituents present in the drug as well as useful in the determination of exhausted or adulterated drugs. The ethyl acetate soluble extractive value of flower petals and the water soluble extractive value of root and rhizome showed higher value when compared to benzene, chloroform and

ethanol soluble extractive values (Table-3). The result indicates the flower petals contain higher flavonoid content and the root and rhizome contains higher content of polar phytoconstituents.

Presence of moisture content activates the enzymatic reaction that leads to the degradation of active constituent. Loss on drying indicates the percentage of moisture content present in a drug. The percentage loss on drying of flower petals was found to be 1.37%w/w and for root and rhizome 3.21%w/w. These values indicate, the plant drug has less moisture content (Table-3).

The therapeutic activity of the plant drug is based upon its active constituent. The flower petals showed the presence of glycosides, steroids, flavonoids, phenols, reducing sugars, proteins and trace amount of alkaloid. The root and rhizome showed the presence of alkaloid, glycosides, flavonoids, phenols, tannins, reducing sugars and proteins (Table-4).

The powdered drug was extracted with the suitable solvent and observed in the short and long UV light and also in the visible light to identify the presence of chromophores. The fluorescence analysis of the powdered drug of *Nymphaea pubescens* showed that the plant contains chromophores (Table-5).

RESULTS & DISCUSSION

Fig.6 *Nymphaea pubescens* Willd. - Habit

Fig.7 Vegetative part of *Nymphaea pubescens*

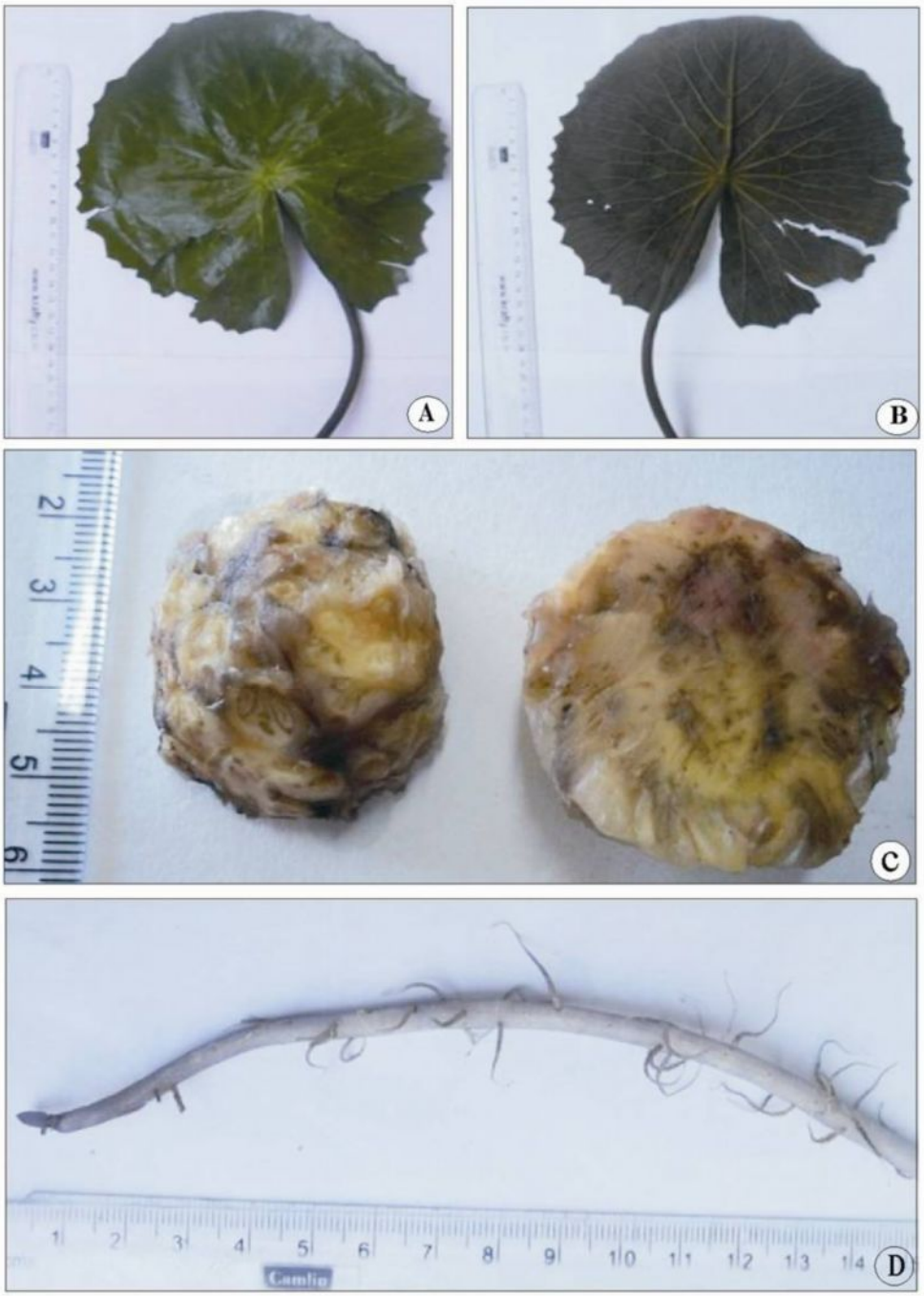

A & B – Dorsal and ventral view of *N. Pubescens* leaf
C – Close view of *N. pubescens* rhizome
D – Tap root with hairs of *N. pubescens*

Fig.8 **Reproductive part of *Nymphaea pubescens***

A – L.S. of *N. pubescens* flower
B – L.S. of *N. pubescens* fruit
C – Close view of *N. pubescens* seeds

Fig. 9 T.S. of *Nymphaea pubescens* anther

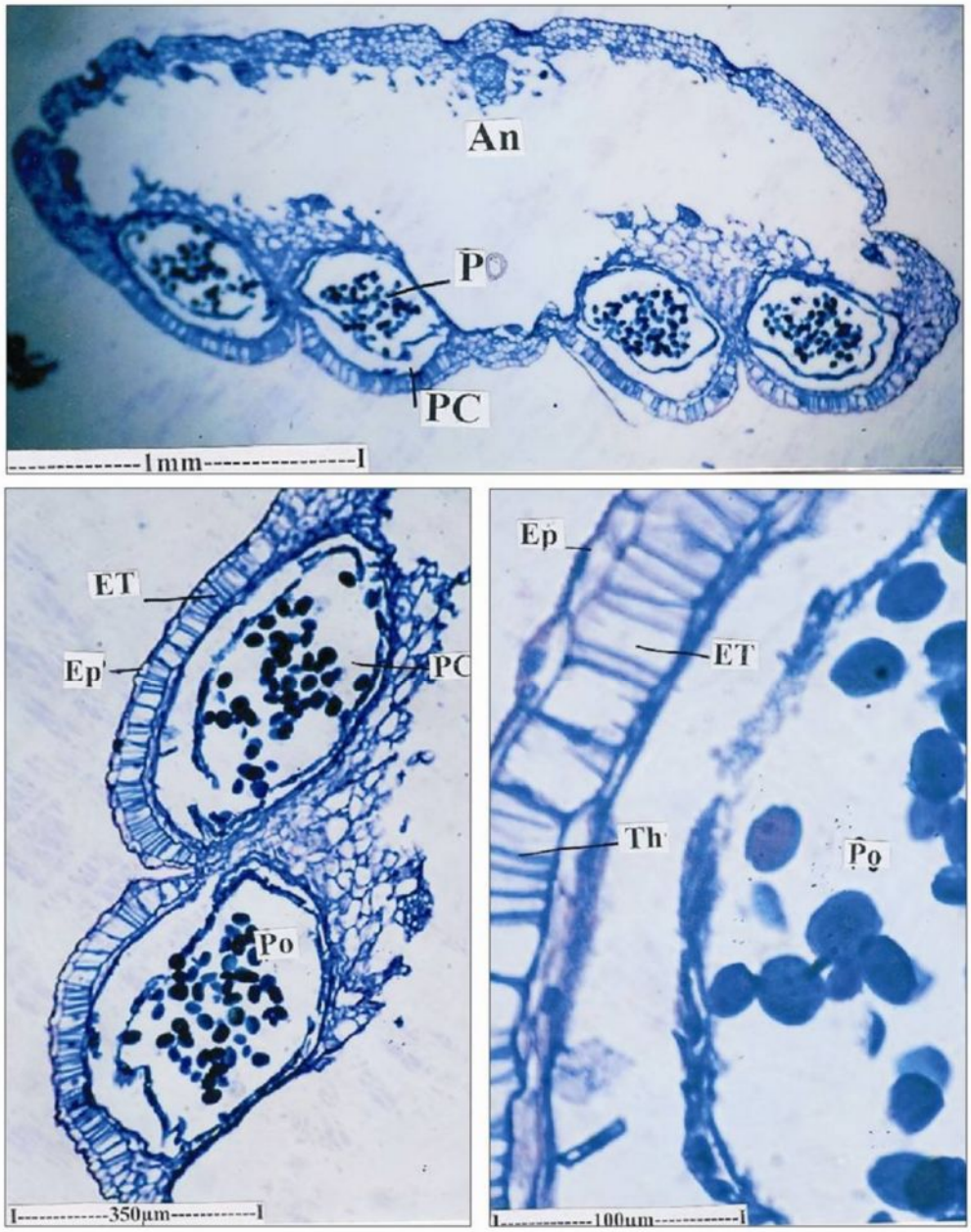

A – TS of anther (4X)
B – Anther chambers (10X)
C – Anther wall and Pollen grains (10X)

An – Anther; **Ep** – Epidermis **Et** – Endothecium
Th – Wall thickenings **Po** – Pollen grains **Pc** – Pollen chamber

Fig.10 T.S of *Nymphaea pubescens* root

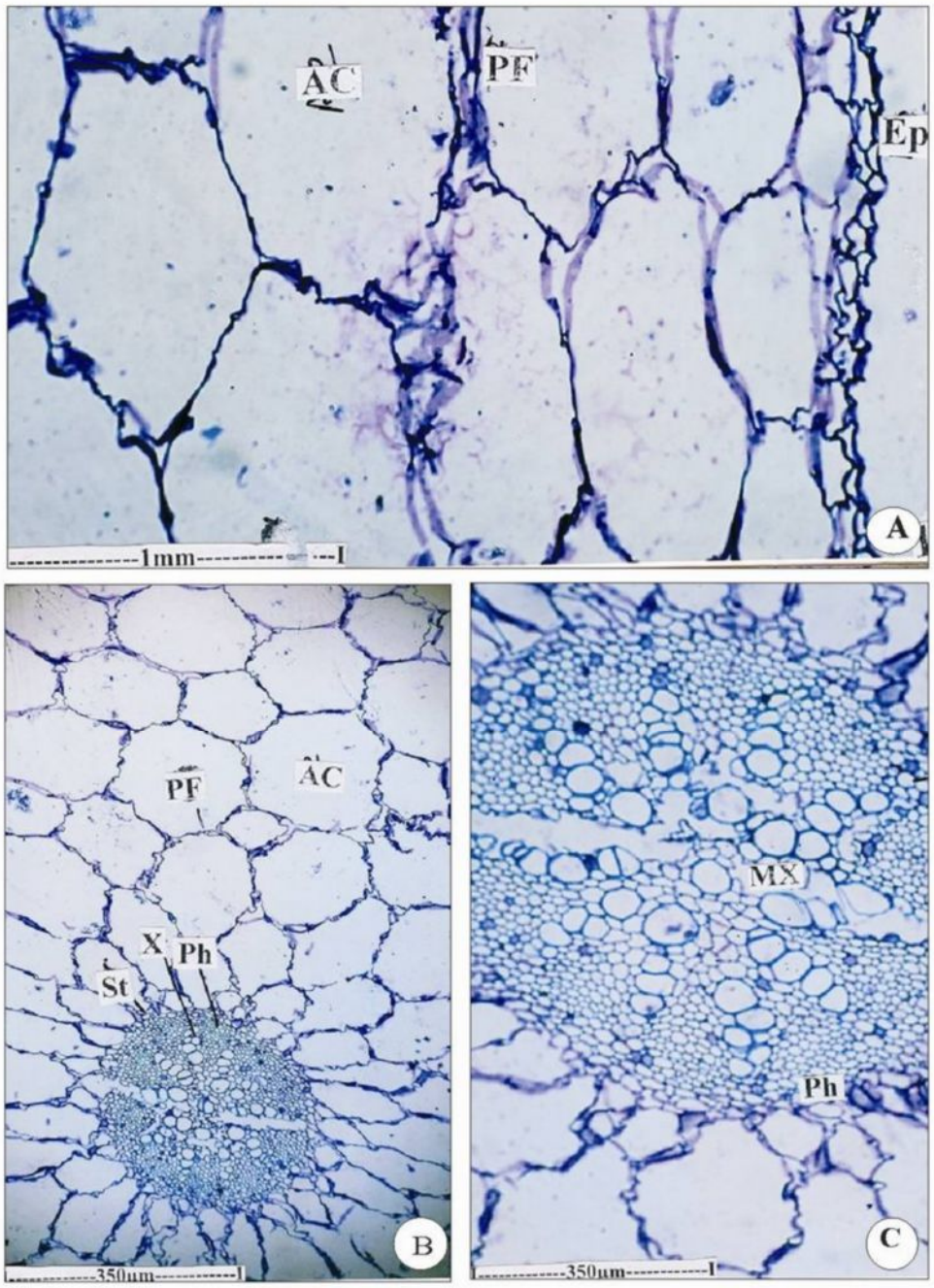

A – TS of root showing cortical air chambers (4X)
B – Cascular cylinder (10X)
C – Cortex and vascular cylinder (10X)

Ac – Air chamber **Mx-** Meta xylem **Pf** – partition filament
St – stele **X-** Xylem **Ph-** Phloem

Fig.11 Anatomy of *Nymphaea pubescens* rhizome

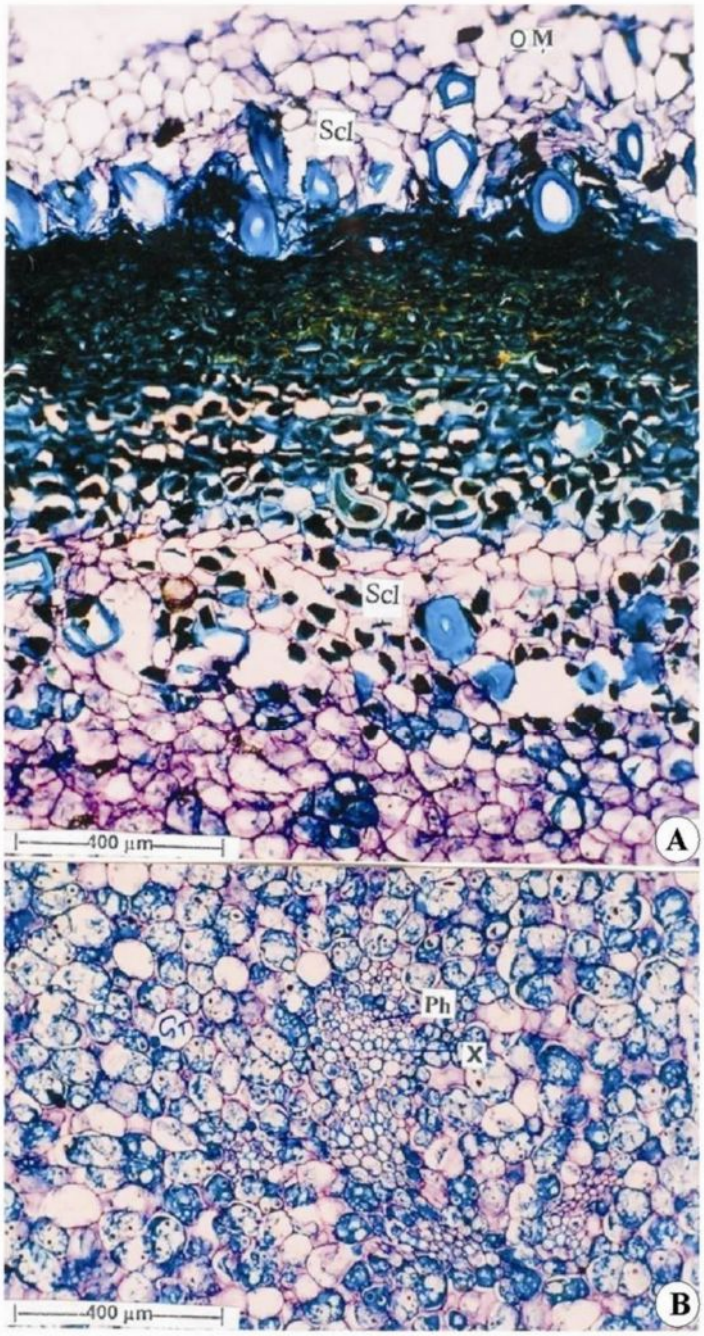

A. Periderm region
B. Central Portion

GT – Ground tissues
Ph – Phloem
OM – Outer membrane
Scl – Sclereids
X – Xylem

Fig.12 T.S. of *Nymphaea pubescens* rhizome (outer portion)

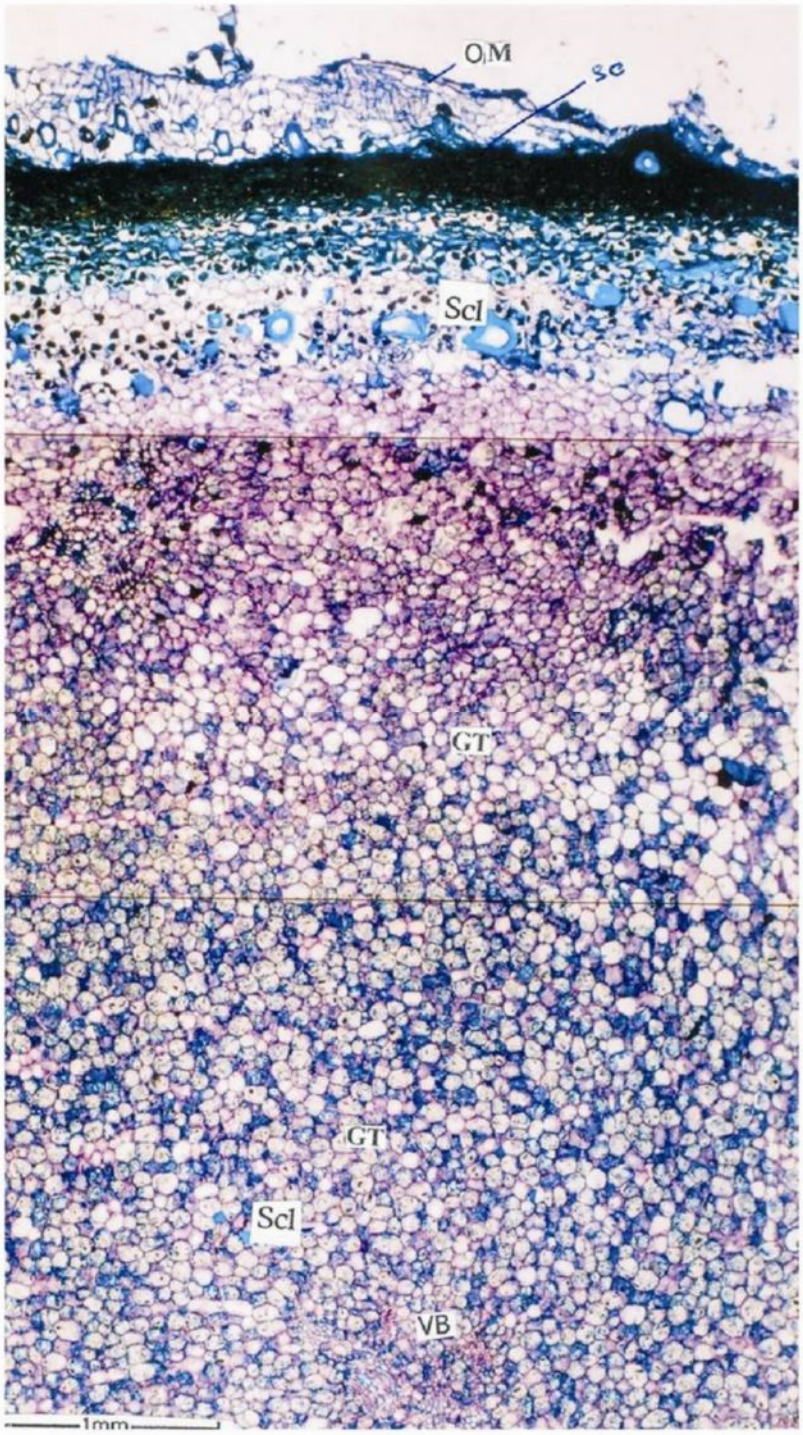

GT – Ground tissues
Scl – Sclereids
OM – Outer membrane
VB – Vascular Bundle
Ph – Phloem
X – Xylem

Fig.13 T.S. of *Nymphaea pubescens* rhizome (inner portion)

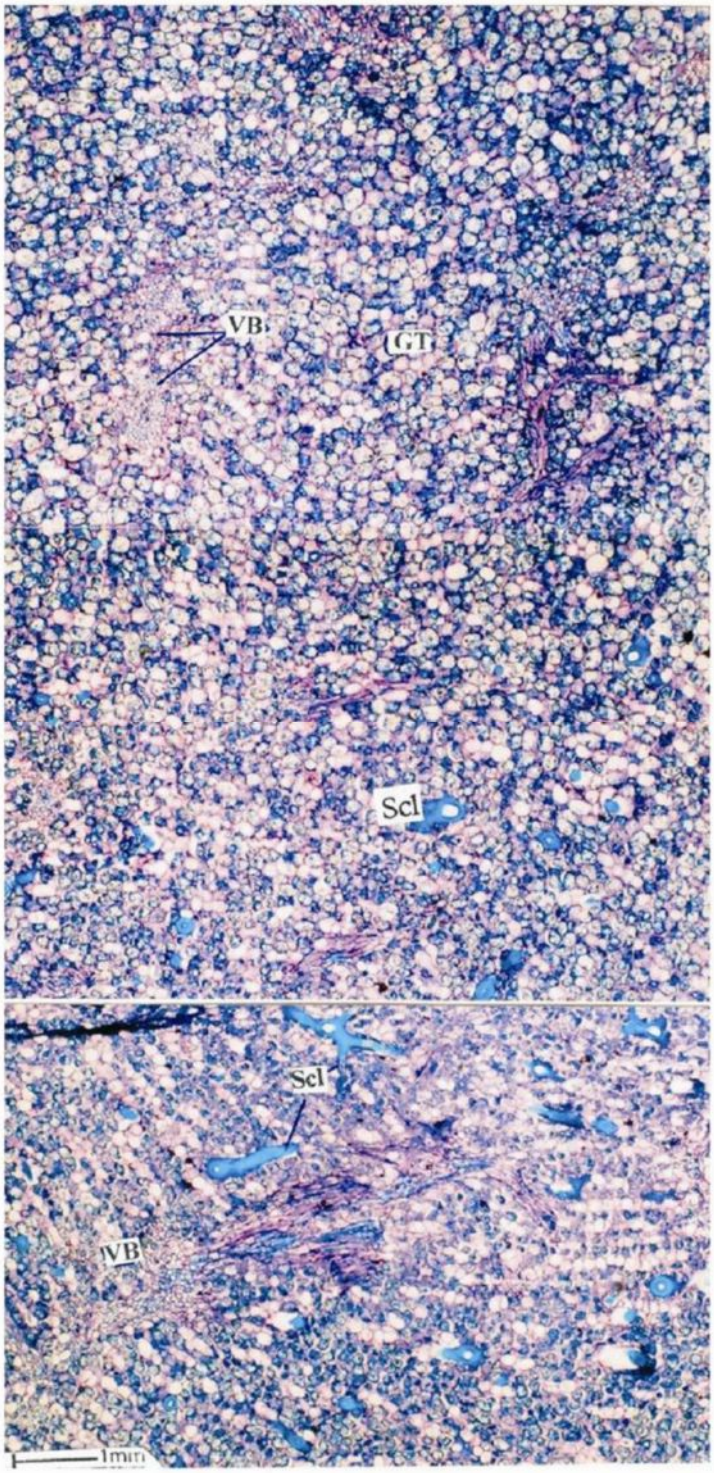

GT – Ground tissues **Scl** – Sclereids **VB** – Vascular Bundle

Fig.14 Starch grains distribution

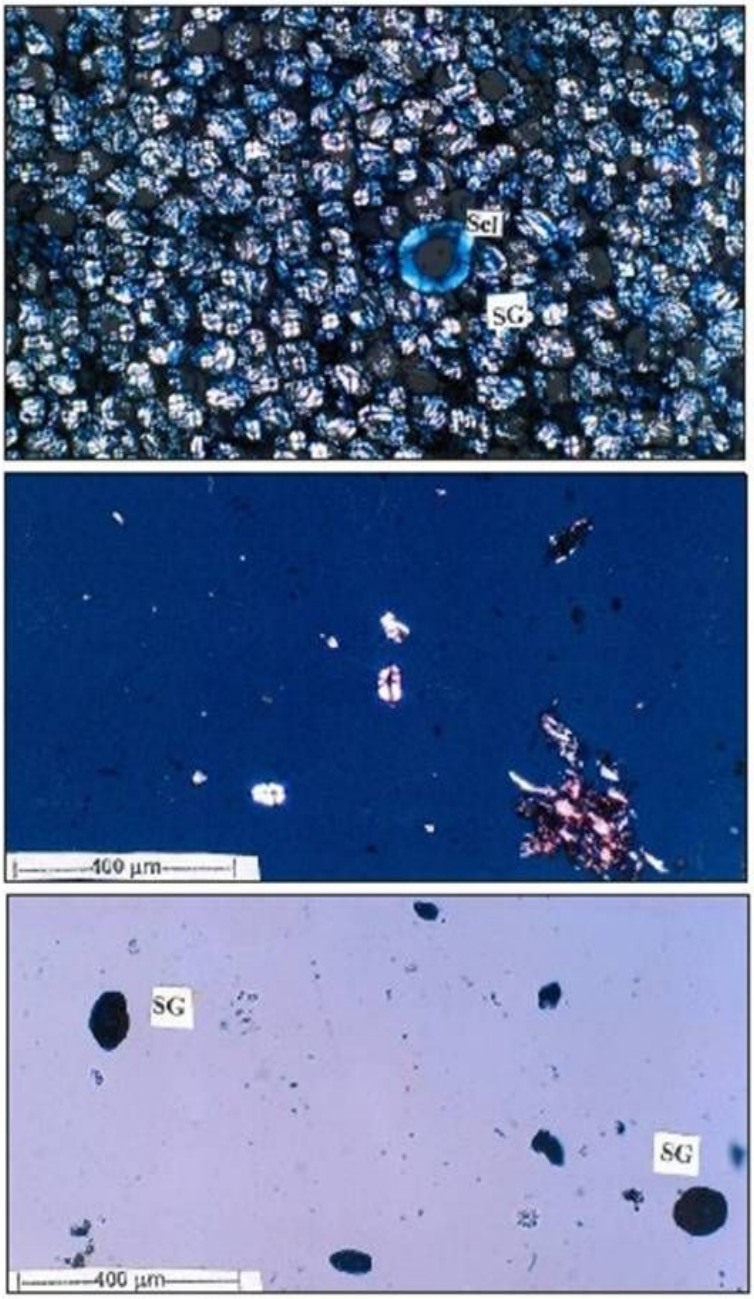

Scl – Sclerenchyma **SG** –Starch grain

Fig.15 Histochemical study of *Nymphaea pubescens* root

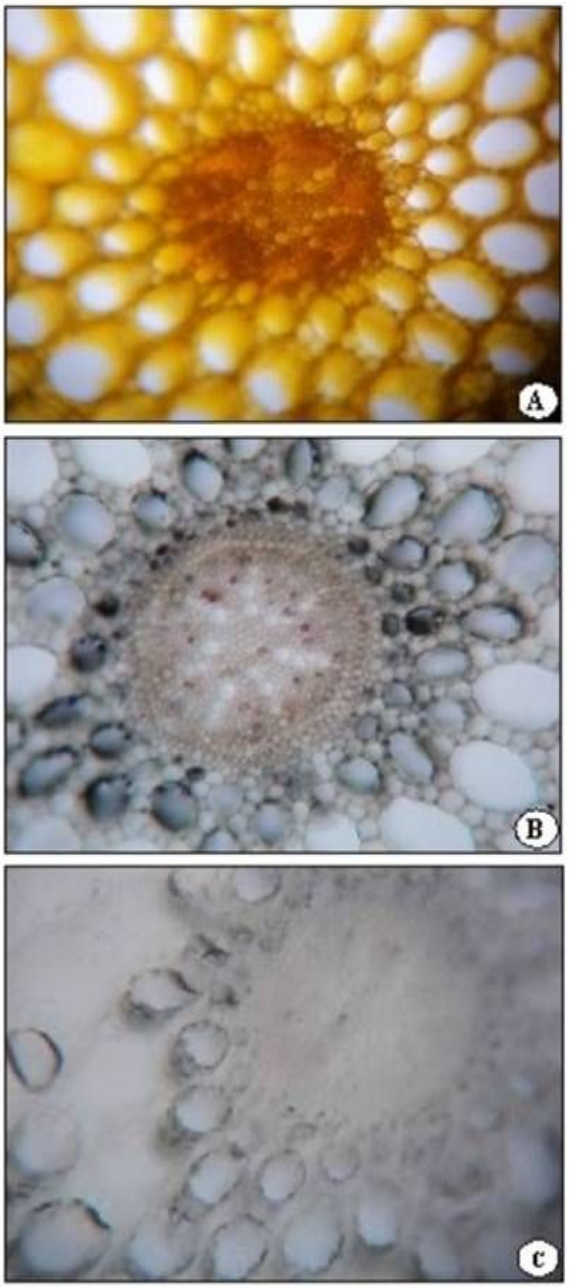

A. Histochemical staining for alkaloids
B. Histochemical staining for proteins
C. Histochemical staining for tannins

Fig.16 Histochemical study of *Nymphaea pubescens* rhizome

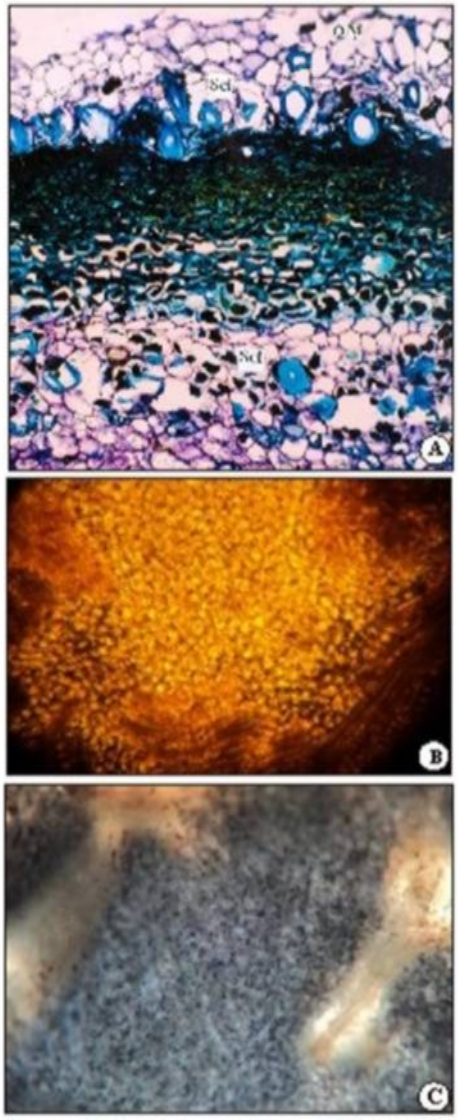

A. Histochemical staining for tannins
B. Histochemical staining for alkaloids
C. Histochemical staining for starch

OM - Outer membrane **Scl** – Sclereids

Table-1 Histochemical colour reaction of roots and rhizome of *Nymphaea pubescens*

S. No.	Reagents used	Test for	Nature of Change	Histological part		Degree of change	
				Root	Rhizome	Root	Rhizome
1.	Dragendorff's	Alkaloid	Reddish orange precipitate	Vascular bundles	Parenchyma cells in the ground tissue	+	++
2.	Ferric chloride	Tannin	Brownish black	Phloem cells and Partition filament	Inner sclerotic zone	+	++
3.	Millon's reagent	Protein	Reddish orange	Phloem and Pith	Parenchyma cells in the ground tissue	++	+
4.	Sulphuric acid	Saponins	Yellow strain	-	-	-	-
5.	Iodine	Starch	Dark blue	Partition filament in the ground tissue	Distributed throughout out in the parenchyma cells in the ground tissue	+	++

+ → Slightly stained ++ → Highly stained

Fig.17. Powder icroscopy of root and rhizome *Nymphaea pubescens*

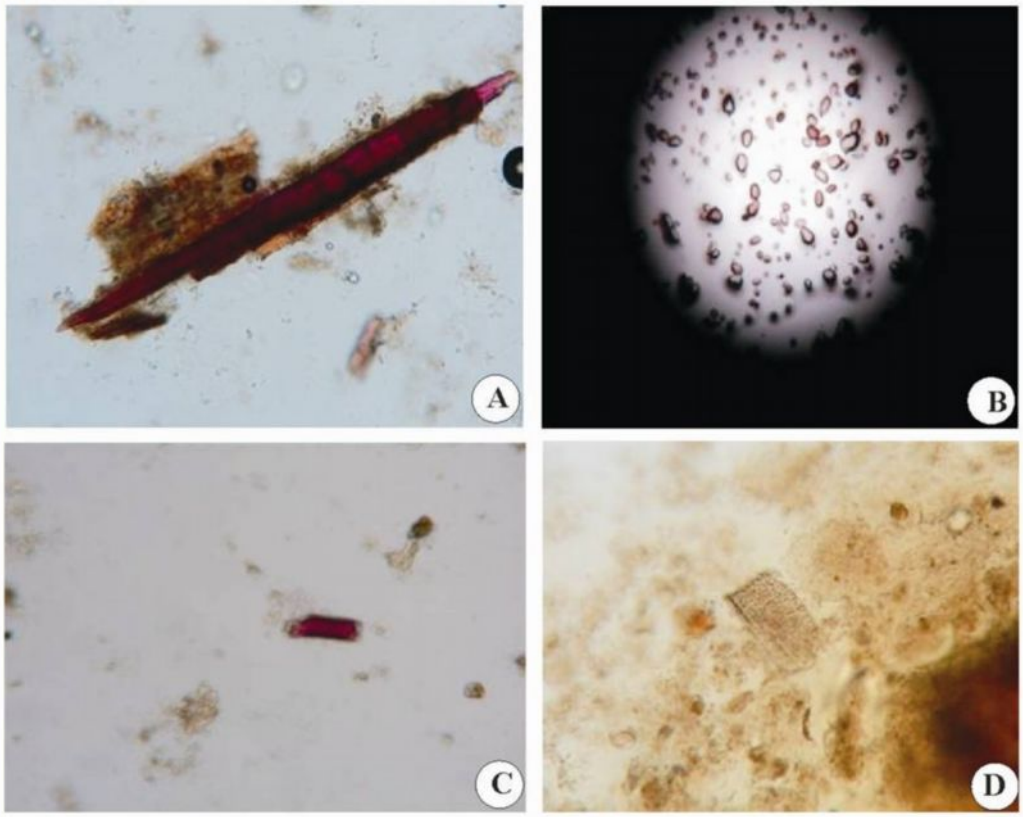

A. Lignified fibre (10X)
B. Starch grains (4X)
C. Sclereids (40X)
D. Xylem Vessels (Pitted-10X)

Table-2 Linear measurement of fibres and starch grains

S .No.	Parameter	Size in µm
1.	Length of fibre	240-560
2.	Width of fibre	64-112
3.	Diameter of starch grains	30-82

Table-3 Physicochemical constants

		Values (% w/w)	
S. No.	**Parameters**	**Flower**	**Root and rhizome**
1.	Ash values		
	Total ash	5.88	11.3
	Sulphated ash	0.04	0.07
	Acid insoluble ash	1.96	0.02
	Water soluble ash	0.03	0.04
2.	Extractive values		
	Benzene soluble extractive	14.4	10.1
	Chloroform soluble	19.2	12.3
	extractive	26.2	16.2
	Ethyl acetate soluble	24.0	26.8
	extractive	19.1	46.7
	Ethanol soluble extractive		
3.	Water soluble extractive	1.37	3.21
	Loss on drying		

Table-4 Behavior of drug powder with different chemical reagents

S. No.	Reagents	Test for	Roots & Rhizome	Flower Petals
1.	Dragendorff's	Alkaloid	++	+
2.	Anthrone + H_2SO_4	Glycoside	+	++
3.	HCl + Ammonia	Anthraquinone	-	-
4.	Tin + Thionyl chloride	Triterpenoid	-	-
5.	Acetic anhydride + Glacial acetic acid + H_2SO_4	Steroid	-	+
6.	Magnesium turnings + HCl	Flavonoids	+	++
7.	Ferric Chloride solution	Phenols	+	+
8.	Lead acetate solution	Tannins	++	-
9.	Fehling's A and B	Reducing sugars	+	+
10.	Water	Saponins	-	-
11.	NaOH and Copper sulphate	Proteins	+	+
12.	Acetic anhydride and sulphuric acid	Resin	-	-

+ → Slightly stained ++ →Highly stained

Table-5 Fluorescence analysis of plant parts with various chemical reagents

S. No.	Reagents	Flower petals			Root and Rhizome		
		Short UV 254 nm	Long UV 366 nm	Visible	Short UV 254 nm	Long UV 366 nm	Visible
1.	Powder drug + 1N Hcl	Yellowish green	Yellowish Green	Yellow	Green	Yellow	Cream yellow
2.	Powder drug + 1 N NaOH	Green	Green	Yellowish brown	Yellowish green	Yellowish green	Yellow
3.	Powder drug + 50% Hcl	Yellowish green	Dark green	Cream yellow	Greyish brown	Yellow	Yellowish brown
4.	Powder drug + 50% NaOH	Yellowish green	Dark green	Yellowish brown	Yellowish green	Yellow	Yellowish brown
5.	Powder drug + 50% HNO_3	Green	Yellow	Yellow	Green	Yellowish green	Yellow
6.	Powder drug + 50% H_2SO_4	Brownish black	Brownish black	Brownish black	Yellowish green	Yellowish green	Yellowish brown
7.	Powder drug + Hexane	Bluish green	Greyish brown	Yellow	Pale yellow	Yellow	Cream yellow
8.	Powder drug + Chloroform	Orange	Yellowish green	Yellowish Green	Yellowish green	Yellow	Cream yellow
9.	Powder drug + Ethyl acetate	Yellow	Greyish brown	Yellow	Yellowish green	Greyish brown	Pale yellow
10.	Powder drug + Methanol	Brown	Green	Cream yellow	Green	Greenish black	Brownish black
11.	Powder drug + Ethanol	Yellow	Yellowish green	Yellowish green	Yellowish orange	Yellowish green	Pale yellow

The pharmacognostic evaluation provides the simplest and quickest means to establish the identity and purity and thereby ensure quality of an herbal drug. It is often necessary to substantiate the findings by morphology, microscopy and physicochemical analysis to obtain the standardization protocol for the evaluation of herbal drug.

Nymphaea pubescens Willd. (Fig. 6) is a perennial aquatic rhizomatous stoloniferous herbs, leaves large orbicular with long fleshy warty petiole and the leaves are green above and pubescent below, sinus to 8cm deep, margins sharply dendate (Fig.7A&B).

The flower consists of numerous stamens, arranged spirally. The stamens are transformed into petals through gradual modifications of the stamens. The stamens are flat and dorsiventral. The filaments and the anthers are equally flat. The pollen chambers are located on the adaxial side of the stamen. The chambers are vertically elongated and dehiscence of the anther is also along vertical line. Sepals are oblong, obtuse and green in colour. Petals are white in colour. The sepals and petals are marked with pink striations in its centre (Fig. 6).

The fruit is a large berry (Fig 8B). The seeds are attached on the surface of septa (Fig. 8C). The rhizome is thick spherical fleshy and soft (Fig. 7C). Roots contains numerous root hairs which tapering towards the end (Fig. 7D).

As seen in transverse section, the anther consists of two adaxial theca (dithecous) and each theca is two chambered (Fig 9A). The outer wall of the pollen chamber consists of outer epidermis, middle layer of endothecium and inner layer of endodermis. The epidermis is thin and the cells are spindle shaped and thin walled (Fig. 9B&C). The endothecial cells are wide and radially elongated. They possess annular thickenings which offer rigidity to the anther wall. The anther wall is 6.0 µm thick; pollen grains are elliptical to spherical. The exine (outer wall) of the pollen is smooth and no distinct marking are evident (Fig. 9C). The starch grains are 30µm in diameter.

The root exhibits hydromorphic features. It consists of a thin epidermal layer of shrunken cells. The cortex is wide and aerenchymatous. Is consists of several layers of

air-chambers, which are large and polygonal in outline. The air-chambers are separated from each other's by thin uniseriate partition filaments (Fig. 10A). The vascular cylinder is circular measuring 700µm in diameter. It consists of about 10 radial arms of exarch xylem strands and 10 clusters of phloem alternating with the xylem. The xylem and phloem strands are radial in arrangement (Fig. 10B&C). The xylem strands have 7-10 cells, which are angular and thin walled. The metaxylem elements are upto 80 µm in diameter. The ground tissue of the vascular cylinder has small, thin walled, compact parenchyma cells.

The rhizome is thick spherical fleshy and soft. It is 1cm in diameter. It is covered by membranous sheath which is peeled off easily. The sheath consists of small thin walled parenchyma cells. Inner to the membranous covering is a dark band of thick walled cells which are compact and dense. The dark zone is 200µm thick. The cells of this zone consist of sclerenchyma with lignified walls filled with dense tannin which renders the zone dark color. Inner to the dark sclerotic zone, the entire rhizome has homogenous parenchymatous tissue. Throughout rhizome are diffusely distributed sclereids of various shape and size, they are circular, amoeboid, elongated and irregular. The sclereids have very thick lignified wall and narrow lumen. Tanniferous cells are also seen, especially along the outer zone (Fig.11,12 &13).

The vascular strands are seen scattered in the ground tissue. They are variable in shape and size. The vascular bundles have a few reduced xylem elements and well developed phloem elements. No bundle sheath is seen.

Almost all ground tissue is filled with dense starch grains. The starch grains are solitary and simple. Some of these are circular and concentric with central hilum and others are elongated, elliptical or spindle shaped with exeutic hilum. When the starch grains are viewed under the polarized light microscope "+" shaped dark marking is seen in the concentric type and "y" shaped markings are seen in the elongated type (Fig.14). The starch grains are 30µm (circular type) and 50µm (elongated type) in size.

The histochemical studies give a preliminary idea about the type of compounds and their accumulation in the plant tissues. Histochemical studies of root showed the

presence of alkaloids inbetween the vascular bundle, tannins in the phloem cells and partition filaments, protein in phloem cells and pith and starch in the partition filament in the ground tissue. In rhizome the alkaloids, proteins and starch histochemically stained in the parenchymatous cells and in the ground tissue and tannin in the inner sclerotic zone (Table-1; Fig. 15 &16). This is of great interest for quality control in basic research and biosynthetic accumulation of phytoconstituent in the aquatic plant *Nymphaea pubescens*.

Powder microscopy is an evaluation parameter in a quality control process used for medicinal plants to study the specific microscopic characters using different staining reagent for the detection of adulterants and its purity. The powder microscopic analysis of the powdered root and rhizome of *Nymphaea pubescens* showed the presence of lignified fibres, starch grains, xylem vessels pitted and sclereids (Fig. 17). These cellular characters give the diagnostic features of *Nymphaea pubescens*.

The linear measurement of fibres showed 240-560 µm in length and 64-112 µm in width. The diameter of starch grains shows 30-82 µm (Table-2). These values are found to be constant for this species. Quantitative microscopic data's are useful for identifying the different species of genus and also helpful in the determination of the authenticity of the plant.

The physico-chemical parameters are mainly used in judging the purity and quality of the drug. Ash values of a drug give an idea about the earthy matter or inorganic composition or other impurities present along with the drug. Total ash value was found to be slightly high (when compared to sulphated ash, acid insoluble ash and water soluble ash (Table-3).

Extractive values give an idea about the chemical constituents present in the drug as well as useful in the determination of exhausted or adulterated drugs. The ethyl acetate soluble extractive value of flower petals and the water soluble extractive value of root and rhizome showed higher value when compared to benzene, chloroform and ethanol soluble extractive values (Table-3). The result indicates the flower petals contain

higher flavonoid content and the root and rhizome contains higher content of polar phytoconstituents.

Presence of moisture content activates the enzymatic reaction that leads to the degradation of active constituent. Loss on drying indicates the percentage of moisture content present in a drug. The percentage loss on drying of flower petals was found to be 1.37%w/w and for root and rhizome 3.21%w/w. These values indicate, the plant drug has less moisture content (Table-3).

The therapeutic activity of the plant drug is based upon its active constituent. The flower petals showed the presence of glycosides, steroids, flavonoids, phenols, reducing sugars, proteins and trace amount of alkaloid. The root and rhizome showed the presence of alkaloid, glycosides, flavonoids, phenols, tannins, reducing sugars and proteins (Table-4).

The powdered drug was extracted with the suitable solvent and observed in the short and long UV light and also in the visible light to identify the presence of chromophores. The fluorescence analysis of the powdered drug of *Nymphaea pubescens* showed that the plant contains chromophores (Table-5).

PART 2 - PHYTOCHEMISTRY

MATERIALS AND METHODS

Natural product represents an extra ordinary reservoir of secondary metabolites. These secondary metabolites are responsible for the therapeutic activity of the plant. Since plants may contain hundreds or even thousands of metabolites, there is currently resurgence of interest in a plant kingdom as a possible source of new lead compounds. There exists a wide field for research in the phytochemistry in such a way that plants are phytochemically screened and documented for its analytical profile. The leads for a significant number of modern synthetic drugs have originated from isolated plant ingredients since the search for newer entities begins from either derivatizing existing drugs or from traditional medicinal systems. Therefore it is important to undertake phytochemical investigations along with biological screening to understand the therapeutic dynamics of medicinal plants and also to develop quality parameters[55].

The methods employed in phytochemical standardization of herbal drugs are chromatographic fingerprinting, isolation and identification of bioactive lead molecules. LCMS, LCMSMS, GCMS, GCMSMS and 2DNMR and FTIR are some of the new generation instrumental techniques in this field. The new generation phytochemical techniques such as hyphenated chromatographic and 2D NMR spectroscopic techniques provide very efficient screening of extracts and also an important tool in identification of bio-active metabolites.

6.1.1 Collection of plant material

The whole plant of *Nymphaea pubescens* was collected throughout the year (2008-2011) from different parts of Tamilnadu (Chennai, Neyveli, and Nagarkoil), India. The different plant parts such as leaves and petiole, flower petals, fruit and underground part (Root and Rhizome) were detached from the whole plant and washed separately in running tap water, cut into small pieces, spread on blotting paper and shade dried for 20 days. The powdered samples were kept in polythene bags, sealed properly and stored at room temperature.

6.1.2 Preparation and selection of extracts for phytochemical screening

The coarsely powdered plant parts such as leaves and petiole, flower petals, fruits and underground part (Root and Rhizome) were separately extracted in a soxhlet extractor with 95% ethanol by hot percolation. After exhaustive extraction, the solvent was completely removed by rotary evaporator under reduced pressure. The crude ethanolic extracts of different plant parts of *Nymphaea pubescens* were comparatively screened for antidiabetic activity (OGTT)[56] and *in-vitro* anticancer activity[57,58] (against *Hela* cell lines). The extracts that showed potent antidiabetic activity and anticancer effect against *Hela* cell lines were selected for phytochemical studies. From the above said preliminary screening the underground part (root and rhizome) and flower petals of *Nymphaea pubescens* were choosen for phytochemical and pharmacological screening.

6.1.3 Preliminary phytochemical screening[55]

The nature (chemical group, specific identity, polarity, etc) of the substances in a mixture can be determined by chemical tests and chromatographic studies. In chemical tests, a colour reaction or precipitate in response to specific reagents may indicate the presence of a particular compound or more usually a class of compounds. Such tests can be useful to investigate the chemical constituents of test organisms and to monitor the effectiveness of an extraction process when a particular chemical class is being sought.

The ethanolic root and rhizome extract and ethanolic flower extract of *Nymphaea pubescens* were subjected for preliminary phytochemical analysis.

Test for Alkaloid

To the test substance a few drops of acetic acid were added, followed by dragendorff's reagent and shaken well. Formation of orange red precipitate indicates the presence of alkaloid.

The substance was mixed with little amount of dilute hydrochloric acid and Mayer's reagent. Formation of white precipitate indicates the presence of alkaloid.

Test for Glycosides

The substance was mixed with a pinch of anthrone on a watch glass. One drop of concentrated sulphuric acid was added, made into a paste and warmed gently over water bath. Dark green coloration is the indication of the presence of glycosides.

Test for Anthraquinones

Borntrager's Test

The substance was macerated with ether and after filtration, aqueous ammonia or caustic soda was added. Pink, red or violet colour in the aqueous layer after shaking indicates the presence of anthraquinones. If present as glycoside then the test should be modified by hydrolysing with hydrochloric acid as the first step.

Test for Flavones

Shinado's Test : To the substance in alcohol, a few magnesium turnings and few drops of concentrated hydrochloric acid were added and boiled for five minutes. Red coloration shows the presence of flavones.

To the substance in alcohol, 10%w/v sodium hydroxide solution or ammonia was added. Dark yellow colour indicates the presence of flavones.

Test for Terpenoids

Noller's Test: The substance was warmed with tin and thionyl chloride. Pink coloration indicates the presence of terpenoids.

Test for Steroids - Libermann Buchard Test

One milligram of the test substances was dissolved in a few drops of chloroform. 3ml of acetic anhydride, 3ml of glacial acetic acid were added, warmed and cooled under tap water and few drops of concentrated sulphuric acid were added along the sides of test tube. Appearance of bluish green shows the presence of steroids.

Test for Tannins

The substance is mixed with basic lead acetate solution. Formation of white precipitate indicates the presence of tannins.

Test for Phenol

To the substance a few drops of alcohol and ferric chloride solution was added. Bluish green or red indicates the presence of phenol.

Test for Saponins

Substance shaken with water, copious lather formation indicates the presence of saponins.

Test for Sugars

The substance was mixed with Fehling's solution I and II. Formation of red coloration indicates the presence of sugars.

Test for Proteins

To 1ml of hot aqueous extract 5-8 drops of 10%w/v sodium hydroxide solution and 1 or 2 drops of 3% w/v copper sulphate were added. Red violet colour develops indicates the presence of proteins.

Test for Resin

To the few ml of ethanolic extract of the drug, 5-10ml of acetic anhydride was added, heated and cooled. To the above solution 0.05ml of sulphuric acid was added. Bright purplish red colour rapidly changing to violet indicates the presence of resins.

Chromatography

Phytochemical evaluation comprises of different chemical tests, physical evaluation, chemical assays, the isolation, purification and identification of active constituents. One of the modern physical standardisation techniques that are widely used is the chromatographic technique. Chromatography comprises a group of

methods for separating molecular mixtures that depend on the different affinity towards the solutes. The behaviour of substances in chromatographic systems is usually highly reproducible and this yield information on their identity and/or physicochemical properties, as well as the identity of the source organism.

6.1.4 Thin layer Chromatography[59]

Thin layer chromatography can be used to identify compounds present in a mixture and to determine the purity of a substance.

Stationary phase	:	The glass plate coated with silica gel G (Merck) was used as stationary phase
Standard solution	:	1 mg of standard substance was dissolved in 10ml of methanol.
Solvent system	:	The appropriate mobile phase for the extracts was chosen by trial and error method.
Saturation of chamber	:	A sheet of filter paper was placed on three sides of the TLC chamber from inside and was allowed to soak in solvent system prior to development of the chromatogram. It was ensured that the paper was fully wet and stuck to the walls of the chamber and left undisturbed before introducing the plates for half an hour, so that the saturation of chamber with solvent was completed.
Application of test & standard solution	:	The extract and standard solution were applied 1.5cm away from the lower edge of the plate with the help of micro-capillary tube. The solvent was allowed to evaporate after each sample application by air drying. On each plate, one spot of test solution and standard solution was loaded.
Development of chromatogram	:	The loaded plates were then placed vertically in the chamber with the bottom edge immersing in developing medium. After

the solvent front moved up to a distance of about 18cm, the plate was taken out, solvent front was marked and the plate was taken out, solvent front was marked and the plate was dried at room temperature.

Detection system : Observation under short and long UV identified the position of spots first if any and then the plates were sprayed with 10% methanolic sulphuric acid, followed by heating at 110ºc for 5 mins. Then the Rf value was calculated.

6.1.5 High Performace Thin Layer Chromatography[60].

HPTLC is an enhanced form of TLC. A number of enhancements can be made to the basic method of TLC to automate the different steps, to increase the resolution achieved for quantitative measurements.

Sample application : Samples were applied in the form of bands using Linomat IV applicator of CAMAG for all the precoated silica gel plates.

Stationary phase : Pre-coated silica gel 60 F254 plate (E merck) of uniform thickness 0.2mm was used for all the HPTLC analysis.

Elution : The plates were eluted in their respective mobile phases in CAMAG twin trough chambers. The chambers were saturated with the respective mobile phases (selected by trial and error method) for a period of 30 minutes before the elution unless chloroform was used as one of the components of the mobile phase in which case no chamber saturation is required.

Scanning : Eluted plates were then densitometrically scanned using CAMAG scanner 3 at the respective wavelengths or at multiwavelengths, for the crude extracts either under UV light using deuterium lamp or after derivatisation using tungsten lamp.

The ethanolic extract from root and rhizome and the ethyl acetate fraction from ethanolic flower extract of *Nymphaea pubescens* were spotted in the concentration of 50mg/ml using the CAMAG Linomat IV applicator onto the precoated silica gel plate (merck). The plate was then eluted with the respective mobile phase. After the elution, the plate was scanned densitometrically using CAMAG TLC scanner 3 at 254nm and 366nm. The R_f value, maximum height, % height, area and % area was calculated from the peak.

6.1.6 Gas Chromatography–Mass Spectrometry anlysis[61]

GCMS is an integrated method for spectrum extraction and compound identification from GCMS data. The GCMS is used for extracting individual component spectra from GCMS data files and then using these spectra in a reference library.

Procedure

GC-MS analysis was carried out on a GC clarus 500 Perkin Elmer system comprising a AOC-20i autosampler and gas chromatograph interfaced to a mass spectrometer (GC-MS) instrument employing the following conditions: Column Elite-1 fused silica capillary column (30 x 0.25 mm ID x 1EM df, composed of 100% Dimethyl poly siloxane), operating in electron impact mode at 70 eV; helium (99.999%) was used as carrier gas at a constant flow of 1ml/min and an injection volume of 0.5 EI was employed (split ratio of 10:1) injector temperature 250°C; ion-source temperature 280°C. The oven temperature was programmed from 110°C (isothermal for 2 min), with an increase of 10°C/min to 200°C/min then 5°C/min to 280°C/min ending with a 9 min isothermal at 280°C.Mass spectra were taken at 70 eV; a scan interval of 0.5 s and fragments from 40 to 550 Da.

Interpretation on mass spectrum of GC-MS was done using the database of National Institute Standard and Technology (NIST) having more than 62,000 patterns. The mass spectrum of the unknown component was compared with the spectrum of the known components stored in the NIST library. The name, molecular weight and structure of the components of the test materials were ascertained.

The ethanolic root and rhizome extract and ethanolic flower extract of *Nymphaea pubescens* were subjected for GCMS analysis.

Column Chromatography[55]

Column chromatography in phytochemistry is a method used to purify individual chemical compounds from mixtures of compounds. It is often used for preparative applications on scales from micrograms up to kilograms. This technique is suitable for the physical separation of gram quantities of material. A solvent acts as the mobile phase while a finely divided solid surface acts as the stationary phase. The stationary phase will adsorb the components of the mixture to varying degrees. As the solution containing the mixture passes over the adsorbent, the components are distributed between the solvent and adsorbent surface. This process may be described by three-way equilibrium between the sample, the solvent and the adsorbent.

6.1.7 Isolation of Compound I and II using column chromatography

Glass column of 100 x 4 cm was packed with 400g silica gel (100-200 mesh, Merck, India) using hexane. 20gms of the crude ethanolic root and rhizome extract of *Nymphaea pubescens* was ground with 2g of silica gel and loaded on the top of the column. Fractions each of 20ml were collected using solvents of increasing order of polarity such as n-hexane, chloroform, ethyl acetate, acetone, ethanol and water. The fractions were collected and subjected to TLC analysis. Fractions yielding single band and exhibiting similar R_f values are pooled and allowed to evaporate to remove the solvent. The pure compounds were subjected to spectroscopic analysis.

6.1.8 Isolation of compound III

Separation of crude alkaloid from powdered root and rhizome of *Nymphaea pubescens* (Stas otto process)[62]

Fifty grams of the powdered root and rhizome of *Nymphaea pubescens* was added with 10 g of sodium carbonate and added sufficient amount of water. Boiled for few minutes and filtered. The filterate was added with few drops of dilute sulphuric acid to remove the excess of sodium carbonate. The filterate was extracted

three times with sufficient amount of chloroform. The chloroform layer was separated, evaporated and the percentage yield of crude alkaloid was calculated. The crude alkaloid is further subjected for column chromatography for the isolation of compound.

Isolation of compound III from crude alkaloid

Glass column of 50 x 20 cm was packed with 200 g neutral alumina (150 mesh, Merck, India) using benzene. 0.12 mgs of crude alkaloid was ground with 1g of alumina and loaded on the top of the column. Fractions each of 20ml were collected using solvents of increasing order of polarity such as benzene, chloroform, ethyl acetate, acetone, ethanol and water. The fractions were collected and subjected to TLC analysis. Fractions yielding single band and exhibiting similar R_f values are pooled and allowed to evaporate to remove the solvent. The pure compounds were subjected to spectroscopic analysis.

6.1.9 Bioassay guided isolation of Compound IV[55]

The path which leads from the intact plant to its pure bioactive constituents is generally known as bio-assay guided fractionation. Following this procedure, crude plant extracts are submitted to different bioassays for a rapid estimation of their bioactivity. The extracts of interest are then fractionated with the help of various chromatographic methods. The bioassays serve as a guide during the isolation process and all fractions continuing to exhibit activity are carried through further isolation and purification until pure active principles are obtained.

Fractionation of ethanolic flower extract from *Nymphaea pubescens*[60]

Glass column of 100 x 4cm was packed with silica gel (100-200 mesh, Merck, India) using hexane. 20g of the ethanolic flower extract of *Nymphaea pubescens* were grounded with 2g of silica gel and loaded on the top of the column. Fraction each of 20ml were collected using solvents of increasing order of polarity such as benzene, chloroform, ethyl acetate, ethanol and water. The fractions in increasing order of polarity are separately collected. The fraction showing potent *in*

vitro anticancer activity against *HeLa* cells was further subjected for isolation of compound.

Isolation of compound IV from active fraction

Glass column of 50 x 2cm was packed with 200g of silica gel (200-400 mesh, Merck, India) using hexane. 2g of active crude fraction was ground with 1g of silica gel and loaded on the top of the column. Fractions each of 10ml were collected using solvents of increasing order of polarity such as n-hexane, chloroform, ethyl acetate and methanol. The fractions were collected and subjected to TLC analysis. Fractions yielding single band and exhibiting similar R_f values are pooled and allowed to evaporate to remove the solvent. The pure compound was subjected to spectroscopic analysis.

6.1.10 Quantification of compound IV in the active fraction

Quantification of compound IV was carried out for the ethyl acetate fraction from the ethanolic flower extract of *Nymphaea pubescens*. The linearity of the HPTLC method was investigated for the applied spot (100mcg/ml) using the CAMAG Linomat IV applicator onto the precoated silica gel plate (merck). The plate was then eluted with the mobile phase n-Hexane: Ethyl Acetate: Formic Acid (4.0: 5.5: 0.5). After the elution the plate was sprayed with 10% methanolic H_2SO_4, heated at 105ºC for 5 minutes and scanned densitometrically using CAMAG TLC scanner 3 at 460nm, 366 nm and 600nm respectively for quercetin. The percentage of compound IV in the fraction was calculated by calibration using peak height and peak area ratio.

6.1.11 Structural elucidation[63]

After a separation of a pure compound, it is necessary to determine the chemical structure of the compound. Spectroscopy includes a variety of analytical techniques for determining the molecular properties and to characterize the molecules isolated by using various chromatographic techniques. The most common techniques that are sufficient to give complete molecular structure of small molecules are UV/Visible, IR, NMR (^{1}H, ^{13}C and 2D NMR) and Mass spectroscopy. However more

emphasis is given to NMR experiments including two dimensional NMR experiments.

UV/Visible spectroscopy

The UV/Visible spectrum gives information about presence and nature of various chromophores such as conjugated dienes, enones and dienones etc., based on the position and intensity of the absorption band. UV spectra was recorded on UV-Vis-NIR spectrophotometer (Make : Varian Model : 5000)

IR spectroscopy

The IR spectrum of an organic molecule can be used as a finger print for molecular identification. IR energy is used to obtain structural information about the functional groups and the nature of bonds present in organic molecule. IR spectra was recorded on a IR spectrometry

Make : Thermo Nicolet Model :6700

Method : KBr Disc method

Wave number : 4000-500 cm^{-1}

NMR Spectroscopy

NMR is the powerful tool in structure elucidation of organic molecules. NMR spectrum gives information about specific chemical environments of observable nuclei in a molecule. It provides information about the number, types and connectivity of particular atoms. ^{1}H and ^{13}C NMR spectral methods are employed and the resonances are assigned. If the information is not sufficient to elucidate the complete structure then advanced and 2 dimensional NMR methods are used. DEPT spectrum is used to determine the number of protons attached to each carbon. HETCOR, HSQC and HMBC helps in assigning all the protons to their respective carbons. This is followed by further 2D experiment that give short and long range correlations (COSY, HMBC etc.) and help to establish the complete structure of the molecule.

^{13}C NMR

Gives a view of the carbon skeleton, shows better resolution as chemical shift are spread over a range from δ0-220. Chemical shift values indicate chemical environment and state of hybridization.

Advanced 1-Dimensional NMR experiments

DEPT-(Distortionless enhancement of polarization technique) experiment is the most commonly used experiment to determine the multiplicity of carbon atoms, in other words it gives information about the number of protons attached to a particular carbon. It involves transfer of magnetization from protons to their respective carbon atoms.

Connectivity spins systems separated by quaternary compounds

Heteronuclear multiple bond coherence (HMBC) represents hetero nuclear long range coupling experiments. These experiments help establish connectivity through quaternary carbons. Normally HMBC experiments shows correlation between proton and carbon separated by two or three bonds. However in conjugated or extended conjugated system correlations even upto five bonds can be seen.

NMR spectra were recorded on Multinuclear FT-NMR spectrometer (Model Avance-II Bruker). The instrument is equipped with a cryomagnet of field strength 9.4T. Its frequency 1H frequency is 400MHZ, while for 13C the frequency is 100MHZ. 1D, ^{13}C, DEPT-135, HMBC NMR spectrums were carried out on the same instrument.

Mass Spectroscopy

The process of fragmentation follows a predictable pathway and the fragment ions that are formed reflect the most stable cations the molecules can form. The highest m/z peak, termed the molecular ion peak, represents the parent molecule less an electron. The molecular ion peak together with analysis of fragment ions gives useful structural information about the molecule. High resolution mass spectroscopy

gives exact mass of the molecules and is useful in establishing correct molecular formula of the molecule.

Instrument used	: Shimadzu QP 5050
Inlet temperature	: 100°c
Flagging	: m/z

6.1.12 Physico-chemical property analysis[64]

The physico-chemical properties were evaluated for the isolated compounds I, II, III and IV by feeding the compounds in the ACD/ilabs software and the parameters such as Lipinski type properties (Molecular weight, number of hydrogen bond donors and acceptors, total polar surface area and number of rotable bonds), Pharmacokinetic properties (absorption, crossing blood brain barrier, volume of distribution, plasma protein binding and bio-availability) and Pharmacodynamic parameters (Ames test, Estrogen receptor binding, hERG inhibition, toxicity catogery and LD50) were evaluated.

6.1.13 Chemotaxonomical analysis[65]

The distribution of secondary metabolites is not random. Once an interesting lead structure was known then it is often possible to direct the search for related compounds.

The genus *Nymphaea* subdivided into five subgenera-*Anecphya*, *Brachyceras*, *Hydrocallis*, *Lotos* and *Nymphaea*. So far no comparative phytochemical studies have been investigated and hence the comparative chemo systematic study was carried out for the five subgeneras in the *Nymphaea* genus.

RESULTES AND DISCUSSION

Table-6 Colour, consistency and % yield of ethanolic extracts of *Nymphaea pubescens*

S. No.	Ethanolic extract	Colour	Consistency	Yield (% w/w)
1.	Root & rhizome	Dark Brown	Greasy	7.31
2.	Flower	Yellowish Brown	Glossy	3.58

Table-7 Preliminary phytochemical analysis of the ethanolic extracts of *Nymphaea pubescens*

S. No.	Test for	Roots & Rhizome	Flower Petals
1.	Alkaloid	++	+
2.	Glycoside	+	++
3.	Anthraquinone	-	-
4.	Triterpenoid	-	-
5.	Steroid	-	+
6.	Flavonoids	+	++
7.	Phenols	+	+
8.	Tannins	++	-
9.	Reducing sugars	+	+
10.	Saponins	-	-
11.	Proteins	+	+
12.	Resin	-	-

+ → Slightly stained ++ →Highly stained

Table-8 TLC Profile for the ethanolic extract from the root and rhizome of *Nymphaea pubescens*

Test sample	Solvent system	Peaks	R_f value (Iodine vapours)
Ethanolic extract	n-Hexane : Ethyl acetate : Formic acid (4 : 5.5 : 0.5)	1	0.15
		2	0.49
		3	0.8

Table-9 TLC Profile for the crude alkaloid fraction from the root and rhizome of *Nymphaea pubescens*

Test sample	Solvent system	Peaks	R_f value (Iodine vapours)
Ethyl acetate fraction	Toluene: Ethyl Acetate: Formic Acid: Methanol (3:3:0.8:0.2)	1	0.14
		2	0.52
		3	0.73

Table-10 HPTLC fingerprint of ethanolic extract from the roots and rhizomes of *Nymphaea pubescens*

Sample	:	Ethanolic extract
Sample prepared in	:	Methanol
Sample concentration	:	Extract (50mg/ml)
Applied volume	:	4 µl
Stationary Phase	:	Silica Gel GF_{254}
Mobile phase	:	n-Hexane : Ethyl acetate : Formic acid (4:5.5:0.5)
Scanning wavelength	:	366nm
Development Mode	:	Ascending mode

Peak	Start Rf	Start Height	Max Rf	Max Height	Height %	End Rf	End Height	Area	Area %
1	0.13	0.2	0.15	31.6	3.13	0.17	0.5	530.7	1.03
2	0.26	4.9	0.33	152	15.04	0.4	1.3	7506.3	14.62
3	0.41	0.1	0.49	456.9	45.2	0.6	27.4	27881.2	54.32
4	0.61	27.9	0.67	344.2	34.05	0.75	0.1	14766.6	28.77
5	0.76	0.3	0.8	11.9	1.18	0.83	0.1	354.2	0.69
6	0.84	0.1	0.87	14.2	1.4	0.89	0	291.7	0.57

Fig.18. Chromatogram of ethanolic extract from root and rhizome of *Nymphaea pubescens*

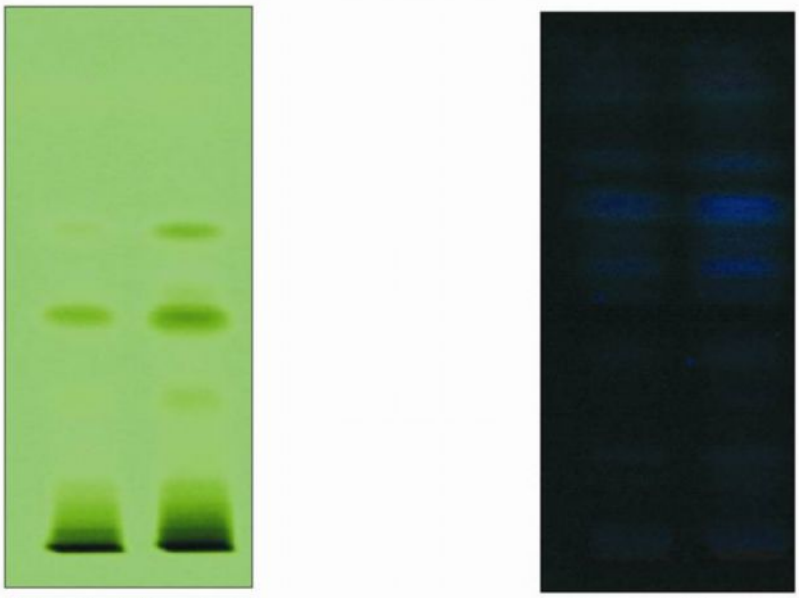

Track **1** Track **2** Track **1** Track **2**

254 nm **366 nm**

Fig.19. Densitogram of ethanolic extract from root and rhizome of *Nymphaea pubescens*

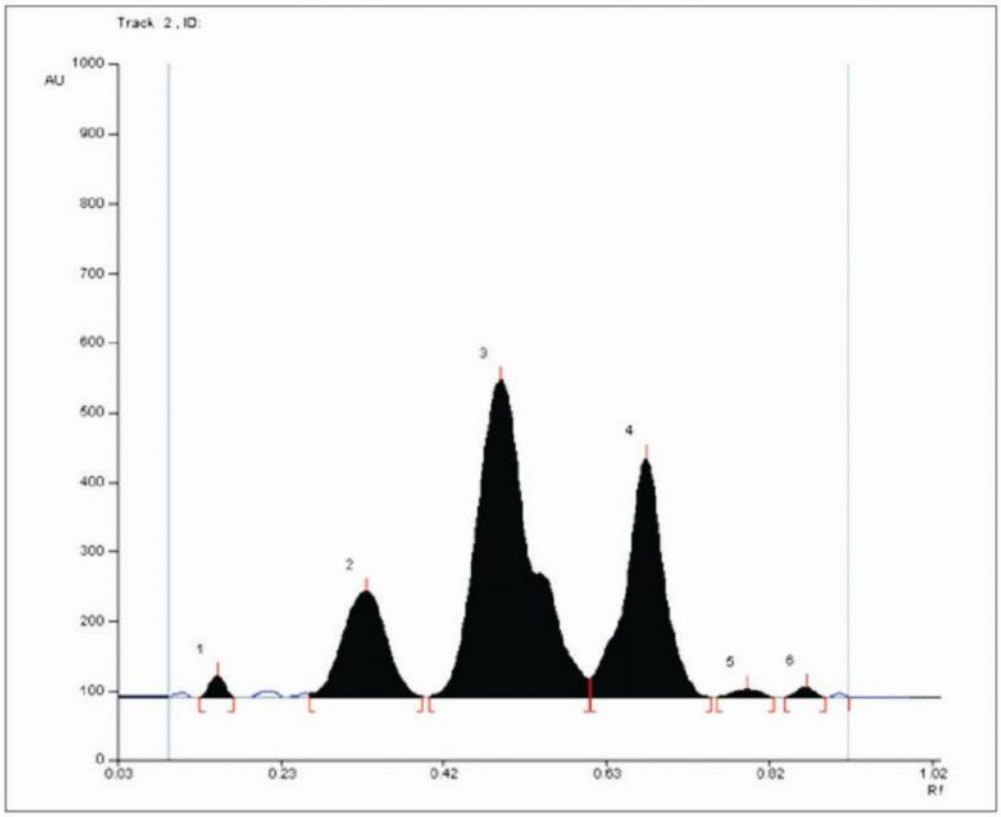

Table-11 HPTLC fingerprint of crude alkaloid fraction from root and rhizome of *Nymphaea pubescens*

Sample	:	Crude alkaloid fraction
Sample prepared in	:	Methanol
Sample concentration	:	Extract (50mg/ml)
Applied volume	:	Track 1 (2µl), Track 2 (4 µl), Track 3 (8 µl), Track 4 (10 µl)
Stationary Phase	:	Silica Gel GF_{254}
Mobile phase	:	Toluene : Ethyl acetate : Formic acid : Methanol (3:3:0.8:0.2)
Scanning wavelength	:	366nm
Development Mode	:	Ascending mode

Peak	Start Rf	Start Height	Max Rf	Max Height	Height %	End Rf	End Height	Area	Area %
1	0.07	0.1	0.10	63.3	4.29	0.12	0.2	1076.9	2.21
2	0.13	0.4	0.14	20.2	1.37	0.15	14.7	279.6	0.57
3	0.17	15	0.17	16.4	1.11	0.21	0.2	278.8	0.57
4	0.33	3.2	0.39	44.2	2.99	0.4	38.1	1637.1	3.36
5	0.42	36.3	0.45	48.9	3.31	0.46	48.3	1256.6	2.58
6	0.47	47.5	0.52	172.6	11.68	0.57	76.8	8749.6	17.97
7	0.57	76.8	0.61	113.0	7.65	0.62	110.4	3926.1	8.06
8	0.62	110.6	0.65	155.7	10.54	0.67	139.2	5236	10.76
9	0.68	139.3	0.71	201.7	13.65	0.72	192.1	5318.9	10.93
10	0.72	193	0.73	247.6	16.76	0.76	146.5	6166.3	12.67
11	0.76	147.3	0.78	315.4	21.34	0.85	49.0	12080.1	24.81
12	0.85	49.3	0.87	78.5	5.31	0.92	0.4	2678.1	5.5

Fig.20 Chromatogram of the crude alkaloidal fraction from root and rhizome of *Nymphaea pubescens*

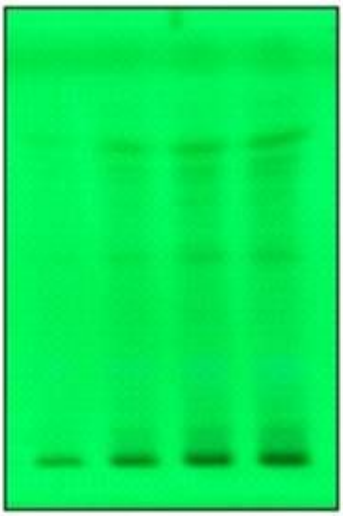

Track1 Track2 Track3 Track4

254 nm

Track1 Track2 Track3 Track4

366 nm

Fig. 21 Densitogram of the crude alkaloidal fraction from root and rhizome of *Nymphaea pubescens*

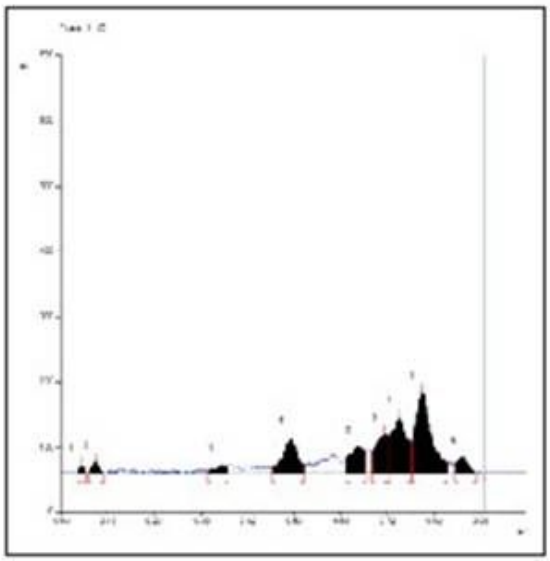

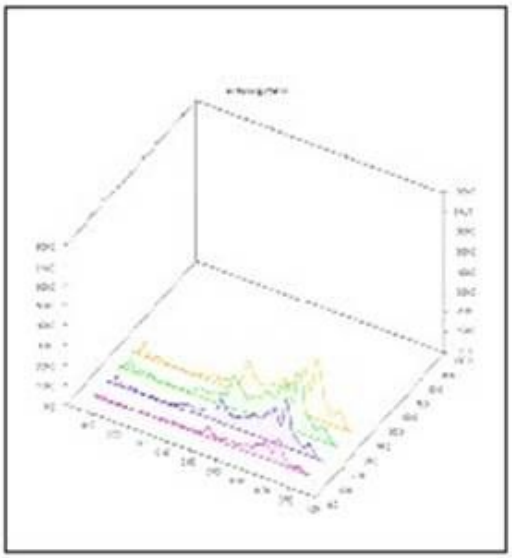

Spectra-1 GCMS of ethanolic extract from root and rhizome of *Nymphaea pubescens*

Sample Information

Sample Name : PF1111-1057-02
Sample ID : NR SAMPLE
Data File : D:\MSDATA\Year 2011\Dec-11\02-12-2011\PF1111-1057-02.QGD

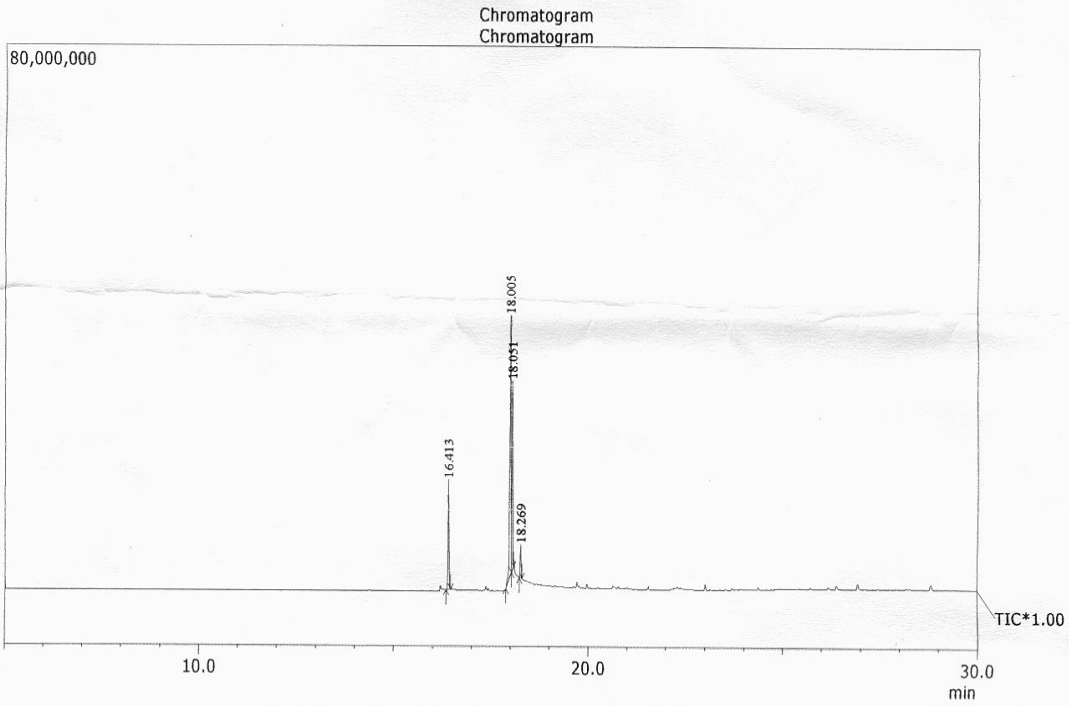

Peak Report TIC

PEAK#	R.TIME	AREA	AREA%	NAME
1	16.413	25618283	15.83	Ethyl palmitate
2	18.005	83308808	51.48	Methyl linoleate
3	18.051	45157021	27.91	Ethyl Oleate
4	18.269	7739785	4.78	Ethyl stearate
		161823897	100.00	

Table-12 GCMS analysis of ethanolic extract from root and rhizome of *Nymphaea pubescens*

S.No	Name	Linear structure	Molecular Formula	Molecular weight	% Area
1	Ethyl palmitate / Palmitic acid ethyl ester	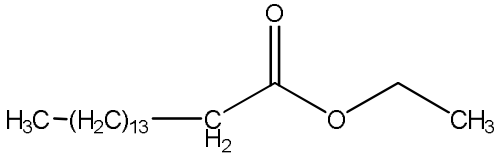	$C_{18}H_{36}O_2$	284.4	15.83
2	Methyl linoleate / Methyl *cis,cis*-9,12-octadecadienoate / Linoleic acid methyl ester	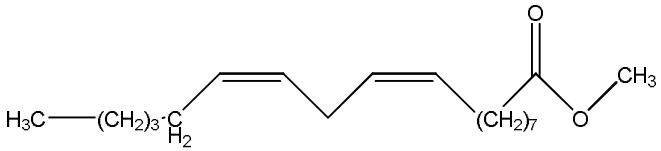	$C_{19}H_{34}O_2$	294.4	51.48
3	Ethyl oleate / Ethyl hexadecanoate / Palmitic acid ethyl ester	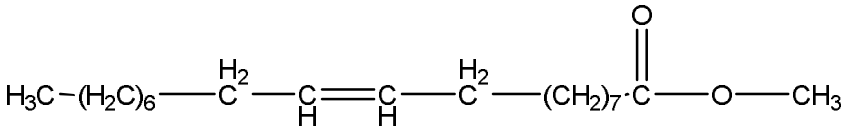	$C_{20}H_{38}O_2$	310.5	27.91
4	Ethyl stearate / Ethyl octadecanoate / Stearic acid ethyl ester	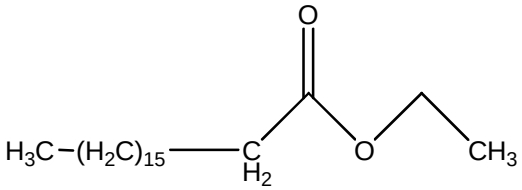	$C_{20}H_{40}O_2$	312.53	04.78

Spectra-2 GCMS of ethanolic flower extract of *Nymphaea pubescens*

Sample Information

Sample Name : PF1111-1057-01
Sample ID : NF SAMPLE
Data File : D:\MSDATA\Year 2011\Dec-11\02-12-2011\PF1111-1057-01.QGD

Chromatogram
Chromatogram

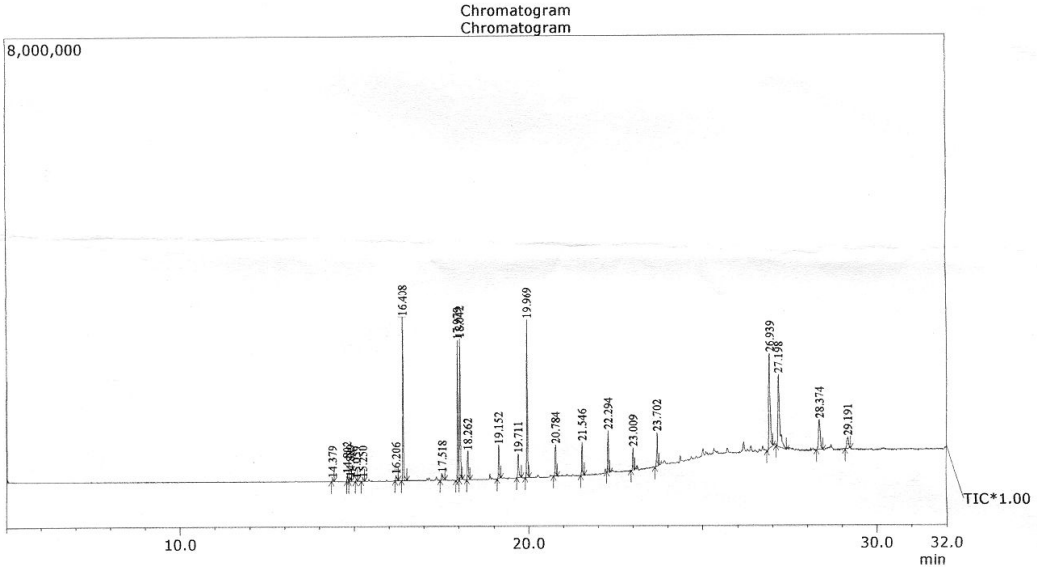

Peak Report TIC

PEAK#	R.TIME	AREA	AREA%	NAME
1	14.379	72796	0.19	Ethyl myristate
2	14.802	222217	0.58	NEOPHYTADIENE
3	14.889	103978	0.27	6,10,14-Trimethyl-2-pentadecanone
4	15.059	63084	0.17	NEOPHYTADIENE
5	15.250	78882	0.21	3,7,11,15-Tetramethyl-2-hexadecen-1-ol
6	16.206	184088	0.48	Ethyl 9-hexadecenoate
7	16.408	4369811	11.50	Ethyl palmitate
8	17.518	246792	0.65	Phytol
9	17.979	4090856	10.76	Methyl linoleate
10	18.042	4032836	10.61	Ethyl linolenate
11	18.262	912903	2.40	Ethyl stearate
12	19.152	1016312	2.67	n-Tetracosane
13	19.711	810410	2.13	(9E)-12-Hydroxy-9-octadecenoic acid
14	19.969	4827394	12.70	ETHYL OCTADECANOATE
15	20.784	899680	2.37	n-Hexatriacontane
16	21.546	1049917	2.76	Ethyl nonadecanoate
17	22.294	1279855	3.37	n-Hexatriacontane
18	23.009	652150	1.72	Ethyl tetracosanoate
19	23.702	1023433	2.69	n-Hexatriacontane
20	26.939	4695354	12.35	gamma.-Sitosterol
21	27.198	4740600	12.47	Pregnan-17,21-diol-9,11-epoxy-3,20-dione, acetate
22	28.374	1868902	4.92	24-Methylenecycloartanol
23	29.191	765974	2.02	(2E)-3,7,11,15-Tetramethyl-2-hexadecen-1-ol
		38008224	100.00	

Table-13 GCMS analysis of ethanolic flower extract of *Nymphaea pubescens*

S. No.	Name	Chemical structure / Linear structure	Molecular Formula	Molecular weight	% Area
1.	Ethyl Myristate / Ethyl tetradecanoate / Myristic acid ethyl ester	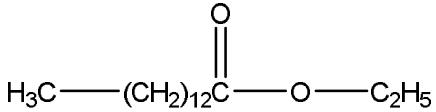	$C_{16}H_{32}O_2$	256.42	0.19
2.	Neophytadiene	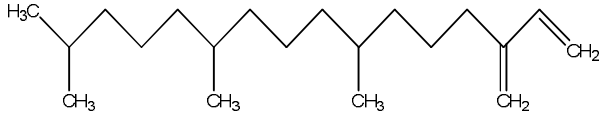	$C_{20}H_{38}$	278.5	0.58
3.	6,10,14-trimethyl-2-pentadecanone	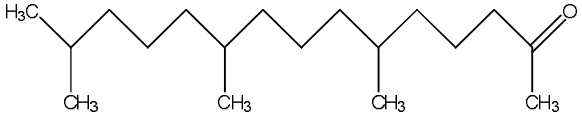	$C_{18}H_{36}O$	268.47	0.27
4.	3,7,11,15-Tetramethyl-2-hexadecen-1-ol / Phytol	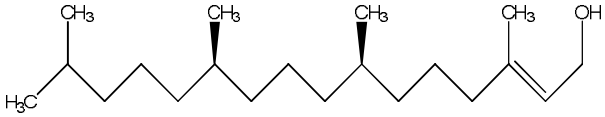	$C_{20}H_{40}O$	296.5	0.21
5.	Ethyl 9-hexadecenoate	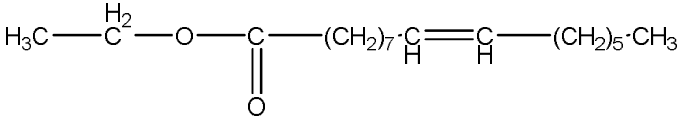	$C_{18}H_{34}O_2$	282.16	0.48
6.	Ethyl palmitate	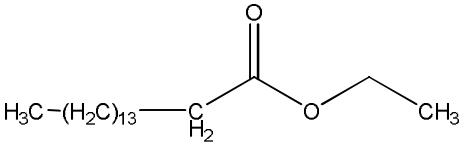	$C_{18}H_{36}O_2$	284.4	11.50

Cont.…

S. No.	Name	Chemical structure / Linear structure	Molecular Formula	Molecular weight	% Area
8.	Ethyl linolenate	$H_3C—(CH_2)_3-(CH_2CH=CH)_2(CH_2)COOC_2H_5$	$C_{21}H_{34}O_2$	308.5	10.61
9.	Ethyl stearate / Ethyl octadecanoate	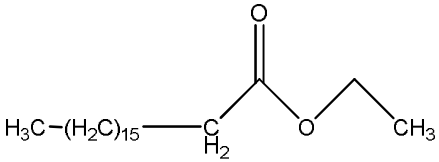	$C_{20}H_{40}O_2$	312.53	12.70
10.	n-Tetracosane	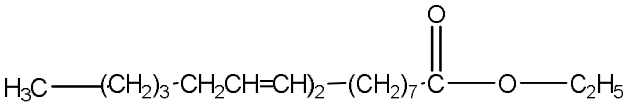	$C_{24}H_{50}$	338.65	2.67
11.	12-Hydroxy-9-octadecenoic acid	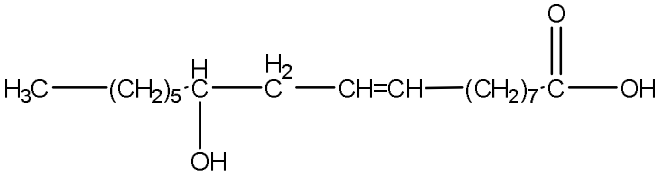	$C_{18}H_{34}O_3$	298.46	2.13
12.	n-Hexa triacontane	$H_3C—(CH_2)_{34}CH_3$	$C_{36}H_{74}$	506.97	2.37
13.	Ethyl Nonadecanoate	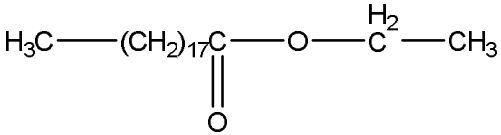	$C_{21}H_{42}O_2$	326.5	2.76
14.	Ethyl tetracosanoate	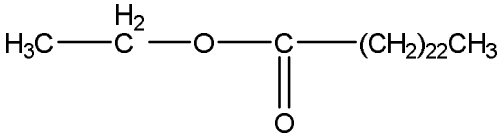	$C_{26}H_{52}O_2$	396.6	1.72

Cont.…

S. No.	Name	Chemical structure / Linear structure	Molecular Formula	Molecular weight	% Area
15.	Gamma-sitosterol	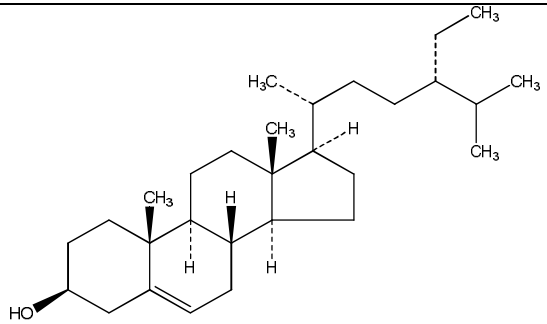	$C_{29}H_{50}O$	414.7	12.35
16.	24-Methylenecycloartanol	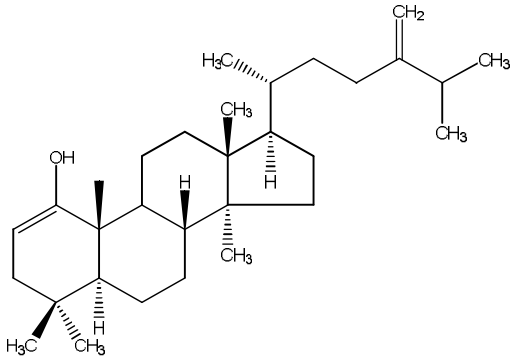	C31H52O	440.7	4.92

Spectra-3 IR Spectrum of compound I

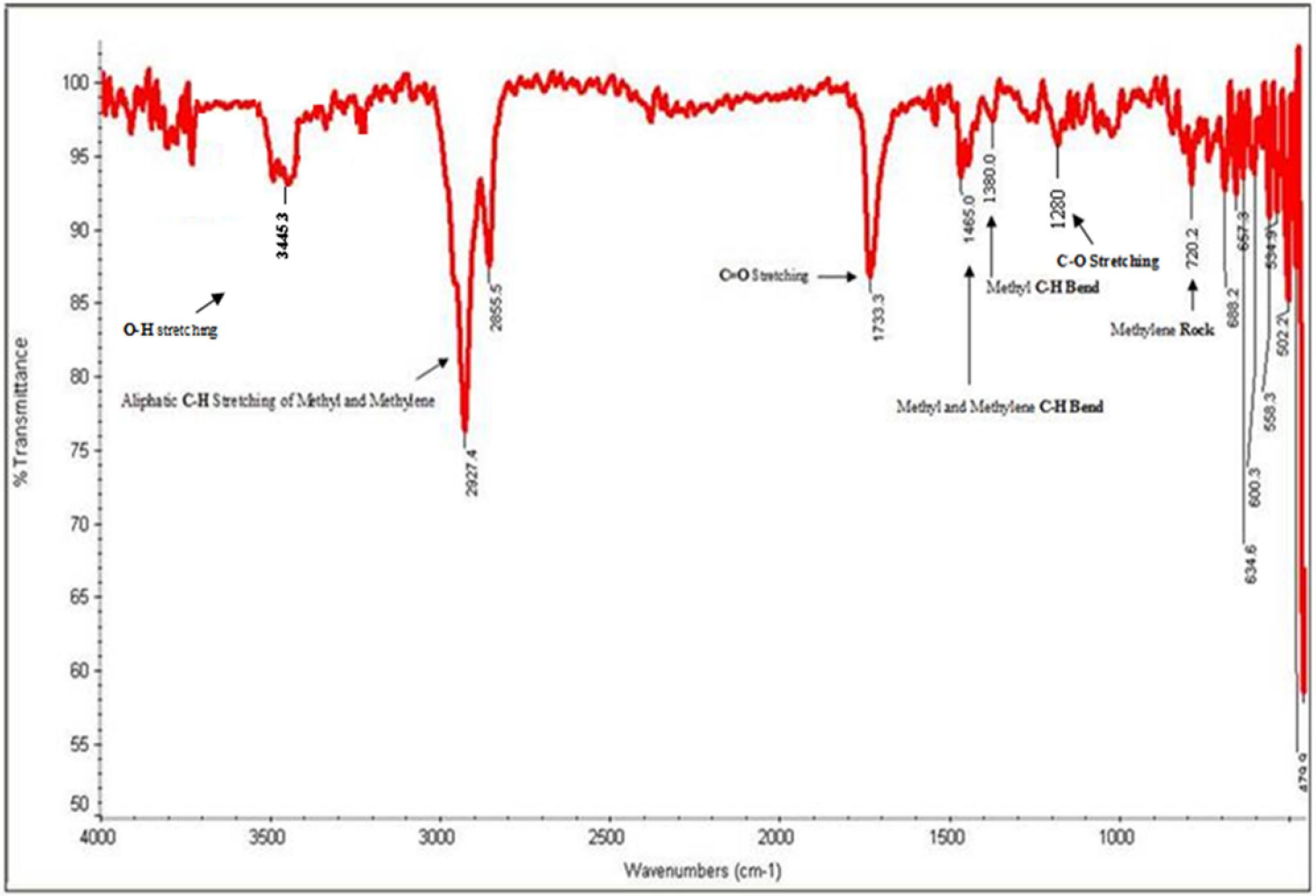

Spectra-4 ^{1}H NMR spectrum of compound I

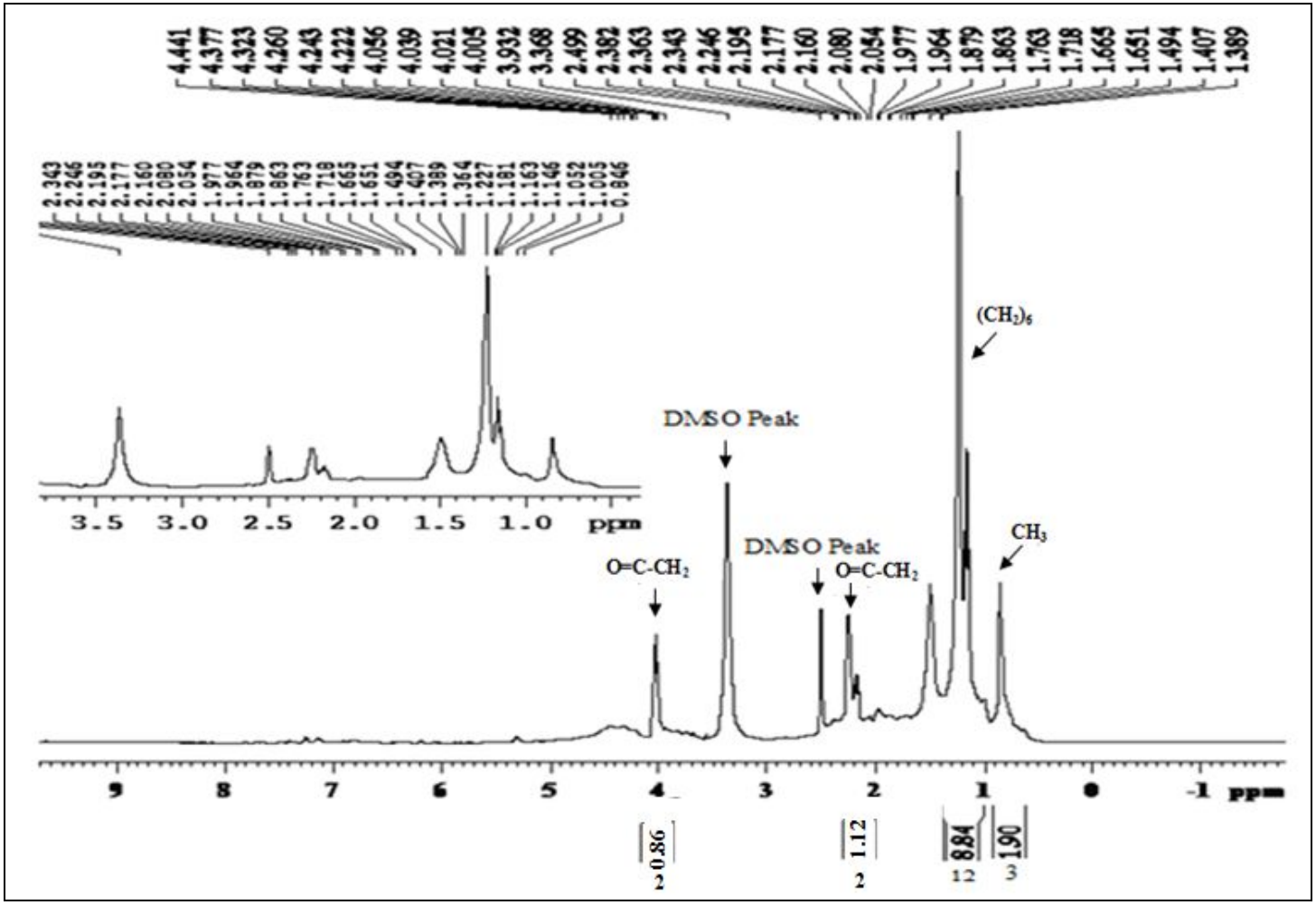

Spectra-5 ^{13}C NMR spectrum of compound I

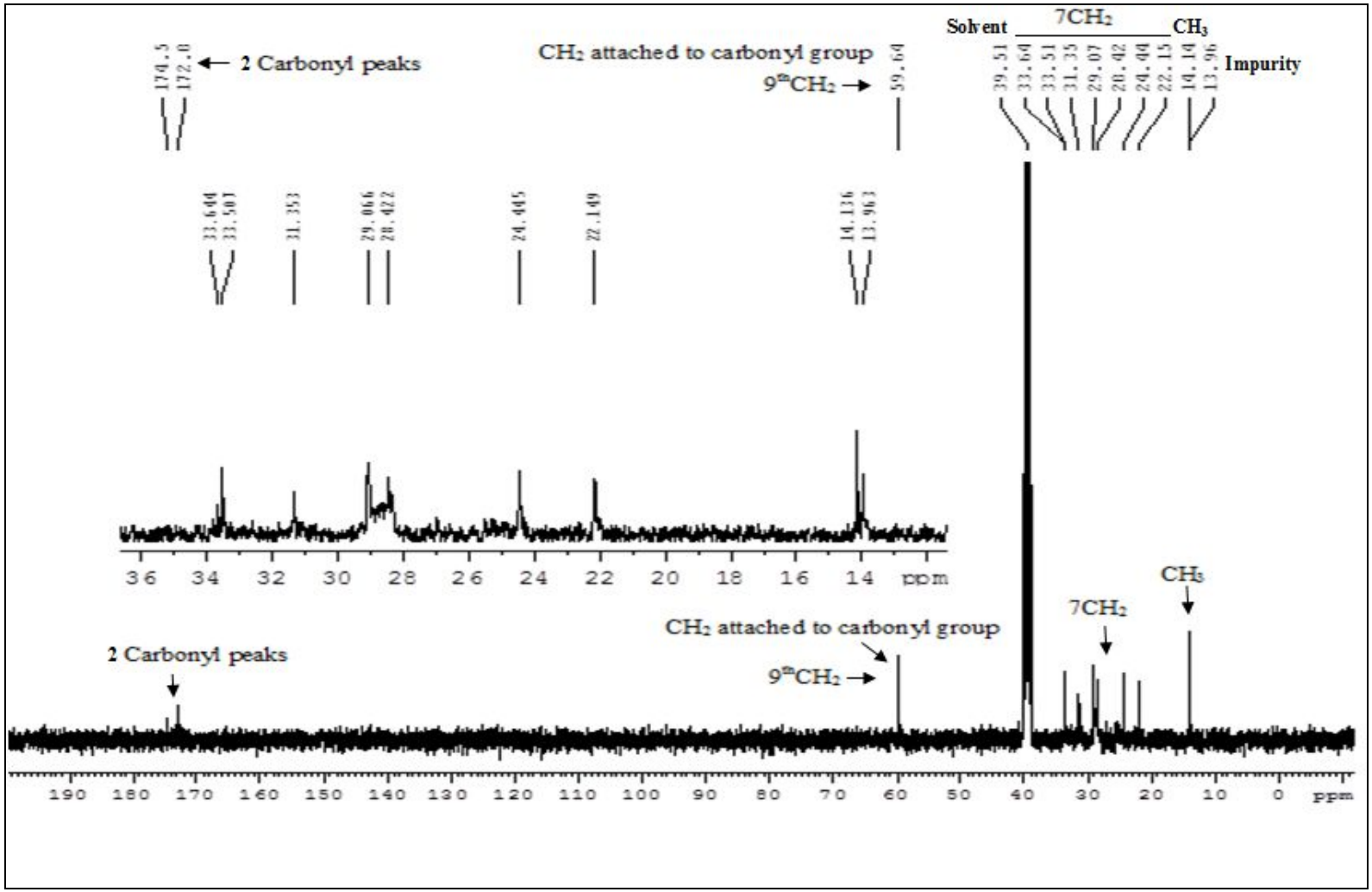

Spectra-6 ^{13}C DEPT-135 NMR Spectrum of compound I

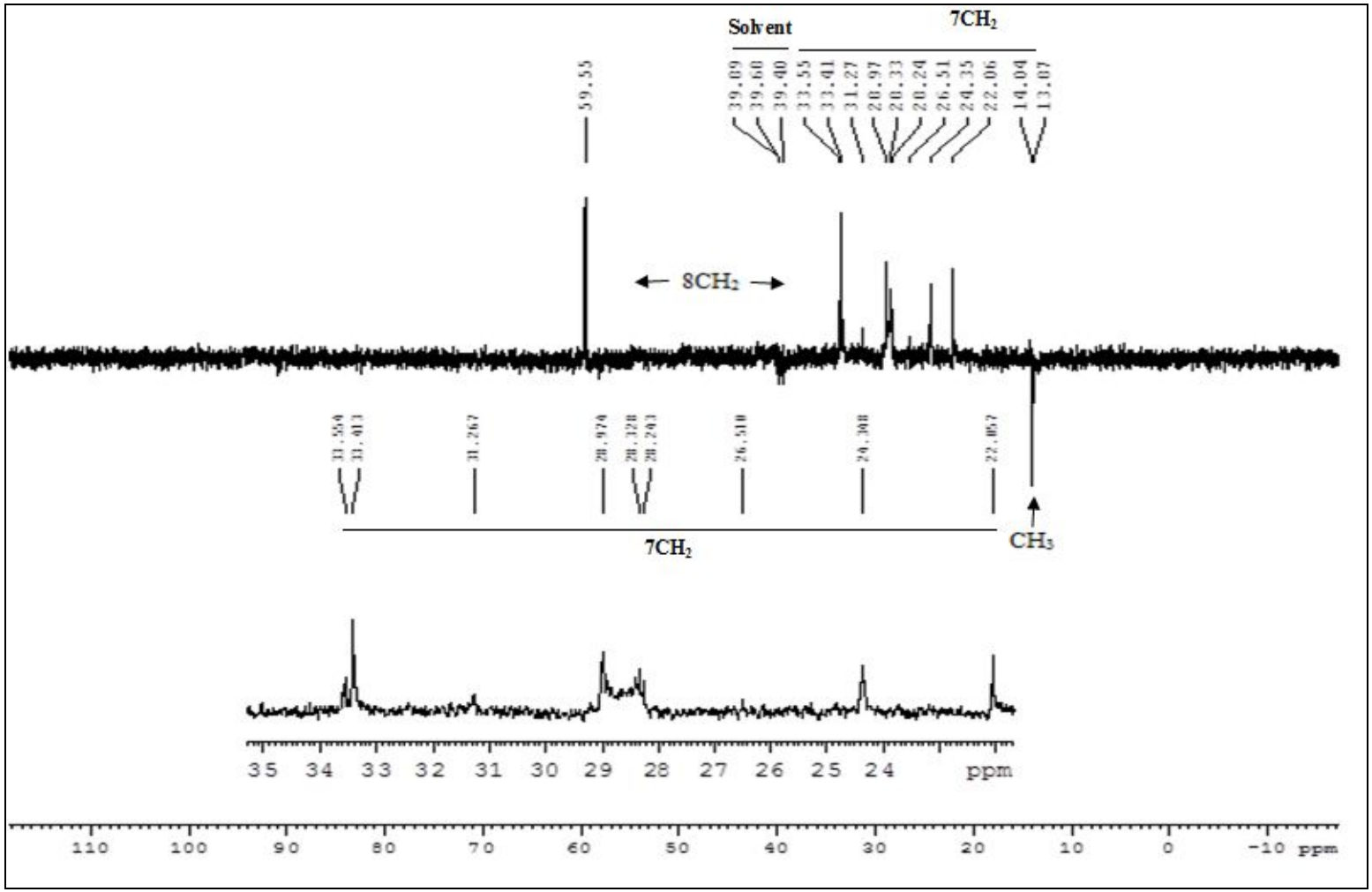

Spectra-7 HMBC Spectrum of compound I

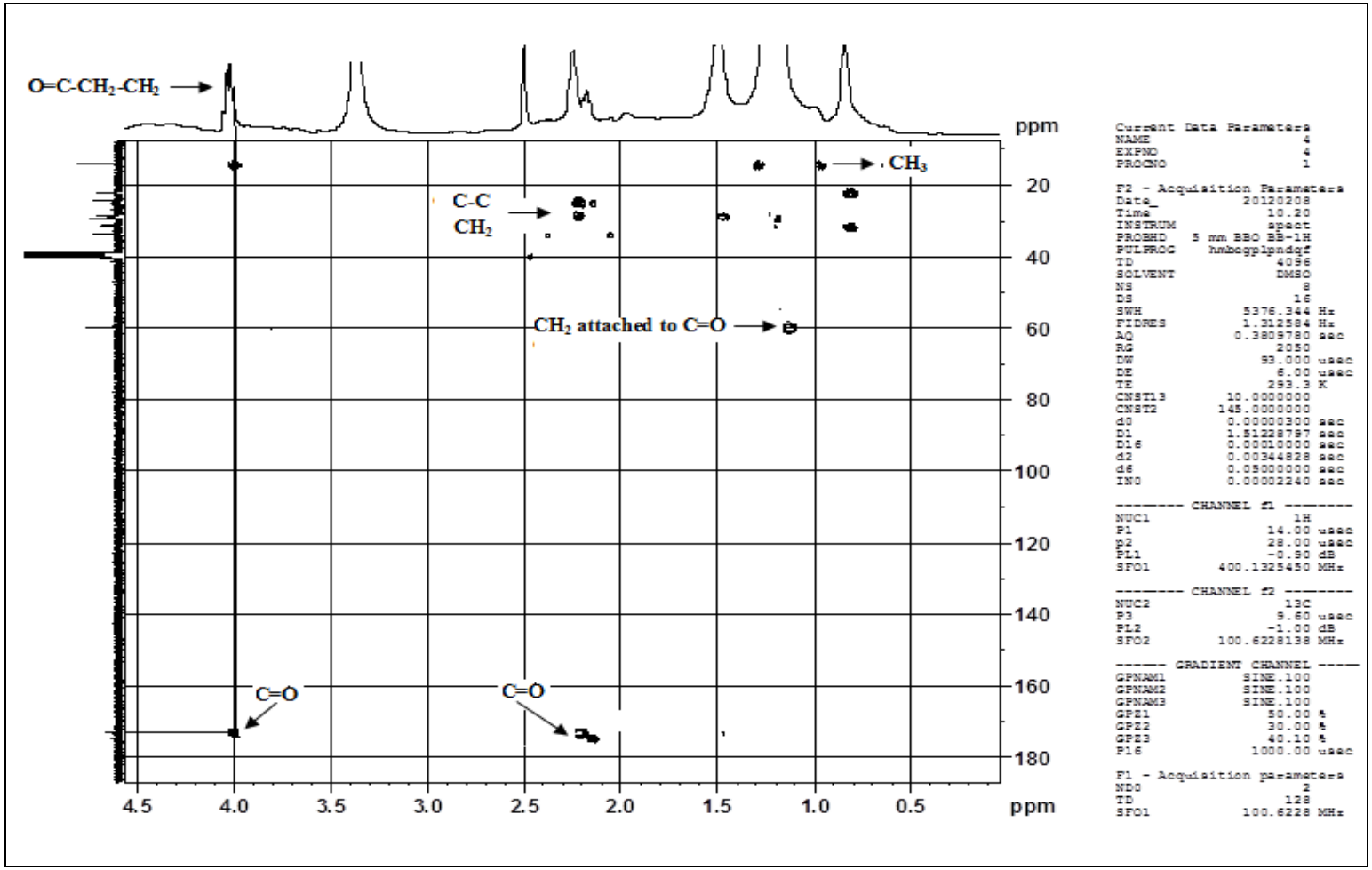

Spectra-8 Mass spectrum of compound I

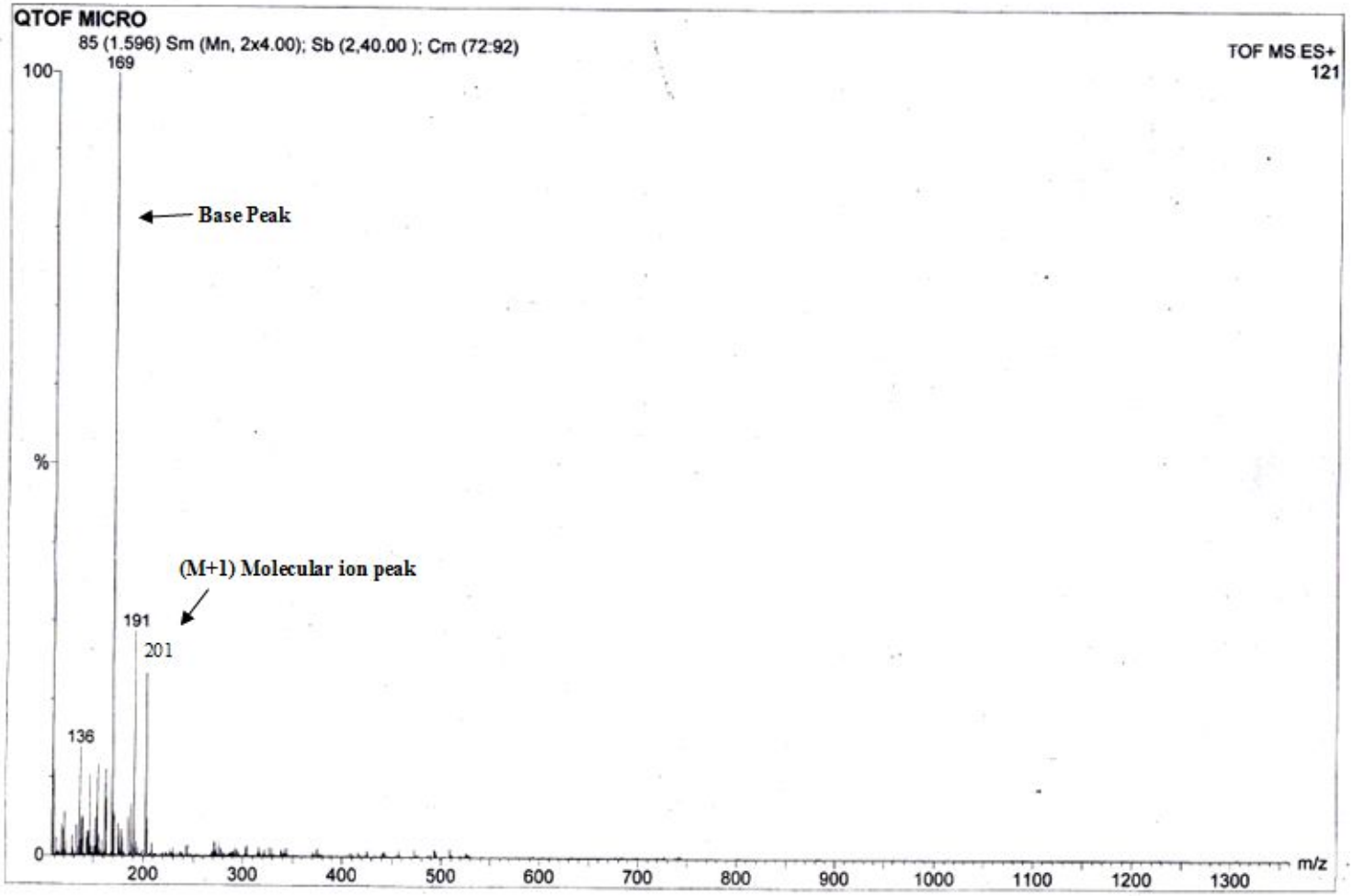

ANALYTICAL SPECTRUM OF COMPOUND I

Table-14 IR Spectroscopic interpretation of compound I

Frequency (cm^{-1})	Functional group
3445.3	O-H Stretching
2925.4 & 2855.5	Aliphatic C-H stretching of Methyl and Methylene
1733.3	C=O Stretching
1465.5	Methyl and Methylene C-H bend
1380.0	Methyl C-H bend
1280.0	C-O stretching
720.2	Methylene rock

Table-15 ^{1}H NMR Spectroscopic interpretation of compound I

δ (ppm)	No. of peaks	J value / coupling constant (Hz)	No. of protons
4.056-4.005	Multiplet	2.0	2
1.227-1.145	Doublet	20	2
1.227-1.145	Multiplet	44.8	12
0.846	Singlet	-	3

Table-16 ^{13}C NMR Spectroscopic interpretation of compound I

δ (ppm)	Carbon atoms
14.14	$-CH_3$
22.15	$-CH_2$
24.44	$-CH_2$
28.42	$-CH_2$
29.07	$-CH_2$
31.35	$-CH_2$
33.51 & 33.64	$-CH_2$
59.64	CH_2 attached to C=O
172.8	carbonyl peak

Table-17 ^{13}C DEPT-135 NMR Spectroscopic interpretation of compound I

δ (ppm)	No. of $–CH_2$	No. of $–CH_3$
14.04	-	$–CH_3$
22.06	$-CH_2$	-
24.35	$-CH_2$	-
26.51	$-CH_2$	-
28.24 & 28.33	$-CH_2$	-
28.97	$-CH_2$	-
31.27	$-CH_2$	-
33.41 & 33.55	$-CH_2$	-
59.55	$-CH_2$ attached to C=O	-

Table-18 HMBC NMR Spectroscopic interpretation of compound I

^{1}H- δ (ppm)	^{13}C- δ (ppm)	Carbon & Hydrogen
1.0	10	$-CH_3$
0.8	20 & 30	$-CH_2$
1.2	30	$-CH_2$
1.5	30	$-CH_2$
2.2	25	$-CH_2$
2.3	25 & 30	$-CH_2$
1.0	60	$-CH_2$ attached to C=O
2.0	175	C=O
4.0	170	C=O

MASS SPECTRUM

Molecular Ion Peak : 201 (M+H)

Base Peak : 169

Spectra-9 IR spectrum of compound II

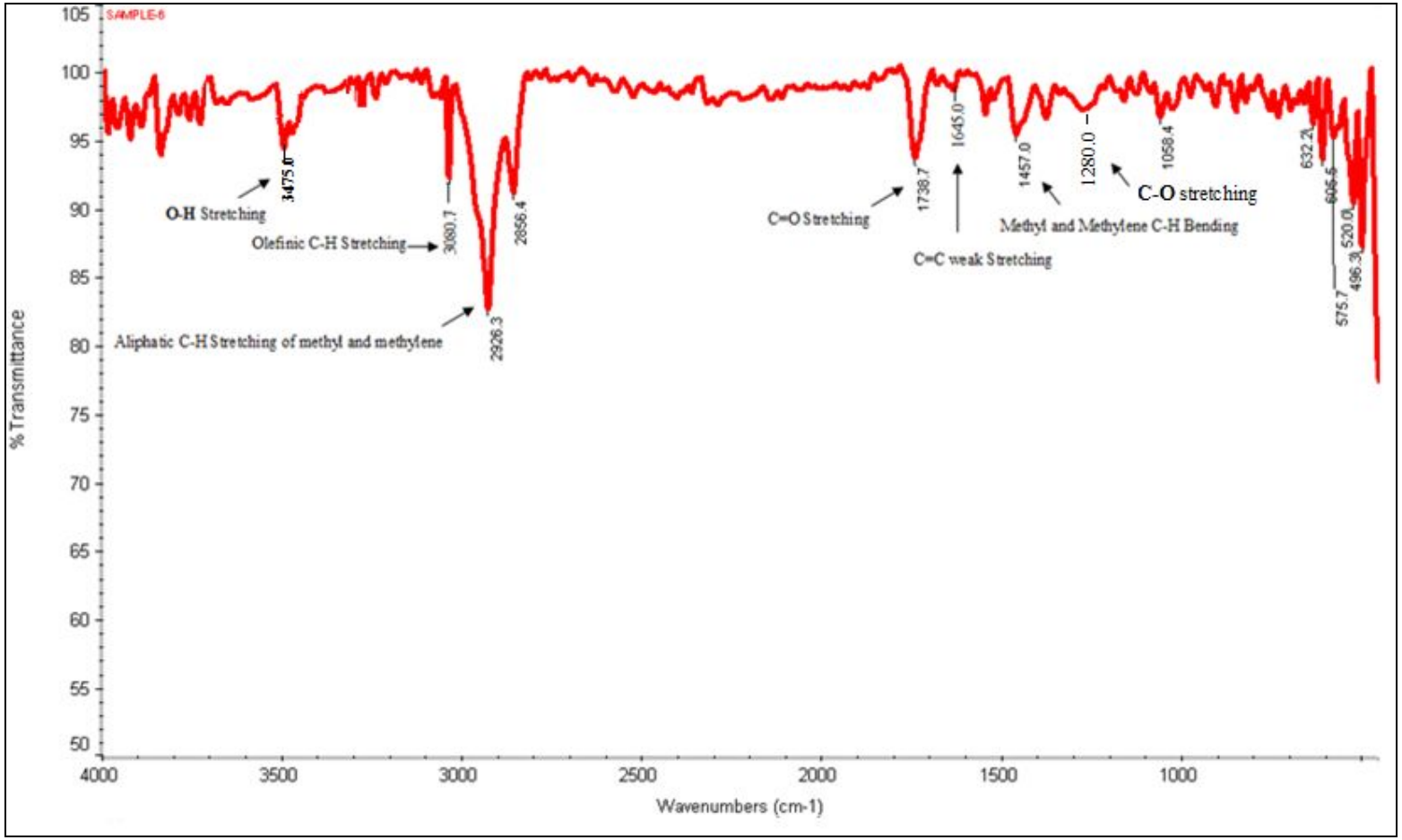

Spectra-10 ^{1}H NMR spectrum of compound II

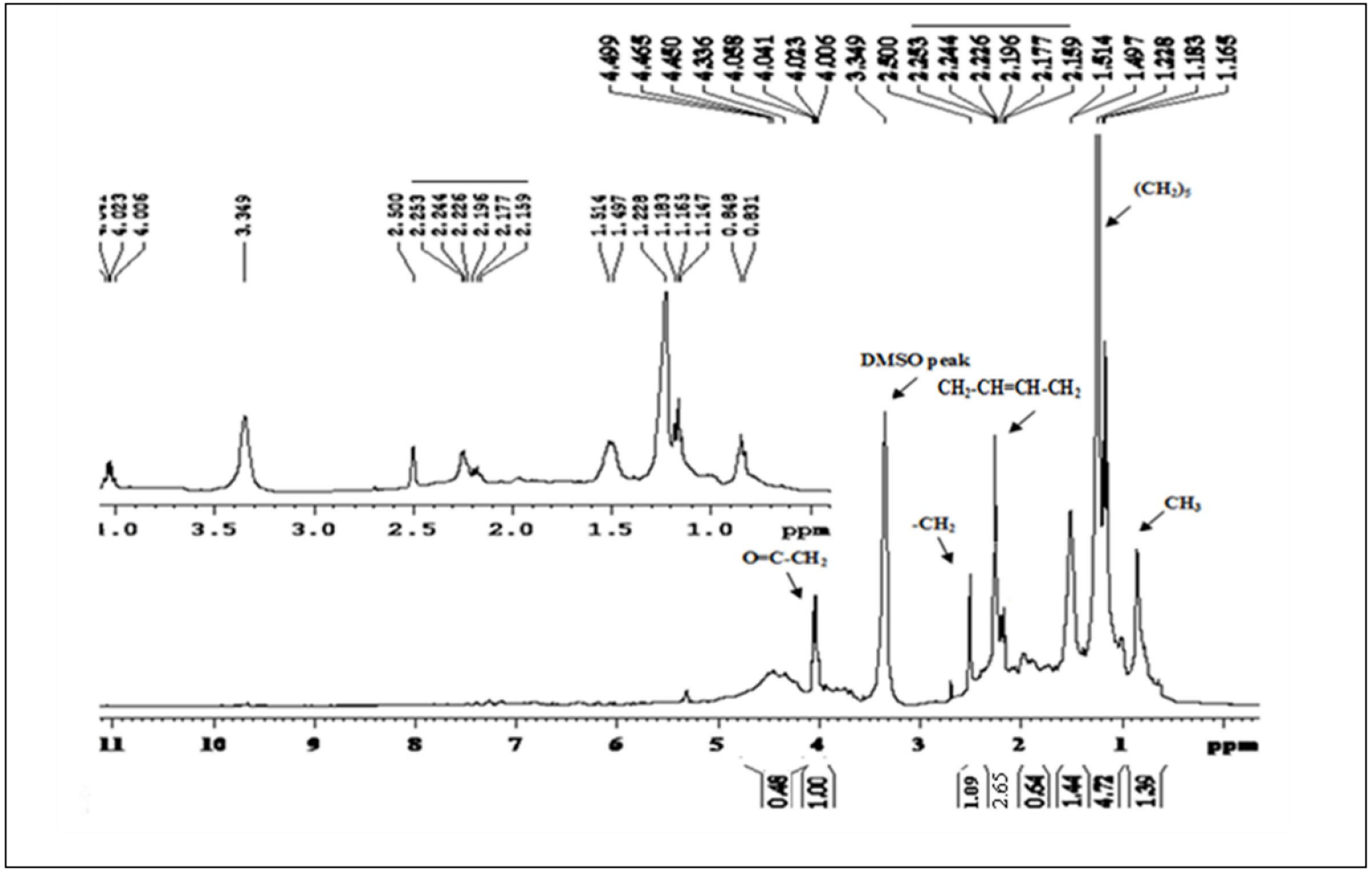

Spectra-11 ^{13}C NMR spectrum of compound II

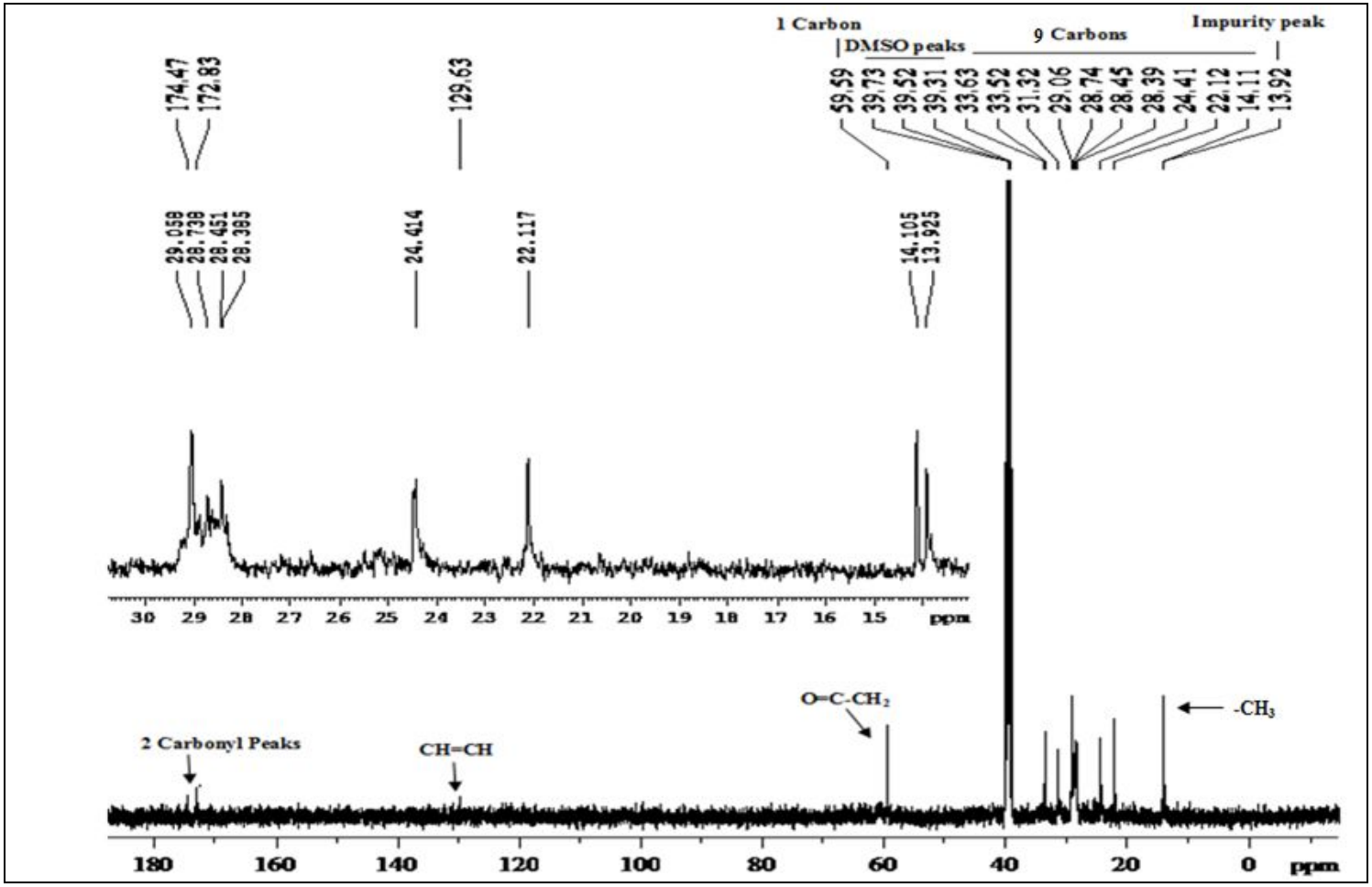

Spectra-12 ^{13}C DEPT-135 NMR spectrum of compound II

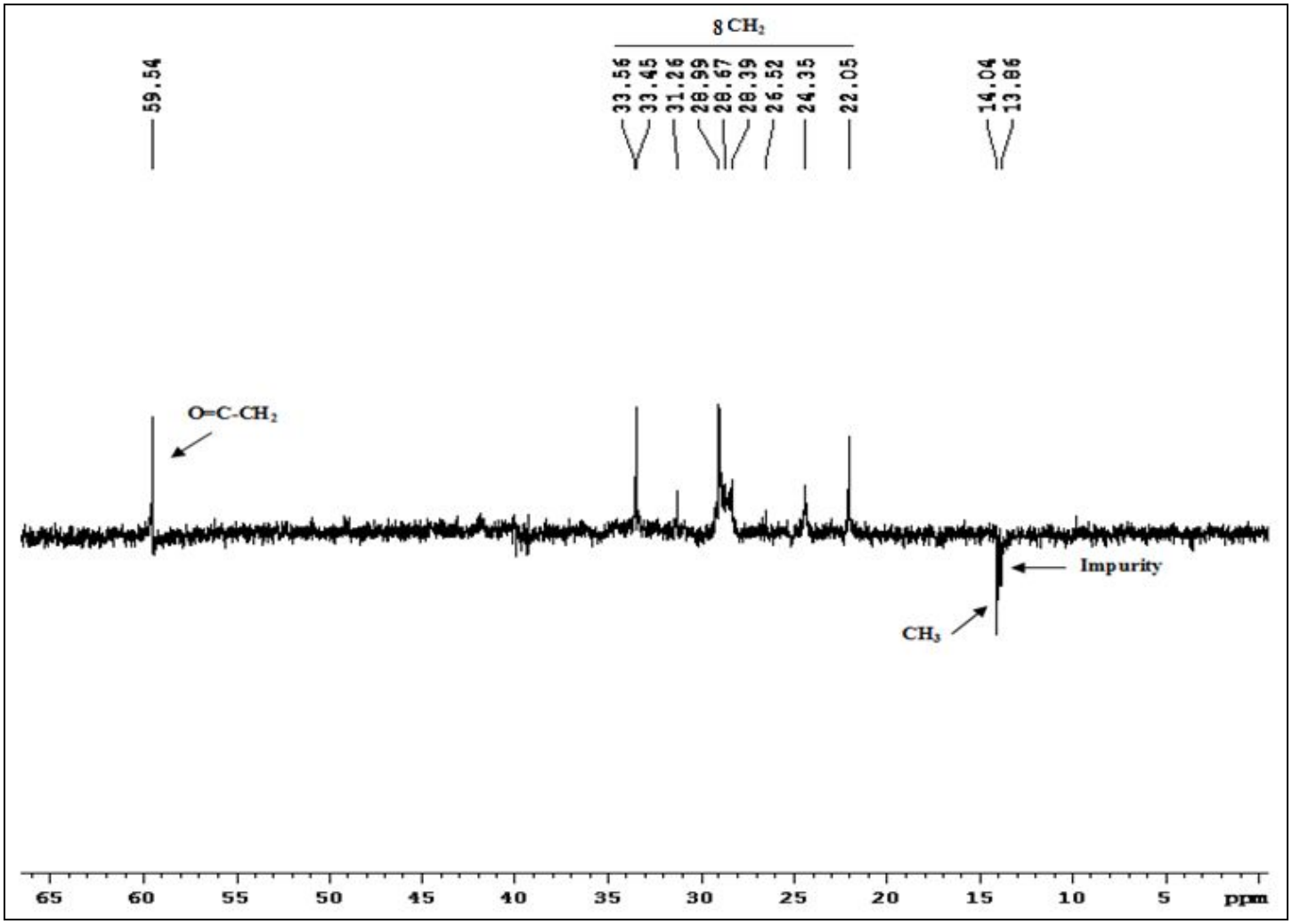

Spectra-13 HMBC spectrum of compound II

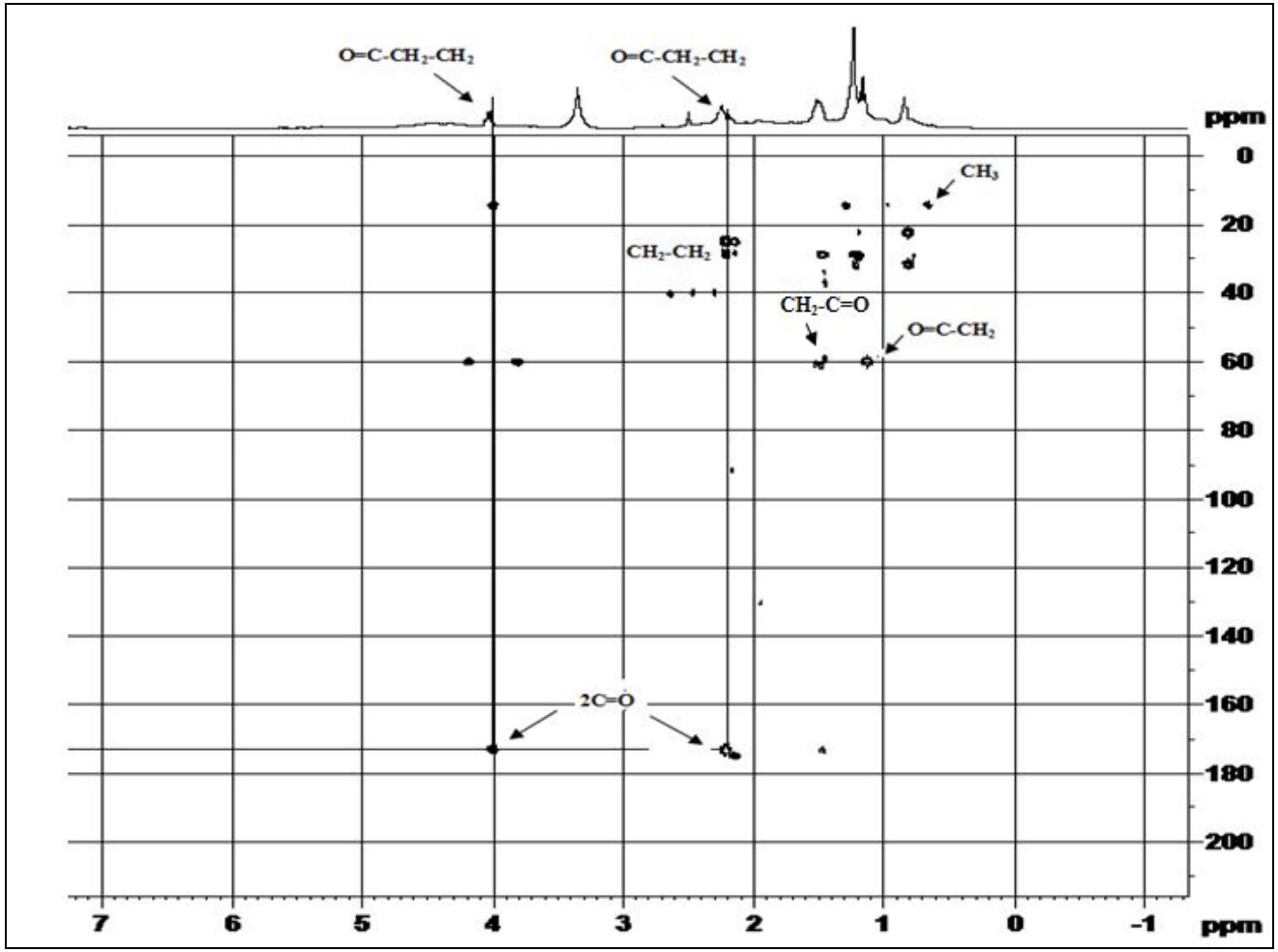

Spectra-14 Mass Spectrum of compound II

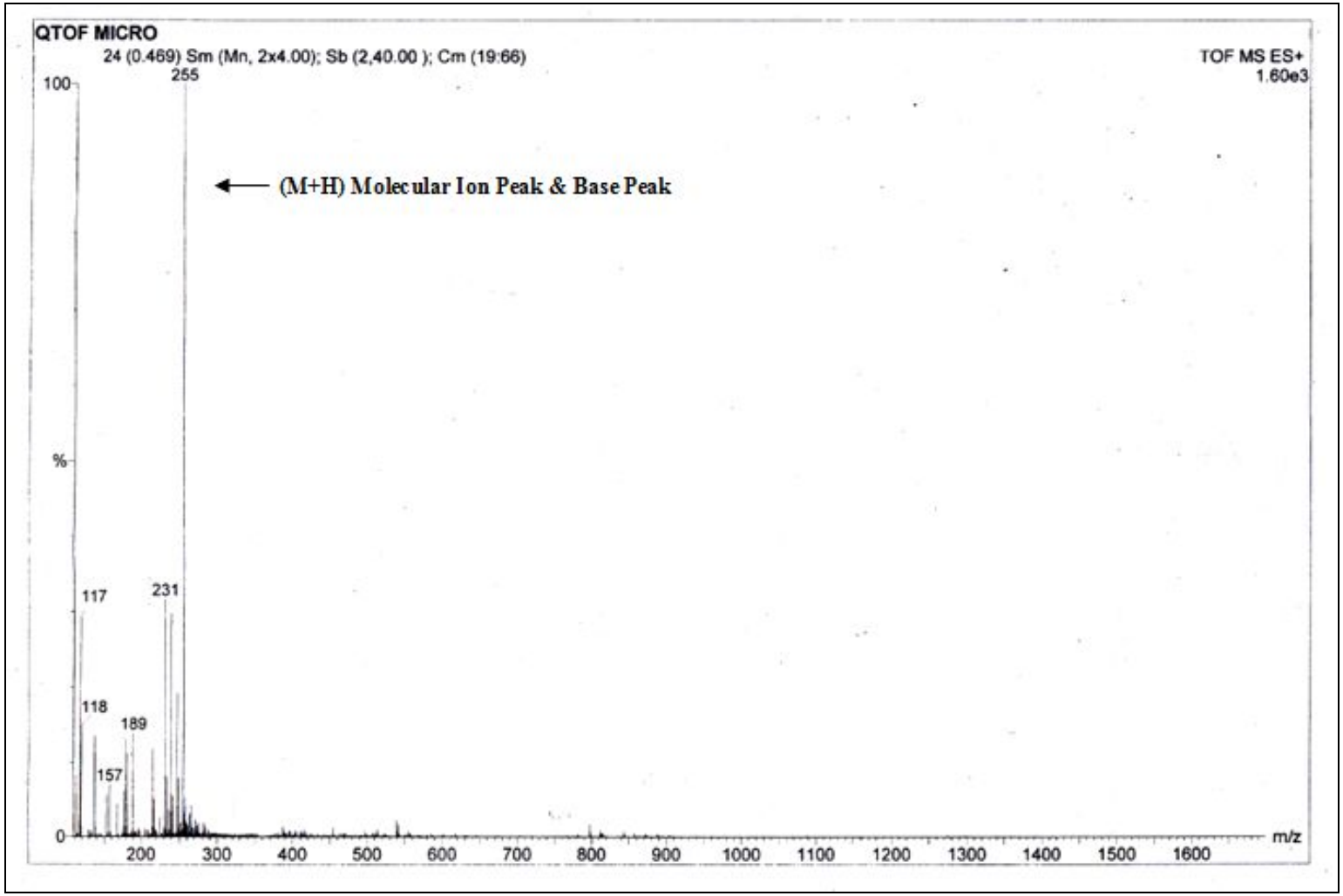

ANALYTICAL SPECTRUM OF COMPOUND II

Table-19 IR Spectroscopic interpretation of compound II

Frequency (cm^{-1})	Functional group
3475.0	O-H Stretching
3080.7	Olefinic C-H Stretching
2926.3 & 2856.4	Aliphatic C-H stretching of Methyl and Methylene
1738.7	C=O Stretching
1645.0	C=C weak stretching
1457.0	Methyl and Methylene C-H bend
1280.0	**C-O** stretching
720.2	Methylene rock

Table-20 ^{1}H NMR Spectroscopic interpretation of compound II

δ (ppm)	No. of peaks	J value / coupling constant (Hz)	No. of protons
0.848	Singlet	-	3
1.228-1.14	Multiplet	16	10
2.25-2.15	Multiplet	40	6
2.50	Singlet	-	2
4.05-4.00	Multiplet	20	4

Table-21 ^{13}C NMR Spectroscopic interpretation of compound II

δ (ppm)	Carbon atoms
14.11	$-CH_3$
22.12	$-CH_2$
24.41	$-CH_2$
28.39	$-CH_2$
28.45	$-CH_2$
28.74	$-CH_2$
29.06	$-CH_2$
31.32	$-CH_2$
33.52 & 33.63	$-CH_2$
59.59	$-CH_2$ attached to C=O
129.63	CH=CH
172.83	C=O
174.47	C=O

Table-22 ^{13}C DEPT-135 NMR Spectroscopic interpretation of compound II

δ (ppm)	No. of $-CH_2$ & $-CH_3$
14.04	$-CH_3$
22.05	$-CH_2$
24.35	$-CH_2$
26.52	$-CH_2$
28.39	$-CH_2$
28.67	$-CH_2$
28.99	$-CH_2$
31.26	$-CH_2$
33.45 & 33.56	$-CH_2$
59.54	$-CH_2$ attached to C=O

Table-23 HMBC NMR Spectroscopic interpretation of compound II

^{1}H- δ (ppm)	^{13}C- δ (ppm)	Carbon & Hydrogen
0.8	15	$-CH_3$
20-40	1.8-2.5	$-(CH_2)_8$
1.1 & 1.6	60	$-CH_2$ attached to C=O
2.2 & 4.0	176	2 C=O

MASS SPECTRUM

Molecular Ion & Base Peak : 255 (M+H)

Spectra-15 UV Spectrum of compound III

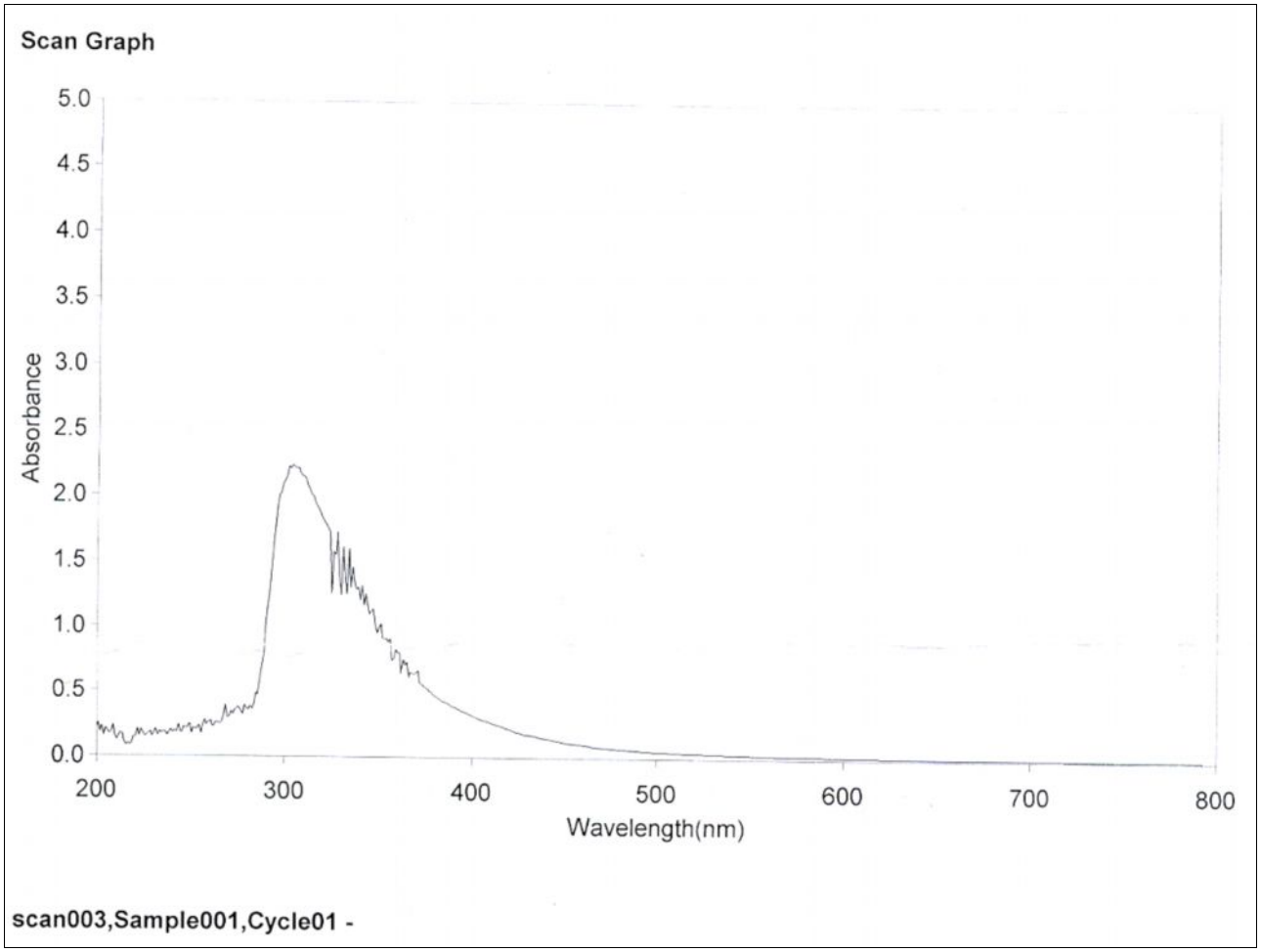

Spectrum-16 IR spectrum of compound III

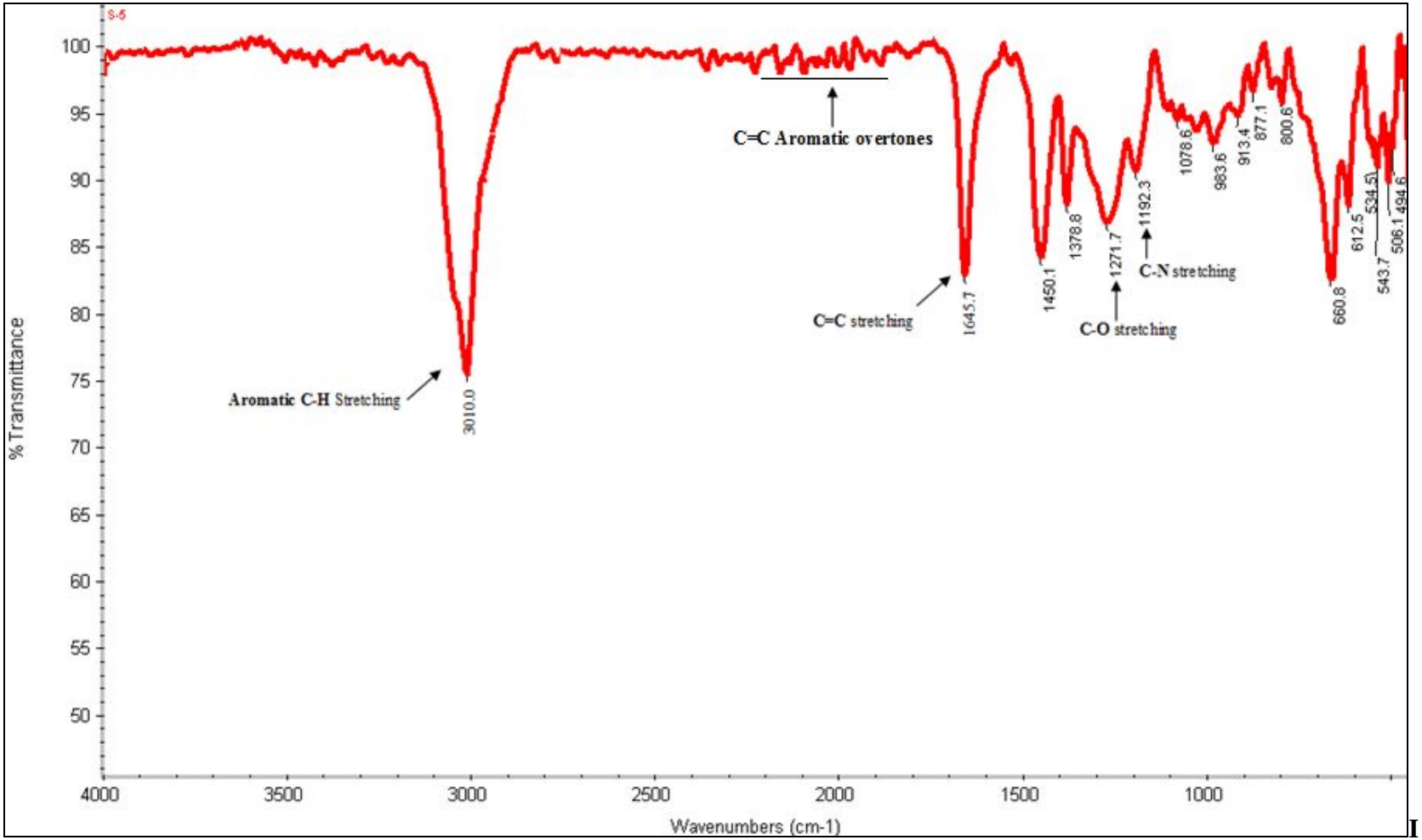

I

Spectra-17 ^{1}H NMR spectrum of compound III

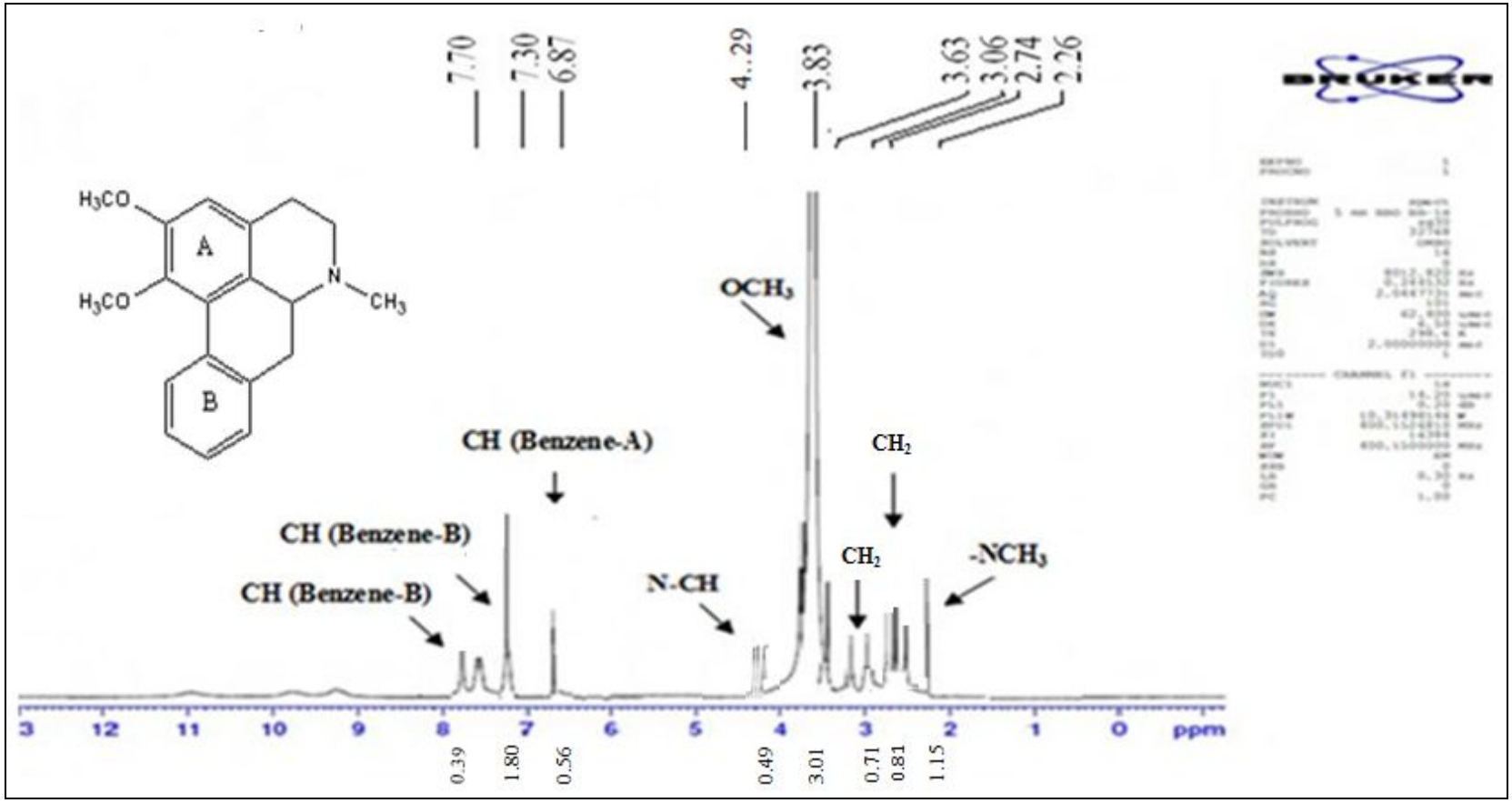

Spectra-18 Mass spectroscopy of compound III

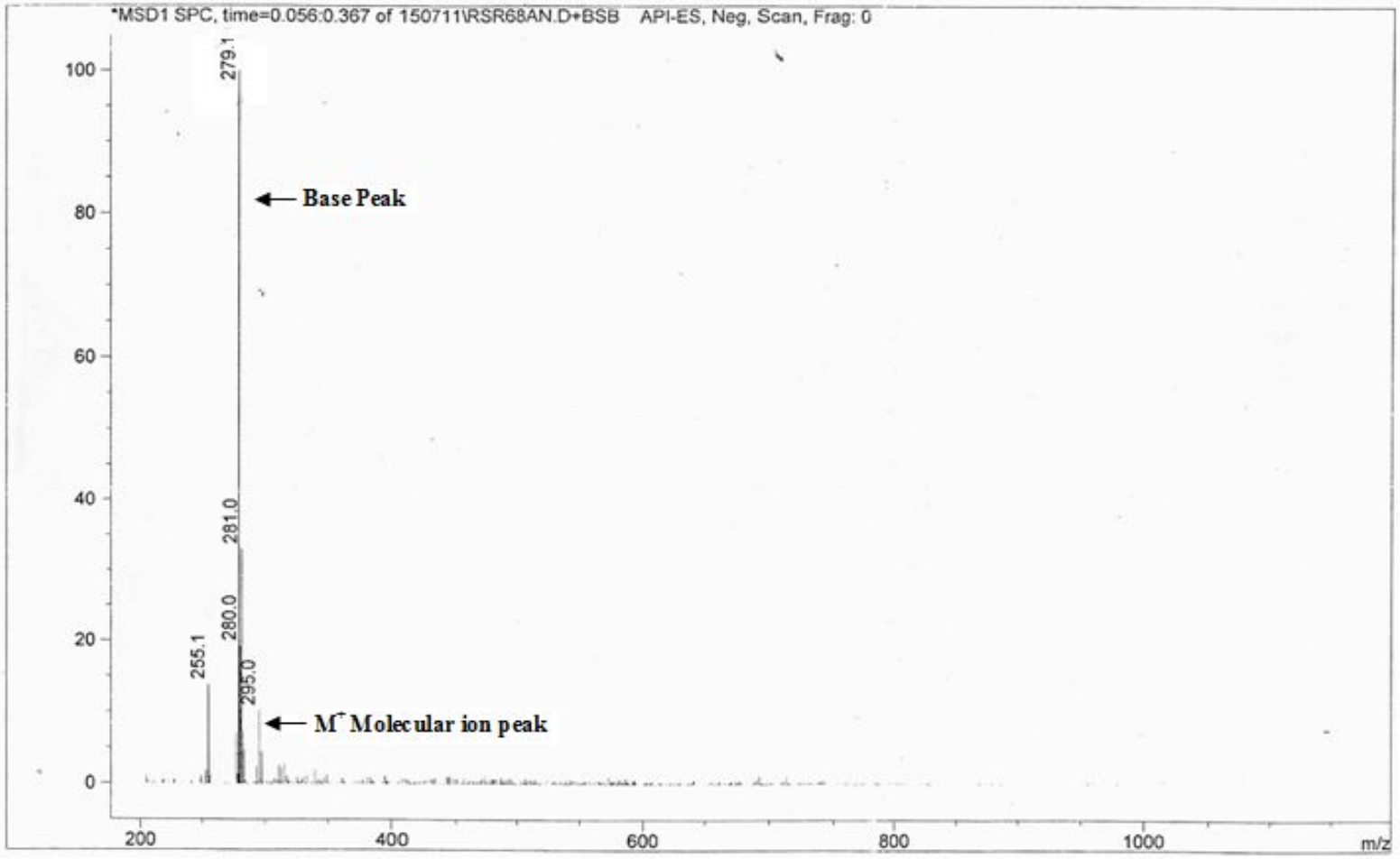

ANALYTICAL SPECTRUM OF COMPOUND III

UV Spectrum : λ_{max} – 310nm

Table-24 IR Spectroscopic interpretation of compound III

Frequency (cm^{-1})	Functional group
3010.0	Aromatic C-H Stretching
1900-2200	C=C Aromatic overtone
1645.7	C=C Stretching
1271.7	C-O Stretching
1192.3	C-N Stretching

Table-25 ^{1}H NMR Spectroscopic interpretation of compound III

	δ (ppm)	No. of peaks	J value / coupling constant (Hz)	No. of protons
$-CH_3$	2.26	Singlet	-	3
$-CH_2$ heterocyclic ring	2.74-2.72	Triplet	8	2
$-CH_2$	3.06-3.26	Doublet	80	2
$-OCH_3$	3.83	Singlet	-	6
-CH	4.31-4.29	Triplet	8	1
-CH Aromatic ring A	6.87	Singlet	-	1
-CH Aromatic ring B	7.30	Singlet	-	3
-CH Aromatic ring B	7.74	Singlet	-	1

MASS SPECTRUM

Molecular Ion Peak : 295 (M^+)

Base Peak : 279.1

Table-26 Colour, Consistency and % yield of fractions from ethanolic flower extract of *Nymphaea pubescens*

S. No.	Fraction	Colour	Consistency	Yield (% w/w)
1.	Hexane	Yellow	Waxy	3.10
2.	Chloroform	Yellowish green	Greasy	22.16
3.	Ethyl acetate	Pinkish brown	Glossy	59.00
4.	Ethanol	Yellowish green	Greasy	13.00
5.	Water	Brownish green	Greasy	1.33

Table-27 Preliminary phytochemical analysis of fractions from ethanolic flower extract of *Nymphaea pubescens*

Chemical test for	Hexane	Chloroform	Ethyl acetate	Ethanol	Water
Glycosides	-	-	+	+	+
Alkaloids	+	-	-	-	-
Flavonoids	-	+	++	-	-
Tannins	-	-	-	+	+
Steroids	+	-	-	-	-
Triterpenes	+	-	-	-	-
Phenols	-	-	+	+	+
Sugars	-	-	-	+	+
Proteins	-	-	-	+	+

+ → Slightly stained ++ →Highly stained

Table-28 TLC Profile for the ethyl acetate fraction from the ethanolic flower extract of *Nymphaea pubescens*

Test sample	Solvent system	Peaks	R_f value (Iodine vapours)
Ethyl acetate fraction	n-Hexane : Ethyl acetate : Ferric chloride (4 : 5.5 : 0.5)	1	0.14
		2	0.30
		3	0.54
		4	0.71

Table-29 HPTLC of ethyl acetate fraction from the ethanolic flower extract of *Nymphaea pubescens*

Sample	:	Ethyl acetate fraction
Sample prepared in	:	Methanol
Sample concentration	:	Extract (50mg/ml)
Applied volume	:	4 µl
Stationary Phase	:	Silica Gel GF_{254}
Mobile phase	:	n-Hexane : Ethyl acetate : Formic acid (4:5.5:0.5)
Scanning wavelength	:	366nm
Development Mode	:	Ascending mode

Peak	Start Rf	Start Height	Max Rf	Max Height	Height %	End Rf	End Height	Area	Area %
1	0.1	0.4	0.14	336.9	32.38	0.17	15.8	8187.4	25.32
2	0.17	16.1	0.19	23.6	2.27	0.21	0.1	375.2	1.16
3	0.25	0.2	0.3	83.8	8.05	0.37	0.9	3292.6	10.18
4	0.4	2.8	0.48	237.6	22.83	0.52	25.4	8879.6	27.46
5	0.52	25.6	0.54	32.8	3.15	0.57	11.3	1000.4	3.09
6	0.59	11.8	0.65	224.9	21.62	0.68	58.7	7341.6	22.7
7	0.69	59.5	0.71	101	9.71	0.76	1.9	3264.8	10.09

Fig.22 Chromatogram of the ethyl acetate fraction from the ethanolic flower extract of *Nymphaea pubescens*

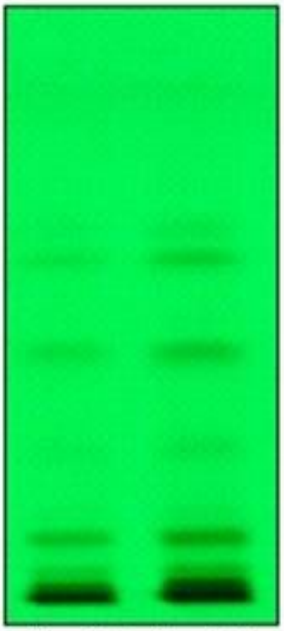

Track 1 Track 2

254 nm

Track 1 Track 2

366 nm

Fig.23 Desitogram of the ethyl acetate fraction from the ethanolic flower extract of *Nymphaea pubescens*

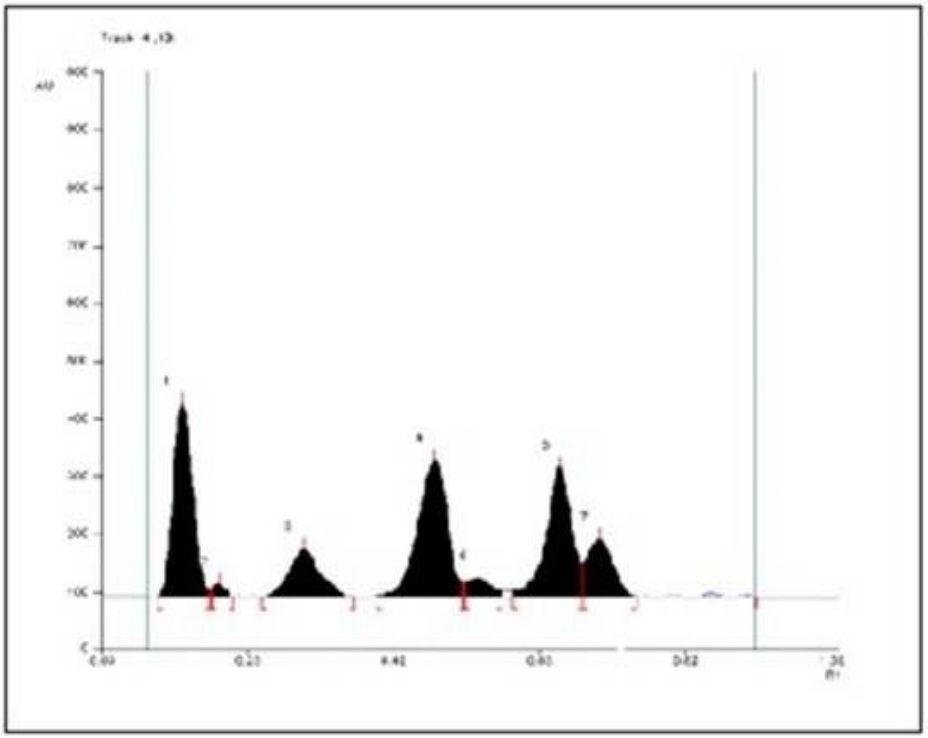

Table-30 Isolation of Compound-IV from the ethyl acetate fraction from ethanolic flower extract of *Nymphaea pubescens*

S.No.	Solvent	Ratio (%)	Nature of residue	Mg/HCl
1.	Benzene	100	Yellow waxy	-
2.	Benzene : Chloroform	75 : 25	Yellow waxy	-
3.	Benzene : Chloroform	50 : 50	Yellow waxy	-
4.	Benzene : Chloroform	25 : 75	Yellow waxy	-
5.	Chloroform	100	Yellowish green waxy	-
6.	Chloroform : Ethyl acetate	75 : 25	Yellowish green waxy	-
7.	Chloroform : Ethyl acetate	50 : 50	Yellow waxy	+
8.	Chloroform : Ethyl acetate	25 : 75	Yellow waxy	+
9.	Ethyl acetate	100	Yellowish purple waxy	+
10.	Ethyl acetate : Methanol	75 : 25	Yellow crystals	++
11.	Ethyl acetate : Methanol	50 : 50	Yellowish orange waxy	-
12.	Ethyl acetate : Methanol	25 : 75	Yellowish green	-
13.	Methanol	100	Greenish brown	-

Spectra-19 UV spectrum of compound IV

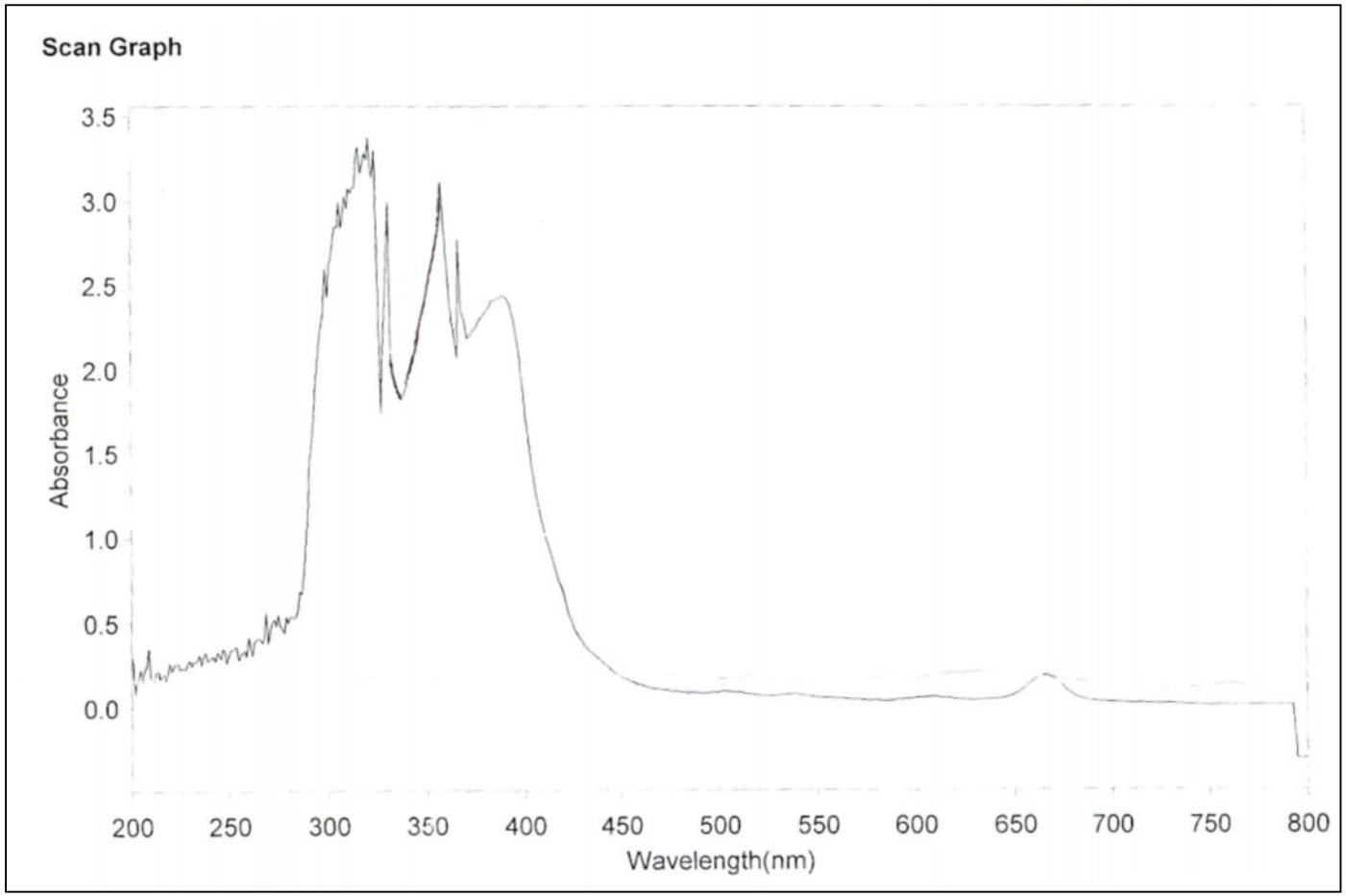

c

Spectra-20 IR spectrum of compound IV

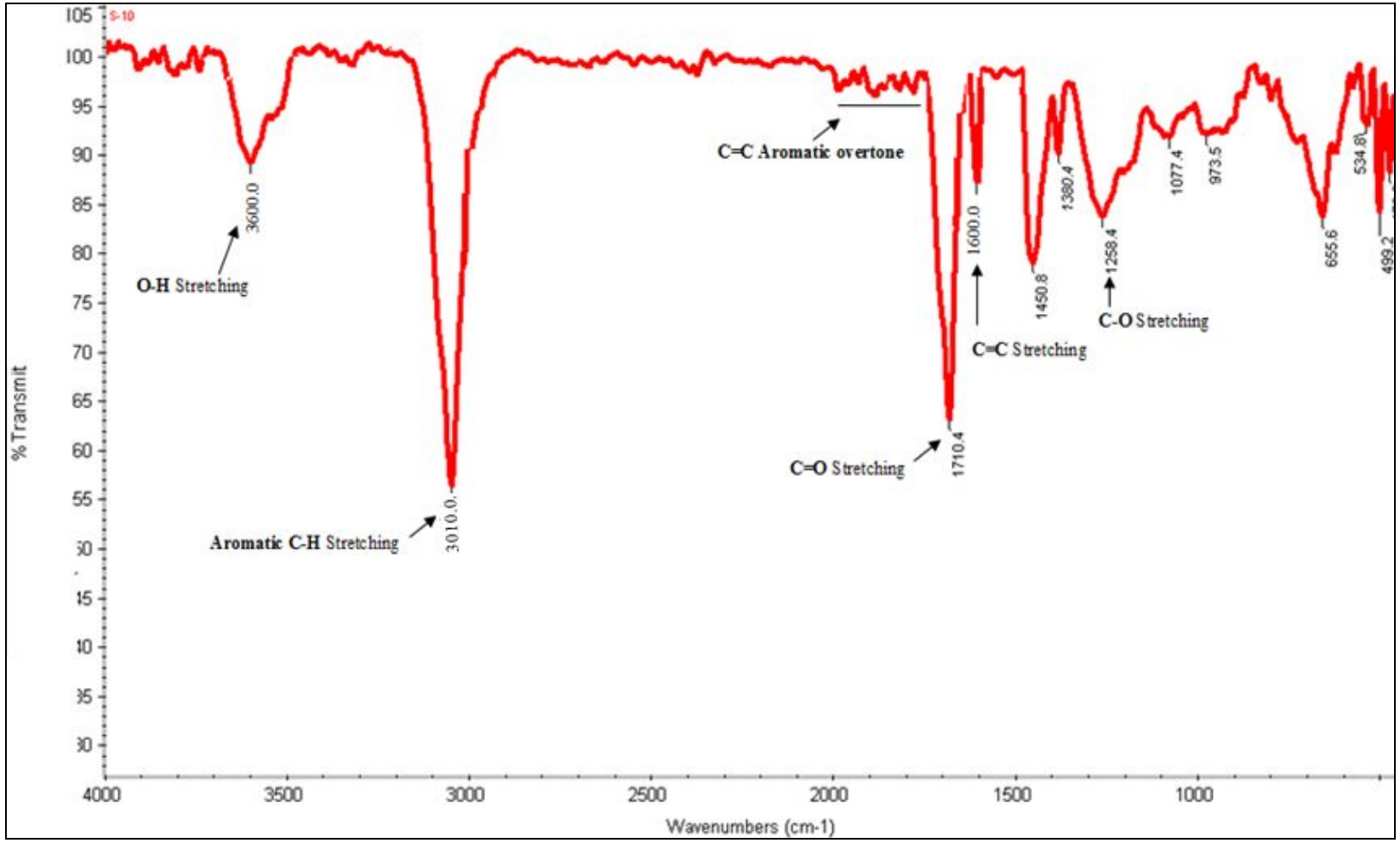

Spectra-21 ^{1}H NMR spectrum of compound IV

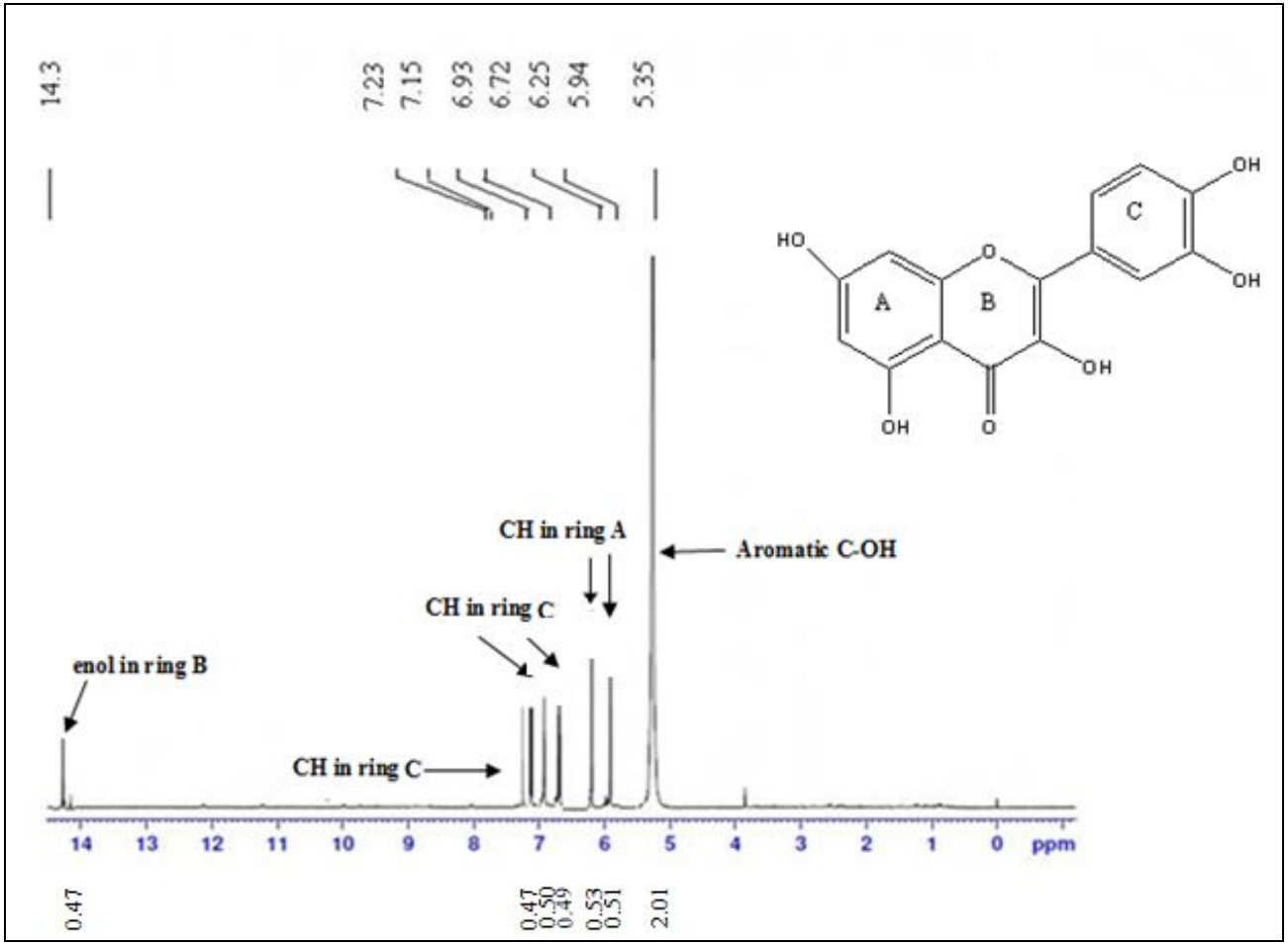

Spectra-22 Mass spectroscopy of compound IV

Mass spectrum
Sample name RSR/604/032/68B
Ionization mode Negative
Sample Information:

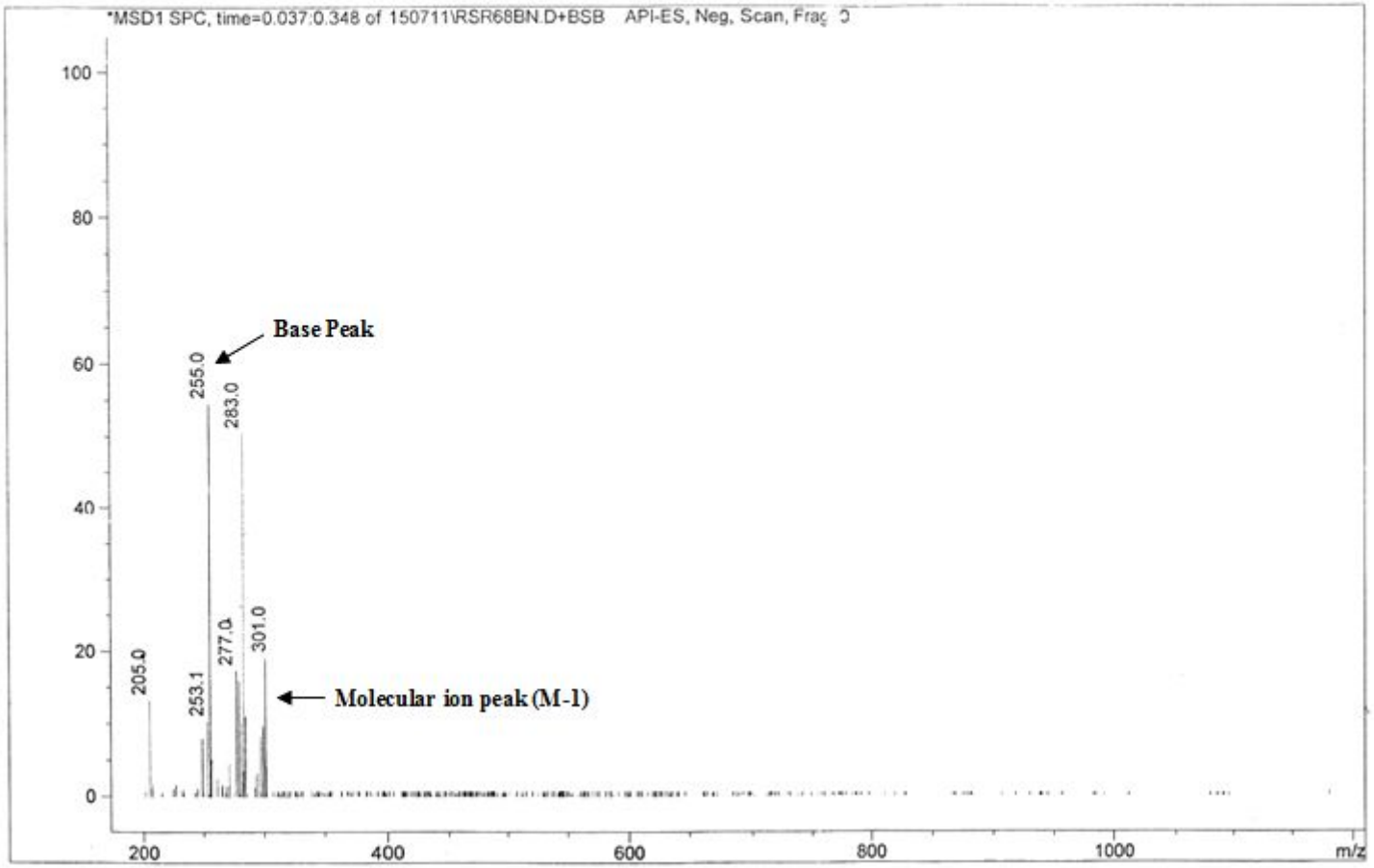

ANALYTICAL SPECTRUM OF COMPOUND IV

UV Spectrum : λ_{max} – 369nm

Table-31 IR Spectroscopic interpretation of compound IV

Frequency (cm^{-1})	Functional group
3600.0	O-H Stretching
3010.0	Aromatic C-H Stretching
1750.0-2000	Aromatic C=C Overtone
1710.4	C=O Stretching
1600.0	C=C Stretching
1258.4	C-O Stretching

Table-32 ^{1}H NMR Spectroscopic interpretation of compound IV

	δ (ppm)	No. of peaks	J value / coupling constant (Hz)	No. of protons
-OH	5.35	Singlet	-	4
-CH	5.94	Singlet	-	1
-CH	6.25	Singlet	-	1
-CH	6.72	Singlet	-	1
-CH	6.93	Singlet	-	1
-CH	7.15-7.23	Doublet	32	2
OH	14.3	Singlet	-	1

MASS SPECTRUM

Molecular Ion Peak : 301 (M-1)

Base Peak : 255

Table-33 Quantification of compound IV in ethyl acetate fraction from the ethanolic flower extract of *Nymphaea pubescens*

Sample	:	Ethyl acetate fraction
Standard	:	Quercetin Eugenol
Sample and standard prepared in	:	Methanol
Sample concentration	:	Extract (50mg/ml)
Applied volume	:	4 µl
Stationary Phase	:	Silica Gel GF_{254}
Mobile phase	:	n-Hexane : Ethyl acetate : Formic acid (4:5.5:0.5)
Scanning wavelength	:	366nm
Development Mode	:	Ascending mode

Track	Peak	Start Rf	Start Height	Max Rf	Max Height	Height %	End Rf	End Height	Area	Area %
Sample	1	0.1	0.4	0.14	336.9	32.38	0.17	15.8	8187.4	25.32
Sample	2	0.17	16.1	0.19	23.6	2.27	0.21	0.1	375.2	1.16
Sample	3	0.25	0.2	0.3	83.8	8.05	0.37	0.9	3292.6	10.18
Sample	4	0.4	2.8	0.48	237.6	22.83	0.52	25.4	8879.6	27.46
Sample	5	0.52	25.6	0.54	32.8	3.15	0.57	11.3	1000.4	3.09
Sample	6	0.59	11.8	0.65	224.9	21.62	0.68	58.7	7341.6	22.7
Sample	7	0.69	59.5	0.71	101	9.71	0.76	1.9	3264.8	10.09
Std.	1	0.62	8.5	0.67	82.2	100	0.71	5.2	2171.3	100

Sample	Quercetin Content	Concentration
Ethyl acetate extract	0.38 mg/ml	50 mg/ml

Fig.24 Chromatogram for the quantification of Compound IV in ethyl acetate fraction from ethanolic flower extract of *Nymphaea pubescens*

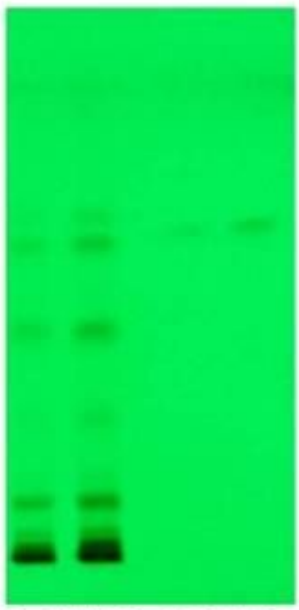

Track1 Track2 STD. STD.

254 nm

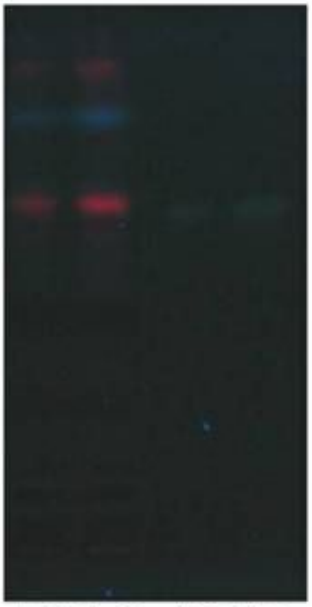

Track1 Track2 STD. STD.

366 nm

Fig.25 Densitogram of quantification of Compound IV in ethyl acetate fraction from ethanolic flower extract of *Nymphaea pubescens*

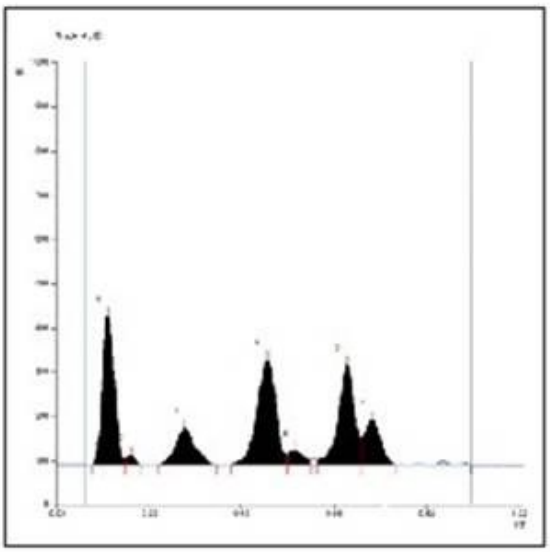

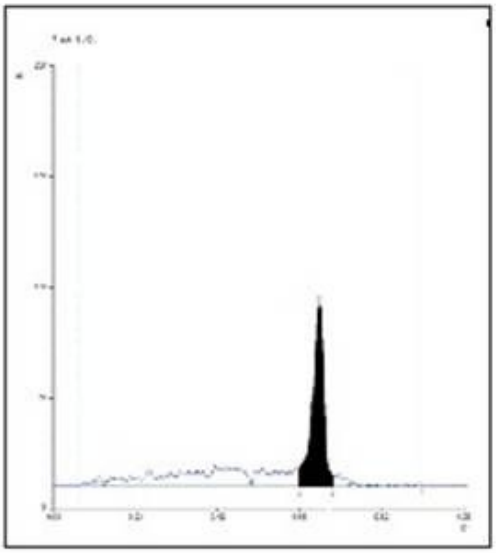

PHYSICO-CHEMICAL PARAMETERS OF ISOLATED COMPOUNDS

Table-34 Lipinski type properties

Isolated compounds	Molecular Weight	No. of Hydrogen Bond Donors	No. of Hydrogen Bond Acceptors	Total Polar Surface Area	No. of Rotatable Bonds
Compound I	200.27	1	3	54.37	9
Compound II	254.36	1	3	54.37	12
Compound III	295.37	0	3	21.7	2
Compound IV	302.24	5	7	127.45	1

Table-35 Pharmacokinetic / ADME properties and absorption parameters

Isolated compound	LogP	pKa (acid)	pKa (base)	Maximum Passive absorption	Permeability pH-6.5 Human Jejunum scale: Pe, Jejunum	Absorption rate Ka
Compound I	2.71	4.90	Nil	100%	6.77×10^{-4} cm/s	0.046 min-1
Compound II	3.96	4.90	Nil	100%	7.80×10^{-4} cm/s	0.053 min-1
Compound III	4.48	Nil	3.60	100%	8.04×10^{-4} cm/s	0.055 min-1
Compound IV	1.82	7.70	Nil	100%	3.37×10^{-4} cm/s	0.023 min-1

Table-36 Blood brain barrier, volume of distribution and plasma protein binding parameters

Isolated compound	Blood Brain Barrier Transport		Apparent Volume of Distribution		Plasma Protein Binding		
	BBB	CNS activity	Vd value (L/Kg)	Range	%PPB	Reliability range	Reliability values
Compound I	Penetrates	CNS active	0.32	Least Vd value	77.68	Moderate	0.65
Compound II	Penetrates	CNS active	0.36	Least Vd value	88.48	Moderate	0.62
Compound III	Penetrates	CNS active	2.91	Moderate value	91.11	Borderline	0.47
Compound IV	Low Penetration	CNS inactive	0.60	Moderate value	93.43	High	0.77

Table-37 Bio-availability parameter

Isolated compound	Oral Bio-availability	Passive Absorption	First Pass Metabolism	Active Transport
Compound I	30-70%	✓	-	-
Compound II	30-70%	✓	-	-
Compound III	30-70%	✓	✓	-
Compound IV	30-70%	✓	-	-

PHARMACODYNAMIC PROPERTIES – TOXICITY PROFILES

Table-38 Ames test & Estrogen receptor binding parameters

Isolated compound	Ames Test		Binding to Estrogen Receptor	
	Probability of positive Ames test	Reliability	Estrogen receptor binding	Binding value
Compound I	0.04	Moderate	Nil	<-3
Compound II	0.05	Moderate	Nil	<-3
Compound III	0.69	Boderline	Nil	<-3
Compound IV	0.85	Boderline	Weak Binding	Between -3 and 0

Table-39 HERG inhibition & toxicity category parameters

Isolated compound	HERG Inhibition		Toxicity Category LD_{50}			
	Reliability	Range	From (mg/kg b.w)	Probability (%)	To (mg/kg b.w)	Probability (%)
Compound I	0.59	Moderate	=< 5000	94	> 300	82
Compound II	0.49	Boderline	=< 5000	94	> 300	82
Compound III	0.65	Moderate	=< 2000	97	> 50	96
Compound IV	0.39	Boderline	=< 2000	87	> 50	97

Table-40 LD_{50} profile

Species	**Administration route**	**Compound I** (mg/kg b.w)	**Compound II** (mg/kg b.w)	**Compound III** (mg/kg b.w)	**Compound IV** (mg/kg b.w)
Mouse	Intraperitoneal	580	420	140	450
Mouse	Oral	1200	700	330	670
Mouse	Intravenous	200	55	59	350
Mouse	Subcutaneous	420	150	320	160
Rat	Intraperitoneal	770	240	110	1200
Rat	Oral	2800	900	350	160

Table-41 Chemotaxonomical analysis of the genus *Nymphaea*

S.No.	Subgenera	Species	Constituent	Isolated compound
1.	*Anecphya*	*Nymphaea gigantea*	Glycosidal anthocyanin	Delphinidine 3 :5 dimonosides
2.	*Brachyceras*	*Nymphaea ampla*	Alkaloid	Nupharidine & Apomorphine based compounds
		Nymphaea tetragona	Hydolysable tannin	Geraniin
		Nymphaea caerulea	Flavonol glycoside	Myricetin 3-rhamnoside Quercetin-3-rhamnoside Kaempferol 3-rhamnoside
		Nymphaea ampla *Nymphaea gracilis* *Nymphaea elegans*	Glycosyl isoflavones, Flavonol glycoside	7,3’,4’-trihydroxy-5-O-β-D- (2”-acetyl)-xylopyranosyl-isoflavone, 7,3’,4’-trihydroxy-5-O-α-L- Rhamnopyranosyl-isoflavone, Kaempferol-3-Rhamnopyranoside, Quercetin-3-Rhamnoside
3.	*Hydrocallis*	-	-	-
4.	*Lotus*	*Nymphaea lotus*	Macrocyclic flavonoidal glycoside	Myricetin-3’-o-(6”-p-coumaroyl) glucoside, Nympholide A, Nympholide B
5.	*Nymphaea*	*Nymphaea candida*	Glycosidal anthocyanin	Delphinidine-3-galactoside Delphinidin-7-galactoside Cyanidin-3-galactoside

Cont….

S.No.	Subgenera	Species	Constituent	Isolated compound
		Nymphaea alba	Alkaloid	Nupharin and Nymphaeine
			Cardiac glycoside	Nymphalin
		Nymphaea odorata	Sterols	Campesterol, Stigmasterol, β-Sitosterol
			Triterpenes	α & β-amyrin, Taraxasterol, Friedlin, Allobetulin, Erythrodiol, Betulin
		Nymphaea x marliacea	Acylated anthocyanin	Delphinidin 3-0-(6”-o-acetyl- β-galactopyranoside)
				Cyanidin 3-0-(2”-0-galloyl-6”-o-acetyl-β-galactopyranoside)
		Nymphaea odorata	Lignans	Nymphaeoside-A & Icariside E_4
			Flavonol glycosides	Kaemferol 3-o-α-rhamnopyranoside
				Quercetin 3-o-α-rhamnopyranoside
				Myricetin 3-o-α-rhamnopyranoside

The plant kingdom represents an enormous reservoir of biologically active molecules and so far only a small fraction of plants with medicinal activity have been assayed. There is therefore much current research devoted to the phytochemical investigation which has ethnobotanical information associated with them. The phytochemical research helps to identify the lead molecule with proven pharmacological activity which may offer scope for development of a drug molecule in the drug discovery process in the field of modern pharmacognosy.

The phytochemical screening of the plant under investigation focused on extraction, separation, isolation, identification of phytoconstituents and also to study the physico-chemical parameters for the isolated compounds from *Nymphaea pubescens* willd.

To identify the phytoconstituent of *Nymphaea pubescens*, the plant material was extracted with 95% ethyl alcohol by using soxhlet apparatus. The percentage yield of the ethanolic root and rhizome extract was found to be higher 7.31%w/w when compared to the ethanolic flower extract of *N.pubescens*, 3.58%w/w (Table-6).

The preliminary phytochemical analysis of the ethanolic extract of root and rhizome, was highly stained for alkaloids and tannins and slightly stained for glycosides, flavonoids, phenols, reducing sugars and proteins. Whereas the ethanolic flower extract was highly stained for flavonoids and glycosides and slightly stained for alkaloids, steroids, phenols, carbohydrates and proteins (Table-7). The result indicated the presence of wide variety of secondary metabolite in *N. pubescens* which is responsible for its folklore claim and ethnomedical uses.

Thin layer chromatographic fingerprinting is one of the most powerful approach for the quality control of herbal medicines. The TLC fingerprint for the ethanolic extract from the root and rhizome of *N. pubescens* showed 3 peaks with R_f values 0.15, 0.49 and 0.8 when exposed to iodine vapours (Table.8).

Preliminary phytochemical analysis of the ethanolic extract showed the presence of alkaloid. The extract gave dense red precipitate with dragendorff's reagent. Hence the crude alkaloid was separated from root and rhizome of *N. pubescens* by stas otto process and the percentage yield is found to be 0.24 %w/w.

The crude alkaloid fraction gave three spots when exposed to iodine vapours with the R_f values 0.14, 0.52 and 0.73respectivelty (Table-9). Thus the TLC fingerprints gave the quality parameter in the physical standardization of *N.pubescens*.

HPTLC provides higher detection sensitivity and separation resolution and reproducibility. The densitometric scanning (366nm) of ethanolic extract from the root and rhizome of *N.pubescens* showed the presence of 6 resolved peaks with the Rf values 0.15, 0.33, 0.49, 0.67, 0.8 and 0.87 respectively eluted with the mobile phase n-Hexane : Ethyl acetate : Formic acid (4:5.5:0.5). Third peak with Rf value 0.49 showed highest peak area 27,881.2 (Table-10; Fig 18&19). HPTLC fingerprint of the crude alkaloid fraction showed the presence of 12 resolved peaks with the Rf values 0.1, 0.14, 0.17, 0.39, 0.45, 0.52, 0.61, 0.65, 0.71, 0.73, 0.78 and 0.87 eluted with the mobile phase Toluene : Ethyl acetate : Formic acid : Methanol (3:3:0.8:0.2). Eleventh peak with the Rf value 0.78 showed highest peak area 12080.1 (Table-11; Fig 20&21). From the HPTLC fingerprints, it is observed that the crude alkaloid fraction contains 12 different alkaloidal compounds.

GCMS is an integrated method for spectrum extraction and compound identification from the spectrum library. The GC-MS analysis is carried out for the ethanolic extract from root and rhizome and ethanolic flower extract from *Nymphaea pubescens*, to identify the phytoconstituent. GCMS analysis of the ethanolic extract from the root and rhizome of *N.pubescens* showed the presence of fatty acid methyl and ethyl esters *viz*., Ethyl palmitate, Methyl linoleate, Ethyl oleate and Ethyl stearate. The percentage area of Methyl linoleate is 51.48% and the value is found to be higher when compared to other phytoconstituents (Spectra.1; Table-12).

The GCMS data of the ethanolic flower extract of *N. pubescens* showed the presence of fatty acid ester compounds *viz*., Ethyl myristate, Ethyl 9-hexadecenoate, Ethyl palmitate, Methyl linoleate, Ethyl linolenate, Ethyl stearate / Ethyl nonadecanoate, n-Tetracosane, 9(E) 12-Hydroxy-9-octadecenoic acid, Ethyl Nonadecanoate, Ethyl tetracosanoate, aliphatic compounds (hydrocarbons and oxygenated hydrocarbons) *viz*., Neophytadiene, 6,10,14-Trimethyl-2-pentadecanone, Phytol, n-Hexatriacontane and steroidal compounds *viz*., gamma-sitosterol and 24-methylenecycloartanol. Among these the percentage area of Ethyl stearate also called

as Ethyl octadecanoate is 12.70% and the value is found to be higher (Spectra.2; Table.13).

The GCMS analysis of the ethanolic extract from the root and rhizome and ethanolic flower extract showed the presence of methyl and ethyl fatty acid ester compounds, hydrocarbons, oxygenated hydrocarbons and steroidal compounds in *N. pubescens*.

The ethanolic root and rhizome extract of *N.pubescens* is subjected for isolation of phytoconstituent by column chromatography. The extract is subjected for gradient elution with mobile phase of increasing order of polarity. The fractions from 29 – 49 eluted with n-Hexane : Chloroform (75 : 25) gave single spot with R_f value-0.55 (mobile phase - Hexane: chloroform - 7:3) and the fractions from 50-61 eluted with the same eluant gave single spot with R_f value 0.62 (mobile phase - Hexane: chloroform - 6:4) when observed in long UV 366nm and exposed to iodine vapours. These fractions 29-49 were pooled together and the fractions 50-61 were pooled together. The solvent is evaporated by rotary evaporator. Yellow semi solid mass of 0.012% w/w obtained from the pooled, concentrated, solvent free fractions from 50-61 named as compound I and creamy yellow semisolid solid mass of 0.25% w/w obtained from the fractions from 29-49 named as compound II and both the compounds were subjected for spectroscopic analysis.

The IR spectrum of compound I showed the presence of O-H Stretching in 3445.3cm^{-1}, aliphatic C-H stretching of Methyl and Methylene groups in 2925.4 cm^{-1} & 2855.5 cm^{-1}, C=O Stretching in 1733.3 cm^{-1}, C-O Stretching in 1280.0 cm^{-}1, Methyl and Methylene C-H bend in 1465.5 cm^{-1}, Methyl C-H bend in 1380.0 cm^{-1} and Methylene rock in 720.0 cm^{-1}(Spectra.3 and Table-14).

The ^{1}H NMR spectrum of compound I showed four different peaks indicates four different sets of protons in its chemical environment. The intensity of the peak corresponds to the number of protons. The singlet peak appeared near to the TMS peak indicates highly shielded. The integrity value and chemical shift value from ^{1}H NMR spectrum of compound I showed the presence of methyl protons and twelve methylene protons (Spectra.4, Table-15).

From the ^{13}C NMR spectrum, each peak identifies a carbon atom in a different chemical environment within the molecule. The spectrum showed the presence of eleven peaks and hence presence of eleven carbon atom. The chemical shift from the spectrum showed the presence of one methyl carbon, six methylene carbons, two methylene carbons attached to carbonyl carbon and two carbonyl carbons (Spectra.5, Table-16).

DEPT is an acronym for Distortionless Enhancement by Polarization Transfer. This experiment allows determining multiplicity of carbon atom substitution with hydrogens. ^{13}C DEPT is an NMR technique for distinguishing among ^{13}C signals for CH_3, CH_2, CH, and quaternary carbons. 135° pulse - carbon signals show different phases. Signals for CH_3 and CH carbons give positive signals and signals for CH_2 carbons give negative signals. The ^{13}C DEPT 135 NMR spectrum of compound I showed one methyl group, seven methylene groups and two methylene groups attached to carbonyl carbon (Spectra.6, Table-17).

Heteronuclear Multiple Bond Coherence (HMBC) is 2-dimensional inverse hydrogen and carbon correlation technique that allow for the determination of carbon (or other heteroatom) to hydrogen connectivity. In HMBC ^{1}H NMR spectrum lies on the X-axis and ^{13}C NMR lies on the Y-axis. The HMBC spectrum of compound I showed the presence of methyl group, methylene groups, methylene groups attached to carbonyl group and two carbonyl groups(Spectra.7, Table-18).

The mass spectrum analysis of the compound I showed (Spectra.8) the molecular ion peak in the ionization mode positive at 201 m/z.

From the IR, ^{1}H, ^{13}C, ^{13}C DEPT-135 and HMBC NMR and Mass spectroscopic interpretation the possible structure of compound I is identified as **10-Oxoundecanoic acid**.

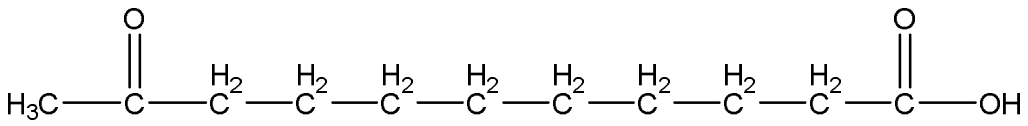

10-Oxoundecanoic acid

The IR spectrum of compound-II (Spectra.9, Table-19) showed the presence of O-H stretching at 3475.0 cm^{-1}, olefinic C-H stretching at 3080.7 cm^{-1}, aliphatic C-H stretching of Methyl and Methylene at 2926.3 & 2856.4 cm^{-1}, C=O Stretching at 1738.7 cm^{-1}, C=C weak stretching at 1645.0 cm^{-1}, C-O stretching at 1280.0 cm^{-1}, Methyl and Methylene C-H bend at 1457.0 cm^{-1} and Methylene rock at 720.2 cm^{-1}.

The ^{1}H NMR spectrum showed five different peaks indicates five different sets of protons in its chemical environment. The singlet peak appeared near to the TMS peak indicates highly shielded. The integrity value and chemical shift values showed the presence of methyl protons, ten methylene protons (CH_2) in chemically equivalent environment, one methylene protons and two methylene protons attached to carbonyl carbon (Spectra.10, Table-20).

The ^{13}C NMR spectrum of compound II showed fifteen peaks and hence presence of 15 carbon atoms. The peak at 14.11 δ ppm appeared near to the TMS peak and it is highly shielded. The spectrum showed the presence of one methyl carbon, eight methylene carbons, two methylene carbons attached to carbonyl carbon, two olefinic carbons and two carbonyl carbons (Spectra.11, Table-21).

The ^{13}C DEPT 135 NMR spectrum of compound II showed one methyl group, eight methylene groups and two methylene group attached to carbonyl groups (Spectra.12, Table-22).

The HMBC spectrum of compound II (Spectra.13, Table-23) showed the chemical shift at 0.8 δ (ppm) (^{1}H NMR) and 15 δ (ppm) (^{13}C NMR) due to high shielding effect of CH_3. The chemical shift from 1.8-2.5 δ ppm (^{1}H NMR) and 20-40 δ ppm (^{13}C NMR) showed the presence of Methylene groups. Presence of methylene group attached to carbonyl group is confirmed by the chemical shift at 1.1 & 1.6 δ ppm and 20-30 δ ppm respectively. The chemical shift at 2.2 & 4.0 δ ppm and 176 δ ppm showed the presence of carbonyl group(Spectra.13, Table-23).

The mass spectrum of compound II (Spectra.14) showed the molecular ion peak in the ionization mode positive at 255 m/z.

From the IR, ^{1}H, ^{13}C, ^{13}C DEPT-135 and HMBC NMR and Mass spectroscopic interpretation the possible structure of the compound II is identified as **14-Oxopentadec-9-enoic acid.**

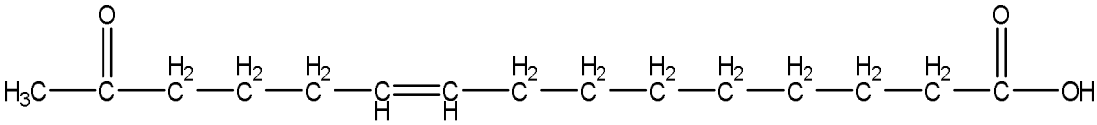

14-Oxopentadec-9-enoic acid

The crude alkaloid is subjected for column chromatography for the isolation of compound. The crude alkaloid is subjected for gradient elution. The fractions from 37–53 eluted with n-Hexane : Chloroform (80:20) gave single spot with R_f value-0.57 (mobile phase - Hexane: chloroform–5:5). The fractions were pooled together and the pooled fraction is subjected for evaporation by rotary evaporator for the removal of the solvent. White needle shaped crystals is obtained and the percentage yield is found to be 0.015% w/w. The melting point of isolated crystals is found to be 297°c and further subjected for spectroscopic studies.

The UV spectrum of compound III (Spectra.15) showed the λ_{max} at 310 nm. The compound is UV active, indicates the presence of conjugated dienes.

The IR spectrum of compound III (Spectra.16, Table-24) showed the presence of aromatic C-H stretching at 3010.0 cm^{-1}, C=C Stretching at 1645.7 cm^{-1}, C-O Stretching at 1271.7 cm^{-1}, C-N Stretching at 1192.3 cm^{-1} and C=C aromatic overtone in the region 1900-2200 cm^{-1}.

The ^{1}H NMR spectrum of compound III (Spectra.17, Table-25) showed eight different peaks indicates the presence of eight different sets of protons in its chemical environment. Singlet peak is observed at 2.26 δ ppm with an integrated value 1.15 showed the presence of methyl proton (CH_3). Triplet is observed at 2.72-2.74 δ ppm. This is due to splitting of signal with respect to nearby proton. Similarly doublet is observed at 3.06-3.26 δ ppm due to splitting of signal with respect to nearby proton. These splitting of signals are due to spin-spin coupling. The integrated value is found to be 0.8 for the triplet and 0.71 for the doublet. This might be due to the presence of methylene proton present adjacent to each other. Singlet is observed at 3.83 δ ppm

with an integrated value 3.01 indicates the presence of six protons. Triplet is observed at 4.31-4.29 δ ppm with an integrated value 0.49. This is due to spin-spin splitting with respect to nearby proton. Peaks observed near to δ ppm 7 showed the presence of aromatic protons. Singlet peak observed at 6.87 δ ppm with an integrated value 0.56 showed the presence of one aromatic proton. The singlet peak is observed at 7.30 and 7.74 δ ppm with an integrated value 1.80 showed the presence of three aromatic protons and 0.39 due to the presence of one aromatic proton.

The mass spectrum of compound III (Spectra.18) showed the molecular ion peak at 295 m/z.

From the UV, IR, ^{1}H and Mass spectroscopic interpretation the possible structure of compound III is identified as an alkaloid **Nuciferine**.

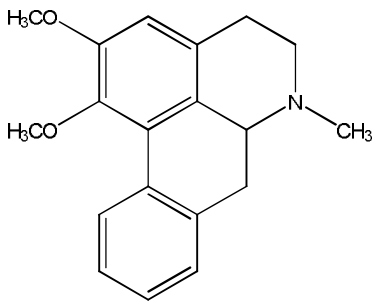

Nuciferine

Bio-assay guided isolation is an important technique in exploring lead moieties. Active extracts are fractionated using bioassay guided fractionation and chromatographic techniques are used to separate the phytoconstituent in the extract into its individual components. The biological activity is checked at all stages until a pure active compound is obtained.

The ethanolic flower extract is preliminarily screened for *in-vitro* anticancer activity against *HeLa* cell lines. The extract induced anticancerous effect to the *HeLa* cell lines and hence it is subjected for bioassay guided fractionation using column chromatographic technique using gradient elution with benzene, chloroform, ethyl acetate, ethanol and water. The fractions were collected separately depending upon the polarity and subjected for *in-vitro* anticancer activity to find out the active fraction against *HeLa* cell lines. Ethyl acetate fraction showed anticancer effect against *HeLa*

cell lines and it is further subjected for phytochemical screening to find out the constituent present in the fraction.

The percentage yield of ethyl acetate fraction (59.0%w/w) is higher when compared to hexane, chloroform, ethanol and aqueous fractions (Table.26). The preliminary phytochemical analysis of the ethyl acetate fraction showed the presence of flavonoids, phenols and glycosides. The ethyl acetate fraction gave dark red color for shinoda test. This indicates that the fraction is having high flavonoid or flavonoidal glycoside content (Table.27).

The TLC chromatographic profile (Table-28) showed the presence of 4 resolved spots with the R_f values 0.14, 0.3, 0.54 and 0.71 respectively when exposed to iodine vapours and examined under UV light (366nm). The HPTLC chromatogram (Table.29; Fig.22&23) showed 7 resolved peaks with the R_f values 0.14, 0.19, 0.3, 0.48, 0.54, 0.65 and 0.71 respectively when eluted with the mobile phase n-Hexane : Ethyl acetate : Formic acid (4:5.5:0.5) and densitometricaly scanned at 366nm. The percentage area of the fourth peak with the Rf value 0.48 was found to be higher 27.46 when compared to other resolved peaks.

The ethyl acetate fraction is subjected for the isolation of phytoconstituent by column chromatography. The fraction is eluted by gradient elution technique. The fractions were collected and subjected to TLC analysis. The fractions from 771 – 795 eluted with Ethyl acetate : Methanol (75 : 25) gave single spot with R_f value- 0.65 (mobile phase - n-Hexane: Ethyl acetate: Formic acid - 4:5.5:0.5). The fractions were pooled together and the pooled fraction is subjected for evaporation by rotary evaporator for the removal of the solvent. Yellow crystals obtained (0.017%w/w) and gave dark reddish colour for shinoda test (Table.30). The melting point of the isolated compound is found to be 316° C and further subjected for spectroscopic studies.

The UV spectrum of compound IV (Spectra.19) showed one of the λ_{max} at 369nm. The compound is UV active, showed the presence of conjugated dienes.

The IR spectrum of compound IV (Spectra.20; Table-31) showed the presence of O-H Stretching at 3600.0 cm^{-1}, aromatic C-H stretching at 3010.0 cm^{-1}, Aromatic

C=C Overtone at 1750.0-2000 cm^{-1}, C=O stretching at 1710.4 cm^{-1}, C=C stretching at 1600.0 cm^{-1} and C-O stretching at 1258.4 cm^{-1}.

The ^{1}H NMR spectrum of compound IV (Spectra.21; Table-32) showed seven different peaks indicate the presence of seven different sets of protons in its chemical environment. Singlet is observed at 5.35 δ ppm with highest integrated value 2.01 indicates the presence of four protons. Two singlets is observed at 5.94 δ ppm and 6.25 δ ppm with an integrated value 0.51 and 0.53 showed the presence of two protons. Two singlets is observed at 6.72 δ ppm and 6.93 δ ppm with an integrated value 0.49 and 0.50 δ ppm respectively. This indicates the presence of two aromatic protons. Doublet is observed at 7.15-7.23 δ ppm with an integrated value 0.47. This is due to splitting of signal with respect to nearby proton and hence showed the presence of one aromatic proton. Singlet is observed at 14.3 δ ppm with an integrated value 0.47. The value is due to the presence of enolic proton.

The mass spectrum of the compound IV (Spectra.22) showed the molecular ion peak in the ionization mode negative at 301 m/z.

From the UV, IR, ^{1}H and Mass spectroscopic interpretation the possible structure is identified as **Quercetin**.

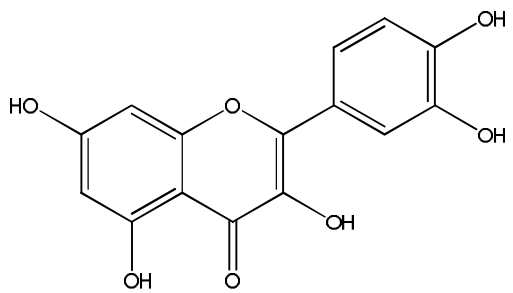

Quercetin

The anticancer effect of ethyl acetate fraction against *HeLa* cell lines may be due to the presence of quercetin and hence it is planned to quantify by HPTLC method. The ethyl acetate fraction is subjected for Co-TLC with the marker compound Quercetin. The standard and sample is eluted with the mobile phase n-Hexane: Ethyl acetate: Formic acid (4:5.5:0.5) and densitometricaly scanned at 366nm. The sixth resolved peak with the Rf value 0.65 matches with the standard

Quercetin with the Rf value 0.67. The quantification of the quercetin from the densitometric scanning is calculated and it is found that the quercetin content in the ethyl acetate fraction is 0.38mg/ml (Table.33; Fig.24&25).

The Lipinski rule of five is to evaluate “drug likeness” or to determine the chemical compound is orally active in humans in drug development process. The Lipinski rule state that not more than 5 hydrogen bond donors (nitrogen or oxygen atoms with one or more hydrogen atoms), not more than 10 hydrogen bond acceptors (nitrogen or oxygen atoms), molecular mass less than 500 daltons, and an octanol-water partition coefficient log *P* not greater than 5. All the isolated compounds 10-Oxoundecanoic acid, 14-oxopentadec-9-enoic acid, Nuciferine and Quercetin obey Lipinski type properties. The molecular weight, number of hydrogen bond donors, number of hydrogen bond acceptors is comparatively higher when compared to 10-Oxoundecanoic acid, 14-Oxopentadec-9-enoic acid and Nuciferine (Table.34).

The total polar surface area of a compound is defined as the overall polar atoms such as oxygen and nitrogen including attached hydrogens. Polar surface is used for the optimization of a drug’s ability to penetrate cell membrane. PSA is a very good indicator characterizing drug absorption including intestinal absorption, bioavailability, Caco-2 permeability and blood-brain barrier penetration. The polar surface area greater than 140 angstrom possesses poor cell permeability. If the value is lesser than 60 angstrom then the molecule penetrate the blood brain barrier and acts on receptors in the central nervous system. The total polar surface area of 10-Oxoundecanoic acid, 14-oxopentadec-9-enoic acid and Nuciferine is found to be less than 60 angstrom and for quercetin greater than 60 angstrom i.e., 127.45 angstrom (Table.34).

The bioavailability of a drug like molecule is related with it rotatable bond number. Less than seven rotatable bonds are essential for good bioavailability. The isolated compound Quercetin and Nuciferine had least number of rotatable bonds. The data predicts these compound may have good oral bioavailability when compared to 10-Oxoundecanoic acid and 14-oxopentadec-9-enoic acid (Table.34).

The relationship between activity and partition co-efficients (logP) is due to the movement of hydrocarbons to the site of action. There is an ideal log p and any deviation from this value results in a slow rate of movement to the site of value results in a slow rate of movement to the site of action and consequently in a decrease in biological activity. It is not desirable to increase the lipid solubility of drugs over a certain value since most of the drug will become stuck to membranes and unable to achieve maximum concentration at the site of action. Conversely, drugs with a low value of logP as washed out since they are not lipophilic enough to stick to biological membranes. The logP of a drug like molecule should be less than 5. The logP value for all the isolated compounds 10-Oxoundecanoic acid, 14-oxopentadec-9-enoic acid, Nuciferine and Quercetin is found to be less than 5 (Table.35).

The acid-base property of a drug molecule is the key parameter for drug development because it governs solubility, absorption, distribution, metabolism and elimination. pKa and pKb is also helpful in screening salts, developing pre-clinical and clinical formulation. It is also necessary in developing analytical methods. Most of the drugs behave in solution as weak acids, weak bases or sometimes as both weak acids and weak bases. The pKa and pKb values give information about the strength of acids and bases and pH at which 50% of the drug is ionized. The pKa value of Quercetin and pKb value of Nuciferine is found to be higher when compared to 10-Oxoundecanoic acid and 14-Oxopentadec-9-enoic acid (Table.35) .

Drug absoption is determined by the drug's physico-chemical properties, formulation and route of administration. A drug must cross several semi-permeable cell membranes before it reaches the systemic circulation. Cell membranes are biologic barriers that selectively inhibit passage of drug molecules. The membranes are composed primarily bi-molecular lipid matrix, which determines membrane permeability characteristics. Drugs may cross cell membrane by passive diffusion, facilitated passive diffusion, active transport or pinocytosis. Sometimes various globular proteins embedded in the matrix function as receptors and help transport molecules across the membrane. Drugs passively diffuse across a cell membrane from a region of high concentration (GI fluids) to one of low concentration (Blood). The isolated compounds 10-Oxoundecanoic acid, 14-oxopentadec-9-enoic acid,

Nuciferine and Quercetin diffuse through a cell membrane by passive transport and maximam passive absorption is found to be 100% for all the isolated compounds (Table.35).

Maximum absorption of drug products takes place in the jejunum and ileum over a period of 3-4 hours in a pH range 4.5-8.0. This suggests that weak acids and weak bases ought to be better absorbed in the jejunum and in the ileum respectively. The surface area available for absorption is highest in the jejunum and ileum respectively. The permeability of drug in the pH 6.5 in the human jejunum for Quercetin is found to higher 8.04×10^{-4} cm/s and lower for Nuciferine 3.37x10-4 cm/s (Table-35).

Absorption is characterized by an absorption rate constant K_a . The absorption rate is found to be higher for Nuciferine followed by 14-oxopentadec-9-enoic acid, 10-Oxoundecanoic acid and Quercetin (Table-35).

Blood Brain Barrier is a separation of circulating blood from the brain extracellular fluid in the central nervous system. It occurs along the capillaries and consists of tight junctions around the capillaries that do not exist in normal circulation. Endothelial cells restrict the diffusion of microscopic objects (eg. bacteria) and larger hydrophilic molecules in the cerebrospinal fluid, while allowing the diffusion of small hydrophobic molecules (O_2, CO_2, hormones). This barrier also includes a thick basement membrane and astrocytic endfeet. Astrocytes are star shaped glial cells in the brain and spinal cord. 10-Oxoundecanoic acid, 14-oxopentadec-9-enoic acid and Nuciferine cross blood brain barrier because of its hydrophobic nature and hence these compounds are CNS active leads. Because of hydrophilic nature of Quercetin the compound had low penetration and hence it is CNS inactive (Table. 36).

Volume of distribution or apparent volume of distribution is the ratio between the total amount of drug in the body and the drug blood plasma circulation. 10-Oxoundecanoic acid and 14-oxopentadec-9-enoic acid possessed least Vd value, Nuciferine and Quercetin possessed moderate Vd value (Table-36).

Drug efficiency may be affected by the degree to which it binds to the proteins within blood plasma. The less bound a drug is the more efficiently it can transverse cell membrane on diffusion. The % plasma protein binding for Quercetin is highest 93.43% whereas comparatively lowest for 10-oxoundecanoic acid 77.68% (Table-36).

Bio-availability is the fraction of administered drug that reaches the systemic circulation in chemically unchanged forms. The bio-availability of 10-Oxoundecanoic acid, 14-oxopentadec-9-enoic acid, Nuciferine and Quercetin is found to be in between 30-70% (Table-37).

After a drug is swallowed, it is absorbed by the digestive system, enters the hepatic portal system. It is carried through the portal vein into the liver before it reaches the rest of the body. The liver metabolizes many drugs and emerge the rest in the circulatory systems. The first pass through the liver thus greatly reduces the bio-availability of the drug. Only Nuciferine undergoes first pass metabolism and hence oral route of administration should not be preferred (Table-37).

Active transport requires energy expenditure and may involve against a concentration gradient. Active transport seems to be limited to drug structurally similar to endogenous substance (eg. ions, vitamins, sugars, amino acids). These drugs are usually absorbed from specific sites in the small intestine. 10-Oxoundecanoic acid, 14-oxopentadec-9-enoic acid, Nuciferine and Quercetin transports to a cell by passive absorption and not by active transport (Table-37).

Ames test, Estrogen receptor binding parameter and hERG inhibition are the parameters to assess the mutagenic potential of chemical compounds. 10-Oxoundecanoic acid, 14-oxopentadec-9-enoic acid, Nuciferine and Quercetin didn’t showed any mutagenic potential (Table-38 &39).

From the toxicity parameter, 10-Oxoundecanoic acid and 14-oxopentadec-9-enoic acid didn’t produce any toxic effect from 300-5000 mg/kg body weight and Nuciferine and Quercetin didn’t produce any toxic effect from 50-2000 mg/kg body weight (Table-39).

Median lethal dose, LD_{50} is the dose required to kill half of the members of tested population after specified test duration. LD_{50} values are frequently used as a general indicator of a substances produce acute toxicity. The LD_{50} value for rat is found to be higher for 10-Oxoundecanoic acid (Table-40).

The chemotaxonomical analysis of the genus *Nymphaea* showed the presence of glycosidal anthocyanin, isoflavone, flavonol glycoside, steroid, alkaloid, cardiac glycoside, lignan and triterpene (Table-41). From the comparative phytochemical studies the genus *Nymphaea* contains wide variety of secondary metabolites which is responsible for the folklore claims.

PART 3 – PHARMACOLOGY

Pharmacology is a lively scientific discipline providing a basis for the use of drugs in therapy. Natural products were widely viewed as templates for structural optimization programs designed to perfect new drugs. The search for new drugs from plant sources is a multidisciplinary endeavour involving the examination of traditional medicine by animal experimentation. Modern chemical methods have led to a dramatic increase in number of natural molecules available for pharmacological research. At the same time, recent developments in cellular and molecular pharmacology and also by computational screening provides an increasing number of selective tests able to identify the activity and the mechanisms of action of biologically active molecules.

The drug action is based upon the selectivity on particular cells and tissues. In other words, it must show a high degree of binding site specificity. Conversely the proteins that function as drug targets generally show a high degree of ligand specificity and they will recognise only ligands of a certain precise type and ignore closely related molecules. The protein targets for drug action on mammalian cells are receptors, ion channels, enzymes and carrier molecules[66].

A comprehensive search of the literature on *Nymphaea pubescens* revealed the aquatic plant is being traditionally used in the treatment of diabetes, bleeding piles and as a cardiotonic in the palpitation of the heart. In Africa *Nymphaea lotus* is given for the management of cancer. Diabetes and cancer are common diseases with tremendous impact on health worldwide. These are heterogeneous, multifactorial, severe and chronic diseases. One of the key factors for the pathogenesis of diabetes and cancer is oxidative stress. Hence the research work on the aquatic plant *Nymphaea pubescens* was selected for antidiabetic, anticancer and anti-oxidant activity. The antidiabetic activity of the *N.pubescens* is planned to screen by molecular method targeting at enzymatic level (including glycolytic and gluconeogenic enzyme and estimating pro and anti-apoptotic protein by western blot analysis) and at receptor level (protein tyrosine phophatase 1B by docking studies).

Diabetes Mellitus

Diabetes is one of the non-communicable disease accounts 366 million people worldwide and by 2030 this will be raised to **552 million.** Diabetes is a chronic disorder of carbohydrates, fat and protein metabolism characterized by fasting elevations of blood glucose levels and an increased risk of cardiovascular disease, renal disease and neuropathy. Diabetes can occur when the pancreas does not secrete enough insulin or if the cells of the body become resistant to insulin and hence the blood glucose cannot enter into the cells leads to serious complications[67].

Major complication of diabetes[68]

Cardiovascular disease	-	Adults with diabetes have death rates from cardiovascular disease about 2-4 times higher than adults without diabetes.
Hypertension	-	About 75% of adults with diabetes have high blood pressure.
Retinopathy	-	Diabetes is the leading cause of blindness among adults.
Nephropathy	-	Diabetes is the leading reason for dialysis treatment accounting for 43% of new cases.
Neuropathy	-	About 60%-70% of people with diabetes have mild to severe forms of nervous system damage. Severe forms of diabetic nerve disease are a major contributing cause of lower extremity amputations.
Amputations	-	More than 60% of lower limb amputations in the United States occur among people with diabetes.
Periodontal disease	-	Almost one third of people with diabetes have severe periodontal (gum) disease.
Pain	-	Many diabetes fall victim to chronic pain due to conditions such as arthritis, neuropathy, circulatory insufficiency or muscle pain (fibromyalgia).
Depression	-	This is a common accompaniment of diabetes. Clinical depression can often begin to occur even years before diabetes is fully evident. It is difficult to treat in poorly controlled diabetes.
Autoimmune disorders	-	Thyroid disease, inflammatory arthritis and other disease of the immune system commonly add to the suffering of diabetes.

Classification of Diabetes Mellitus

Diabetes is divided into two major categories, one associated with insulin deficiency called type-I or Insulin dependent diabetes mellitus (IDDM) and the other associated with insulin resistant called type-II or non insulin dependent diabetes (NIDDM). Type –I is associated with a specific and complete loss of pancreatic beta cells. Type – II diabetes is the most common type and is associated with obesity, hyperinsulinemia and insulin resistance. Insulin resistance may be due to the defect at receptor level or at the post receptor level. This defect may be in the effector cell or in the beta islet cell causing insulin resistance.

Present global prevalence of Type II Diabetes Mellitus[69]

According to International Diabetes Federation, the enormity of the Type II Diabetes Mellitus is epidemic. Disease now affects a staggering 246 million people worldwide with 46% of all those affected in the 40–59 age group and the total number of people living with diabetes will skyrocket to 380 million within 20 years if nothing is done. Type II Diabetes Mellitus now affects 5.9% of the world's adult population with almost 80% of the total in developing countries. The regions with the highest rates are the Eastern Mediterranean and Middle East where 9.2% of the adult population is affected and North America (8.4%). The highest numbers however are found in the Western Pacific where 67 million peoples suffering from diabetes followed by Europe with 53 million known patients. India leads the global top ten in terms of the highest number of people with diabetes with a current figure of 40.9 million, followed by China with 39.8 million. Behind them come USA, Russia, Germany, Japan, Pakistan, Brazil, Mexico and Egypt. Developing countries account for seven of the world's top. Diabetes has now exploded with the force felt greatest in the Middle East, India, China and USA.

Pathogenesis of Type II diabetes

The pathogenesis of type 2 diabetes mellitus is characterized by peripheral insulin resistance, impaired regulation of hepatic glucose production and declining ß-cell function eventually leading to ß-cell failure and relative insulin deficiency in association with peripheral insulin resistance. Multiple risk factors are involved in the

pathogenesis of type II diabetes including classical genetic risk (family history) as well as a prominent contribution from multiple environmental risk factors which had been shown in Fig.22.

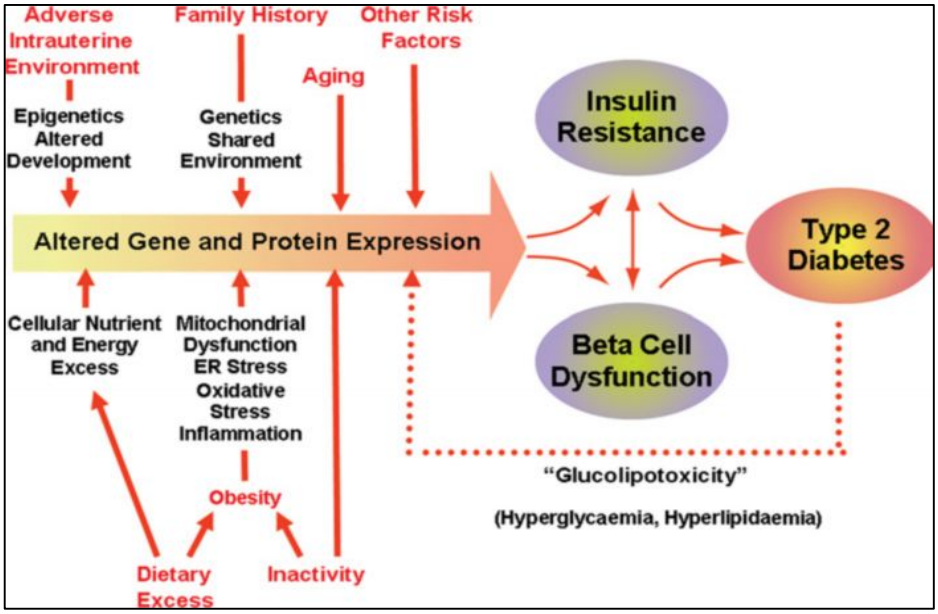

Normal insulin secretion[70]

Glucose is rapidly taken up by the pancreatic beta cell via the glucose transporter 2 (GLUT2) upon which it is phosphorylated via glucokinase which is the rate limiting step of beta cell glucose metabolism (fig.23). Further degradation leads to formation of pyruvate which is then taken up in the mitochondria in which further metabolism leads to ATP formation. ATP is necessary for the delivery of energy needed for the release of insulin but it is also involved in the cell membrane depolarisation. The ADP/ATP ratio leads to activation of the sulphonyl urea receptor 1 (SUR1) protein which will lead to closure of the adjacent potassium channel (potassium inward rectifier-KIR 6·2 channel). The closure of the potassium channels will alter the membrane potential and open calcium channels which trigger the release of preformed insulin-containing granules (fig. 23).

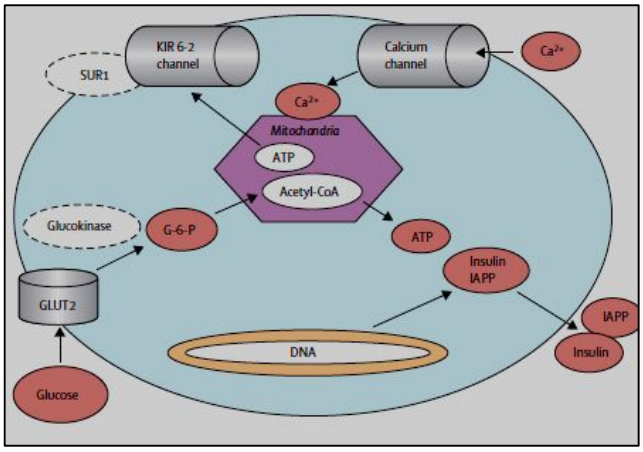

Fig.27 Normal glucose-induced insulin secretion

Glucose Toxicity

In beta cells oxidative glucose metabolism will always lead to production of reactive oxygen species normally detoxified by catalase and superoxide dismutase. Beta cells are equipped with a low amount of these proteins and also redox regulating enzyme glutathione peroxidase. Hyperglycaemia has been proposed to lead to large amounts of reactive oxygen species in beta cells with subsequent damage to cellular components (figure 24). Loss of pancreas duodenum homeobox 1(PDX-1) a critical regulator of insulin promoter activity has also been proposed as an important mechanism leading to beta cell dysfunction

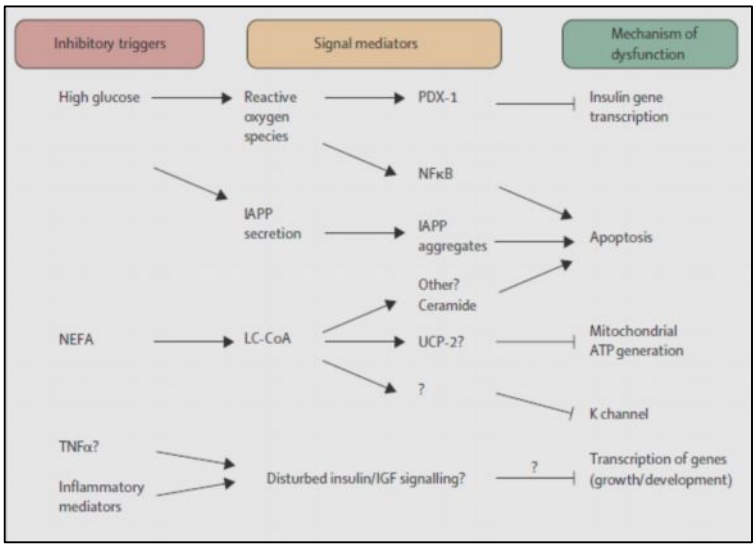

Fig.28. Possible negative effects of hyperglycaemia and various modulators involved in insulin resistance on Beta cell dysfunction

Insulin resistance

Insulin elicits its pleiotropic metabolic responses by binding and activating a specific plasma membrane receptor with tyrosine kinase activity. Cellular substrates of the insulin receptor kinase most prominently the Insulin Receptor Substrate (IRS) proteins are efficiently tyrosine phosphorylated on several sites which serve as binding scaffolds for various adaptor proteins and lead to the downstream signalling cascade. Insulin activates a series of lipid and protein kinase enzymes linked to the translocation of glucose transporters to the cell surface, synthesis of glycogen, protein, mRNAs, and nuclear DNA which affect cell survival and proliferation[71].

Phosphorylation and dephosphorylation of IRS proteins

In states of insulin resistance one or more of the following molecular mechanisms to block insulin signalling are likely to be involved. The positive effects on downstream responses exerted by tyrosine phosphorylation of the receptor and the IRS proteins are opposed by dephosphorylation of these tyrosine side-chains by cellular protein-tyrosine phosphatases and by protein phosphorylation on serine and threonine residues which often occur together. Phospho Tyrosine Phosphatase 1B (PTP1B) is widely expressed and has an important role in the negative regulation of insulin signalling.

Serine or threonine phosphorylation of IRS1 reduces its ability to act as a substrate for the tyrosine kinase activity of the insulin receptor and inhibits its coupling to its major downstream effector systems. Several IRS serine kinases have been identified including various mitogen activated protein kinases, c-Jun NH_2-terminal kinase, atypical protein kinase C and phosphatidylinositol 3-kinase. Signal down regulation can also occur through internalisation and loss of the insulin receptor from the cell surface and degradation of IRS proteins. Members of the Suppressor of Cytokine Signalling (SOCS) family of proteins participate in IRS protein degradation through an ubiquitin-proteosomal pathway (fig.29)

Negative modulation of insulin action can be mediated via various pathways leading to insulin resistance. Various inhibitory triggers affect their respective signal modulators (partly via transcription factors) which lead through deactivating

pathways (tyrosine phosphatases, serine kinases, lipid phosphatases and degradation pathways) to inhibitory actions on insulin signalling (activation pathways)[72] (fig.29).

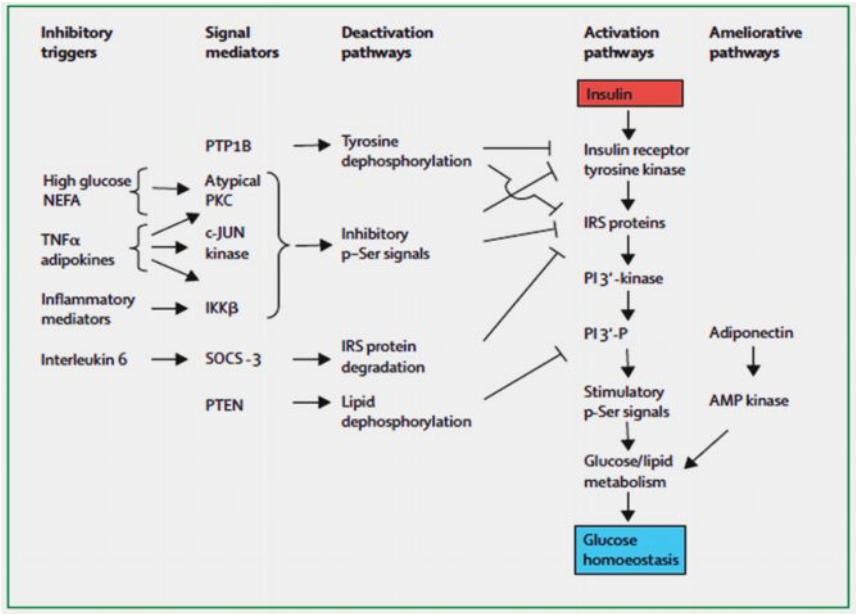

Fig. 29 Activation and deactivation pathways of insulin signalling

Mitochondrial dysfunction induces insulin resistance in skeletal muscle

A decrease in mitochondrial fatty acid oxidation caused by mitochondrial dysfunction or reduced mitochondrial content produces increased levels of intracellular fatty acyl CoA and diacylglycerol. These molecules activate novel protein kinase C which in turn activates a serine kinase cascade (possibly involving inhibitor of nuclear factor kB kinase-IKK and c-Jun N-terminal kinase–1) leading to increased serine phosphorylation (pS) of insulin receptor substrate–1 (IRS-1). Increased serine phosphorylation of IRS-1 on critical sites (e.g., IRS-1 Ser307) blocks IRS-1 tyrosine (Y) phosphorylation by the insulin receptor which in turn inhibits the activity of phosphatidyl inositol 3-kinase (PI 3-kinase). This inhibition results in suppression of insulin-stimulated glucose transport.

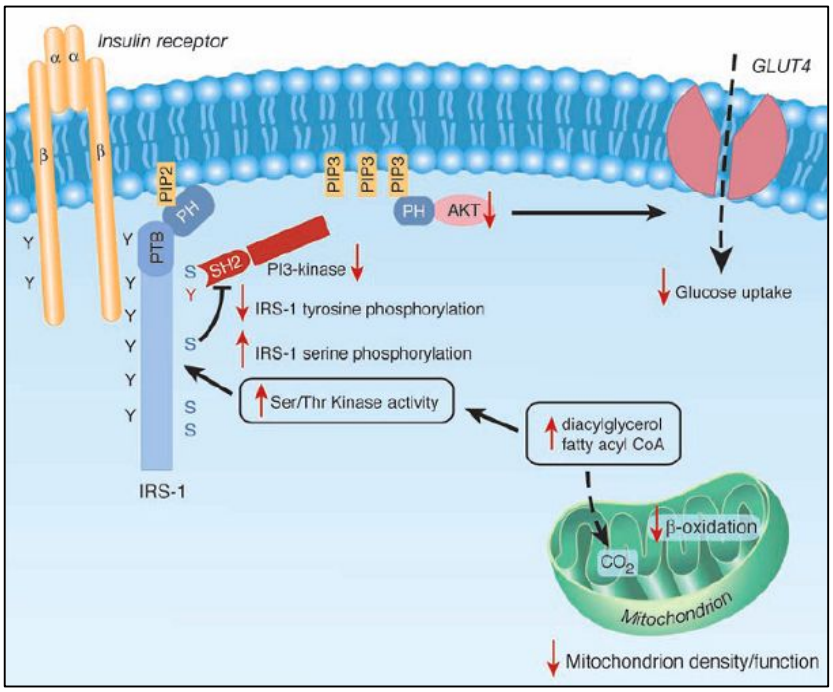

Fig.30 Mitochondrial dysfunction induces Insulin resistance in skeletal muscle

Management of hyperglycaemia

The modern drugs insulin and other oral hypoglycaemic agents such as biguanides (reduce hepatic glucose production), sulphonylureas (stimulates pancreatic insulin secreation), α-glucosidase inhibitors (delay digestion and absorption of intestinal carbohydrate) have characteristic profile of adverse effects which include frequent diarrhoea, hypoglycaemia, hepatotoxicity, lactic acidosis, dyslipidemia, hypertension and hypercoagulability. Significantly for effective control of diabetes combination therapy is being considered because no single drug is able to target diabetes and its associated complications. This necessitates the identification of novel drugs which might function in a mechanistically distinct fashion to the existing drug targets. Hence, the search for a definitive cure for diabetes mellitus is being pursued vigorously by the scientific community[69].

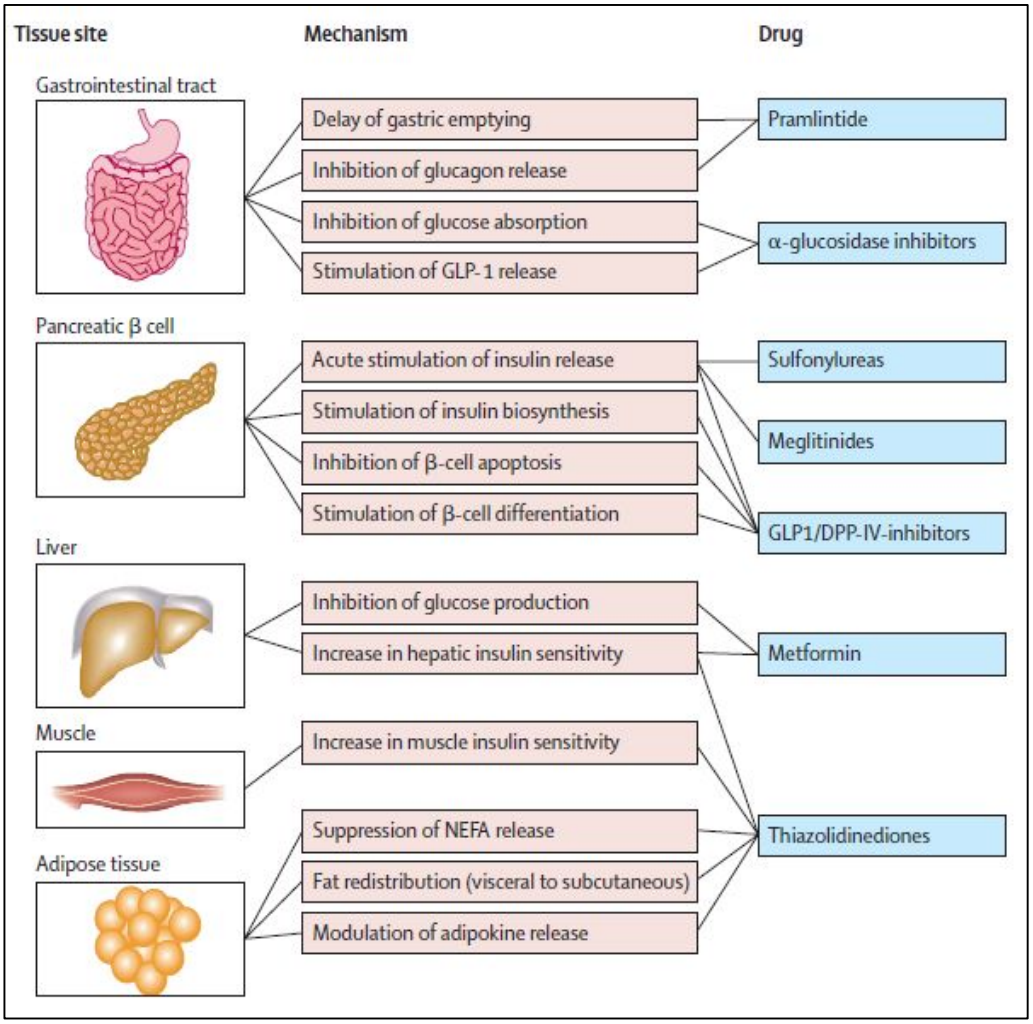

Fig. 31 Pharmacological treatment of hyperglycaemia according to site of action

The detailed investigations in the diabetic animal species are required for better understanding of the disease mechanisms in much closely similar human situation as well as for discovering newer targets and drugs for the treatment of type II diabetes and its complications. Appropriate experiment models are essential tools for understanding the pathogenesis, complications and genetic or environmental influences that increase the risk of type II diabetes and testing of various therapeutic agents. The animal models of type II diabetes can be obtained either spontaneously or induced by chemical or dietary or surgical manipulations.

Table-42 Models for Type II Diabetes Mellitus[74]

S.No.	Model category	Type II diabetes model	
		Obese	**Non obese**
I	Spontaneous or genetically derived diabetic animals	*Ob/ob* mouse Db/db mouse KK mouse KK/A^y mouse NZO mouse NONCNZO10 mouse TSOD mouse M16 mouse Zucker fatty rat ZDF rat SHR/N-cp rat JCR/LA-cp rat OLETF rat Obese rhesus monkey	Cohen diabetic rat GK rat Torri rat Non obese C57BL/6 (Akita) mutant mouse ALS/Lt mouse
II	Diet/nutrition induced diabetic animals	Sand rat C57/BL 6J mouse Spiny mouse	-
III	Chemically induced diabetic animals	GTG treated obese mice	Low dose ALX or STZ adult rats, mice etc Neonatal STZ rat
IV	Surgical diabetic animals	VMH lesioned dietary obese diabetic rat	Partial pancreatectomized animals. e.g. dog, primate, pig and rats

V	Transgenic/knock-out diabetic animals	β_3 receptor knockout mouse Uncoupling Protein (UCP1) knock-out mouse	Transgenic or knock out mice involving genes of insulin and insulin receptor and its components of downstream insulin singnaling e.g. IRS-1, IRS-2, GLUT-4, PTP-1B and others PPAR-γ tissue specific knockout mouse Glucokinase of GLUT 2 gene knockout mice Human Islet Amyloid Polypeptide over expressed rat (HIP rat)

Mechanism of action of Streptozotocin and Nicotinamide induced type II diabetes mellitus[75]

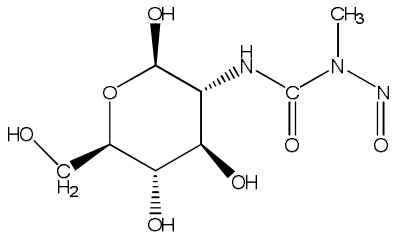

Fig.32 Structure of Streptozotocin

Streptozotocin (STZ, 2-deoxy-2-(3-(methyl-3-nitrosoureido)-D-glucopyranose) is synthesized by *Streptomycetes achromogenes* and is used to induce both insulin-dependent and non-insulin-dependent diabetes mellitus (IDDM and NIDDM respectively). Methylating agent streptozotocin [2-deoxy-2-(3-methyl-3-nitrosourea)-1-d-glucopyranose] (STZ) is actively transported into pancreatic β cells via the Glut-2 glucose transporter. It reacts at many sites in DNA but in particular at

the ring nitrogen and exocyclic oxygen atoms of the DNA bases predominantly producing 7-methylguanine, 3-methyladenine (3-meA), and O^{6}-methylguanine adducts leads to DNA Damage.

STZ is a Nitric Oxide (NO) donor and it was proposed that, this molecule contributes to STZ-induced DNA damage. It was demonstrated that STZ decreases the activity of aconitase that inhibits the krebs cycle and substantially decreases oxygen consumption by mitochondria and increases the activity of xanthine oxidase. This enhances the production of superoxide anion, hydrogen peroxide, hydroxyl and peroxy nitrate radicals. Thus synergistic action of both NO and reactive oxygen species may also contribute to DNA fragmentation and other deleterious changes caused by STZ.

Thus the alkylating property and the free radical formation results in DNA damage. DNA strand breaks leads to overactivation of Poly Adenine Ribosyl Polymerase Enzyme (PARP). PARP is a nuclear enzyme which detects DNA single or double strands break residues. This enzyme metabolizes NAD^{+} into nicotinamide and branched polymers of ADP ribose that are transferred to nuclear proteins. This results in catastrophic fall in NAD^{+} and ATP and thus leads to β cell apoptosis.

It has been reported that adiminstration of nicotinamide partially inhibits the β cell apoptosis by the following mechanism. It is a weak PARP inhibitor, precursor for NAD^{+}, coenzyme for ATP production and as an antioxidant. The above mentioned actions of nicotinamide prevent the aggravation of experimental diabetes[76]. This condition contributes a number of features similar to type II diabetes and is exemplified by stable hyperglycemia, glucose intolerance and significantly altered glucose-stimulated insulin secretion. The threshold value of fasting plasma glucose to diagnose type II diabetes was $\geq$ 126mg /dl[77].

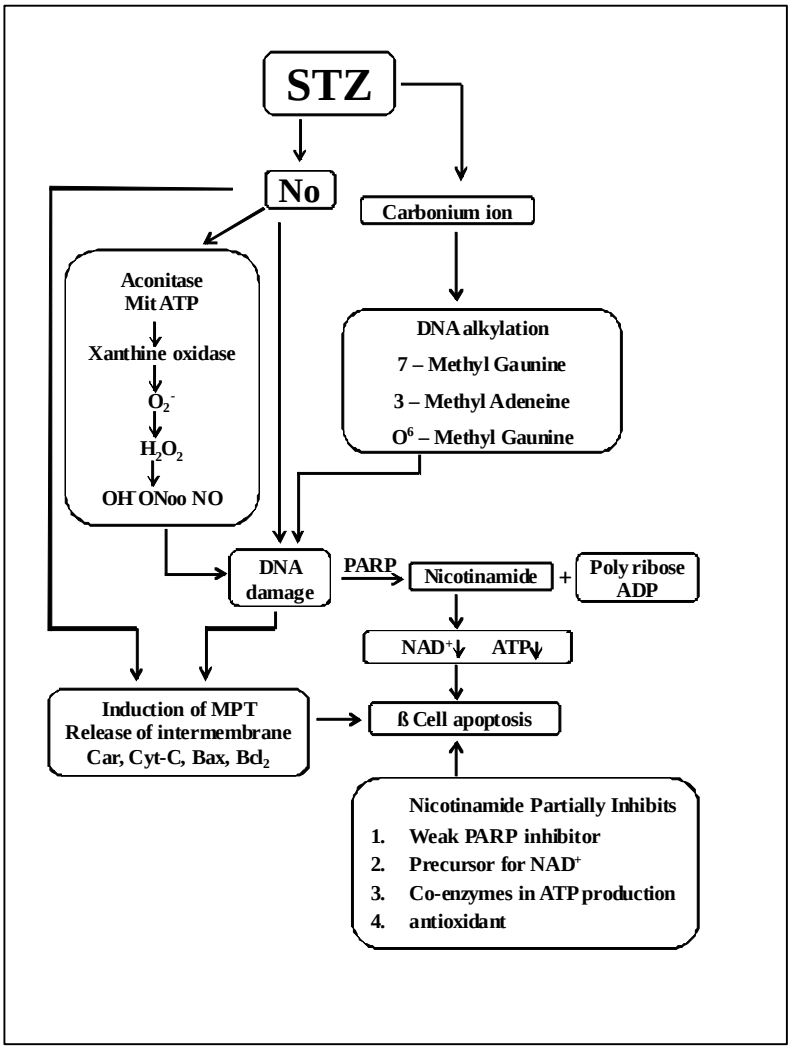

Fig.33 Mechanism of action of Streptozotocin and Nicotinamide induced type II diabetes

Role of Apoptosis in Type II Diabetes Mellitus

Apoptosis or programmed cell death is an essential physiological process that plays a critical role in development and tissue homeostasis. There are a number of mechanisms through which apoptosis can be induced in cells. Some of the major stimuli that can induce apoptosis include viral infection, cellular stress and DNA damage. The sensitivity of cells to any of these stimuli can vary depending on a number of factors such as the expression of pro- and anti-apoptotic proteins (eg. Bcl-2, Bax, Cytochrome C and Caspase etc.), the severity of the stimulus and the stage of the cell cycle (www.sgul.ac.uk/dept/immunology/~dash).

Loss of insulin effect on the liver leads to glycogenolysis, an increase in hepatic glucose and free fatty acid production. The excess in free fatty acids found in the insulin resistant state is known to be directly toxic to hepatocytes. Putative mechanisms include cell membrane disruption at high concentration that leads to cellular stress and mitochondrial dysfunction[78].

Role of mitochondria in apoptosis

Mitochondrial dysfunction has been linked to a wide range of regenerative and metabolic diseases, cancer and aging. All these clinical manifestations arise from the central role of bioenergetics in cell biology[79].

Mitochondria play an important role in the regulation of cell death. They contain many pro-apoptotic proteins such as Apoptosis Inducing Factor (AIF) and cytochrome C. These factors are released from the mitochondria following the formation of a pore in the mitochondrial membrane called the Permeability Transition pore or PT pore. These pores are thought to form through the action of the pro-apoptotic members of the bcl-2 family of proteins which in turn are activated by apoptotic signals such as cell stress, free radical damage or growth factor deprivation (www.sgul.ac.uk/dept/immunology/~dash).

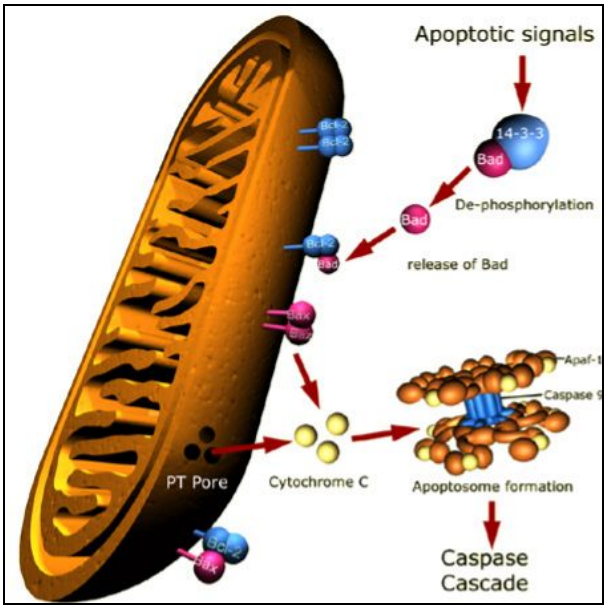

Fig.34 Illustration of the main apoptotic signalling pathways involving in mitochondria

Mitochondrion-mediated procaspase-activation pathway of caspase-9[80]

When cellular stress (e.g. DNA damage) occur proapoptotic proteins in the cytosol will be activated, which will in turn induce the opening of Mitochondrion Permeability Transition Pores (MPTPs). As a result cytochrome c localized in mitochondria will be released to the cytosol. With the presence of cytosolic dATP (Deoxyadenosine Triphosphate) or ATP, apoptotic protease activation factor-1 (Apaf-1) oligomerizes. Together with cytosolic procaspase-9, dATP and cytochrome c oligomerized Apaf-1 can result in the formation of a massive complex known as apoptosome. The N-terminal of Apaf-1 and the prodomain of procaspase-9 both have CARDs with complementary shapes and opposite charges. They interact with each other by CARDs and form a complex in the proportion of 1:1. Activated caspase-9 can in turn activate procaspase-3 and procaspase-7. The activated caspase-3 will then activate procaspase-9 leads to apoptosis.

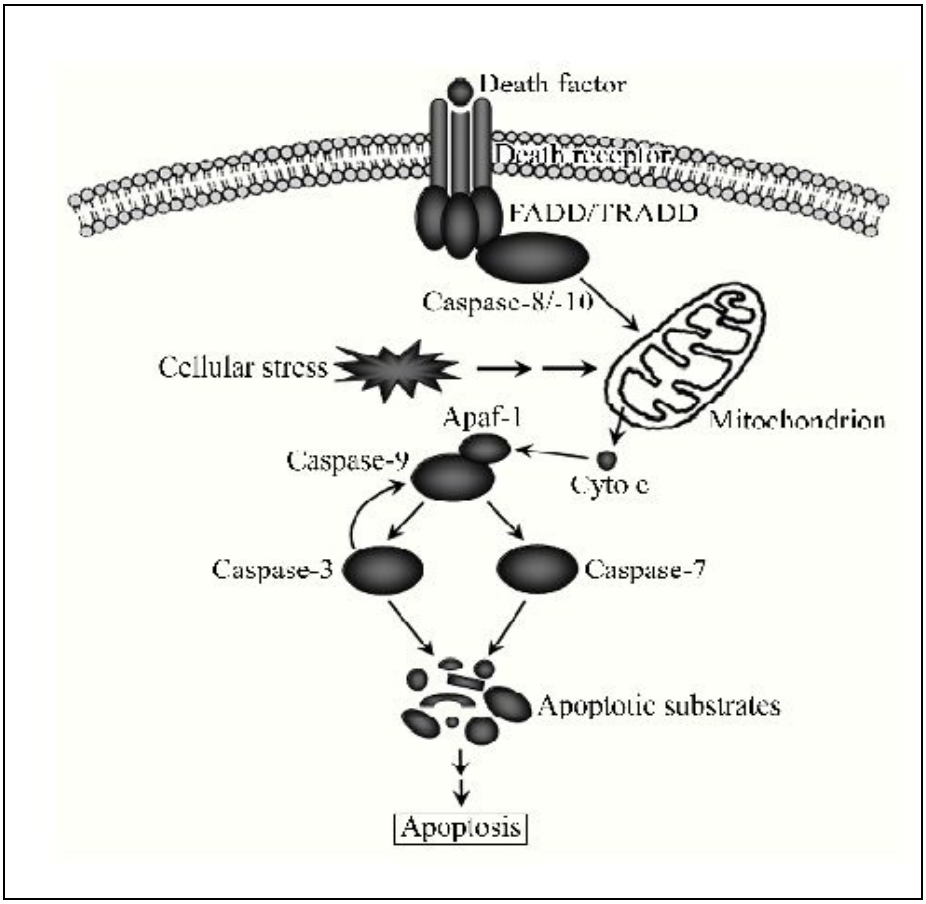

Fig.35 Mitochondrion-mediated caspase dependent pathway

Role of Bcl-2 proteins in apoptosis

The Bcl-2 proteins are a family of proteins involved in response to apoptosis. Some of these proteins (such as Bcl-2 and Bcl-XL) are anti-apoptotic while others (such as Bad, Bax or Bid) are pro-apoptotic. The sensitivity of cells to apoptotic stimuli can depend on the balance of pro- and anti-apoptotic bcl-2 proteins. When there is an excess of pro-apoptotic proteins the cells are more sensitive to apoptosis, when there is an excess of anti-apoptotic proteins the cells will tend to be more resistant. An excess of pro-apoptotic bcl-2 proteins at the surface of the mitochondria is thought to be important in the formation of the PT pore.

The pro-apoptotic bcl-2 proteins are often found in the cytosol where they act as sensors of cellular damage or stress. Following cellular stress they relocate to the surface of the mitochondria where the anti-apoptotic proteins are located. This interaction between pro- and anti-apoptotic proteins disrupts the normal function of the anti-apoptotic bcl-2 proteins and can lead to the formation of pores in the mitochondria and the release of cytochrome C and other pro-apoptotic molecules from the intermembrane space. This in turn leads to the formation of the apoptosome and the activation of the caspase cascade.

The release of cytochrome C from the mitochondria is a particularly important event in the induction of apoptosis. Once cytochrome C has been released into the cytosol it is able to interact with a protein called Apaf-1. This leads to the recruitment of pro-caspase 9 into a multi-protein complex with cytochrome C and Apaf-1 called the apoptosome. Formation of the apoptosome leads to activation of caspase 9 and the induction of apoptosis (www.sgul.ac.uk/dept/immunology/~dash).

Role of Caspase proteins in apoptosis

The caspases are a family of proteins that are one of the main executors of the apoptotic process. They belong to a group of enzymes known as cysteine proteases and exist within the cell as inactive pro-forms or zymogens. These zymogens can be cleaved to form active enzymes following the induction of apoptosis[80].

Induction of apoptosis via death receptors typically results in the activation of an initiator caspase such as caspase 8 or caspase 10. These caspases can then activate

other caspases in a cascade. This cascade eventually leads to the activation of the effector caspases such as caspase 3 and caspase 6. These caspases are responsible for the cleavage of the key cellular proteins such as cytoskeletal proteins that leads to the typical morphological changes observed in cells undergoing apoptosis[80].

PROTEIN TYROSINE PHOSPHATASE 1B

Non-insulin-dependent diabetes mellitus (type II) represents 80–90% of the human population. However clinically useful type-II antidiabetic drugs based on PTP1B inhibition are not available at present. Protein Tyrosine Phosphatases (PTPs) act in opposition with protein tyrosine kinases to control the tyrosine phosphorylation levels of proteins. Reversible tyrosine phosphorylation plays an important role in signal transduction and regulation of cell processes such as growth, differentiation, and proliferation. As anticipated from the importance of tyrosine phosphorylation, PTPases are implicated in diverse human diseases including diabetes, obesity, autoimmune diseases, and neurodegeneration. Type II diabetes is believed to be associated with a defect in insulin receptor signaling which begins with the receptor autophosphorylation and the receptor tyrosine kinase activation.

Insulin signaling is negatively regulated by dephosphorylation of the receptor by PTPases and therefore the defect in insulin sensitivity is possibly reversed by the inhibition of the relevant PTPases. The most likely candidates include PTP1B, LAR, PTPa, and SHP-2. Among those, protein tyrosine phosphatase 1B (PTP1B) has been most intensively studied as a target for the development of inhibitors aiming at the treatment of type II diabetes and obesity[81].

Insulin resistance is evident in many tissues that are important for glucose homeostasis including muscle, liver and in fat and at the level of the central nervous system. Metabolic insulin signal transduction occurs through activation of the insulin receptor including autophosphorylation of tyrosine (Tyr) residues in the insulin-receptor activation loop. This leads to recruitment of insulin receptor substrate (IRS) proteins followed by activation of phosphatidylinositol 3-kinase (PI3K) and downstream protein kinase B (PKB also known as AKT) and activation and subsequent translocation of the glucose transporter GLUT4. This process is negatively regulated by Protein Tyrosine Phosphatases (PTPs) and is a general mechanism for

down regulation of Receptor Tyrosine Kinase (RTK) activity. Several PTPs including receptor protein tyrosine phosphatase-α (rPTP-α), leukocyte antigen-related tyrosine phosphatase (LAR), SH_2-domain-containing phosphotyrosine phosphatase (SHP_2) and protein tyrosine phosphatase 1B (PTP1B) have been implicated in modulating insulin signal transduction. PTP1B seems to be a key regulator of insulin-receptor activity that acts at the insulin receptor and at downstream signalling components such as IRS1[82,83].

Genetic evidence

Further evidence links PTP1B to insulin resistance, obesity and type II diabetes mellitus in humans. Reduced insulin sensitivity in omental fat has been thought to contribute to overall insulin resistance and PTP1B expression and activity is elevated in this tissue.

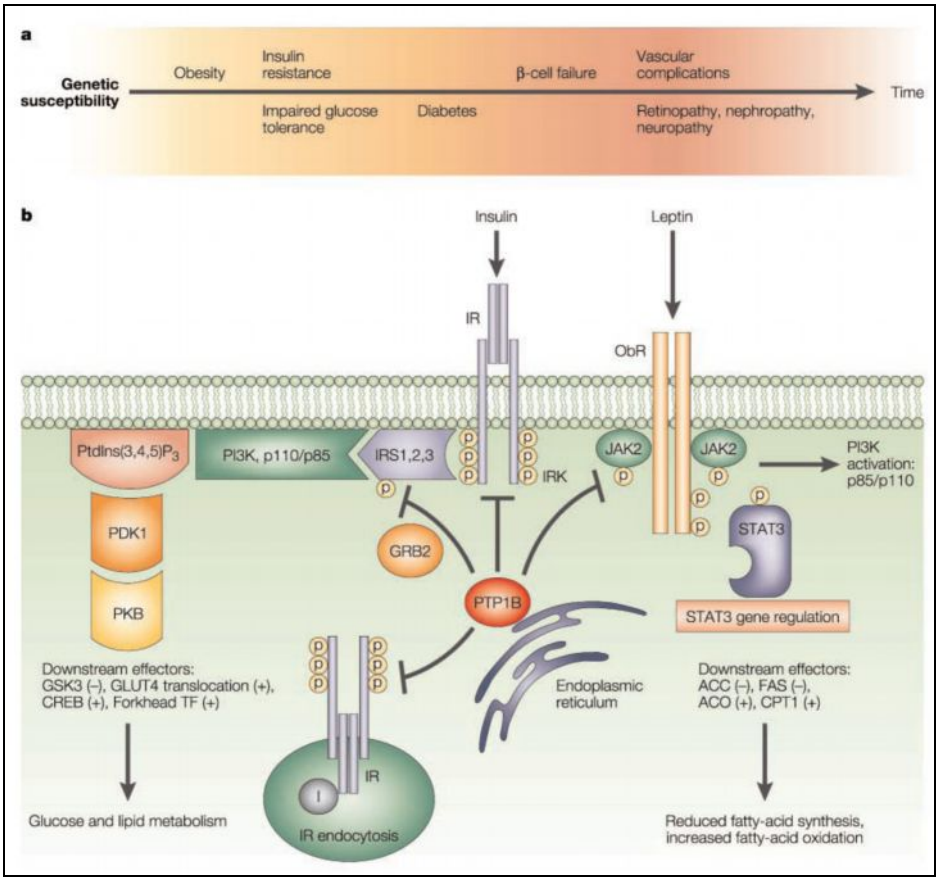

Fig.36 Type 2 diabetes disease-state continuum and regulation of the leptin and insulin signalling pathways by PTP1B - Type 2 diabetes disease-state continuum

The stress of obesity combined with a genetically susceptible background produces insulin resistance and impaired glucose tolerance. Continued stress from hyperinsulinaemia, gluco and lipotoxicity on the pancreatic islet alpha cells results in failure to maintain sufficient insulin levels to compensate for the insulin resistance leading to elevated glucose levels and the diagnosis of diabetes. Microvascular complications become apparent over time depending on how well glucose levels can be controlled. Leptin resistance might have a role in the linkage between obesity and insulin resistance.

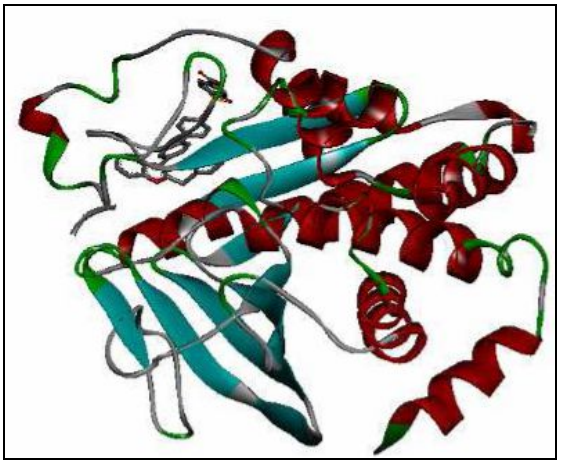

Fig. 37 3D structure of Protein Tyrosine Phosphatase 1B (PTP1B 1SUG)

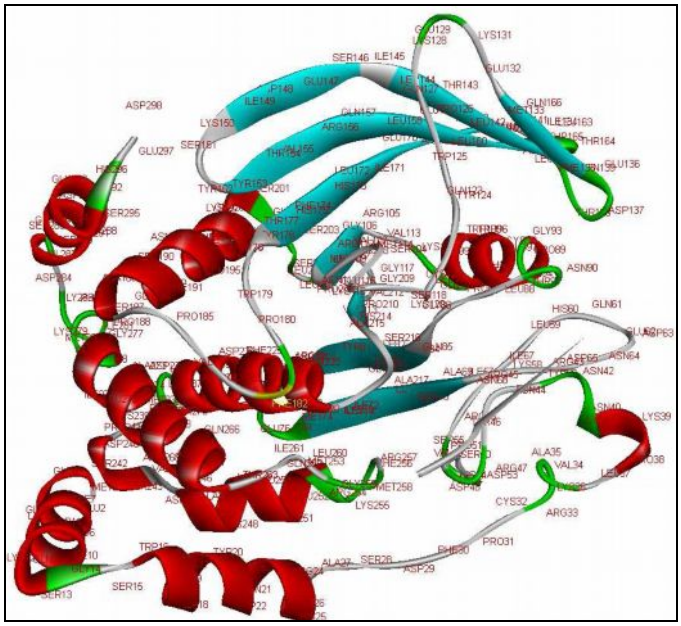

Fig.38 Receptor with all the residue locations labeled

CANCER

In addition to diabetes, cancer is responsible for about one in every four deaths in the United States and is therefore a major public health burden. The American Cancer Society projects that in 2008 over 1.4 million new cases of invasive cancer diagnosed and over 5,65,000 deaths from cancer or more than 1,500 deaths each day. The major cancer mortalities in the U.S. result from cancers of the lung and bronchus, prostate, colon and rectum in men and lung, bronchus, breast, colon and rectum in women. Developing countries are being increasingly afflicted with cancer as their populations live longer and make lifestyle changes associated with increased cancer risk. Accordingly the threat of cancer will be of major concern for the foreseeable future for those in both developed and developing countries[84].

Cancer chemotherapy is an important alternative to surgery and radiation to treat successfully some types of solid tumors, lymphomas and leukemias and many clinically approved cytotoxic and anticancer drugs are available both of synthetic and natural product (microbial and plant) origin. However much progress need to be made to overcome the problems of resistance and toxicity of existing cancer chemotherapeutic agents. It is expected that in the future anticancer drug discovery will need to focus on mechanism-based agents that act on specific molecular targets associated with the etiology of cancer.

Natural product compounds have substantial structural diversity and frequently afford new mechanisms of biological activity. As a result, natural products are used widely in cancer chemotherapy. Accordingly, there is a continued interest in the investigation of extracts of microorganisms, terrestrial plants, and marine life forms to search for further compounds of this type. In a recent analysis of the antineoplastic agents marketed in western countries and Japan, it was revealed that 155 compounds (47%) in total introduced since the 1940s were either unmodified natural products (25 compounds, 16.1%) or semi-synthetic derivatives of natural products (48 compounds, 31.0%). In a recent major volume on promising compounds from nature as anticancer agents there were six major classes from plants, seven from marine organisms and ten from microbes indicating that all types of organisms should be accessed to maximize the likelihood of discovering effective new cancer drugs.

Natural products are recognized as occupying a different region of "chemical space" than typical synthetic compounds and are an excellent source of novel chiral structures for synthetic and combinatorial chemistry modification for drug development. Over 50% of the drugs in clinical trials for antitumor activity were isolated from natural source or related to them. Plant-derived compounds have been an important source of several clinically useful anti-cancer agents. These include vinblastine, vincristine, the camptothecin derivatives, topotecan and irinotecan, etoposide, derived from epipodophyllotoxin, and paclitaxel. A number of promising new agents are in clinical development based on selective activity against cancer-related molecular targets including flavopiridol and combretastin A_4 phosphate[85].

Table-43 Plant derived anticancer agents in clinical use

S.No.	Constituent	Biological source (Family)	Uses
1.	Vincristin & Vinblastin	*Catharanthus roseus* (Apocynaceae)	Lung cancer, Leukemias, Lymphomas
2.	Etoposide & Teniposide Semisynthetic derivative Epipodophyllotoxin	*Podophyllum peltatum* *Podophyllum emodii* (Podophylaceae)	Skin, bronchial & testicular cancer
3.	Taxol	*Taxus brevifolia* (Taxaceae)	Lymphomas, bronchial & testicular
4.	Topotecan & Irinotecan – Derivative of camptothecin	*Camptotheca acuminate* (Nyssaceae)	Ovarian & Lung cancer

One of the best approach in the search for antitumour agents from plant resources is the selection of plant based on ethnomedical leads and testing the selected plants efficacy in appropriate animal model and safety through modern scientific methods.

Table-44 Commonly used Transplantable Tumors[86]

Cancer cells	Animal model	Route of administration
Sarcoma 180/Crocker sarcopme	BALB/C and Random-bred Swiss mice	Subcutaneous
Carcinoma 755/adeno carcinoma 755	Mouse	Subcutaneous
Leukaemia 1210 (L1210)	Mouse DBA strains	Intra peritoneal subcutaneous
Ehlrich ascites	Mouse various strains	Intra peritoneal subcutaneous
Dalton ascites	Mouse various strains	Intra peritoneal subcutaneous
$6C_3$ H-ED, Lymphosarcoma	Mouse C_3 H strains	Injection subcutaneous
Walker adenocarcinoma 256	Rat various strains including Wistar	Subcutaneous

Oxidative stress

Involvement of free radicals and oxidative stress-induced expression of red-ox sensitive factors, cytokines and adhesion molecules leads to the development of various diseases. Free radicals act as signalling intermediate and initiate receptor-mediated activation of intracellular signalling pathways that activate the production of inflammatory chemokines and cytokines. MAPk cascades are activated by various free radicals, cellular stress and growth factors and are involved in several biological responses like cytokines production, differentiation, proliferation and cell death. TNF exerts a variety of biological effects like production of inflammatory cytokines, up-regulation of adhesion molecules, proliferation, differentiation and cell death. It induces free radicals accumulation and also acts as a strong activator of NF-kB. NF-kB is a transcriptional factor that regulates expression of various inflammatory cytokines, chemokines and adhesion molecules and plays an important role in vascular cell functions[86,87].

Free radicals and their generation sites

Hyperphysiological burden of free radicals causes imbalance in homeostatic phenomena between oxidants and antioxidants in the body. This phenomenon leads to oxidative stress that is being suggested as a root cause of various human diseases. Oxidants are generated as a result of normal intracellular metabolism in mitochondria and peroxisomes as well as from a variety of cytosolic enzyme systems. In addition a number of external agents can trigger ROS production. A sophisticated enzymatic and non-enzymatic antioxidant defence system including catalase (CAT), Superoxide Dismutase (SOD) and Glutathione Peroxidase (GPx) counteracts and regulates overall ROS levels to maintain physiological homeostasis. Lowering ROS levels below the homeostatic set point may interrupt the physiological role of oxidants in cellular proliferation and host defence. Similarly increased ROS may also be detrimental and lead to cell death or to acceleration in ageing and age-related diseases. Traditionally, the impairment caused by increased ROS is thought to result from random damage to proteins, lipids and DNA. In addition to these effects, a rise in ROS levels may also constitute a stress signal that activates specific redox-sensitive signalling pathways. Once activated, these diverse signalling pathways may have either damaging or potentially protective functions. (Fig.39)

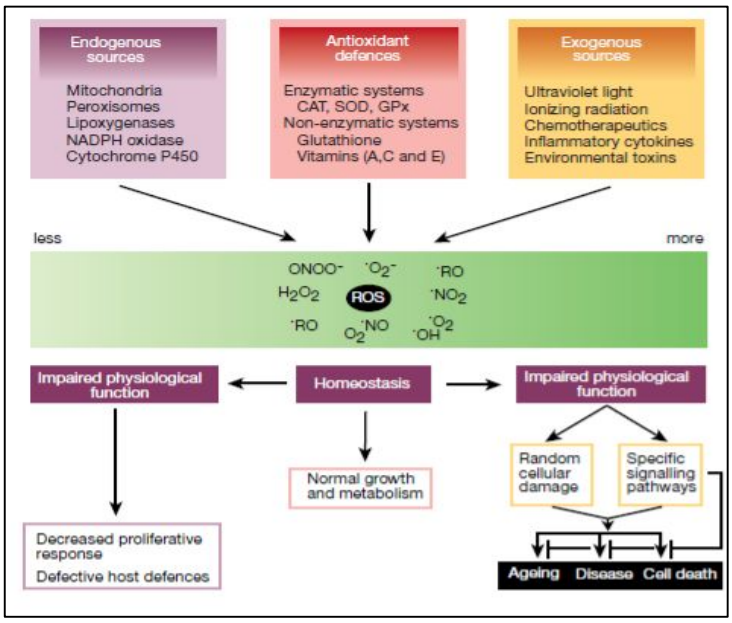

Fig.39 Free radicals and their generation sites

Major signalling pathways activated in response to oxidative stress

ROS can originate outside the cell or may be generated intracellularly in response to external stimuli. Heat shock transcription factor 1 (HSF1), NF-kB and p53 are themselves transcription factors while the PI(3)K/Akt and MAPK pathways regulate transcription factors through phosphorylation. The degree to which a given pathway is activated is highly dependent on the nature and duration of the stress as well as the cell type. The consequences of the response vary widely with the ultimate outcome being dependent on the balance between these stress-activated pathways. HSF1 is responsible for activation of the heat-shock response. Factors depicted in pink represent those pathways whose activities are altered with ageing (Fig.40)[88,89].

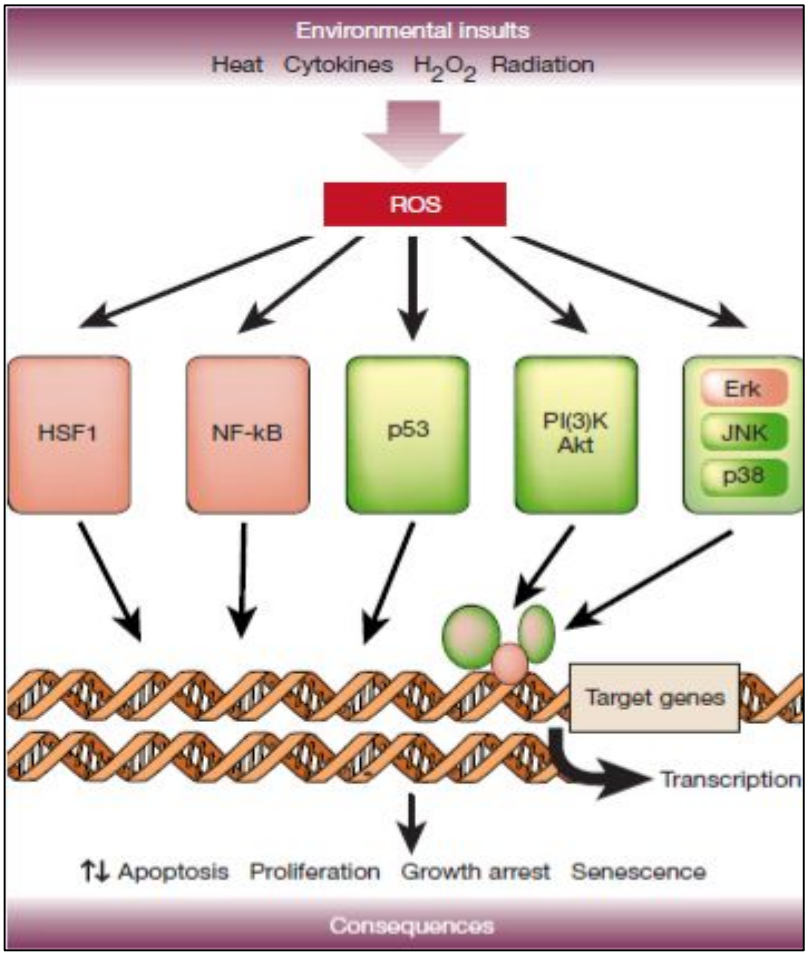

Fig.40 Major signalling pathways activated in response to oxidative stress
Oxidants - Superoxide anions

Super oxide anion is highly reactive and toxic to cell membranes. When oxygen molecule takes up one electron by the univalent reduction it becomes superoxide anion $O_2^{-\cdot}$ It can capture further electrons to form hydrogen peroxide. H_2O_2 is toxic and injurious. Whenever superoxide anion (O_2^-) is formed in tissues, it will lead to the formation of other free radicals like hydroperoxy radical, hydroxyl free radical and hydrogen peroxide[90].

Formation of superoxide anion in metabolic pathways

Cytosolic oxidations by auto oxidizable FP dependent enzymes like xanthine oxidase and aldehyde dehydrogenase. Oxidative deamination by L-amino acid oxidase superoxide anion may be formed when reduced flavins are reoxidised univalently by molecular O_2. It is also formed during univalent oxidations with molecular oxygen in respiratory chain. It can be formed during methaemoglobin formation. It may also form during cytosolic hydroxylation of steroid drugs and xenobitics by Cytochrome P_{450} or Cytochrome P_{448} system. It is also produced during phagocytosis by NADPH oxidase system during respiratory burst when O_2 consumption is increased[91].

Hydrogen peroxide (H_2O_2)

Hydrogen peroxide is the most stable ROS. It is the less reactive and the most readily detected. H_2O_2 may be generated directly by divalent reduction of O_2 or indirectly by univalent reduction of O_2. H_2O_2 is the primary product of the reduction of O_2 by numerous oxidases such as xanthine oxidase, uricase and α-hydroxy acid oxidase localizes in peroxisome. The H_2O_2 is decomposed to H_2O and O_2. H_2O_2 like most peroxides is very sensitive to decomposition by the species that react with it. The reaction is catalysed by redox-active metal complexes of which catalase and peroxidase are the most effective exponents. Experiments with antioxidants enzymes show that hydrogen peroxide rather than super oxide anion is the most essential species to induce cell injury. H_2O_2 has been known to cause DNA damage in the form of chromosomal aberrations.

Hydroxyl radical (OH)

Hydroxyl is highly reactive**.** It can react with practically any molecule present in cells and is short lived. This insufficient stability does not allow it to diffuse through the cells. Therefore it reacts with organic substrates at the sites or near the sites of its formation. The life span of OH radical at 370˚C is 10^{-9} seconds. The reactions of OH radical are thus site specific. OH radical is produced following the reaction of O_2 and H_2O_2 in presence of metallic ions like ferrous and copper ions. They are very susceptible to OH radical attack and initiates LPO. OH radical is the most potent among ROS reacting with a wide lipid range of macromolecules at a high rate constant. OH radical is known to induce conformational changes in DNA including strand breaks base modifications.

Nitric oxide (NO)

Nitric oxide is an inorganic free radical gas containing odd number of electrons and can form covalent link with other molecules by sharing a pair of electrons. It is synthesized by a family of isoenzymes called nitric oxide synthase located in various tissues and play an active role in free radical mediated diseases. It regulates numerous physiological process including neurotransmission, smooth muscle contractility, platelet reactivity and the cytotoxic activities of immune cells. Moreover it may have a role in carcinogenesis by inducing DNA strand breaks. NO can stimulate O_2, H_2O_2 and OH induced Lipid Peroxidation.

Lipid peroxidation

Lipid peroxidation (LPO) can be defined as the oxidative deterioration of lipids that contain a large number of carbon-carbon double bonds. Toxic by products called “second messengers” are formed due to LPO as membrane lipids are susceptible to it. Since membranes form the basis of cellular organelles like mitochondria, endoplasmic reticulum, plasma membrane, peroxisomes, lysozomes etc. The damage caused by the LPO is highly detrimental to the functioning of the cell and its survival LPO alters the biophysical properties of the cell membranes, decreases the membrane fluidity and decreases the electrical resistance. Cross linking also occurs which resists the mobility of the membrane proteins. Leakage of cytosolic

enzymes may also occur on extensive peroxidative attack. An iron induced lipid peroxidation process is described as peroxidative sequence initiated by the attack of an unsaturated lipid by any species that attracts hydrogen atom from a methylene group which leaves an unpaired electron to the carbon atom. The resultant carbon radical is stabilized by molecular rearrangement to produce a conjugated diene. It readily reacts with an oxygen molecule forming peroxyl radical that attracts hydrogen from the lipids which is further degraded in presence of iron and breaking into malondialdehyde and other such end products.

RESULTS AND DISCUSSION

Table-45 Acute toxicity study

S. No.	Group (n=6)	Dose	Signs of toxicity	On set of toxicity	Duration of observation
1.	Ethanolic extract	2 gms/kg	No toxicty	Nil	3 days
2.	Ethyl acetate fraction	2 gms/kg	No toxicty	Nil	3 days

Table-46 Effect of ethanolic extract from the root and rhizome of *Nymphaea pubescens* on oral glucose tolerance test

Groups (n=6)	**Treatment**	**Blood glucose level** (mg/dl)			
		30 mins.	**60 mins.**	**90 mins.**	**120 mins.**
I	Normal control (5ml-0.05% Tween 80/ kg b.w)	85.00 ± 0.81	111.13 ± 0.60	105.27 ± 0.76	97.2 ± 1.30
II	Glibenclamide (0.25mg/kg b.w)	183.00 ± 0.81	94.30 ± 0.71	82.00 ± 0.82	73.30 ± 0.66**
III	Ethanolic extract (200mg/Kg b.w)	193.2 ± 0.19	156.30 ± 1.11	126.00 ± 0.51	94.67 ± 1.16**
IV	Ethanolic extract (400mg/Kg b.w)	186.50 ± 0.76	155.20 ± 0.94	120.70 ± 1.90	83.17 ± 0.61**

Values given as Mean ± SEM, p** → <0.05 when compared with normal control

Fig.41 Effect of ethanolic extract from the root and rhizome of *Nymphaea pubescens* on oral glucose tolerance test

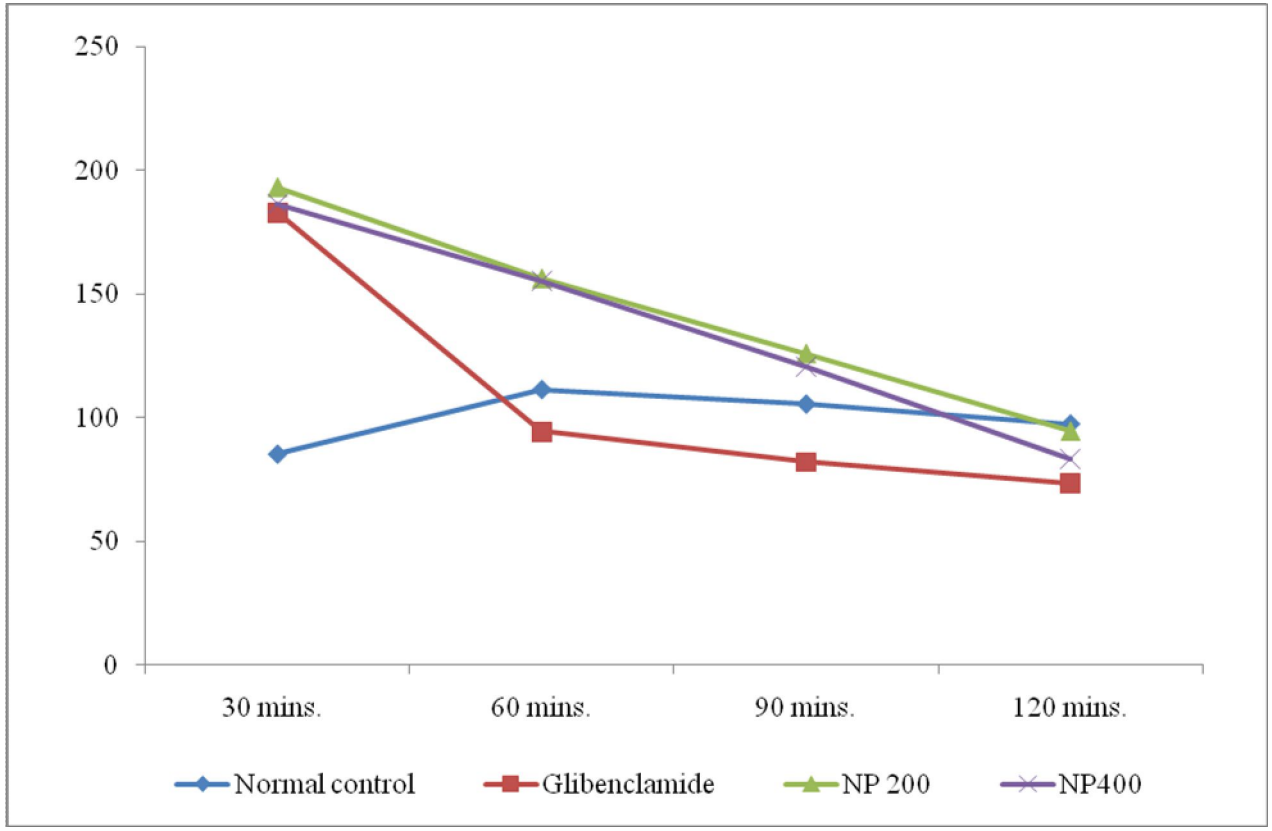

Table-47 Effect of the ethanolic extract from the root and rhizome of *Nymphaea pubescens* on blood sugar level and glycosylated Hemoglobin

Groups (n=6)	Treatment	Blood sugar level (mg/dl)		Glycosylated Hemoglobin
		0 day	21st day	(% Hb)
I	Normal control (5ml-0.05% Tween 80/ kg b.w)	85.00 ± 0.81	82.83 ± 0.60	7.05 ± 0.05
II	Diabetes induced (5ml-0.05% Tween 80 / kg b.w)	183.00 ± 0.81	201.30 ± 0.71	14.12 ± 0.41
III	Diabetes induced+ Glibenclamide (0.25mg/kg b.w)	186.50 ± 0.76	75.20 ± 0.94***	6.13 ± 0.21***
IV	Diabetes induced+ Ethanolic extract (200mg/Kg b.w)	185.8 ± 0.60	95.00± 0.57***	8.28 ± 0.56***
V	Diabetes induced+ Ethanolic extract (400mg/Kg b.w)	193.2 ± 0.19	86.30 ± 1.11***	7.18 ± 0.37***

Values given as Mean ± SEM, p*** → <0.001 when compared with diabetic control

Fig.42 Effect of the ethanolic extract from the root and rhizome of *N. pubescens* on blood sugar level and glycosylated Hemoglobin

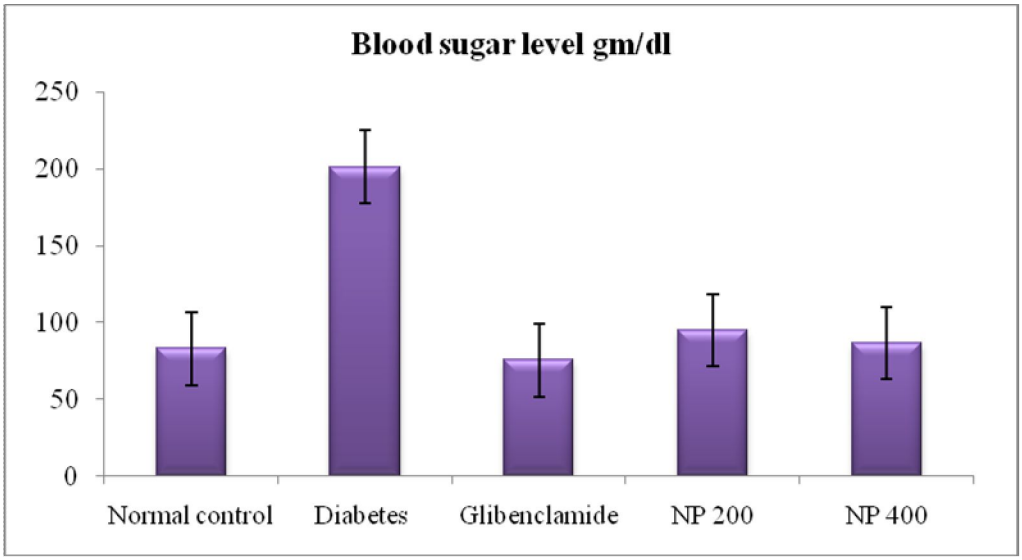

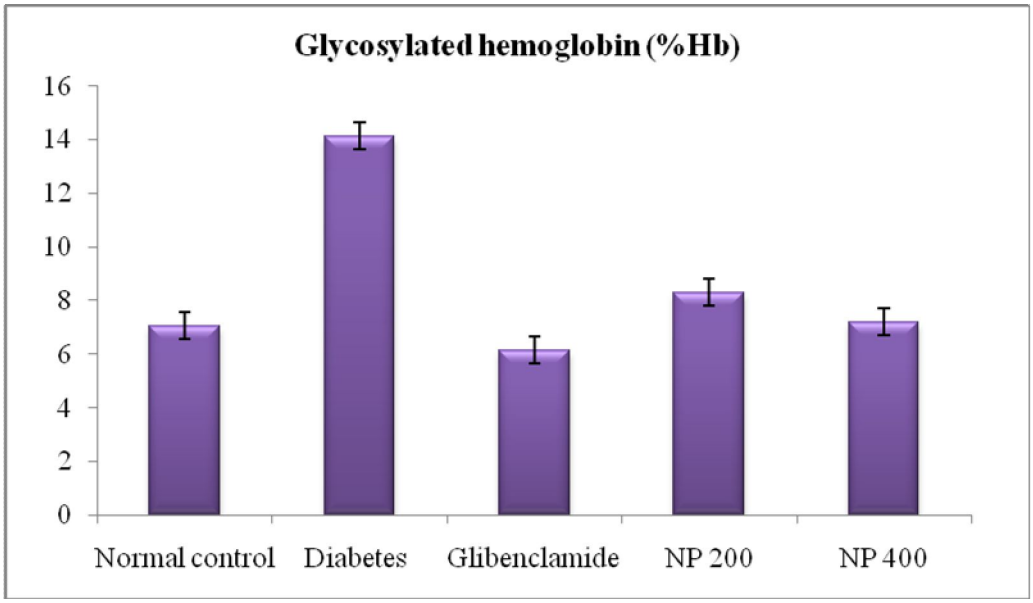

Table-48 Effect of ethanolic extract from the root and rhizome of *Nymphaea pubescens* on body weight, urine sugar and glycogen content

Groups (n=6)	Treatment	Body weight (g)		Urine sugar		Glycogen content (mg/g)
		0 day	21st day	0 day	21st day	
I	Normal control (5ml-0.05% Tween 80/ kg b.w)	130.80 ± 0.61	130.00 ± 0.57	Nil	Nil	12.50 ± 0.76
II	Diabetes induced (5ml-0.05% Tween 80 / kg b.w)	195.40 ± 0.61	161.00 ± 0.57	+	+	5.16 ± 0.60
III	Diabetes induced + Glibenclamide (0.25mg/kg b.w)	120.40 ± 0.73	135.30 ± 0.42***	+	Nil	12.17 ±0.60***
IV	Diabetes induced + Ethanolic extract (200mg/Kg b.w)	130.50± 0.76	137.00 ± 0.57***	+	Nil	10.50 ± 0.42***
V	Diabetes induced + Ethanolic extract (400mg/Kg b.w)	121.80 ± 0.61	133.30 ± 0.42***	+	Nil	11.51 ± 0.42***

Values given as Mean ± SEM, p*** → <0.001 when compared with diabetic control

Fig.43 Effect of ethanolic extract from the root and rhizome of *N. pubescens* on body weight, urine sugar and glycogen content

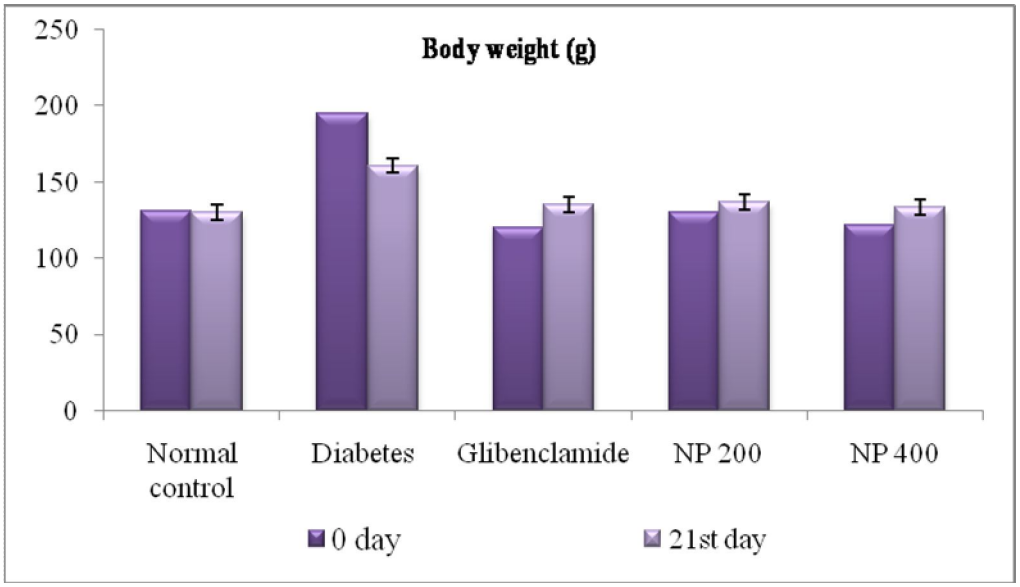

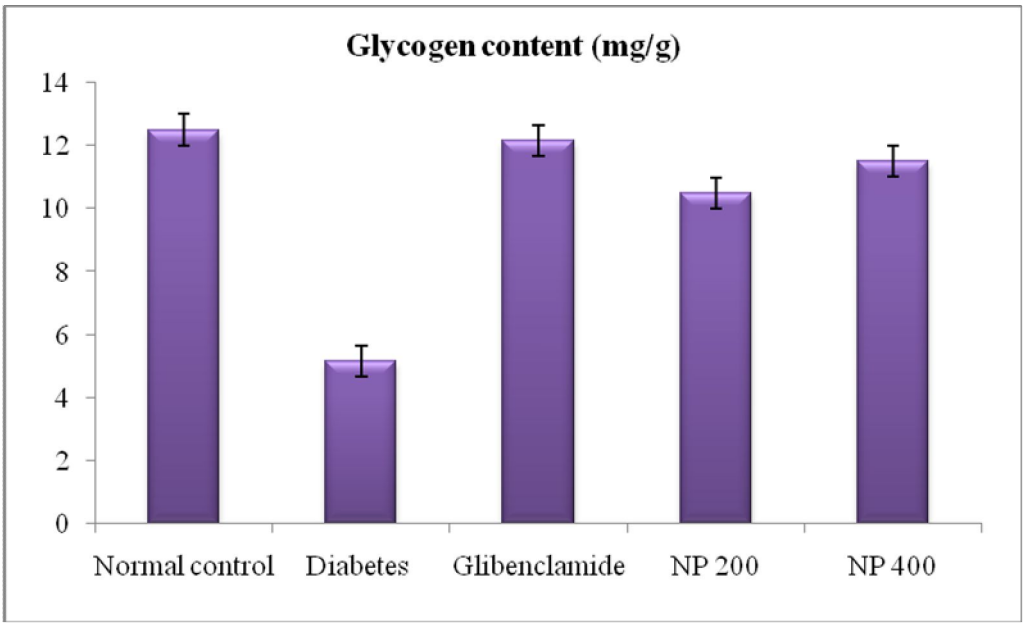

Table-49 Effect of the ethanolic extract from the root and rhizome of *Nymphaea pubescens* on lipid profile

Group (n=6)	**Treatment**	**Triglycerides** (mg/dl)	**Total cholesterol** (mg/dl)	**High density lipoprotein** (mg/dl)	**Low density lipoprotein** (mg/dl)	**Very low density lipoprotein** (mg/dl)
I	Normal control (5ml-0.05% Tween 80/ kg b.w)	77.0±0.57	57.17±0.47	78.5±0.76	47.83±0.60	16.17±0.60
II	Diabetes induced (5ml-0.05% Tween 80 / kg b.w)	150.2±0.60	120.2±0.60	30.67±0.42	160.2±0.60	27.00±0.58
III	Diabetic + Glibenclamide (0.25mg/kg b.w)	78.33±0.76***	55.5±0.76***	75.5±0.42***	54.33±0.47***	16.71±0.60***
IV	Diabetic + Ethanolic extract (200mg/Kg b.w)	86.00±1.26***	67.00±0.57***	64.83±0.71***	68.50±0.42***	19.67±0.49***
V	Diabetic + Ethanolic extract (400mg/Kg b.w)	84.50±0.42***	60.17 ±0.60***	70.50±0.42***	61.50±0.42***	18.83±0.30***

Values given as Mean ± SEM, p*** → <0.001 when compared with diabetic control

Fig.44 Effect of the ethanolic extract from the root and rhizome of *Nymphaea pubescens* on lipid profile

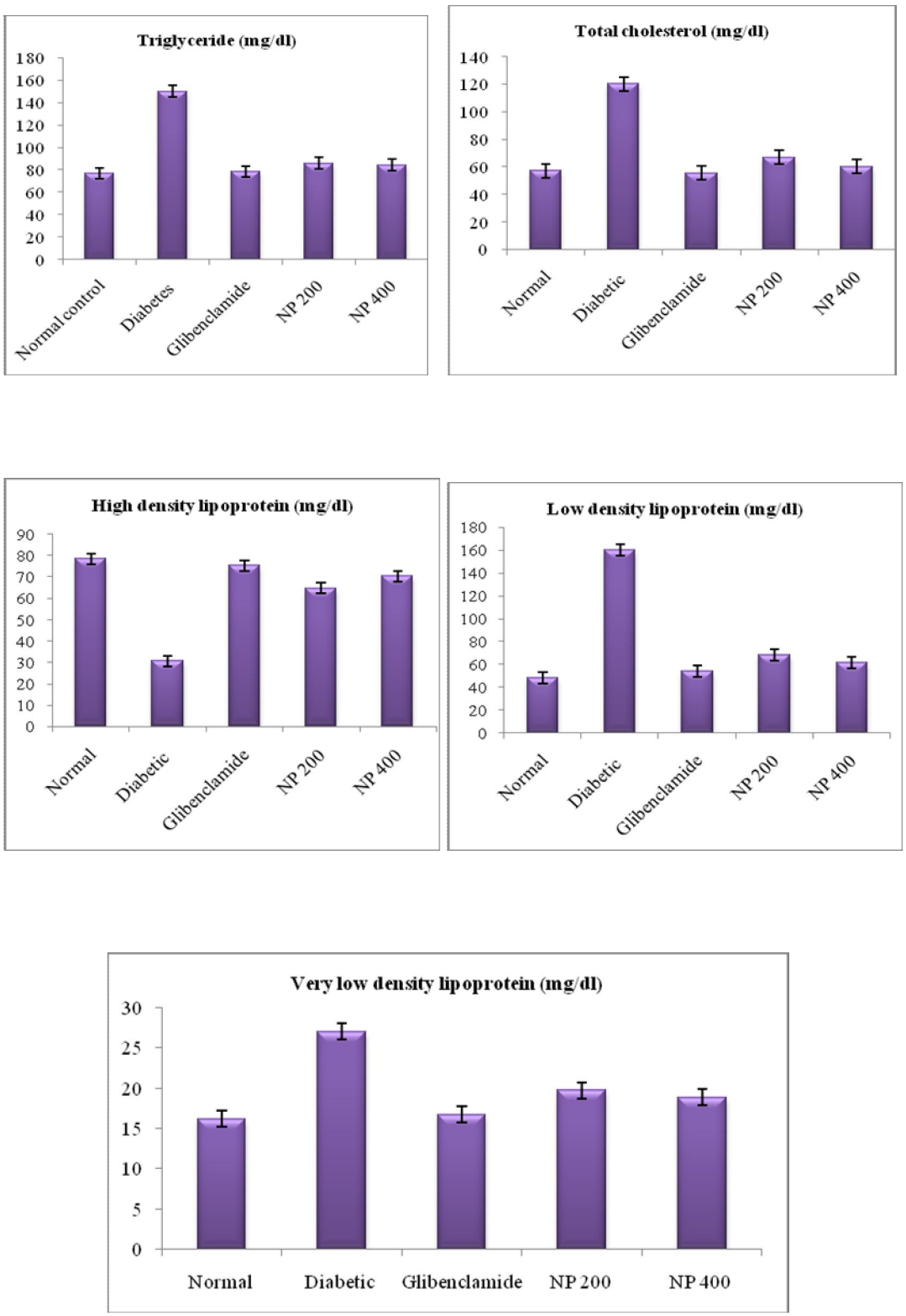

Table-50 Level of protein, urea, creatinine and uric acid in control and experimental groups of rats

Groups (n=6)	**Treatment**	**Total Protein** (gm/dl)	**Blood urea** (mg/dl)	**Serum creatinine** (mg/dl)	**Uric acid** (mg/dl)
I	Normal control (5ml-0.05% Tween 80/ kg b.w)	9.00±0.57	23.50±0.76	0.48±0.042	2.52±0.075
II	Diabetes induced (5ml-0.05% Tween 80 / kg b.w)	6.00±0.51	43.67±0.71	1.22±0.04	6.36±0.049
III	Diabetes induced + Glibenclamide (0.25mg/kg b.w)	8.83±0.54***	23.67±0.66***	0.51±0.06***	2.63±0.061***
IV	Diabetes induced + Ethanolic extract (200mg/Kg b.w)	7.61±0.66***	26.33±0.88***	0.58±0.06***	3.86±0.06***
V	Diabetes induced + Ethanolic extract (400mg/Kg b.w)	8.16±0.60***	24.50±0.76***	0.55±0.04***	3.08±0.03***

Values given as Mean ± SEM, p*** → <0.001 when compared with diabetic control

Fig. 45 Level of protein, urea, creatinine and uric acid in control and experimental groups of rats

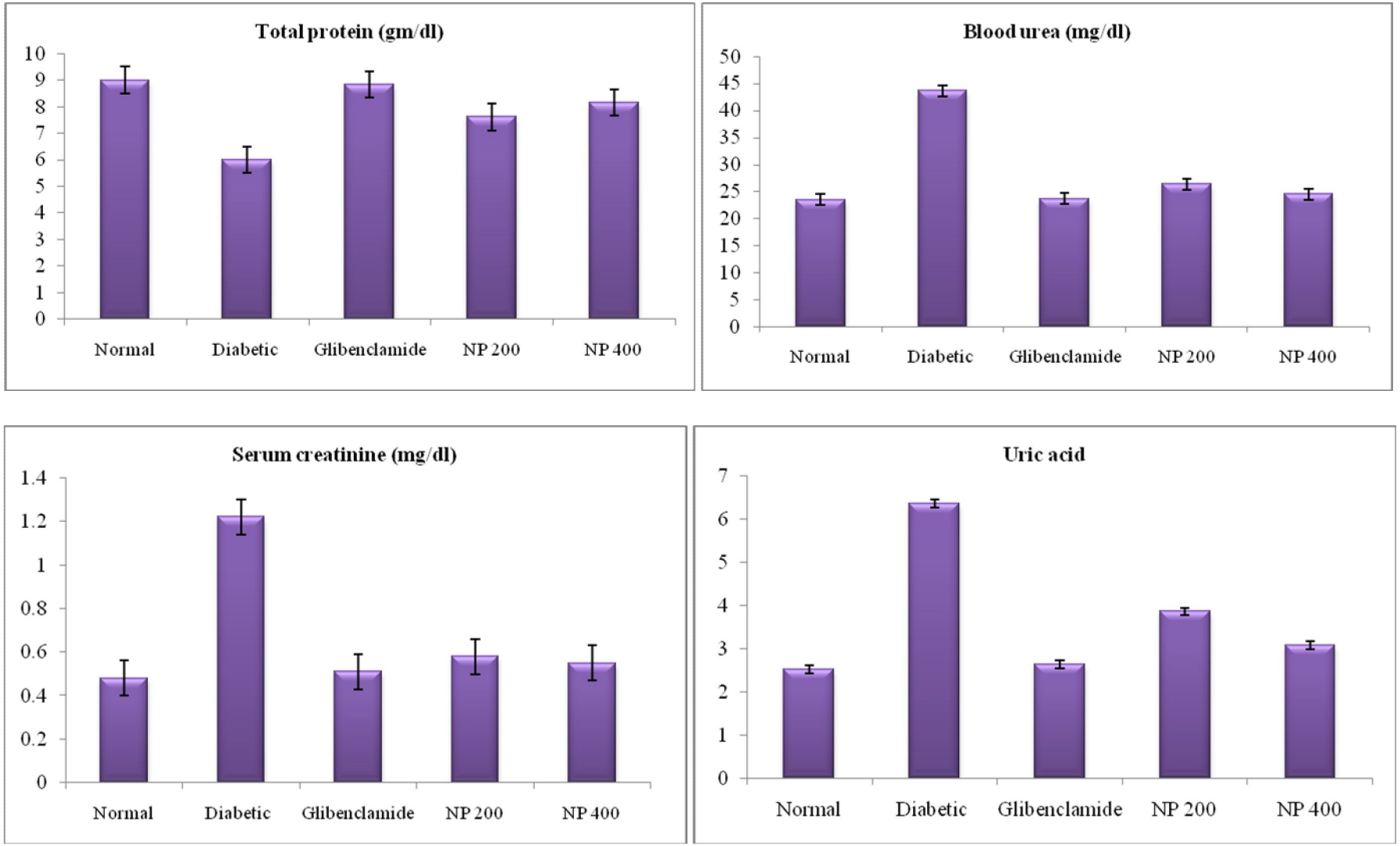

Table-51 Changes in the activities of hepatic and renal glycolytic enzymes in control and experimental animals

Groups (n=6)	Treatment	Hexokinase (n moles of glucose utilised/min/mg protein)		Phosphoglucoisomerase (n moles of fructose formed/min/mg protein)		Aldolase (n moles of glyceraldehydes formed/min/mg protein)	
		Hepatic	**Renal**	**Hepatic**	**Renal**	**Hepatic**	**Renal**
I	Normal control (5ml-0.05% Tween 80/ kg b.w)	1.58±0.04	0.29±0.05	4.45±0.08	7.12±0.116	71.72±0.78	77.55±0.69
II	Diabetes induced (5ml-0.05% Tween 80 / kg b.w)	0.83±0.03	0.13±0.006	0.68±0.047	2.53±0.170	23.30±0.35	36.80±0.64
III	Diabetic + Glibenclamide (0.25mg/kg b.w)	1.7±0.08***	0.29±0.006***	4.88±0.175***	6.51±0.07***	71.42±0.49***	79.28±0.58***
IV	Diabetic + Ethanolic extract (200mg/Kg b.w)	1.43±0.08***	0.19±0.003**	4.18±0.079***	5.87±0.059***	69.82±0.51***	68.52±1.16***
V	Diabetic + Ethanolic extract (400mg/Kg b.w)	1.51±0.05***	0.25±0.007***	4.31±0.11***	6.43±0.09***	70.84±0.39***	76.81±0.78***

Values given as Mean ± SEM, p*** → <0.001 when compared with diabetic control, p** → <0.05 when compared with diabetic control

Fig.46 Changes in the activities of hepatic and renal glycolytic enzymes in control and experimental animals

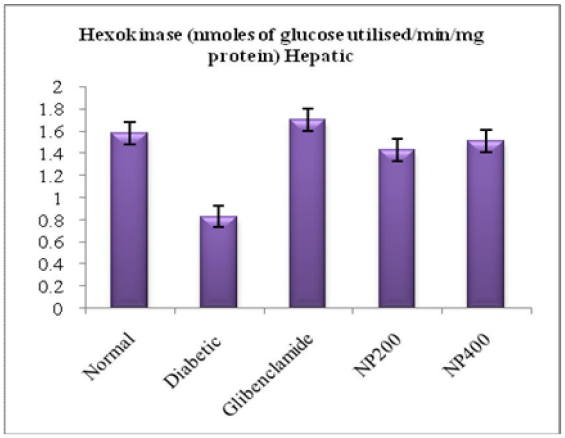

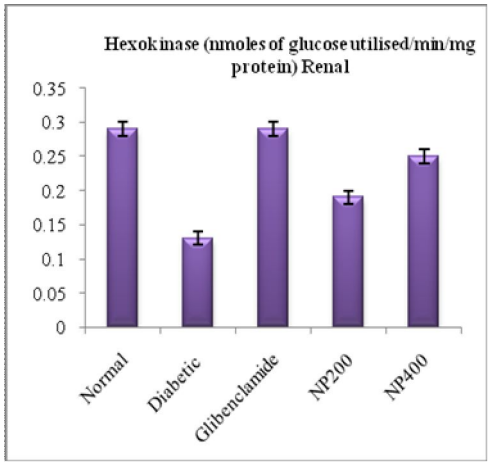

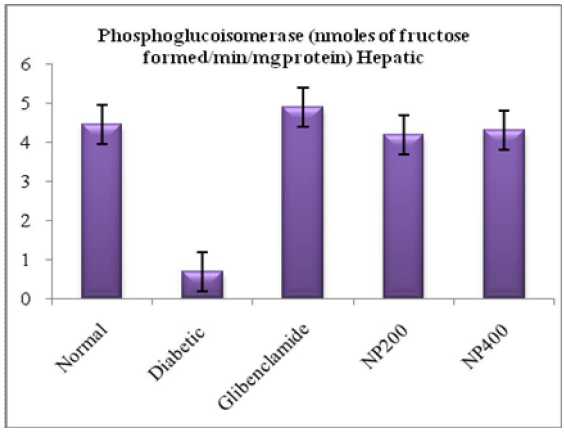

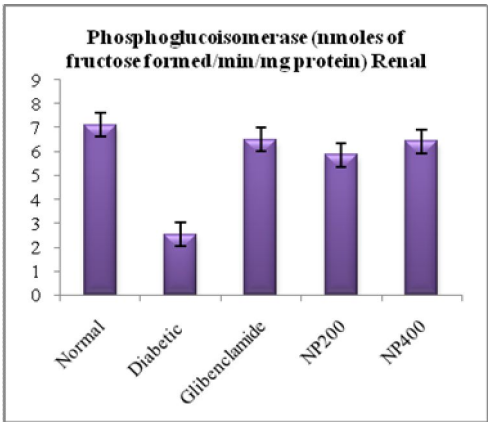

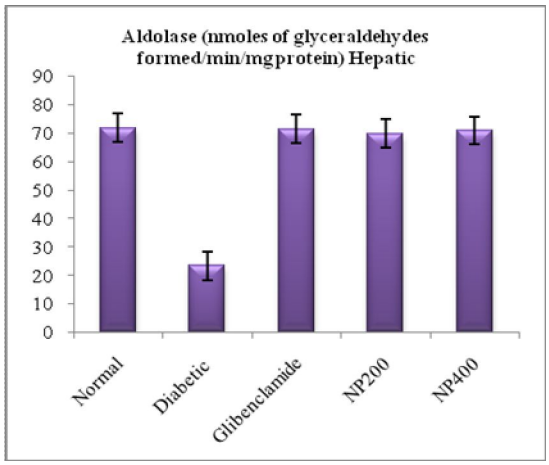

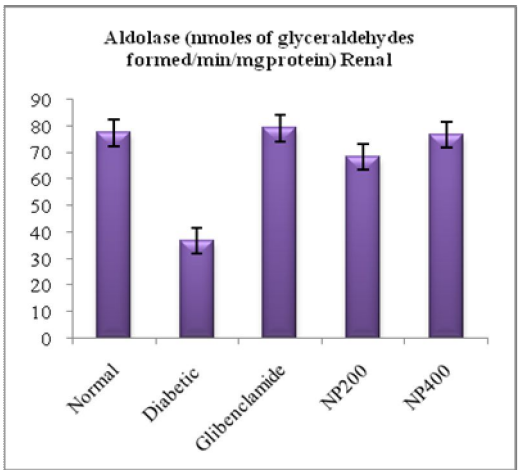

Table-52 Changes in the activities of hepatic and renal gluconeogenic enzymes in control and experimental animals

Groups (n=6)	Treatment	Fructose 1,6-bis phosphatase (µ moles of PO_4 liberated/min/mg protein)		Glucose 6 phosphatase (n moles of PO_4 liberated/min/mg protein)
		Hepatic	**Renal**	**Hepatic**
I	Normal control (5ml-0.05% Tween 80/ kg b.w)	0.0043±0.0004	0.0087±0.0031	1.24±0.019
II	Diabetes induced (5ml-0.05% Tween 80 / kg b.w)	0.0086±0.0002	0.0103±0.00023	1.95±0.013
III	Diabetes induced + Glibenclamide (0.25mg/kg b.w)	0.0032±0.00019***	0.0082±0.00015***	1.23±0.0414***
IV	Diabetes induced + Ethanolic extract (200mg/Kg b.w)	0.0053±0.00027*	0.0069±0.00027***	1.33±0.0115***
V	Diabetes induced + Ethanolic extract (400mg/Kg b.w)	0.004±0.0017***	0.0075±0.00013***	1.26±0.0167***

Values given as Mean ± SEM,
p*** → <0.001 when compared with diabetic control
p* → <0.01 when compared with diabetic control

Fig.47 Changes in the activities of hepatic and renal gluconeogenic enzymes in control and experimental animals

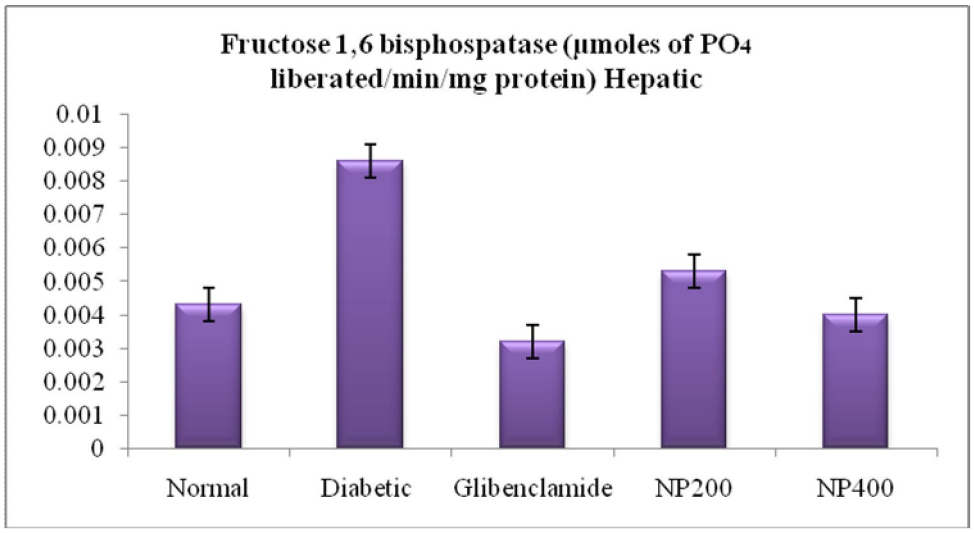

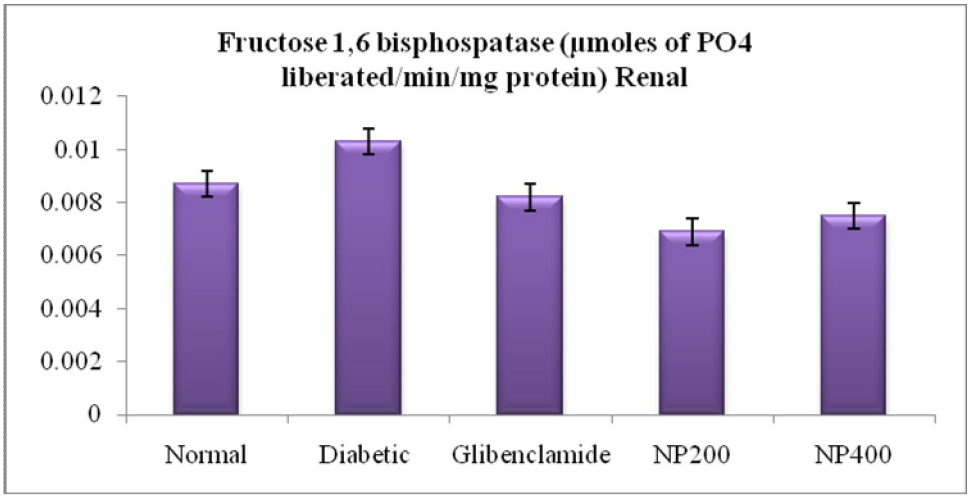

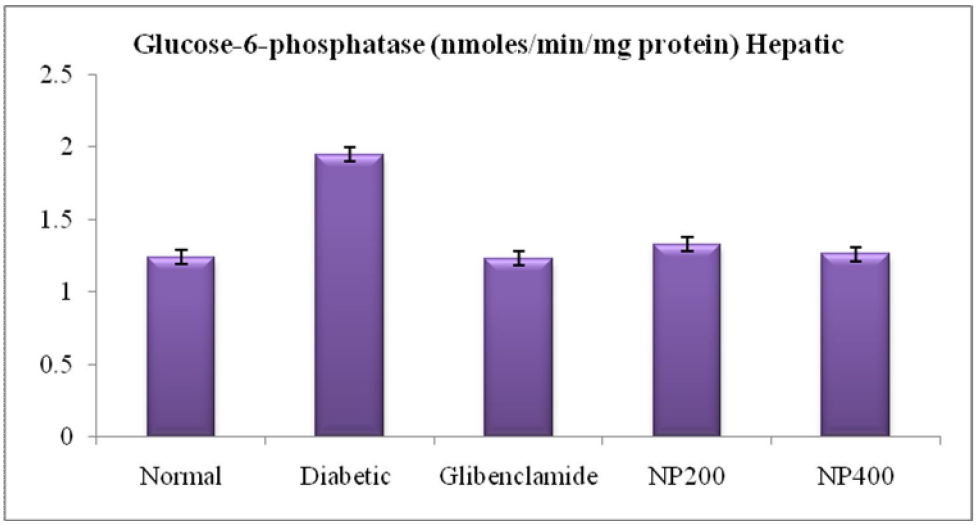

Fig.48 Histopathology of pancreas

(Haematoxylin and Eosin stained)

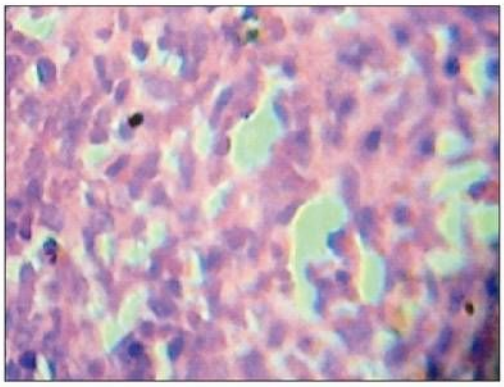

Histology of the pancreas of control rat showing normal cell Architecture (45X)

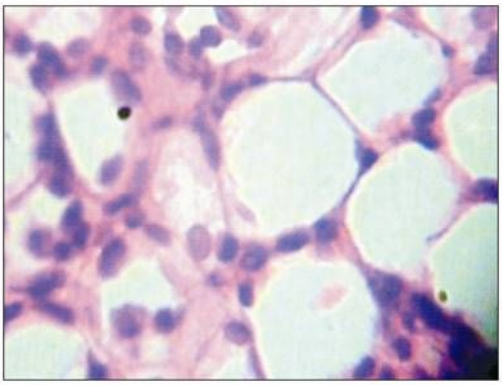

Histology of the pancreas of diabetic rats shows massive cell Necrosis (10X)

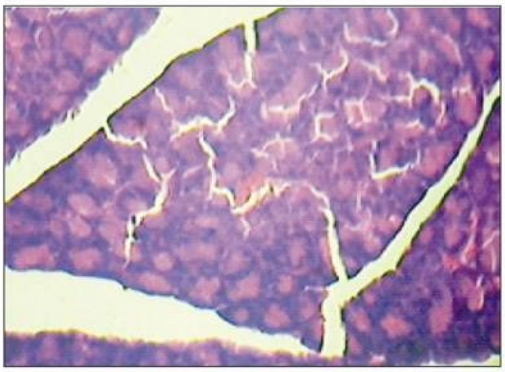

Histology of the pancreas of diabetic rats administered with Glibenclamide shows regeneration of cells (10X)

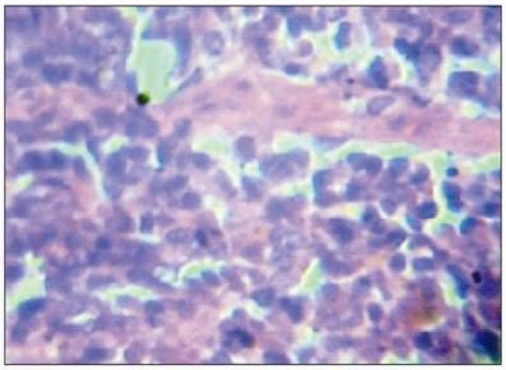

Histology of pancreas of diabetic rats administered with *N. pubescens* (200mg) shows regeneration with patchy necrosis (10X)

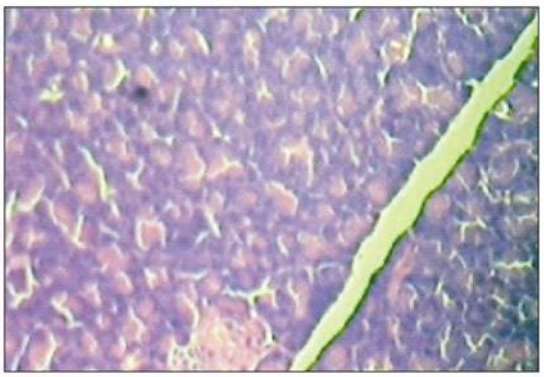

Histology of pancreas of diabetic rats administered with *Nymphaea pubescens* (400mg) shows regeneration of cells similar to Glibenclamide (10X)

Fig. 49 Polyacrylamide Gel Electrophoresis of tissue homogenate

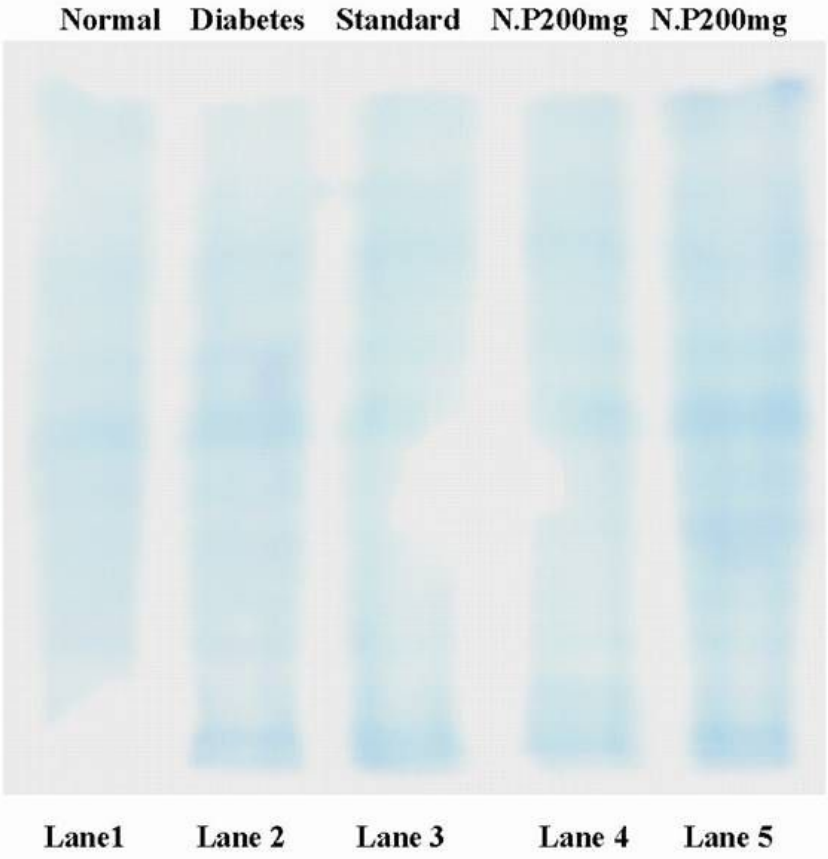

Fig. 50 Western Blot of Caspase-3

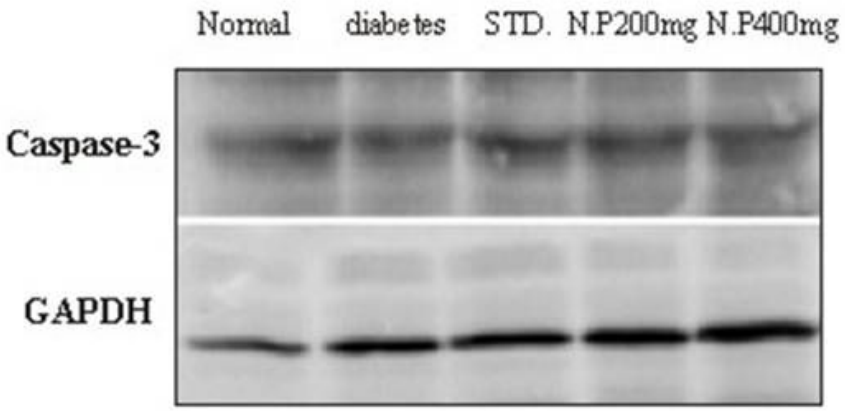

Fig. 51 Western Blot of Bcl-2

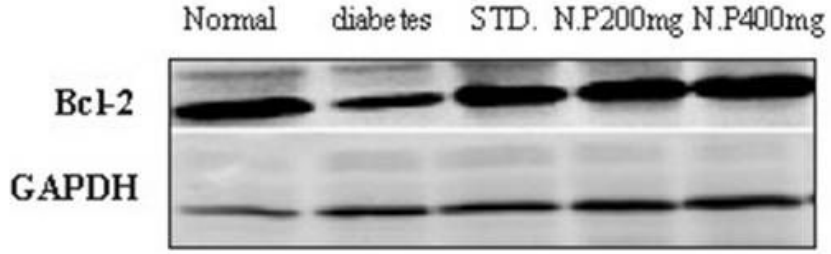

Table-53. Intensity of proteins

Groups (n=6)	Treatment	Bcl-2 µg protein	Caspase-3 µg protein	GAPDH µg protein
I	Normal control (5ml-0.05% Tween 80/ kg b.w)	8103.93	8328.84	12550.19
II	Diabetes induced (5ml-0.05% Tween 80 / kg b.w)	4126.28	10446.64	13120.00
III	Diabetic + Glibenclamide (0.25mg/kg b.w)	8962.36	11387.12	22746.91
IV	Diabetic + Ethanolic extract (200mg/Kg b.w)	8089.15	11726.66	24713.82
V	Diabetic + Ethanolic extract (400mg/Kg b.w)	7845.48	11151.91	21008.29

Values given as an average of triplicate

Table-54 Relative intensity of proteins

Groups	Treatment	BCl-2 (%)	Caspase-3 (%)
I	Normal control (5ml-0.05% Tween 80/ kg b.w)	44.5±7.71	66.36±7.37
II	Diabetes control (5ml-0.05% Tween 80 / kg b.w)	31.45±3.49	79.62±8.84
III	Diabetic + Glibenclamide (0.25mg/kg b.w)	39.40±4.37*	50.06±5.56***
IV	Diabetic + Ethanolic extract (200mg/Kg b.w)	40.81±3.31*	53.08±5.89***
V	Diabetic + Ethanolic extract (400mg/Kg b.w)	39.23±4.14***	42.49±4.72***

Values given as Mean ± SD,

p*** → <0.001 when compared with diabetic control

p** → <0.05 when compared with diabetic control

p* → <0.01 when compared with diabetic control

Fig.52 Relative intensity of proteins

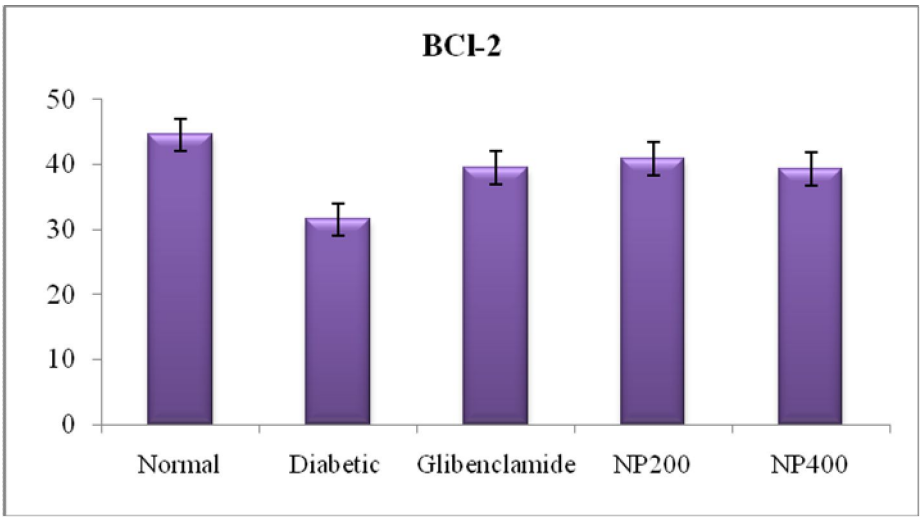

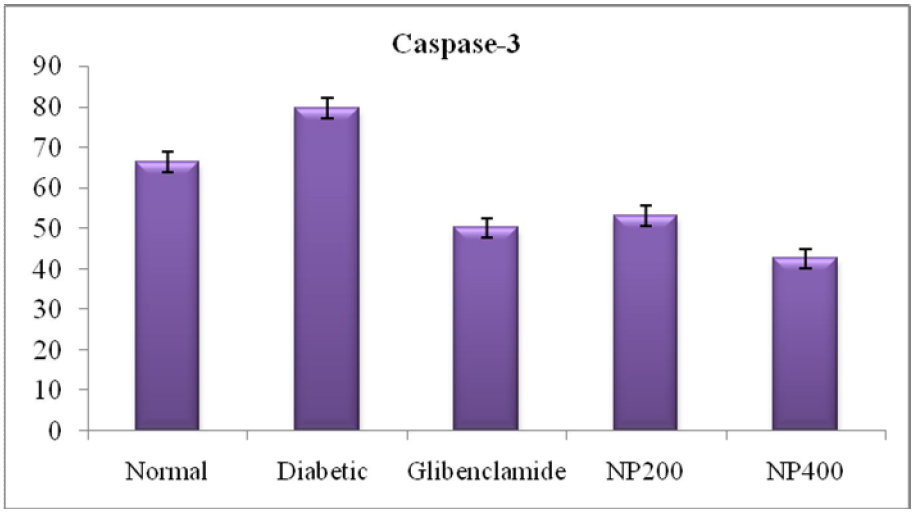

Fig.53 Binding mode of 10-Oxoundecanoic acid in the active site of PTP1B viewed through autodock 4.0.1

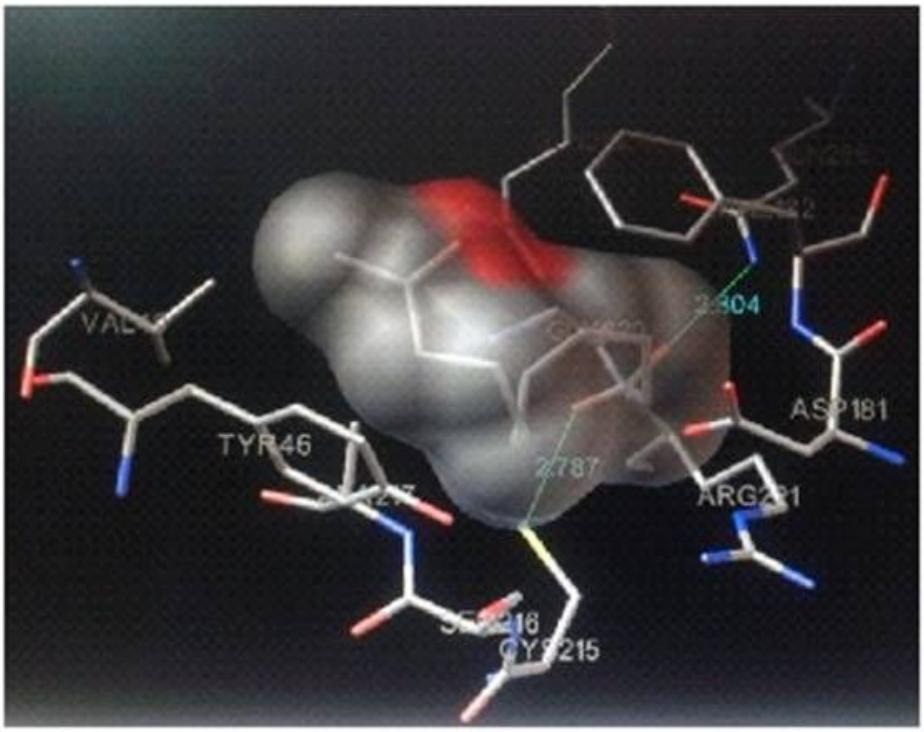

Fig.54 Binding mode of 10-oxoundecanoic acid in the active site of PTP1B viewed through USF chimera software

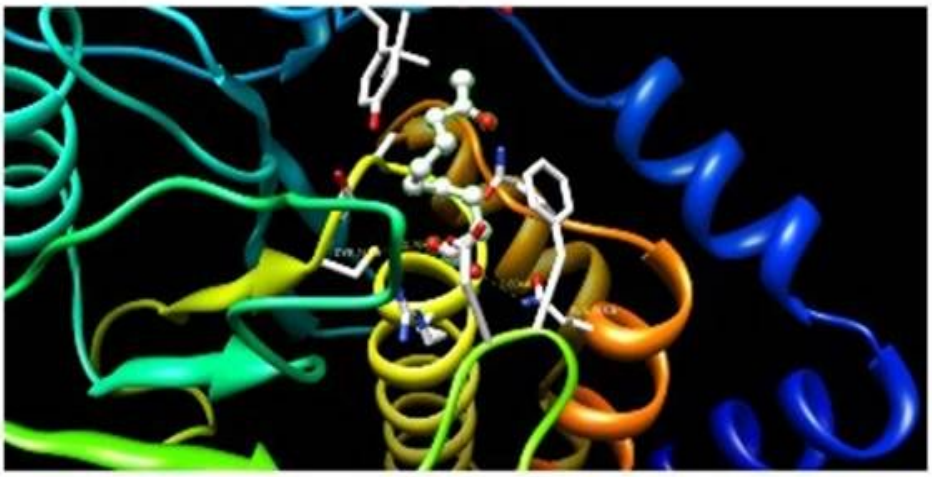

Fig.55 Enlarged view of 10-Oxoundecanoic acid in the active site of PTP1B through USF Chimera software

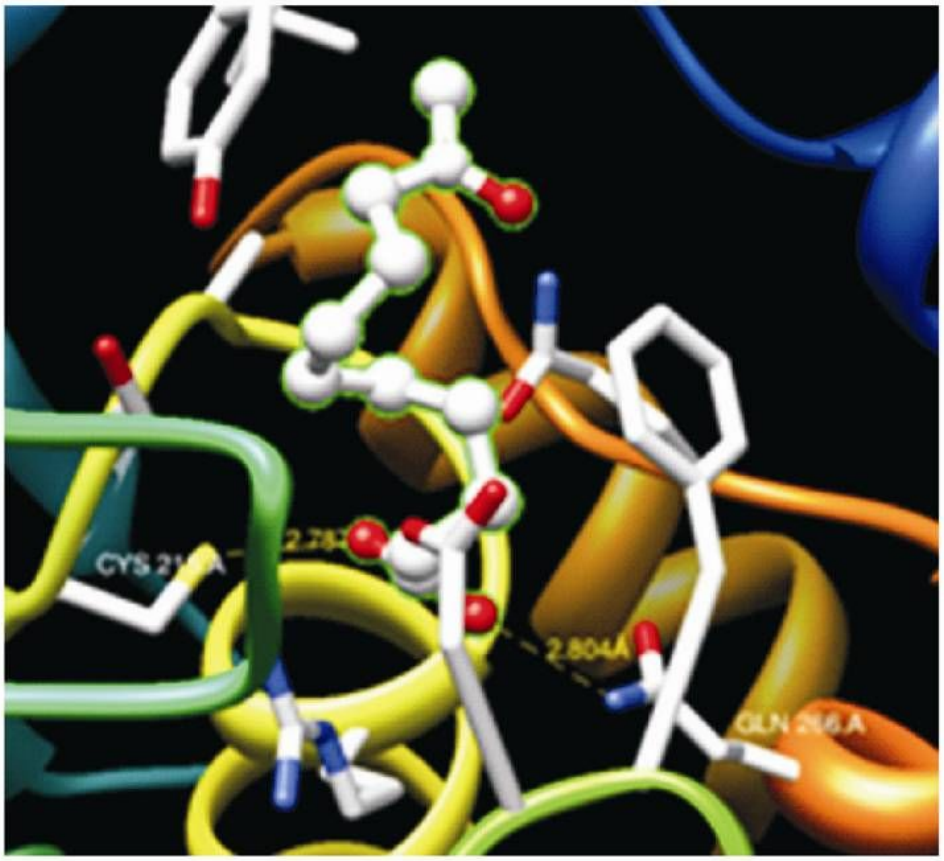

Fig. 56 Binding mode of 14-Oxopentadec-9-enoic acid in the active site of PTP1B viewed through autodock 4.0.1

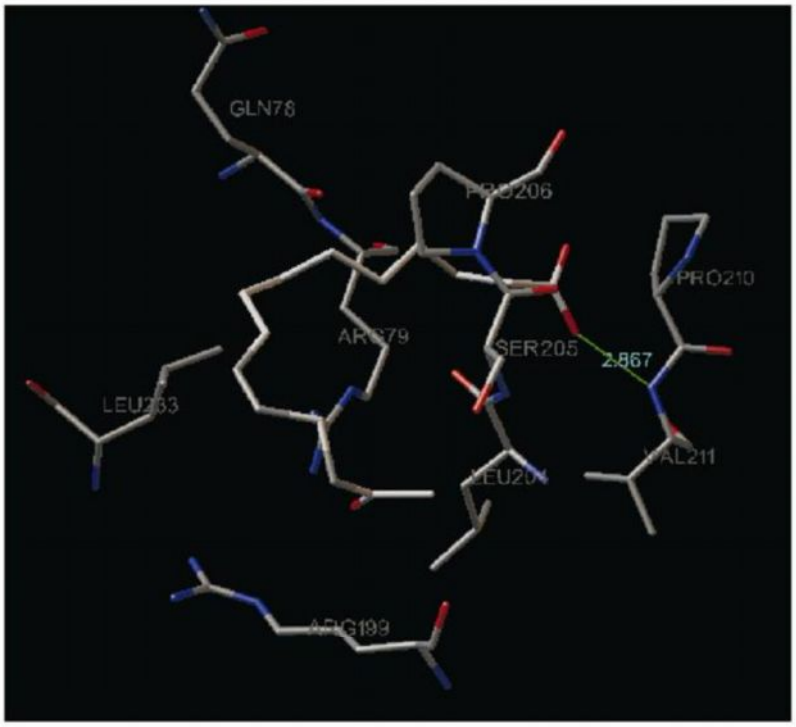

Fig.57 Binding mode of 14-Oxopentadec-9-enoic acid in the active site of PTP1B viewed through USF chimera softeware

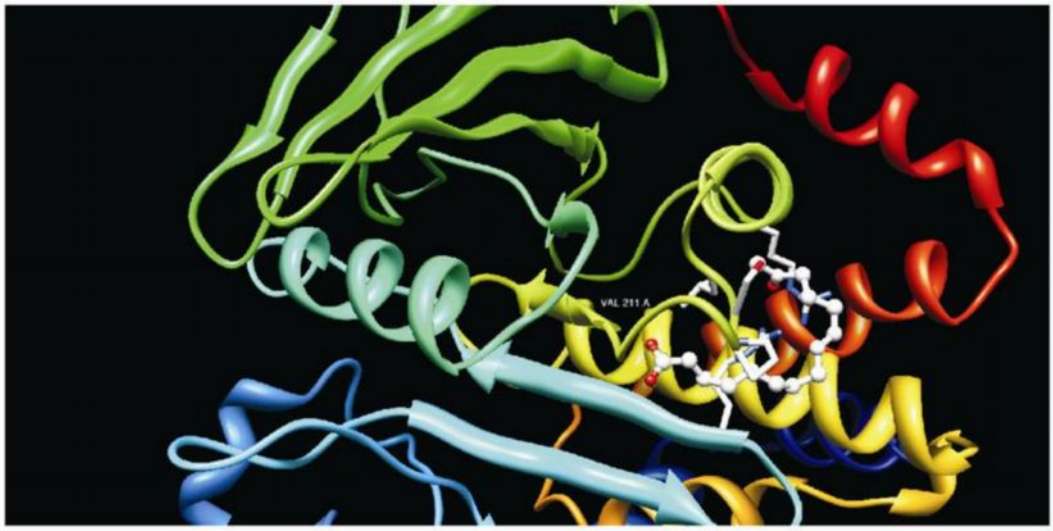

Fig.58 Enlarged view of 14-Oxopentadec-9-enoic acid in the active site of PTP1B through USF chimera software

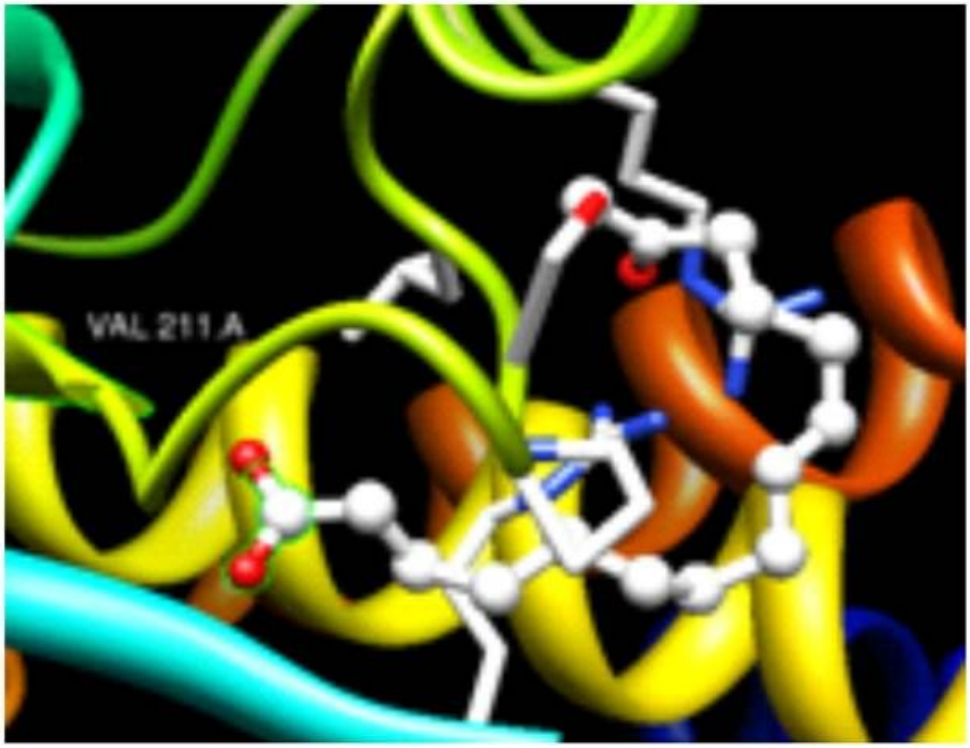

Fig. 59 Binding mode of nuciferine in the active site of PTP1B viewed through autodock 4.0.1

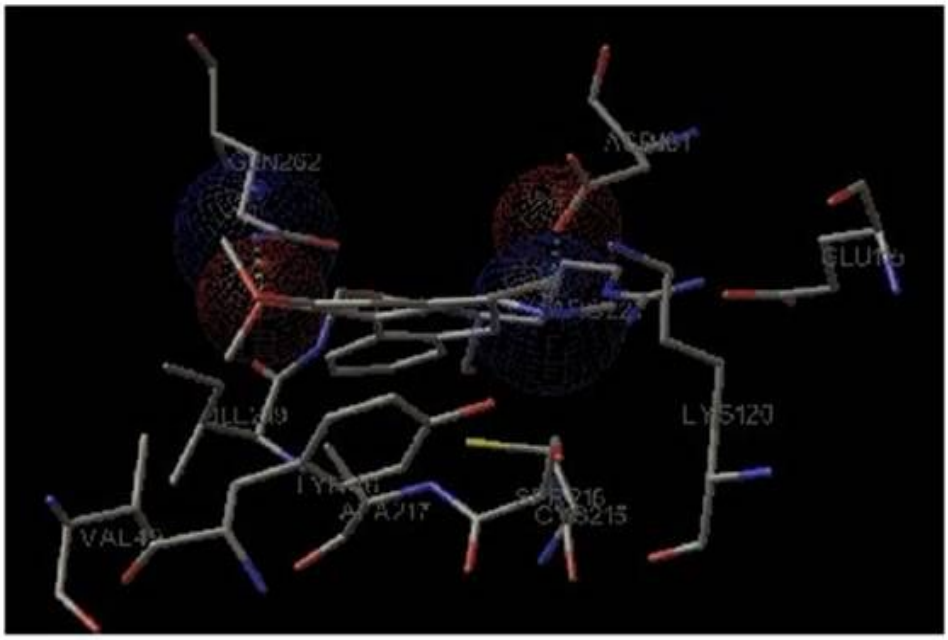

Fig.60 Binding mode of Nuciferine in the active site of PTP1B viewed through USF chimera softeware

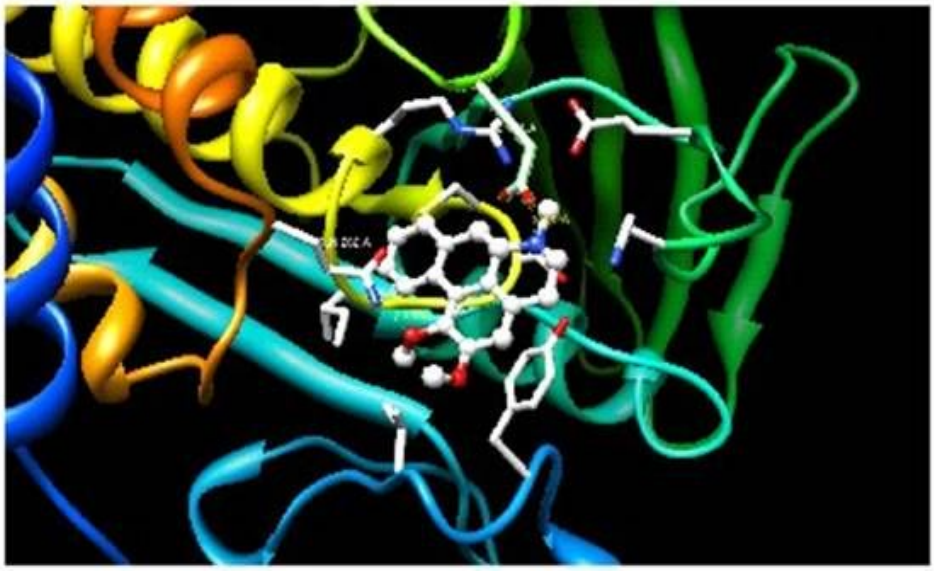

Fig.61. Enlarged view of Nuciferine in the active site of PTP1B through USF chimera software

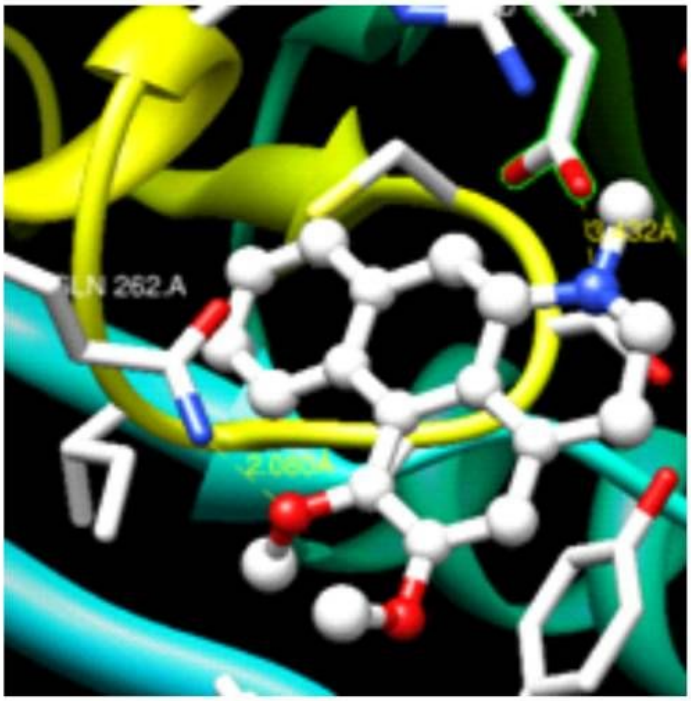

Table-55 Docking energies for protein inhibitor complex

S. No.	Compound	Binding energy	No. of Hydrogen bonds formed
1.	Nuciferine	-18.33	2
2.	10-oxoundecanoic acid	-3.56	2
3.	14-oxopentadec-9-enoic acid	-4.31	1

Table-56 Interactions of the isolated compounds with amino acids at the active site of the protein (PTP1B)

Compound	Hydrogen bonds formed	Aminoacid involved in hydrogen bond interactions	Distance between Donor & Acceptor (Å)	Aminoacid involved in van der waals interactions
Nuciferine	2	GLN-262 (N)	2.08 Å	TYR-46, VAL-49, LYS-120, ALA-217, ILE-219, GLY-220, SER-216, CYS-215, ARG-221, GLU-115
10-oxoundecanoic acid	2	GLN-266 (N)	2.804	TYS 46, VAL 49, ASP 181, PHE 182, SER 216, ALA 217, ARG 221, GLY 262
		CYS-215 (S)	2.787	
14-oxopentadec-9-enoic acid	1	VAL-211 (N)	2.867	GLN 78, ARG 79, ARG 199, LEU 204, SER 205, PRO 210, LEU 233

Table-57 *In vitro* anticancer activity of ethanolic flower extract of *Nymphaea pubescens* against *HeLa* cells

Concentration (µg/ml)	Absorbance			Average
9.3	0.309	0.328	0.323	0.32
18.75	0.288	0.293	0.295	0.292
37.5	0.209	0.212	0.232	0.217
75	0.148	0.152	0.145	0.148
150	0.059	0.057	0.066	0.060

Table-58 Percentage of cell inhibition of ethanolic flower extract against *HeLa* cells

Concentration (µg/ml)	**% Cell inhibition** (µg/ml)
9.3	4.09
18.75	12.48
37.5	34.76
75	55.54
150	81.81
5 – Fluro uracil	19.60

Fig.62 Non linear regression curve

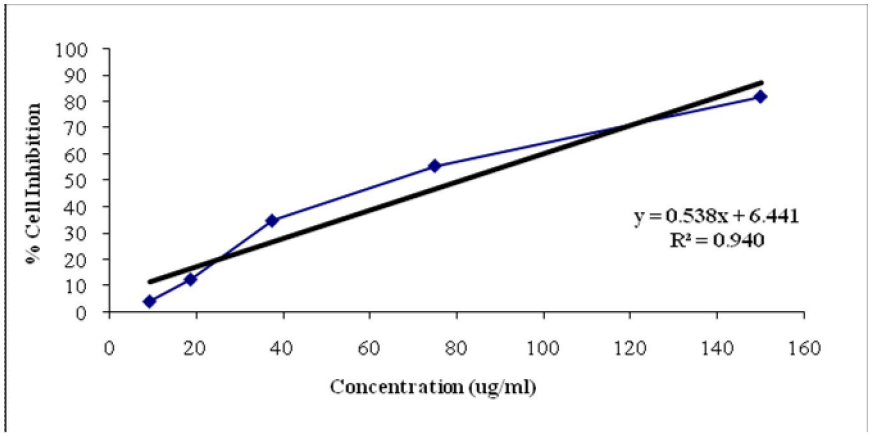

IC_{50} value – 80.96 µg/ml

Table-59 *In vitro* anticancer activity of ethanolic flower extract of *Nymphaea pubescens* against Hep 2 cells

Concentration (µg/ml)	Absorbance			Average
25	0.19	0.21	0.20	0.20
50	0.19	0.17	0.18	0.18
75	0.14	0.14	0.15	0.14
100	0.11	0.10	0.12	0.11
150	0.07	0.06	0.07	0.07
200	0.05	0.04	0.03	0.04

Table-60 Percentage of cell inhibition of ethanolic flower extract against Hep-2 cell lines

Concentration (ug)	% Cell Inhibition
25	15.22
50	22.05
75	36.41
100	52.35
150	70.13
200	81.93
5-Fluoro uracil	20.71

Fig.63 Non linear regression curve

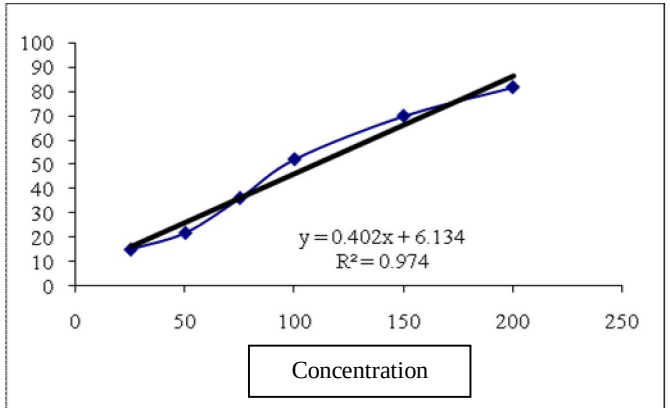

IC_{50} value – 109.12 µg/ml

Table-61 *In-vitro* anticancer activity of ethyl acetate fraction from the ethanolic flower extract of *Nymphaea pubescens* against *HeLa* cells

Concentration (µg/ml)	Absorbance			Average
25	0.22	0.19	0.20	0.20
50	0.16	0.17	0.16	0.16
75	0.09	0.11	0.12	0.11
100	0.08	0.08	0.07	0.08
150	0.06	0.05	0.04	0.05
200	0.02	0.02	0.02	0.02

Table-62 Percentage of cell inhibition of ethyl acetate fraction against *HeLa* cells

Concentration (ug)	% Cell Inhibition
25	12.78
50	28.97
75	52.13
100	66.33
150	77.41
200	90.62
5-Fluoro uracil	19.60

Fig.64 Non linear regression curve

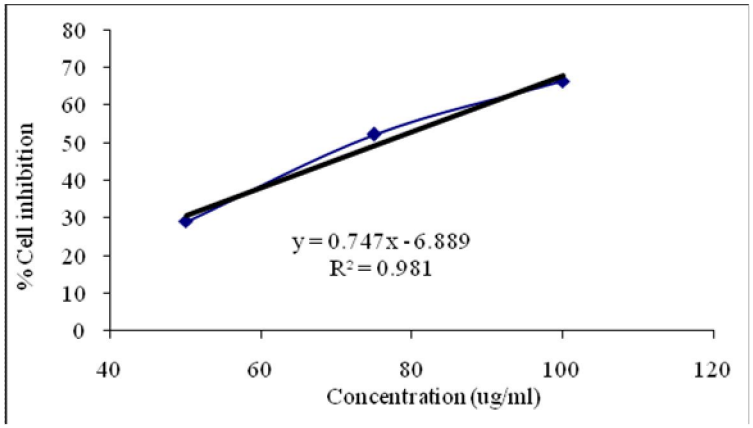

IC_{50} value – 57.71 µg/ml

Table-63 Antitumor activity of ethyl acetate fraction of *nymphaea pubescens* on tumour volume, packed cell volume and cell count

Groups (n=8)	**Treatment**	**Tumor Volume** (ml)	**Packed cell volume** (ml)	**Viable cell count** (cells x 10^6 cells/mouse)
I	Normal control (5ml-0.05% Tween 80/ kg b.w)	-	-	-
II	Dalton ascitic lymphoma induced (5ml-0.05% Tween 80 / kg b.w)	3.03 ± 0.06	2.15 ± 0.14	19.43 ± 0.59
III	DAL + 5-Fluorouracil (20 mg/kg b.w)	0.80 ± 0.05***	0.30 ± 0.05***	1.53 ± 0.31***
IV	DAL + Ethyl acetate fraction (125mg/Kg b.w)	2.10 ± 0.10***	0.68 ± 0.06***	8.76 ± 0.26***
V	DAL + Ethyl acetate fraction (250mg/Kg b.w)	1.70 ± 0.05***	0.4 ± 0.05***	4.16 ± 0.19***

Values given as Mean ± SEM; p***→<0.001 when compared with DAL control

Fig.65 Microscopic observation of cell lines treated with ethyl acetate fraction

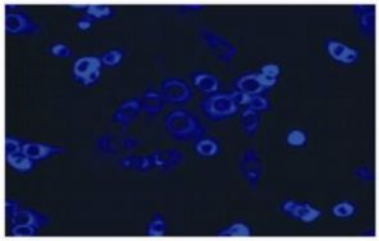

NIH-3T3 treated with ethyl acetate fraction (320X)

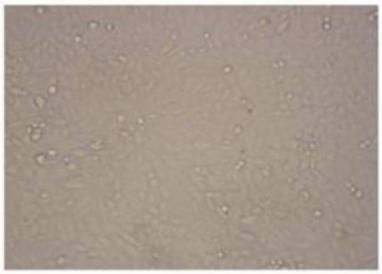

***HeLa* cells treated with 9.3µg of ethyl acetate fraction** (10X)

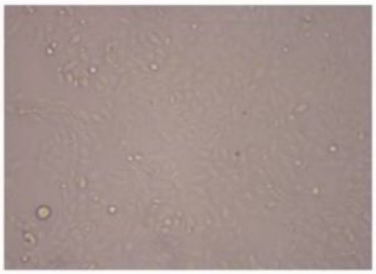

***HeLa* cells treated with 18.75µg of ethyl acetate fraction** (10X)

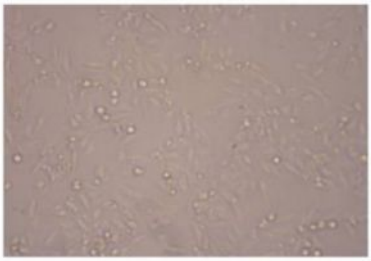

***HeLa* cells treated with 37.53µg of ethyl acetate fraction** (10X)

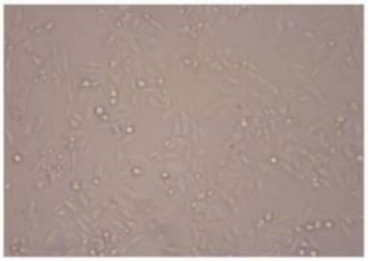

***HeLa* cells treated with 75 µg of ethyl acetate fraction** (10X)

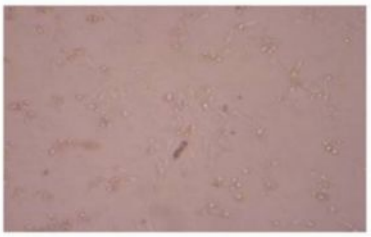

***HeLa* cells treated with 150µg of ethyl acetate fraction** (10X)

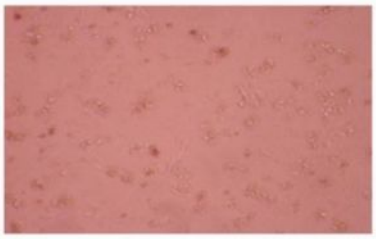

***HeLa* cells treated with 300µg of ethyl acetate fraction** (10X)

Fig.66 Antitumor activity of ethyl acetate fraction of *nymphaea pubescens* on tumour volume, packed cell volume and cell count

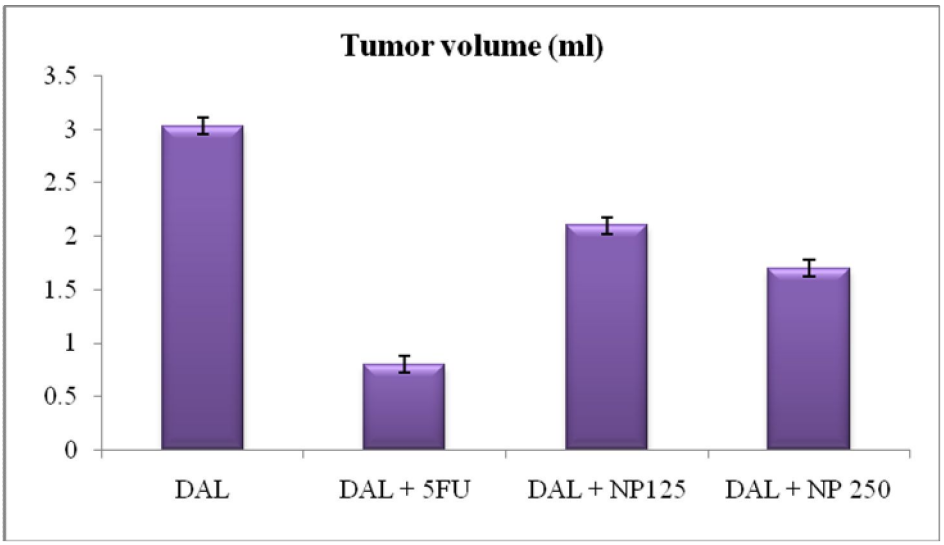

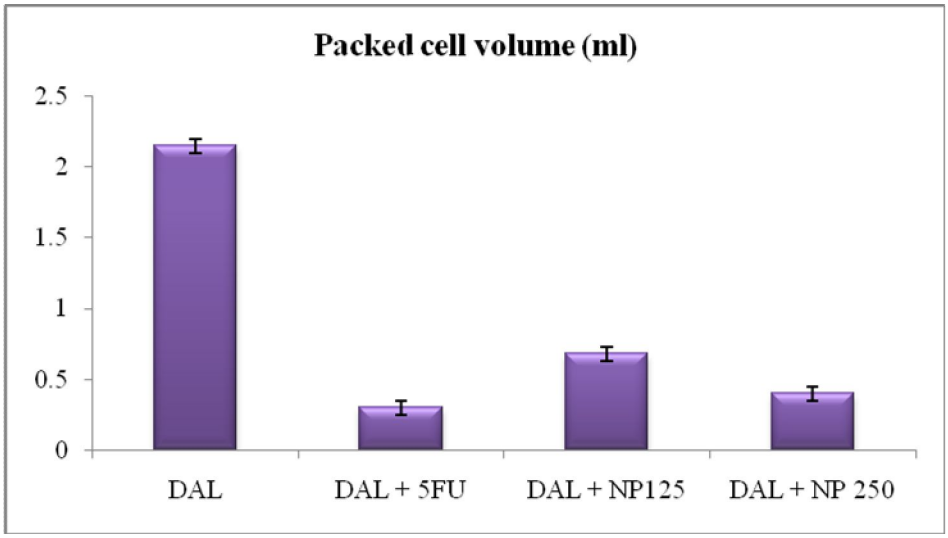

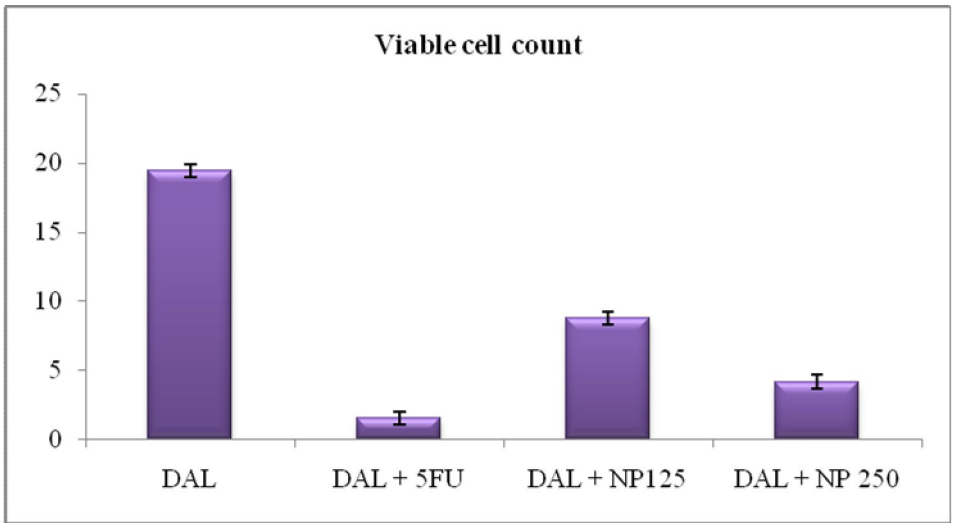

Table-64 Antitumor activity of ethyl acetate fraction of *Nymphaea pubescens* on body weight, mean survival time and % increased life span

Groups (n=8)	**Treatment**	**Body weight** (gms)	**Mean survival time** (Days)	**% Increased life span**
I	Normal control (5ml-0.05% Tween 80/ kg b.w)	24.81 ± 0.13	-	-
II	Dalton ascitic lymphoma induced (5ml-0.05% Tween 80 / kg b.w)	37.50 ± 0.76	7.5	-
III	DAL + 5-Fluorouracil (20mg/kg b.w)	25.50 ± 0.75***	18.5	80.01
IV	DAL + Ethyl acetate fraction (125mg/Kg b.w)	29.83 ± 0.47***	11.5	53.33
V	DAL + Ethyl acetate fraction (250mg/Kg b.w)	26.17 ± 0.47***	12.5	66.67

Values given as Mean ± SEM; p*** → <0.001 when compared with DAL control

Fig.67 Antitumor activity of ethyl acetate fraction of *Nymphaea pubescens* on body weight, mean survival time and % increased life span

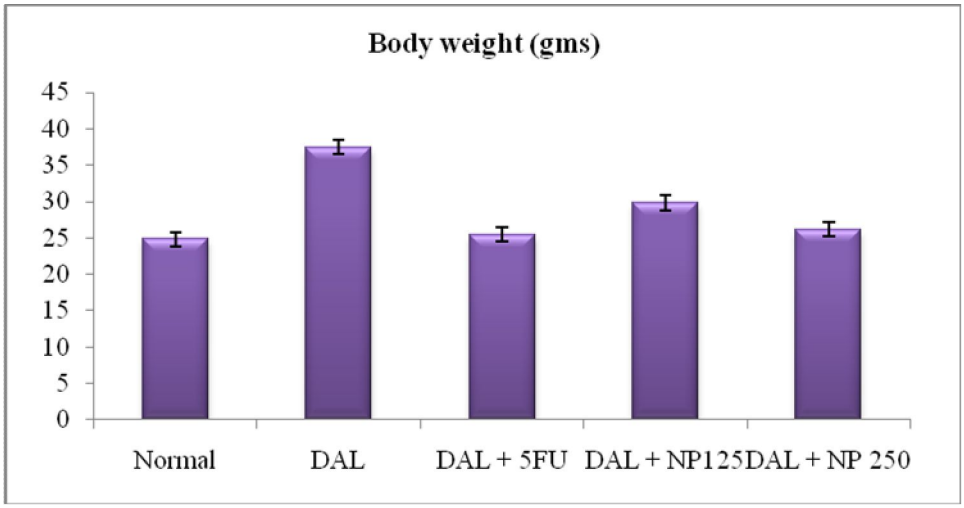

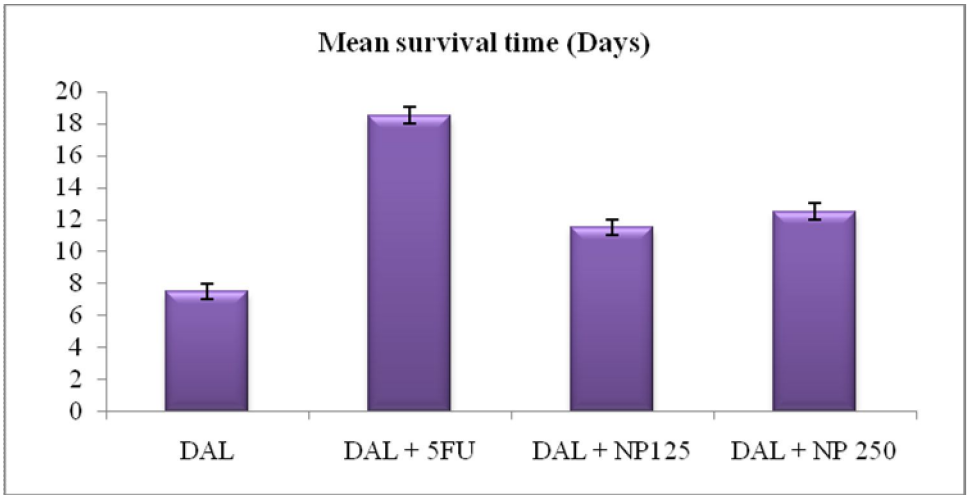

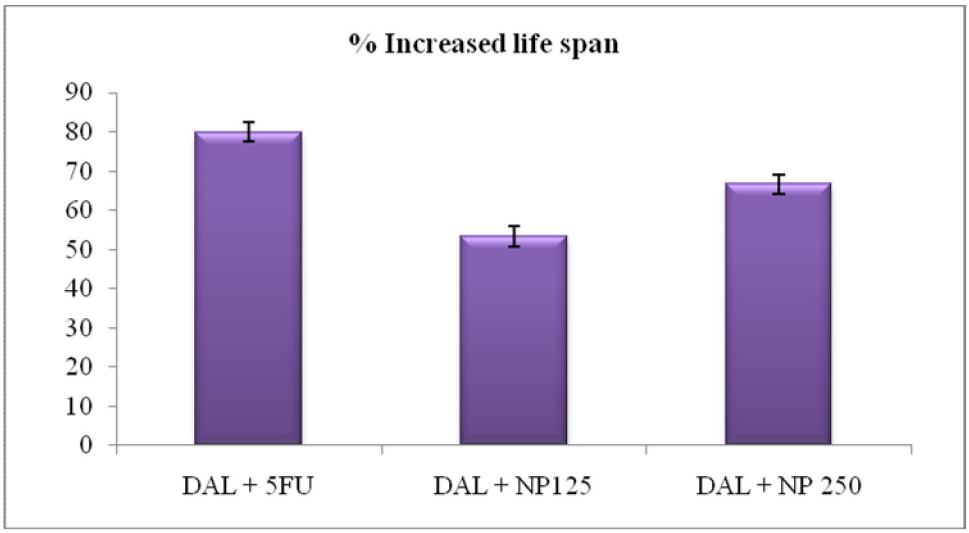

Table-65 Antitumor activity of ethyl acetate fraction of *Nymphaea pubescens* on hematological parameters

Groups (n=8)	**Treatment**	**Hb content**	**RBC** (Cells/ml x 10^6)	**WBC** (Cells/ml x 10^3)
I	Normal control (5ml-0.05% Tween 80/ kg b.w)	13.50 ± 0.76	5.58 ± 0.37	7.3 ± 0.27
II	Dalton ascitic lymphoma induced (5ml-0.05% Tween 80 / kg b.w)	10.00 ± 0.57	3.25 ± 0.25	16.10 ± 0.23
III	DAL + 5-Fluorouracil (20mg/kg b.w)	14.15 ± 0.42***	5.4 ± 0.13***	7.65 ± 0.16***
IV	DAL + Ethyl acetate fraction (125mg/Kg b.w)	11.37 ± 0.42***	4.40 ± 0.16***	12.62 ± 0.39***
V	DAL + Ethyl acetate fraction (250mg/Kg b.w)	13.57 ± 0.20**	5.36 ± 0.15***	8.46 ± 0.35***

Values given as Mean ± SEM; p*** → <0.001 when compared with DAL control; p** → <0.05 when compared with DAL control

Fig.68 Antitumor activity of ethyl acetate fraction of *Nymphaea pubescens* on hematological parameters

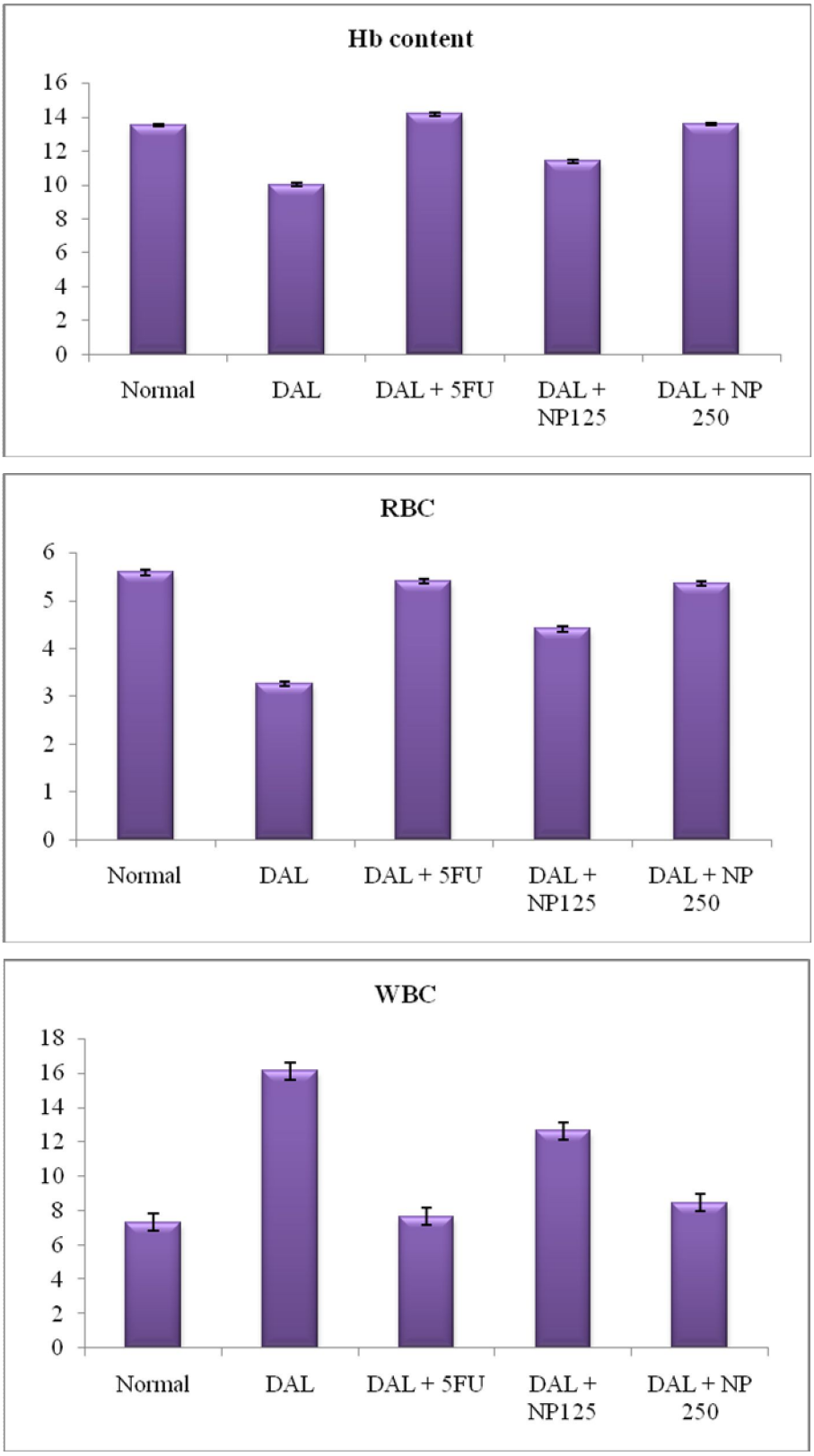

Table-66 Effect of ethyl acetate fraction on scavenging of free radicals by ABTS radical cation method

S. No.	Concentration (µg/ml)	% of Activity	
		Ascorbic acid	**Ethyl acetate fraction**
1	10	13.86 ± 0.19	11.32 ± 0.12
2	20	28.71 ± 0.22	25.31 ±0.27
3	40	47.96 ± 0.40	29.28 ± 0.13
4	80	55.14 ± 0.25	40.13 ± 0.11
5	160	78.79 ± 0.18	53.11 ± 0.18
IC_{50} value		**43.50**	**78.20**

All values are expressed as mean ± SEM for three determinations

Fig.69 Graphical representation of ethyl acetate fraction on scavenging of free radicals by ABTS radical cation method

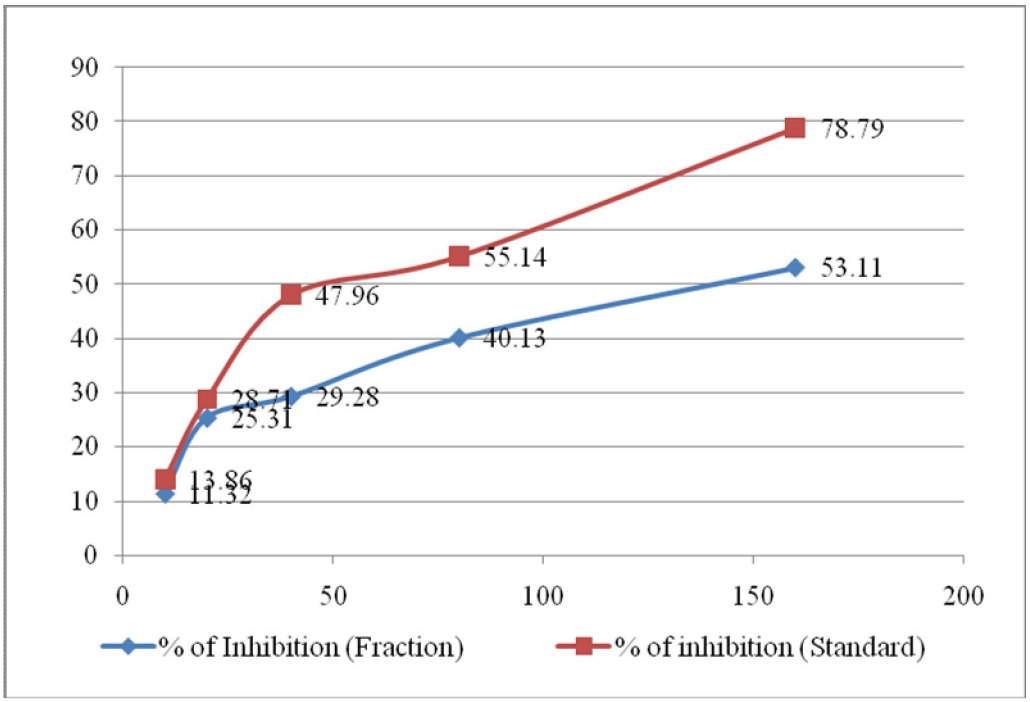

Table-67 Effect of ethyl acetate on scavenging of free radicals by DPPH radical Scavenging Method

S. No.	Concentration (µg/ml)	% of Activity	
		Ascorbic acid	Ethyl acetate fraction
1	10	27.56 ± 0.11	25.33 ± 0.28
2	20	35.17 ±0.25	34.31 ± 0.17
3	40	40.26 ± 0.31	69.32 ± 0.25
4	80	51.81 ± 0.22	75.28 ± 0.31
5	160	75.81 ± 0.14	76.01 ± 0.12
IC_{50} value		**42.30**	**74.37**

All values are expressed as mean ± SEM for three determinations

Fig.70 Graphical representation of ethyl acetate on scavenging of free radicals by DPPH radical Scavenging Method

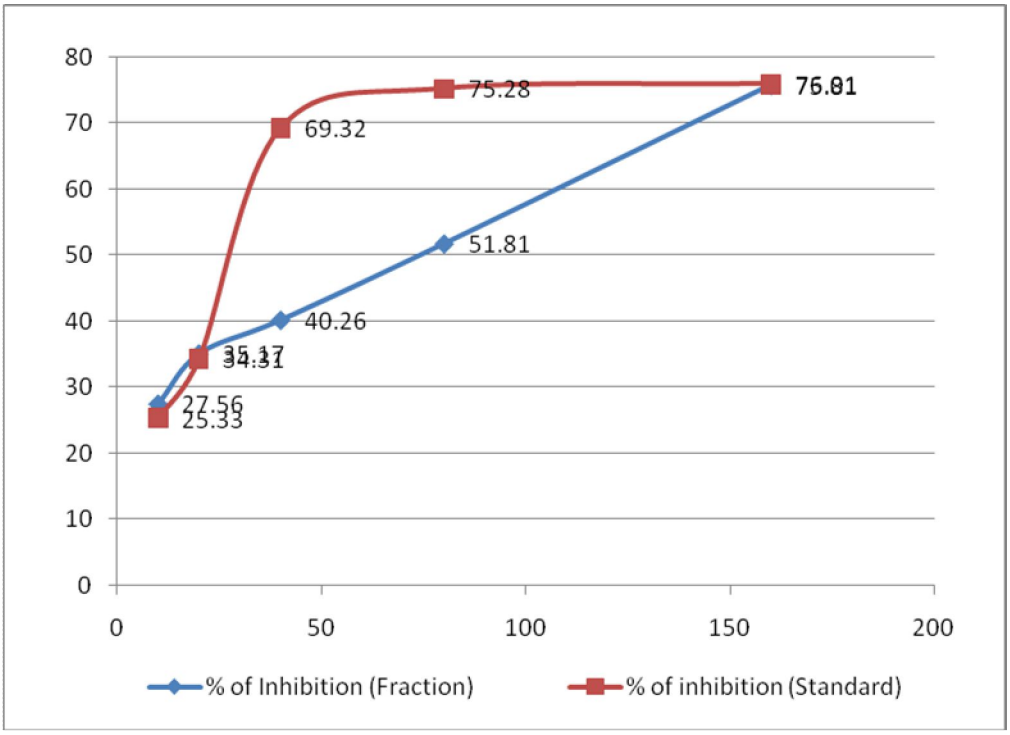

Table-68 Effect of ethyl acetate fraction on scavenging of hydrogen Peroxide

S. No.	Concentration (µg/ml)	% of Activity	
		Ascorbic acid	**Ethyl acetate fraction**
1	10	26.52 ± 0.15	17.70 ± 0.12
2	20	38.35 ± 0.23	28.70 ± 0.21
3	40	59.16 ± 0.25	38.20 ± 0.51
4	80	79.91 ± 0.38	62.29 ± 0.42
5	160	91.53 ± 0.15	88.9 ± 0.27
IC_{50} value		**22.29**	**75.23**

All values are expressed as mean ± SEM for three determinations

Fig.71Graphical representation of ethyl acetate fraction on scavenging of hydrogen Peroxide

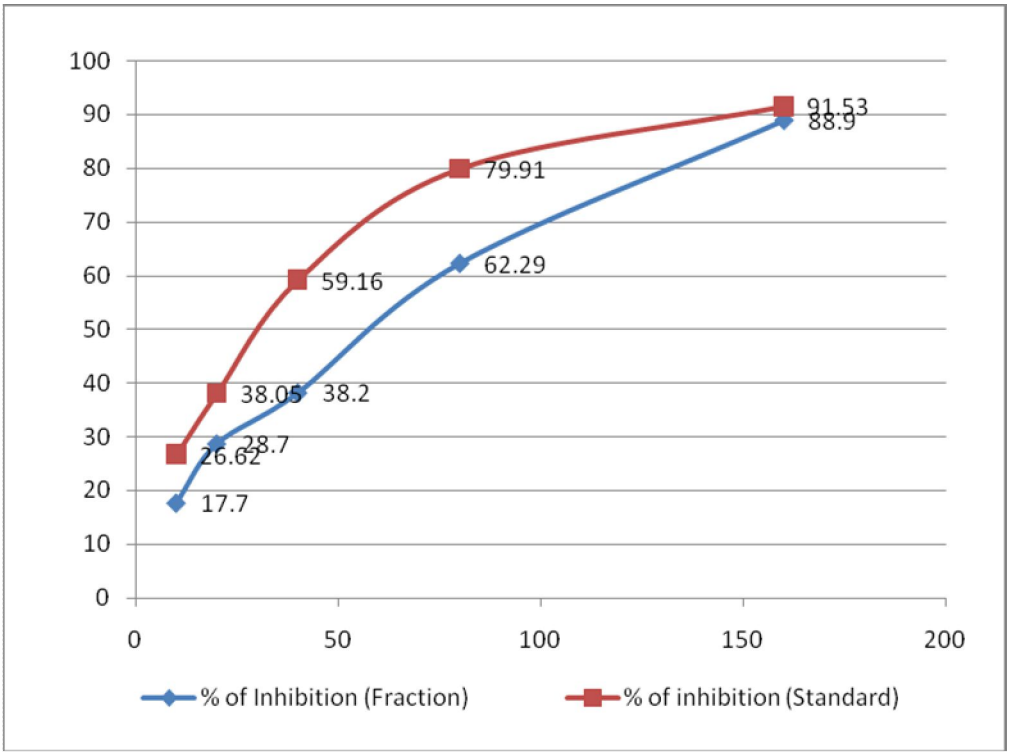

Table-69 Effect of ethyl acetate fraction on scavenging of hydroxyl radical by the *p*-Nitroso Dimethyl Aniline (*p*-NDA)

S. No.	Concentration (µg/ml)	% of Activity	
		Ascorbic acid	Ethyl acetate fraction
1	10	12.70 ± 0.12	26.74 ± 0.44
2	20	25.32 ± 0.09	59.06 ± 0.27
3	40	40.10 ± 0.32	67.91 ± 0.18
4	80	55.02 ± 0.17	68.37 ± 0.21
5	160	68.10 ± 0.25	73.02 ± 0.51
IC_{50} value		**15.6**	**69.37**

All values are expressed as mean ± SEM for three determinations

Fig.72 Graphical representation of of ethyl acetate fraction on scavenging of hydroxyl radical by the *p*-Nitroso Dimethyl Aniline (*p*-NDA)

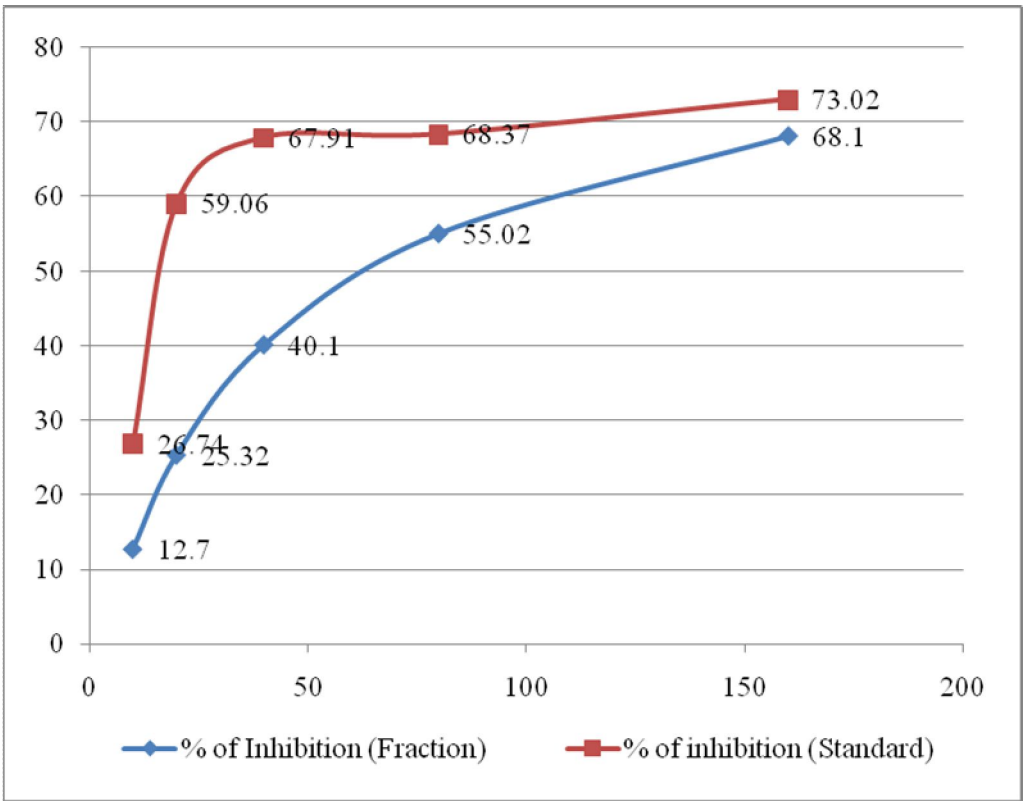

Pharmacological assay is used for qualitatively assessing or quantitatively measuring the presence or amount or the functional activity of a target entity. The classical way of pharmacological screening involves sequential testing of new chemical entities or extracts from biological origin in isolated organ followed by testing in whole animal.

The pharmacological screening of the *Nymphaea pubescens* is done, to scientifically prove the folklore claims of the aquatic plant. The whole plant of *N. pubescens* is being used in the treatment of diabetes[10] and the species *N. alba* is reported for the management of cancer[11]. Hence the aquatic plant *N.pubescens* is screened for antidiabetic, anticancer and anti-oxidant activity.

The action of the drug not only judged by its useful properties but also by its toxic effects. Acute toxicity studies revealed the non toxic nature of the ethanolic extract of roots & rhizome and ethyl acetate fraction from ethanolic flower extract of *Nymphaea pubescens* administered with a dose of 2000mg/kg b.w to the experimental animals. There was no lethality or any toxic reactions found for the dose selected until the end of the study period (Table 45). Hence the dose $1/10^{th}$ and $1/20^{th}$ i.e., 200 and 400 mg/kg b.w is selected for ethanolic extract from root and rhizome for the antidiabetic activity and the dose 125 and 250 mg/kg b.w is selected for ethyl acetate fraction (active fraction against *HeLa* cell line) from ethanolic flower extract of *N.pubescens* for the anticancer activity.

The protein target for drug action on mammalian cells is receptors, ion channels, enzymes and carrier molecules[66]. The antidiabetic activity of the ethanolic extract from root and rhizome of *N.pubescens* is screened by molecular method targeting at enzymatic level such as glycolytic and gluconeogenic enzyme, apoptotic protein such as Caspase-3 and BCl-2 and at the receptor level Protein tyrosine phosphatase 1B by docking with the isolated compound.

An oral glucose tolerance test is a more sensitive measure of early abnormalities in glucose regulation than fasting plasma glucose or glycosylated hemoglobin. Impaired glucose tolerance reflects hepatic gluconeogenesis and reduced uptake of glucose from blood into skeletal muscle and adipose tissue following a meal. It serves as a marker for the state of insulin resistance and predicts both large

and small vessel vascular complications[103]. The ethanolic extract administered with 200 & 400 mg/kg b.w showed a significant reduction in blood glucose levels from 30min onwards in oral glucose tolerance test similar to the standard drug Glibenclamide (Table-46; Fig.41).

Streptozotocin is 1-methyl-1-nitrosourea attached 2nd position of glucose that causes β cell necrosis and induces experimental diabetes in animals. The glucose moiety of STZ allows preferential uptake of STZ into the β-cells probably via the glucose transporter-2 (GLUT-2). STZ is an alkylating agent, it causes DNA strand breaks that induce the activation of islet nuclear poly-ADP-ribose synthetase followed by lethal Nicotinamide Adenine Dinucleotide (NAD) depletion. Intracellular metabolism of STZ aggravates the free radicals such as nitric oxide which also causes the additional DNA strand breaks[104].

It has been reported that administration of Nicotinamide, a poly ADP-ribose synthetase inhibitor, protected the islets functionally by protecting the decrease in the levels of NAD and proinsulin thereby partially reversing the inhibition of insulin secretion to prevent the aggravation of experimental diabetes following the administration of β-cell toxins such as Streptozotocin and Alloxan. This condition contributes a number of features similar with type II diabetes and is exemplified by stable hyperglycemia, glucose intolerance and significantly altered glucose stimulated insulin secretion both *in-vivo* and *in-vitro*[105]. Hence STZ – Nicotinamide induced diabetes in experimental rats was chosen as the animal model to evaluate the antihyperglycemic potential of *Nymphaea pubescens* in the molecular level.

STZ-nicotinamide induced diabetes is mainly attributed to diabetic oxidative stress brought about by overproduction of free radicals which in turn exerts deleterious effect on the function of β-cells. Insulin deficiency ultimately results in increased production of glucose by the liver and decreased utilization of glucose in peripheral tissues[106]. The elevated blood glucose level observed in the diabetic rats 201.30 mg/dl was significantly decreased to 95.00 mg/dl and 86.30 mg/dl administered with the ethanolic extract 200 and 400 mg/kg b.w respectively (Table-47; Fig.42).

Glycosylated haemoglobin is an easily measurable biochemical marker that strongly correlated with the glycemic level during a 2 to 3 month period and is a more accurate and reliable measure than fasting blood glucose level. The observed increase in the level of glycosylated haemoglobin 14.12 % in the experimental diabetic rats implies the oxidation of sugars, extensive damage to both sugars and proteins in the circulation, vascular walls and lens proteins, continuing a re-inforcing the cycle of oxidative stress and damage[107]. Oral treatment with ethanolic extract from the root and rhizome of *Nymphaea pubescens* 200 and 400 mg/kg b.w. significantly decreased the levels of glycosylated haemoglobin 8.28 and 7.18 % Hb respectively in the experimental diabetic rats (Table-47; Fig.42) suggesting that it may prevent oxidative damage caused by the glycation reaction in diabetic conditions.

These results on glucose and glycosylated haemoglobin levels indicate the beneficial effects of *Nymphaea pubescens* in preventing the pathogenesis of diabetic complications caused by impaired glucose metabolism.

The destruction of β-cells during diabetes ultimately causes physico-metabolic abnormalities such as a decrease in body weight gain and increase in food and water intake. These changes were related to important alterations in protein level in skeletal muscle. Hence a notable decrease in the body weight change observed in the diabetic group of rats might be the result of protein wasting due to the unavailability of carbohydrates for energy metabolism and loss of degradation of structural proteins. The gain in the body weight was observed in groups of diabetic rats received the ethanolic extract 200 and 400mg/kg b.w suggesting that carbohydrates are utilized by the cells for the production of energy (Table-48; Fig. 43).

The major symptoms and signs of diabetes is polyuria i.e., excess glucose in renal tubules causes osmotic diuresis. Absence of urine sugar in the groups administered with ethanolic extract of *Nymphaea pubescens* and standard drug Glibenclamide whereas diabetes induced groups showed the presence of urine sugar (Table-48).

Decrease in hepatic glycogen content 5.16mg/g is observed for the group of diabetes induced animals and this is probably due to lack of insulin in the diabetic state which results in the inactivation of glycogen synthase enzyme. The significant

increase in the hepatic glycogen content 10.50 and 11.15mg/g observed for the groups administered with ethanolic extract 200 and 400mg/kg b.w similar to the standard drug Glibenclamide (Table-48; Fig.43). The effect may be due to the increased activity of glycogen synathase enzyme[108].

There are two terms glycation and glycosylation. Both mean addition of sugar (glucose / fructose) to proteins or collagen. Glycation is non-enzymatic while glycosylation is enzymatic[107]. Long standing diabetes mellitus particularly improperly treated ones are characterized by glycation of proteins (albumin or hemoglobin or collagen). Ultimately, the glycated proteins become advanced gycated end products AGE. These AGE's can bind with some receptors and this leads to release of cytokines, initiation of coagulation and formation of white thrombus formation known as atherosclerosis. In diabetes some glucose molecules are converted into sorbitol which is toxic to tissues. Long continued stay of sorbital, as stated above, may be the major cause of retinopathy, nephropathy and neuropathy. The incidence of death due to atherosclerotic lesion in diabetes is very high. Lipids and cholesterol are transported through the bloodstream as macromolecular complexes of lipid and protein known as lipoproteins. The lipoproteins are high density lipoprotein, Low density lipoprotein, very low density lipoprotein and chylomicrons. The cholesterol and triglycerides absorbed from the ileum are transported as chylomicrons in lymph and the blood to capillaries in muscle and adipose tissue. The altered levels of triglycerides, total cholesterol, high density lipoprotein and very low density lipoprotein in the diabetic state reverted back to normal after administration with ethanolic extract similar to the standard drug Glibenclamide (Table-49; Fig.44).

Decrease in insulin secretion in diabetic state causes increase in protein catabolism especially in skeletal muscle. The total muscle protein catabolism is due to increase in protein breakdown rather than a decline in protein synthesis[109]. The decreased level of plasma protein 6.00 mg/dl is observed for diabetes induced group whereas the plasma protein level increased to 7.61 and 8.16mg/dl administerd with ethanolic extract 200 and 400mg/kg b.w similar to the standard drug Glibenclamide (Table-50; Fig.45).

Urea is the end product of protein catabolism in the liver and plasma proteins. Nitrogen homeostasis alterations lead to increased hepatic elimination of urea nitrogen and increased peripheral release of nitrogenous substances[110]. The oral administration of ethanolic extract of *Nymphaea pubescens* 200mg and 400mg/kg b.w significantly decreased the elevated levels of blood urea from 43.67mg/dl in the diabetes induced group to 26.33 and 24.50 µg/dl suggesting the prophylactic role of *Nymphaea pubescens* in protein metabolism (Table-50; Fig. 45).

Creatinine is a byproduct of the breakdown of creatine and phosphocreatinine which are the energy storage molecules in muscle. Serum creatinine values also depend on the kidney to excrete creatinine[111]. Creatinine concentration is used to assess the impairment of kidney function. The elevated level of serum creatinine 1.22mg/dl in diabetes induced group of rats is reduced 0.58 and 0.55mg/dl for the groups of animals administrated with ethanolic extract of *Nymphaea pubescens* 200mg and 400mg/kg b.w (Table-50; Fig.45).

Uric acid is the one of the major endogenous water soluble antioxidants has been thought to be a metabolically inert end product of purine metabolism. Increased oxidative stress is closely related to diabetes and its vascular complications. The elevated levels of circulating uric acid levels is an indicator that the body is trying to protect itself from the deleterious effects of free radicals by increasing the products of endogenous antioxidants such as uric acid. Uric acid prevents oxidative modification of endothelial enzymes and preserves the ability of endothelium to mediate vascular dilation in the oxidative stress[112]. The increased levels of serum uric acid 6.36µg/dl observed in diabetes induced group of rats and after the administration of 200 and 400 mgs of ethanolic extract decreases serum uric acid level to 3.86 and 3.08µg/dl indicates the free radical scavenging activity of *N. pubescens* (Table-50; Fig.45).

Hyperglycemia in type II diabetes is due to the lack of suppression of hepatic glucose production in the absorptive state and excessive glucose production in the post absorptive state. Enzymes that regulates hepatic glucose metabolism are potential targets for controlling hepatic glucose balance and thereby blood glucose levels in type II diabetes[113].

In diabetic state the activities of glycolytic enzymes are decreased which is due to the insufficiency of insulin. Hexokinase, phosphoglucoisomerase, aldolase are some of the enzymes that involved in glucose metabolism. Hexokinase phosphorylates hexoses forming hexose phosphate. Phosphoglucoisomerase are a group of enzymes of the isomerase family convert glucose-6-phosphate to fructose 6-phosphate. Aldolase is an enzyme that catalyses a reversible aldol reaction. The substrate fructose 1,6-bisphosphate is broken down into glyceraldehyde 3-phosphate and dihydroxyacetone phosphate. This reaction is a part of glycolysis. The ethanolic extract from the root and rhizome of *Nymphaea pubescens* upregulates the activities of glycolytic enzymes such as hexokinase, phosphoglucoisomerase, aldolase in hepatic and renal tissues thereby it enhances the utilization of glucose for cellular biosynthesis which is marked by the significant decrease in plasma glucose levels (Table-51; Fig.46).

It has been demonstrated that in diabetes mellitus the increased rate of gluconeogenesis is related to increased expression of gluconeogenic enzymes such as glucose-6-phosphatase, fructose-1,6-bisphosphatase in hepatic and renal tissues. The ethanolic extract of *N.pubescens* significantly decreased the activities of glucose-6-phosphatase and fructose-1,6-bisphosphatase in diabetes induced rats (Table-52; Fig.47).

These results prove that the aquatic plant *N.pubescens* normalizes the disturbed carbohydrate metabolism by enhancing glucose utilization and by decreasing hepatic glucose production and indicates its beneficial effect in the treatment of diabetes mellitus.

From the histopathological studies of the pancreas, the control group showed the normal cellular architecture whereas the diabetic induced group showed massive cellular necrosis. The groups received standard drug Glibenclamide showed regeneration of cells. The groups administered with 200 mg showed regeneration of cells with patchy necrosis whereas groups receive with 400 mg showed regeneration of cells similar to the standard drug Glibenclamide (Fig.48).

Apoptosis or programmed cell death can be initiated by intrinsic signals that are produced by cellular stress. Cellular stress may occur from exposure to radiation or chemicals or viral infection or oxidative stress by free radicals. In general intrinsic

signals initiate apoptosis via releasing the apoptotic factors from mitochondrial membrane called the permeability transition pore or PT pore. Mitochondrial permeability transition causes rapid swelling of the mitochondria, rupture of the outer membrane and releasing intermembrane proteins like cytochrome-c, Bax, Bcl_2 to cytosol leading to apoptosis. In diabetes loss of insulin effect on the liver leads to glycogenolysis, an increase in hepatic glucose and free fatty acid production. The excess in free fatty acids found in the insulin resistant state is known to be directly toxic to hepatocytes and also in streptozotocin-Nicotinamide induced diabetes leads to oxidative stress by overproduction of free radicals[78]. Toxicity of hepatocytes and free radicals plays an important role in cellular stress leads to apoptosis in hepatic cells (www.sgul.ac.UK/dept/Immunology/-dash).

The molecular estimation of pro-apoptotic protein Caspase-3 and anti-apoptotic protein Bcl-2 was done by gel electrophoresis (Fig.49) followed by western blot analysis (Fig.50&51)) in the experimental animals. In the diabetes induced group, the hepatic pro-apoptotic protein expression Caspase-3 is increased and the hepatic anti-apoptotic protein expression Bcl-2 decreased whereas the groups received the standard drug Glibenclamide and ethanolic extract decreases the expression of Caspase-3 and increases the expression of Bcl-2 (Table-54; Fig.52). The result suggests that *Nymphaea pubescens* promotes the synthesis of anti-apoptotic protein and inhibits the pro-apoptotic protein in hepatic cells.

Resistance to insulin is the hallmark of type 2 diabetes. Drugs that can ameliorate this resistance should be effective in treating type 2 diabetes. Protein tyrosine phosphatase 1B is thought to function as a negative regulator of insulin signal transduction. Hence the isolated compounds from the root and rhizome of *Nymphaea pubescens* is planned to dock with the receptor PTP1B as a novel target for type 2 diabetes and looks at the challenges in developing small-molecule inhibitors of this phosphatase.

From the docking studies the isolated compound Nuciferine showed highest binding energy when compared to 10-oxoundecanoic acid and 14-oxopentadec-9-enoic acid. All the three isolated compounds from the root and rhizome of *N.pubescens* showed the negative binding energy value (Table-55). The formation of

hydrogen bonds between the amino acid in the receptor and the docked compound and also the amino acid involved in the vander vaals or hydrophobic interaction with the docked compound is given in Table-56. When there is a high negative binding energy value there will be a high inhibitory effect results in good biological activity. The result showed the inhibitory action of the isolated compounds to the receptor PTP1B (Fig. 53-61) and the compounds may produce good biological activity.

The antidiabetic activity of the root and rhizome from *N. pubescens* acts in a multiple target by increasing the glycolytic enzyme, decreasing the gluconeogenic enzyme and the expression of pro-apoptotic protein Caspase-3, increasing the expression of anti-apoptotic protein BCl-2 in hepatic cells and inhibiting the Protein tyrosine phosphatase 1B. The mechanism based evaluation suggests that in future *Nymphaea pubescens* will provide a multiple target lead compound against type-II diabetes mellitus.

In Africa the genus *Nymphaea* is reported for management of cancer and hence the aquatic plant *N.pubescens* is planned to prove scientifically[11]. To examine whether the plant shows anticancer property, it is preliminarly screened for *in-vitro* anticancer activity against *HeLa* and *Hep-2* cell lines.

The different parts such as root and rhizome, flower, fruit and leaves is extracted with 95% ethyl alcohol and the concentrated solvent free extracts is subjected for *in-vitro* anti-cancer activity by MTT assay. The ethanolic flower extract showed anticancerous effect and the IC_{50} value is found to be 80.96µg/ml against *HeLa* cell lines (Fig. 62) and 109.12µg/ml against Hep-2 cell lines (Fig. 63). Hence ethanolic flower extract is subjected for bioassay guided fractionation by column chromatography using solvent of increasing order of polarity to find out the active fraction. The fractions such as n-Hexane, chloroform, ethyl acetate and ethanol were collected, solvents evaporated and again screened for *in-vitro* anticancer activity against *HeLa* cell lines. The ethyl acetate fraction showed the anticancerous effect and the IC_{50} value is found to be 57.7µg/ml (Fig. 64). When the concentration of the ethyl acetate fraction increases necrotic *HeLa* cells is observed whereas the fraction didn't produce cytotoxic effect to the normal cell NIH-3T3 (Fig. 65). From the *in-vitro* anticancer studies it is found that the ethyl acetate fraction is active against *HeLa* cell

lines and hence the fraction is subjected for *in-vivo* anticancer activity and *in-vitro* anti-oxidant activity.

The ethyl acetate fraction didn't show any toxic reaction for the experimental animals administered with the dose of 2000mg/kg b.w (Table-45). Hence from the *in-vitro* anticancer studies the ethyl acetate fraction from the ethanolic flower extract of *N.pubescens* is found to be active fraction and therefore the dose selected for the *in-vivo* studies is 125mg and 250mg/kg b.w. Cancer is induced by intraperitonial injection of Dalton ascitic lymphoma cells.

Ascitic fluid is the nutritional source for tumor cells and a rapid increase in ascitic fluid will increase the tumor growth[114]. In DAL tumour bearing mice increase in ascitic tumor volume is observed 3.03ml whereas the ethyl acetate fraction treated groups, showed the decreased tumor volume 2.10ml for the groups administered with 125mg and 1.70ml administered with 250mg/kg b.w. (Table-63; Fig. 66).

Packed cell volume is the volume of cells that sediments at the bottom after centrifuging the ascitic fluid. Increased Packed cell volume is observed for DAL bearing group of mice 2.15ml whereas the ethyl acetate fraction treated groups showed the decreased packed cell volume 0.68ml and 0.4ml for groups administered with 125mg and 250mg/kg b.w (Table-63; Fig. 66).

Viable cells are live cells that are capable of growth. The DAL bearing group of mice showed increased viable cell count 19.43 x 10^6cells/mouse indicates the proliferation of DAL cells and the groups received ethyl acetate fraction decreases the viable cell count upto 4.16.x 10^6cells/mouse. The result indicates that ethyl acetate fraction has antiproliferative action against DAL cells (Table-64; Fig. 67).

Proliferation of DAL cells in the experimental animals increases the ascitic fluid and hence body weight increases. The ethyl acetate fraction decreases the body weight of the experimental animals indicate the antitumor activity of *N.pubescens*. Similarly the ethyl acetate fraction increases the mean survival time and percentage increased life span suggesting that the aquatic plant *N.pubescens* has antitumor activity against DAL bearing mice (Table-65; Fig. 68).

The major problem faced during cancer is myelosuppression and anemia. Treatment with ethyl acetate fraction for the DAL bearing mice reverted back Hemoglobin content, RBC and WBC count to normal. The result indicates the ethyl acetate fraction possess protective action on the hemopoietic system (Table-65).

Free radicals are the well known inducers for the pathogenesis of various diseases such as cancer, inflammatory diseases, diabetes mellitus, atherosclerosis and arthirits etc., Plant derived phytoconstituents are the rich source of free radical scavengers. The ethyl acetate fraction is subjected for the free radical scavenging assay by four different methods along with the standard drug ascorbic acid. The IC_{50} value of the ethyl acetate fraction showed 78.20µg/ml for ABTS radical cation method, 74.37µg/ml for DPPH radical scavenging method, 75.23µg/ml for hydrogen peroxide method and 69.37µg/ml for scavenging of hydrogen peroxide by p-NDA method (Table-66-69; Fig. 69-72).

The ethyl acetate fraction showed significant anticancer activity against DAL induced mice similar to the standard drug 5-Fluoro uracil. The fraction also exhibits anti-oxidant effect by scavenging the free radicals depending on the specific assay methodology indicate the complexity of the mechanisms and diversity of the chemical nature of the phytoconstituent present.

SUMMARY

The research work entitled "Studies on *Nymphaea pubescens* Willd (Nymphaeaceae)-A plant drug of aquatic flora interest". The genus *Nymphaea* is a group of fascinating aquatic plants with potent medicinal properties. There are about fifty species from the genus *Nymphaea* and six species occurs in India such as *Nymphaea pubescens*, *N.rubra*, *N.tetragonna*, *N.alba*, *N.stellata* and *N.candida*.

From the review of literature the genus *Nymphaea* is subdivided into five subgenera such as *Anecphya*, *Brachyceras*, *Hydrocallis*, *Lotus and Nymphaea*. With regard to chemical constituents, presence of glycosidal anthocyanins in *N.gigantea* belong to the subgenera *Anecphya*, presence of isoflavones, flavonol glycosides in *N.elegans*, *N.ampla* and *N.caerulea*, steroidal glycoside in *N.gracilis* and *N.elegans*, alkaloid- Nupharidine and aporphine like compounds in *N.ampla* belong to the subgenera *Brachyceras*, presence of Nupharidine alkaloid, Nymphaeine cardiac glycosides, steroid and gallic acid in *N.ampla*, hydrolysable tannin-Gerannin in *N.tetragonna*, two lignans Nymphaeoside and Icaroside, flavanol glycoside, steroid and triterpene in *N.odorata* belong to the subgenera *Nymphaea* and two macrocyclic flavonoid in *N.lotos* belong to the subgenera *Lotus*.

A comprehensive search of the literature revealed that, there is a lacuna in pharmacognostical, phytochemical and pharmacological studies of *N.pubescens* which is not been explored scientifically.

The research work encompases the pharmacognostic standardization, phytochemical studies such as chromatographic studies, bio-assay guided isolation, isolation of phytoconstituent, structural elucidation (by UV, IR, ^{1}H NMR, ^{13}C NMR, DEPT NMR, HMBC NMR and Mass spectrometry), analyzing physico-chemical parameters for the isolated compounds including pharmacokinetic and pharmacodynamic properties, toxicity studies, *In-vitro* and *In-vivo* pharmacological bio-assays, molecular studies and screening of isolated compounds by computational molecular docking studies. The above mentioned studies reveal the novel lead molecule from *N.pubescens*, since scientific standardization including molecular

target studies and computational screening for the receptor and lead molecule is the need of the hour in modernizing pharmacognosy.

Pharmacognostic studies

Nymphaea pubescens is a perennial aquatic rhizomatous stoloniferous herb, leaves orbicular with long fleshy warty petiole. Leaves are green above and pubescent below. Flowers consist of numerous stamens, arranged spirally. The stamens are transformed into petals. The sepals and petals are marked with pink striations in the centre. The fruit is a large berry. Seeds are attached on the surface of septa.

The transverse section of anther consists of two adaxial theca and each theca is two chambered. The outer wall of the pollen chamber consist of outer epidermis with spindle shaped thin walled cells, middle endothecium possess wide cells with annular thickening. The endodermis consists of pollen grains and starch grains.

The root consists of outer thin epidermal layer of shrunken cells, middle cortex layer consists of polygonal aerenchymatous cells. The air chambers are separated from each other by uniseriate partition filaments. The inner ground tissue consists of vascular cylinder with compact parenchymatous cells.

The rhizome has membranous outer covering, thick dark periderm zone and wide homogenous parenchymatous ground tissue. Abundant brachy sclereids and starch grains present throughout the ground tissue.

The histochemical studies of root showed the presence of alkaloids in vascular bundle, tannin in the phloem cells and partition filaments, protein in the phloem cells and pith and starch grains in the partition filament and in the ground tissue. In rhizome the alkaloids, proteins and starch histochemically stained in the parenchymatous cells and in the ground tissue and tannin in the inner sclerotic zone.

The powder microscopy showed the presence of lignified fibres, pitted xylem vessels and sclereids.

The linear measurement of fibres showed 240-560µm in length and 64-112 µm in width. The diameter of starch grains showed 32-80µm.

Total ash value is found to be higher when compared to sulphated ash, acid insoluble ash and water soluble ash.

The ethyl acetate soluble extractive value of flower petals and the water soluble extractive value of root and rhizome showed higher value when compared to benzene, chloroform and ethanol soluble extractive values. This indicates that the flower petals contain higher flavonoid content and the root and rhizome contains higher content of polar phytoconstituents.

The percentage loss on drying of flower petals was found to be 1.37%w/w and for root and rhizome 3.21%w/w.

The flower petals showed the presence of glycosides, steroids, flavonoids, phenols, reducing sugars, proteins and trace amount of alkaloid and the root and rhizome showed the presence of alkaloid, glycosides, flavonoids, phenols, tannins, reducing sugars and proteins when the drug powder is treated with various chemical reagents.

The fluorescence analysis of the powdered flower petals and root and rhizome of *Nymphaea pubescens* showed the presence of chromophoric molecules.

Thus the various parameters examined in the present study provide a base for botanical identification and standardization protocol for *Nymphaea pubescens* Willd.

Phytochemical studies

The preliminary phytochemical analysis showed the presence of alkaloids, tannins, glycosides, flavonoids, phenols, reducing sugars and proteins for the ethanolic extract from the root and rhizome and flavonoids, glycosides, alkaloids, steroids, phenols, carbohydrates and proteins for the ethanolic flower extract from *Nymphaea pubescens*.

The thin layer chromatographic studies of the ethanolic extract from the root and rhizome of *Nymphaea pubescens* showed 3 resolved peaks (0.15, 0.49 and 0.8) eluted with the mobile phase n-hexane : ethyl acetate : formic acid (4:5.5:0.5).

The crude alkaloid is separated from the root and rhizome by stass otto process and the thin layer chromatogram showed 3 resolved peaks (0.14, 0.52 and 0.73) eluted with the mobile phase n-hexane : ethyl acetate : formic acid (4:5.5:0.5).

The HPTLC fingerprint of the ethanolic extract from root and rhizome showed six resolved peaks with R_f value 0.15, 0.33, 0.49, 0.67, 0.8 and 0.87 respectively. Third peak with Rf value 0.49 showed highest peak area 27,881.2.

HPTLC fingerprint of the crude alkaloid fraction showed the presence of 12 resolved peaks with the Rf values 0.1, 0.14, 0.17, 0.39, 0.45, 0.52, 0.61, 0.65, 0.71, 0.73, 0.78 and 0.87. Eleventh peak with the Rf value 0.78 showed highest peak area 12080.1.

The GCMS analysis of the ethanolic extract from the root and rhizome and ethanolic flower extract of *N.pubescens* showed the presence of methyl and ethyl fatty acid ester compounds, hydrocarbons, oxygenated hydrocarbons and steroidal compounds.

Two aliphatic compounds 10-Oxoundecanoic acid and 14-Oxopentadec-9-enoic acid were isolated from the root and rhizome by column chromatography and the structure were elucidated by spectral details such as UV, IR, ^{1}H NMR, ^{13}C NMR, ^{13}C DEPT-135 NMR, HMBC NMR and mass spectroscopy.

From the crude alkaloid, Nuciferine is isolated by column chromatography using alumina neutral as a stationary phase. The structure of Nuciferine is interpreted by spectral details such as UV, IR, ^{1}H NMR and mass spectroscopy.

The ethyl acetate fraction from the ethanolic flower extract is found to be active and it showed the presence of flavonoids, phenols and glycosides. The thin layer chromatogram showed the presence of 4 resolved spots with the R_f values 0.14, 0.3, 0.54 and 0.71. The HPTLC chromatogram showed 7 resolved peaks with the R_f values 0.14, 0.19, 0.3, 0.48, 0.54, 0.65 and 0.71 respectively. The percentage area of the fourth peak with the Rf value 0.48 was higher 27.46 when compared to other resolved peaks.

The ethyl acetate fraction is subjected for isolation of phytoconstituent using column chromatography yielded Quercetin confirmed by melting point, UV, IR, ^{1}H NMR and mass spectroscopic studies.

The isolated compounds are subjected for physico-chemical analysis viz., Lipinski rule of five, pharmacokinetic and pharmacodynamic parameters. The results suggest that the isolated compounds 10-Oxoundecanoic acid, 14-oxopentadec-9-enoic acid, Nuciferine and Quercetin showed the drug likeness property.

The chemotaxonomic analysis of the genus *Nymphaea* showed wide variety of secondary metabolites such as glycosidal anthocyanin, isoflavone, flavonol glycoside, steroid, alkaloid, cardiac glycoside, lignan and triterpene.

Pharmacologic studies

Acute toxicity studies showed the non toxic nature of ethanolic root and rhizome and ethyl acetate fraction from the ethanolic flower extract of *Nymphaea pubescens*.

The antidiabetic activity of ethanolic extract from root and rhizome *Nymphaea pubescens* evaluated in the Streptozotocin and Nicotinamide induced type II diabetic rats.

The ethanolic extract from root and rhizome showed a significant reduction in blood glucose levels from 30min onwards in oral glucose tolerance test similar to the standard drug Glibenclamide.

The elevated blood glucose level and glycosylated hemoglobin, decreased body weight and hepatic glycogen content observed in the diabetic rats significantly reverted back to normal value administered with the ethanolic extract 200 and 400 mg/kg b.w respectively at the end of the experimental study.

The altered levels of triglycerides, total cholesterol, high density lipoprotein and very low density lipoprotein in the diabetic state reverted back to normal after administration with ethanolic extract similar to the standard drug Glibenclamide.

The ethanolic extract from root and rhizome of *N.pubescens* normalizes the disturbed carbohydrate metabolism in the group of diabetic rats by enhancing glycolytic enzyme and decreasing the gluconeogenic enzyme indicates its beneficial effect in the treatment of diabetes mellitus.

The histopathological studies showed the regeneration of pancreatic cells in the group of diabetes induced rats administered with ethanolic extract similar to the standard drug Glibenclamide.

In the diabetes induced group the pro-apoptotic protein expression Caspase-3 is increased and the anti-apoptotic protein expression Bcl-2 decreased whereas the groups received the standard drug Glibenclamide and ethanolic extract decreases the expression of Caspase-3 and increases the expression of Bcl-2. The result suggests that *Nymphaea pubescens* promotes the synthesis of anti-apoptotic protein and inhibits the pro-apoptotic protein in the hepatocytes..

The isolated compounds Nuciferine, 10-oxoundecanoic acid and 14-oxopentadec-9-enoic acid is docked with the insulin designalling receptor Protein Tyrosine Phosphatase 1B. Nuciferine showed highest binding energy when compared to 10-oxoundecanoic acid and 14-oxopentadec-9-enoic acid.

The antidiabetic activity of the root and rhizome from *N.pubescens* acts in a multiple target such as increases the glycolytic enzyme, decreases the gluconeogenic enzyme, decreases the expression of pro-apoptotic protein Caspase-3, increases the expression of anti-apoptotic protein BCl-2 and inhibits the Protein tyrosine phosphatase 1B, designaling pathway for the insulin secreation. The antidiabetic activity of root and rhizome from *N.pubescens* showed high significant activity similar to the standard drug Glibenclamide.

The ethyl acetate fraction from ethanolic flower extract of *N.pubescens* showed anticancer activity against *HeLa* cell lines. The invivo anticancer activity of ethyl acetate fraction against Dalton ascitic lymphoma induced swiss albino mice showed decreased tumor volume, packed cell volume, viable cell count, body weight and increased mean survival time and % increased life span. Treatment with ethyl acetate fraction for the DAL bearing mice reverted back Hemoglobin content, RBC

and WBC count to normal. The result suggests the ethyl acetate fraction showed significant anticancer activity similar to the standard drug 5-Fluoro uracil.

The ethyl acetate fraction showed the antioxidant activity against various free radicals depending on the specific assay methodology indicate the complexity of the mechanisms and diversity of the chemical nature of the phytoconstituent present.

CONCLUSION

The present study was aimed at establishing scientific validation with supporting data of the aquatic plant *Nymphaea pubescens* Willd family Nymphaeaceae on its pharmacognosy, phytochemistry and pharmacological activities.

The study for the first time designed to focus on the pharmacognostic standardization, systematic isolation of the phytoconstituents, identification by spectroscopic interpretation including 2D NMR studies and subjecting the same for physico-chemical analysis like Lipinski rule of five, pharmacodynamic and pharmacokinetic parameters, screening the plant extracts and the isolated compounds for the target based antidiabetic activity in the type II diabetic animal model enzymatically and also at the receptor level, anti-cancer activity and *In-vitro* anti-oxidant activity in order to establish and standardize the folklore claims.

The pharmacognostic standardization helps to differentiate between the species and adulterants or substitutes. The study revealed the macroscopic, microscopic identification, physico-chemical constants, powder and fluorescence analytical datas that provides the standardizing protocol for *Nymphaea pubescens*.

Thoroughly investigated the literature, presence of macrocyclic flavonol Nympholide A and Nympholide B in *Nymphaea lotus* and Nuciferine in *Nelumbo nucifera* were isolated and reported. But so far no such compounds were isolated and scientifically proved from *Nymphaea pubescens*.

The phytochemical studies of the aquatic plant for the first time focused mainly on identification and isolation of two aliphatic compounds 10-oxoundecanoic acid and 14-oxopentadec-9-enoic acid, one aporphine based alkaloid Nuciferine and one flavonol Quercetin. The studies supported by TLC, HPTLC, UV, IR, ^{1}H NMR, ^{13}C NMR, ^{13}C DEPT-135 NMR, HMBC 2D NMR, Mass spectroscopic and melting point data's. In addition the isolated compounds are subjected for physico-chemical analysis by feeding the structure of the compound in the database ACD/ilabs. The

physico-chemical studies revealed all the isolated compounds exhibits drug likeness property.

The literature has thus so far documented no pharmacological and systematic study has been attempted to confirm the traditional practice of using *Nymphaea pubescens* in the treatment of diabetes and cancer.

The pharmacological studies of the root and rhizome showed that the ethanolic extract acts mechanistically by increasing the glycolytic enzymes, anti-apoptotic protein Bcl-2 expression and decreasing the gluconeogenic enzymes, pro-apoptotic protein expression in hepatic cells. The isolated compounds 10-oxoundecanoic acid, 14-oxopentadec-9-enoic acid and Nuciferine inhibit the Protein tyrosine phosphatase 1B receptor involved in the insulin signaling deactivation pathway. The ethanolic extract from the root and rhizome of *Nymphaea pubescens* screened for the first time for antidiabetic activity in the type II diabetes induced animal models and the compounds 10-oxoundecanoic acid, 14-oxopentadec-9-enoic acid and Nuciferine was isolated from root and rhizome and molecularly docked for the first time.

The ethyl acetate fraction from ethanolic flower extract of *N.pubescens* showed significant anticancer and anti-oxidant activity and the activities may be due to the presence of Quercetin which is isolated and reported for the first time.

We conclude that the aquatic plant *Nymphaea pubescens* is scientifically proved by isolating the compounds 10-oxoundecanoic acid, 14-oxopentadec-9-enoic acid, Nuciferine and Quercetin and validating by physico-chemical property analysis, chemotaxonomical analysis, molecular studies of the extracts for the antidiabetic activity, molecular docking for the isolated compounds with the receptor Protein Tyrosine Phosphatase 1B, biological assay for active fraction in the DAL induced animal model and its free radical scavenging effect, since scientific validation is the hour of the day.

The aquatic plant *Nymphaea pubescens* also gives the chemotaxonomical significance due to the presence of aporphine based alkaloid Nuciferine and flavonol Quercetin to the Nymphaeaceae family.

In future, large scale isolation of 10-oxoundecanoic acid, 14-oxopentadec-9-enoic acid and Nuciferine and screening the isolated compounds for *in-vivo* antidiabetic activity including apoptotic studies, *in-vivo* assay for PTP1B, QSAR studies may provide potent lead molecules for the treatment of type II diabetes mellitus.

REFERENCES

1. Qadry JS. *Pharmacognosy*, 1st ed. Delhi: Somya printers; 2010.

2. Sheetal Verma, Singh SP. Current and future status of herbal medicines. *Veterinary World* 2008; 1: 347-350.

3. Chyuan-Chuan Wu, Tsai-Kun Li, Lynn Farh, Li-Ying Lin, Te-Sheng Lin, Yu-Jen Yu, Tien-Jui Yen, Chia-Wang Chiang, Nei-Li Chan. Structural Basis of Type II Topoisomerase Inhibition by the Anticancer Drug Etoposide. *Science* 2011; 333: 459-462.

4. Edward Giovannucci,. Harlan DM, Archer MC, Bergenstal RM, Gapstur SM, Habel LA, Pollak M, Regensteiner JG, Yee D. Diabetes and Cancer: A Consensus Report. *CA. A Cancer Journal for Clinicians* 2010: 60; 207-221.

5. Borsch T, Hiluy KW, Wiersema JH, Cornelia Lo¨hne Z, Barthlott W, Wildes V. Phylogeny of *Nymphaea* (Nymphaeaceae): evidence from substitutions and microstructural changes in the chloroplast trnT-trnF region. *International journal of Plant Science* 2007; 168: 639-671.

6. Nayar MP, Thothathri K, Sanjappa M. Fascicles of flora of India. *Botanical survey of India* 1990: 14-15.

7. Bhattacharjee SK. *Hand book of medicinal plants*. London: Pointer publisher; 2001. p239-240.

8. Nadkarni KM, *Materia Medica* India. Bombay: Popular Prakashan; 1988. p858-860

9. Jayaweera DMA. *Medicinal plants (Indigenous and Exotic) used in Ceylon, Part-IV*. Colombo: The national council of Srilanka; 1982. p134-135.

10. Yoganarasiman SN. *Medicinal plants of India*. Tamil Nadu-Bangalore: Cybermedia; 2000. p380.

11. Sowemimo, Fakoya, Awopetu, Omobuwajo, Adesanya. Toxicity and Mutagenic activity of some selected Nigerian plants. *Journal of Ethnopharmacology* 2007; 113: 427-432.

12. Chopra RN, Nayar SL. *Glossary of Indian medicinal plants*. Delhi: Council of Scientific & Industrial Research; 1956. p162.

13. Robinson GM, Robinson R. A survey of anthocyanins. IV. *Biochemistry Journal* 1934; 28**:** 1712-1720.

14. Bendz G, Jonsson B. Anthocyanins in leaves of *Nymphaea candida, Phytochemistry* 1971; 10: 471-472.

15. Vidya Joshi JR, Merchant V, Nadkariny V, Krishnan Namboori D, Vaghani D. Chemical components of some Indian medicinal plants. *Indian Journal of Chemistry* 1974; 12: 226.

16. William A. Emboden. The mushroom and the water lily, literary and pictorial evidence for *Nymphaea* as a ritual psychogen in Meso America. *Journal of Ethnopharmacology* 1982; 5: 139-148.

17. Shirly NH, Frank chandler R. Herbal remedies of the maritime Indians : Phytosterols and triterpenes of 67 plants. *Journal of Ethnopharmacology* 1984; 10: 181-194.

18. Kurihara H, Kawabata J, Hatano M. Geraniin, a hydrolysable tannin from *Nymphaea tetragona* Georgi (Nymphaeaceae). *Bioscience, Biotechnology and Biochemistry* 1993; 57: 1570-1571.

19. Fossen T, Andersen OM. Acylatedanthocyanins from leaves of the water lily *Nymphaea*x *marliaceae*. *Journal of Phytochemistry* 1997; 46: 353-357.

20. Fossen T, Harsen AA. Anthocyanins from flowers and leaves of *Nymphaea* x *marliaceae* cultivars. *Journal of Phytochemistry* 1998; 48: 823-827.

21. Fossen T, Larsen A, Kiremire BT, Andersen EM. Flavonoids from blue flowers of *Nymphaea caerulea*. *Journal of Phytochemistry* 1999; 51: 1133-1137.

22. Zhang Z, Elsohly HN, Cong Li X, Khan SI, Broedel SE, Rauli RE, Cihlar RL, Burandt C, Walker LA. Phenolic compounds from *Nymphaea odorata*. *Journal of Natural Products* 2003; 66: 548-550.

23. Elegami AA, Bates C, Gray AI, Macky SP, Skellern GG, Waigh RD. Two very unusual macrocyclic flavonol glycoside from the water lily *Nymphaea lotus*. *Journal of Phytochemistry*. 2003; 63: 727-731.

24. Marquina S, Barbosa JB, Alvarez L. Comparative phytochemical analysis of four Mexican *Nymphaea* species. *Journal of Phytochemistry* 2005; 69: 921-927.

25. Agnihotri VK, Elsohly HN, Khan SI, Smillie TJ, Khan IA, Walker LA. Antioxidant activity of *Nymphaea caerulea* flowers. *Phytochemistry* 2008; 69: 2061-2066.

26. Raja MM, Sethiya NK, Mishra SH. A comprehensive review on *Nymphaea stellata*: A traditionally used bitter. *Journal of Advanced Pharmaceutical Technology and Research* 2010; 3: 311-319.

27. Verma A, Ahmed B, Rucha, Soni N. Nymphasterol, a new steroid from *Nymphaea stellata*. *Journal of medicinal chemistry research* 2011; 10: 1-5.

28. Yang TH, Chen CM, Lu CS, Liao CL. Studies on the alkaloids of lotus receptacle. *Journal of Chinese chemical Society* 1972; 19: 143-147.

29. Kunitomo J, Yoshikawa S, Tanaka S, Imori, Isoi K. Alkaloids of *Nelumbo nucifera*. *Phytochemistry* 1973; 12: 699-701

30. Yang J, and Zhou K. Spectral assignments and reference data. *Magnetic resonance chemistry* 2004; 42: 994-997.

31. Wu S, Sun C, Cao X, Zhou H, Zhang H, Pan Y. Preparative counter current chromatography isolation of liensinine and its analogs from embryo of the seed of *Nelumbo nucifera* using upright coil planet centrifuge with four multilayer coils connected in series. *Journal of chromatography A* 2004; 1041: 153-162.

32. Yang J, Zhou K, Spectral assignments and reference data, Magnetic resonance in chemistry-II, *Magnetic resonance chemistry* 2005; 43: 845-849.

33. Kashiwada Y, Aoshima A, Ikeshiro Y, Chen YP, Furukawa H, Itoigawa M, Fujioka T, Mihashi K, Cosentino M, Morris-Natschke SL, Lee KH. Anti-HIV benzylisoquinoline alkaloids and flavonoids from the leaves of *Nelumbo nucifera* and structure activity correlations with related alkaloids, *Bioorganic and Medicinal chemistry* 2005; 13: 443-448.

34. Wrobel JT, Iwanow A. the structure of Nupharolutine, an alkaloid of *Nuphar luteum*. *Canadian Journal of chemistry* 1972; 50: 1831-1833

35. Wrobel TJ, Iwanow A, Szychowski J, Poplawski J. Neothiobinupharidine sulfoxide. *Canadian journal of chemistry* 1972; 50: 1968-1972

36. Agnieszka, Wojtasiewicz K, Wrobel JT. Sulphoxides of thiobinupharidine thiohemiaminals from *Nuphar lutea*. *Phytochemistry* 1986; 25: 2227-2231

37. Cybulski, Babel K, Wojtasiewicz K, Wrobel JT, Maclean DB. Nuphacristine-an alkaloid from *Nuphar luteum*. *Phtochemistry* 1988; 27: 3339-3341

38. Nishizawa K, Nakata I, Kishida A, Ayer WA, Browne LM. Some biologically active tannins of *Nuphar variegatum*. *Phytochemisty* 1990; 29: 2491-2494.

39. Zhao H, Zhao S. New cerebrosides from *Euryale ferox*, Journal of natural products. 1994; 57:138-141.

40. Miyazawa M, Yoshio K, Ishikawa Y, Kameoka H, Insecticidal alkaloids against *Drosophila melanogaster* from *Nuphar japonicum* DC. *Journal of agriculture and Food Chemistry* 1998; 46: 1059-1063.

41. Bhandarkar MR, Khan A. Antihepatotoxic effect of *Nymphaea stellata* Willd. against carbon tetra chloride induced hepatic damage in albino rats. *Journal of Ethnopharmacology* 2004; 91: 61-64.

42. Khan N, Sultana S. Chemomodulatory effect of *Ficus racemos*a extract against chemically induced renal carcinogenesis and oxidative damage response in Wistar rats. *Life Science.* 2005; 29: 1194-210.

43. Rajagopal and Sasikala, Antidiabetic activity of hydro-ethanolic extracts of *Nymphaea stellata* flowers in normal and alloxan induced diabetes rats. *African Journal of pharmacy and pharmacology* 2008; 2: 173-178.

44. Karthiyayini T, Sindu NR, Senthilkumar KL. Antidiabetic activity on the flowers of *Nymphaea pubescens* Willd. *Research Journal of Pharmaceutical, biological and Chemical Sciences* 2011; 2: 866-873.

45. Shajeela PS, Kalpana Devi V, Mohan VR. Potential antidiabetic, hypolipidaemic and antioxidant effects of *Nymphaea pubescens* extract in alloxan induced diabetic rats. *Journal of applied pharmaceutical science* 2012; 2: 83-88.

46. Rajan Rushender C, Madhavi eerike, Madhusudhanan N, Venugopala Rao K. Antidiabetic activity of *Nymphaea pubescens* ethanolic extract - *in vitro* study. *Journal of Pharmacy Research* 2012; 5: 3807-3809.

47. Dalmeida DE, Mohan VR, Total phenolics, flavonoids and in vitro antioxidant activity of *Nymphaea pubescens* Wild rhizome. *Asian Pacific Journal of Tropical Biomedicine* 2012; 2: 1-5.

48. Sass JE. *Elements of Botanical Microtechnique*. New York: McGraw Hill Book Co; 1940.

49. Johansen D. *Plant Microtechnique*. New York: MC Graw Hill Book; 1940. p1-30.

50. O'Brien, TP, Feder N, Mc Cull ME. Polychromatic staining of plant cell walls bytoluidine blue-O. *Protoplasma* 1964; 59: 364-373.

51. Easu K. *Anatomy of seed plants*. New York: John wiley and sons; 1979. p550-767.

52. Kokate CK. *Practical Pharmacognosy*, 4th ed. Delhi: Vallabh Prakashan; 1994. p108-109.

53. Pulok K. Mukerjee. *Quality control of herbal drugs, an approach to evaluation of botanicals, Business Horizons*. New Delhi: Pharmaceutical publishers; 2002. p181-357.

54. Chase CR, Pratt RJ. Fluorescence of powdered vegetable drugs with particular reference to development of a system of identification. *Journal American Pharmacology Association* 1949; 38: 32.

55. Harborne JB. Methods of extraction and isolation In: Harborne JB (ed.) *Phytochemical methods*. 2nd Ed. London; Chapman and Hall: 1998. p60-66.

56. Robinson Singleton J, Gordon Smith A, Russell JW, Feldman EL. Microvascular Complications of Impaired Glucose Tolerance. *Diabetes* 2003; 52: 2867-2873.

57. Mosamann T. Rapid Colorimetric assay for cellular growth and survival; application to proliferation and cytotoxicity assays. *Journal of Immunological Methods* 1983; 65: 55-63.

58. Monks A, Scudiero D, Skehan P, Shoemaker R, Paull K, Vistica D, Hose C, Langley J, Cronise P, Vaigro-Wolff A, Gray-Goodrich M, Campbell H, Mayo J, Boyd M. Feasibility of high flux anticancer drug screen using a diverse panel of cultured human tumour cell lines. *Journal of the National Cancer Institute* 1991; 83: 757-766.

59. Wagner HH, Bladt S, *Plant Drug Analysis: A Thin Layer Chromatography Atlas*. 2nd ed. London: Springer; 1996.

60. Reich E, Schibli A. *High-Performance Thin-Layer Chromatography for the Analysis of Medicinal Plants*. New York: Thieme medical publisher; 2007.

61. Kitson FG, Larsen BS, McEwen CN. *Gas Chromatography and Mass Spectrometry: A Practical Guide follows the highly successful*. Oxford: Academic press; 1996.

62. Madhu C. Diwakar., Plant Drug Evaluation, A laboratory guide, 1st ed. p.27.

63. Kalsi PS. *Spectroscopy of organic compounds.* New Delhi: New age international Pvt. Ltd. Publishers; 2010. p9-512.

64. Veber DF, Johnson SR, Cheng HY, Smith BR, Ward KW, Kopple KD. 2002. Molecular properties that influence the oral bioavailability of drug candidates. *Journal of Medical Chemistry* 2002; 45: 2615-2623.

65. Leland J. Cseke. *Natural Products from Plants.* 2nd ed. New York: Taylor and Francis group; 2006.

66. Humphrey P. Rang and Maureen M. Dale, *Pharmacology*. 7th ed. London: Elsevier; 2011.

67. World Health Oorganization *Definition, Diagnosis and Classification of Diabetes Mellitus and its Complications Report of a WHO Consultation Part 1: Diagnosis and Classification of Diabetes Mellitus*. Geneva: World Health Organization Department of Noncommunicable Disease Surveillance; 1999.

68. Kenneth M. Shaw, Michael H. Cummings. *Diabetes Chronic Complications.* 3rd ed. Portsmouth: Willy Blackwell; 2005. p27-29.

69. Jain S, Saraf S. Type II diabetes mellitus-its global prevalence and therapeutic strategies, Diabetes and Metabolic syndrome. *Clinical Research Reviews* 2010; 204: 48-56.

70. Hiriart M, Aguilar-Bryan L. Channel regulation of glucose sensing in the pancreatic beta-cell. *American Journal of Physiology and Endocrinology Metabolism* 2008; 295: E1298-306

71. Mlinar B, Marc J, Janez A, Pfeifer M. Molecular mechanisms of insulin resistance and associated diseases. *Clinincal Chimical Acta* 2007; 375: 20-35.

72. White MF. IRS proteins and the common path to diabetes. *American journal of Physiology Endocrinology Metabolism* 2002; 283: E413-22.

73. Kim JA, Wei Y, Sowers JR. Role of Mitochondrial Dysfunction in Insulin Resistance. *Circtical Research* 2008;102: 401-414.

74. Srinivasan K, Ramarao P. Animal models in type 2 diabetes research: an overview. *Indian Journal of Medical Research* 2007; 125: 451-472.

75. Szkudelski T. The mechanism of alloxan and streptozotocin action in B cells of the rat pancreas. *Physiological Research* 2001; 50: 537-46.

76. Ibrahim SS, Rizk SM. Nicotinamide: A cytoprotectant against streptozotocin-induced diabetic damage in Wister rat brains. *African Journal of Biochemistry Research* 2008; 2: 174-180.

77. Shirwaikar A, Rajendran K. Barik R. Effect of aqueous bark extract of *Garuga pinnata* Roxb. in streptozotocin-nicotinamide induced type-II diabetes mellitus. *Journal of Ethnopharmacology* 2006; 107: 285-290.

78. Palsamy P, Subramanian S. Resveratrol, a natural phytoalexin normalizes hyperglycemia in streptozotocin-nicotinamide induced experimental diabetes rats. *Biomedicine and Pharmacotherapy* 2008; 62: 598-605.

79. Wallace DC, Fan W, Vincent P. Mitochondrial and therapeutics, *Annual review Pathological Mechanical disease* 2010; 5: 297-348.

80. Fan TJ, Han LH, Cong RS, Liang J. Caspase family proteases and apoptosis. *Acta Biochimical Biophys Sinica* 2005; 37: 719-27.

81. Jung M, Lee Y, Park M, Kim H, Kim H, Lim E, Tak J, Sim M, Lee D, Park N, Oh WK, Hur KY, Kang ES, Lee HC. Design, synthesis, and discovery of stilbene derivatives based on lithospermic acid B as potent protein tyrosine

phosphatase 1B inhibitors. *Bioorganic Medical Chemistry Letter*s 2007; 17: 4481-4486.

82. Theodore O. Johnson, Jacques Ermolieff and Michael R. Jirousek. Protein tyrosine phosphatase 1b inhibitors for diabetes. *Nature reviews drug discovery* 2002; 1:698-709.

83. Popov D. Novel protein tyrosine phosphatase 1B inhibitors: interaction requirements for improved intracellular efficacy in type 2 diabetes mellitus and obesity control. *Biochemistry Biophysical Research Communication* 2011; 410:377-81.

84. Balachandran P, Govindarajan R. 2005 Cancer--an ayurvedic perspective. *Pharmacological Research* 2005; 51: 19-30.

85. Hans G. Vogel. *Drug Discovery and Evaluation: Pharmacological Assays.* 2nd edn. New York: Springer; 2002.

86. Halliwell B, Gutteridge JMC. Free Radicals in Biology and Medicine, 3rd edn. Oxford: Clarendon Press; 1999.

87. Sies H. *Oxidative Stress. Oxidants and Antioxidants.* New York: Academic Press; 1991.

88. Evans Jl, Ira D, Goldfine, Maddux BA, Grodsky GM. Oxidative Stress and Stress-Activated Signaling Pathways: A Unifying Hypothesis of Type 2 Diabetes. *Endocrine Reviews*; 23: 599-622.

89. Halliwell B. The role of oxygen radicals in human disease,with particular reference to the vascular system. *Haemostasis* 1993; 23(Suppl 1):118-126.

90. Fridovich I. 1997 Superoxide Anion Radical (O_2), Superoxide Dismutases, and Related Matters. *The Journal of Biological Chemistry* 1991; 272: 18515-18517.

91. Birnboim HC. A superoxide anion induced DNA strand-break metabolic pathway in human leukocytes: effects of vanadate. *Biochemistry and Cell Biology* 1988; 66: 374-81.

92. Shirwaikar A, Rajendran K, Punitha ISR. Antidiabetic activity of alcoholic stem extract of *Coscinium fenestratum* in streptozotocin-nicotinamide induced type 2 diabetic rats. *Journal of Ethnopharmacology* 2005; 111: 369-374.

93. Lowry OH, Rosenbrough NJ, Farr A. Randall RJ. Protein measurement with the Folin phenol reagent. *Journal of Biological Chemistry* 1951; 193*:*265-275.

94. Leelavinothan P, Sankaranarayanan C. Beneficial effects of thymoquinone on hepatic key enzymes in streptozotocin-nicotinamide induced diabetic rats. *Life sciences* 2009; 85: 830-834.

95. Fiske CH, Subbarow Y. The colorimetric determination of phosphorus *Journal of. Biological Chemistry* 1925; 66: 375-400.

96. Hannah Rachel Vasanthi, Subhendu Mukherjee B, Diptarka R, Shanmugasundara Pandian K, Jayachandran, Lekl I, Dipak Kumar D. Protective role of air potato (*Dioscorea bulbifera*) of yam family in myocardial ischemic reperfusion injury. *Food and function* 2010; 1: 278-283.

97. Doman TN, McGovern SL, Witherbee BJ, Kasten TP, Kurumbail R, Stallings WC, Connolly DT, Shoichet BK. Molecular Docking and High-Throughput Screening for Novel Inhibitors of Protein Tyrosine Phosphatase-1B. *Journal of Medical Chemistry* 2002; 45: 2213-2221.

98. Lengauer T, Rarey M. Computational methods for biomolecular docking. *Current Opinion Structural Biology* 1996; 6: 402-406.

99. Xie J, Tian J, Sua L, Huang M, Zhu X, Ye F, Wana Y. Pyrrolo[2,3-c] azepine derivatives: A new class of potent protein tyrosine phosphatase 1B inhibitors. *Bioorganic and Medicinal Chemistry Letters* 2011; 21: 4306-4309.

100. Rajeshwari Y, Gupta M, Mazumden UK. Antitumor activity and *in vivo* antioxidant status of *Mucuna pruriens* (Fabaceae) seeds against Ehlrich Ascites carcinoma in swiss albino mice. *Iranian Journal of Pharmacology and Therapeutics* 2005; 4: 46-53.

101. Jaishree, V., Badami, S. and Suresh, B. *In vitro* antioxidant activity of *Enicostemma arillare*. *Journal of Health Science* 2008; 54: 524-528.

102. Rao V. 2007. *Biostatistics - A manual of statistical methods for use in Health, Nutrition and Anthropology*, Delhi: Rajkamal Electrical press; 2007. p226-312.

103. Singleton JR, Smith AG, Russell JW, Feldman EL. Microvascular complications of impaired glucose tolerance. *Diabetes* 2003; 52: 2867-2873.

104. Yang H, Wright JR Jr. Human beta cells are exceedingly resistant to streptozotocin in vivo. *Endocrinology* 2002; 143: 2491-2495.

105. Shima K, Zhu M, Kuwajima MA. Role of nicotinamide-induced increase in pancreatic beta-cell mass on blood glucose control after discontinuation of the treatment in partially pancreatectomized OLETF rats. *Diabetes Research Clinical Practice* 1998; 41: 1-8.

106. Giugliano D, Ceriello A, Esposito K. Glucose metabolism and hyperglycemia. *American journal of Clinical Nutrition* 2008; 87: 217S-222S.

107. Sujit K. Chaudhuri. *Quintessence Of Medical Pharmacology* 1st edn. Calcutta: New central book agency ;1997. p704-705.

108. Whitton PD, Hems DA. Glycogen synthesis in the perfused liver of streptozotocin-diabetic rats. *Biochemistry Journal* 1975; 150: 153-165.

109. Møller N, Sreekumaran Nair K. Diabetes and Protein Metabolism. *Diabetes* 2008; 57: 3-4.

110. Green M, Miller LL. Protein Catabolism and Protein Synthesis in Perfused Livers of Normal and Alloxan-Diabetic Rats. *The Journal of Biological Chemistry* 1960; 235: 3202-3208.

111. Travlos GS, Morris RW, Elwell MR, Duke A, Rosenblum S, Thompson MB. Frequency and relationships of clinical chemistry and liver and kidney histopathology findings in 13-week toxicity studies in rats. *Toxicology* 1996; 107:17-29.

112. Becker BF. Towards the physiological function of uric acid. *Free Radical Biology Medicine* 1993; 14: 615-631.

113. Meyer1 C, Dostou1 JM, Welle SL, John E. Gerich1Role of human liver, kidney, and skeletal muscle in postprandial glucose homeostasis. *American Journal Physiology Endocrinology Metabolism* 2002; 282: E419-E427.

114. Prasad SB, Giri. A, Antitumour effect of cisplatin against murine ascites dalton's lymphoma, *Indian Journal Experimental Biology* 1994; 32: 155-62.